THE ROLE OF TYROSINE PHOSPHORYLATION DURING DSCAM1-SIGNALING

Der Einfluss von Tyrosin-Phosphorylierung auf den Dscam1-Signalweg

DE ROL VAN TYROSINE-FOSFORYLERING TIJDENS DSCAM1 SIGNALISATIE

- Dissertation -

zur Erlangung des Doktorgrades
der Mathematisch-Naturwissenschaftlichen Fakultät der
Christian-Albrechts-Universität zu Kiel

und zusätzlich des

Doctor in de biomedische wetenschappen
Doctor of Biomedical Sciences (PhD)
Katholieke Universiteit Leuven

vorgelegt von

Maria-Luise Erfurth

Leuven / Kiel, January 2016

Advisors:

Prof. Dr. Stefan Rose- John (CAU Kiel)

Prof. Dr. Dietmar Schmucker (KU Leuven)

Erster Gutachter/in:	Prof. Dr. Stefan Rose-John
Zweiter Gutachter:	Prof. Dr. Thomas Roeder
Dritter Gutachter:	Prof. Dr. Dietmar Schmucker
Tag der mündlichen Prüfung:	18.4.2016
Zum Druck genehmigt:	

SCHRIFTLICHE ERKLÄRUNG

nach § 8 S. 2 Nr. 1 der Promotionsordnung

der Mathematisch-Naturwissenschaftlichen Fakultät und Technischen Fakultät der Christian-Albrechts-Universität zu Kiel (nachfolgend „PromotionsO “)

Betrifft: **Promotionsverfahren Maria-Luise Erfurth**

an der Mathematisch-Naturwissenschaftlichen Fakultät der CAU zu Kiel
und der KU Leuven
auf Grundlage der diesbezüglichen dreiseitigen Vereinbarung

Hier: Erklärung zur dem Antrag auf Zulassung zum Promotionsprüfungsverfahren nach § 8 S. 2 Nr. 1 PromotionsO beigefügten Dissertation

In meiner vorbezeichneten Promotionsprüfungsangelegenheit erkläre ich hiermit zu meiner als Dissertation beigefügten Abhandlung,

a) dass diese Ausarbeitung – abgesehen von der Beratung durch die Betreuerin oder den Betreuer – nach Inhalt und Form meine eigene Arbeit ist. Für folgende Bestandteile gilt dies nur im nachfolgend nach § 7 Abs. 2 S. 2 PromotionsO dargestellten Eigenanteilsumfang, weil es sich hierbei um bereits veröffentlichte Publikationen im Sinne von § 7 Abs. 2 PromotionsO handelt, an denen mehrere Autoren im Sinne von § 7 Abs. 2 S. 2 PromotionsO beteiligt waren:

   i. Die in Kapitel 1 dargestellte Ausarbeitung „*Cell-intrinsic requirement of Dscam1 isoform diversity for axon collateral formation*” ist in Co-Autorenschaft entstanden und am 6.6.2014 in ***Science*** veröffentlicht worden. Zur Erklärung über meinen eigenen Anteil nehme ich auf meine diesbezügliche Angabe auf Seite 108 der Dissertation Bezug und bestätige diese.

   ii. Die in Kapitel 2 dargestellte Ausarbeitung „*Slit and Receptor Tyrosine Phosphatase 69D Confer Spatial Specificity to Axon Branching via Dscam1*“ ist in Co-Erstautorenschaft entstanden und am 27.8.2015 in ***Cell*** veröffentlicht worden. Zur Erklärung über meinen eigenen Anteil nehme ich auf meine diesbezügliche Angabe auf Seite 124 der Dissertation Bezug und bestätige diese.

b) Der vorstehend unter lit. a) Nr. 2 genannte Bestandteil lag bereits einer Prüfungsstelle als Bestandteil einer Dissertation im Rahmen eines Prüfungsverfahrens des o.a. Co-Erstautors vor (Dissertation Dan Dascenco, KU Leuven, Oktober 2015). Darüber hinaus hat die Arbeit bisher weder in Gänze noch in Teilen einer anderen Stelle im Rahmen eines Prüfungsverfahrens vorgelegen. Hinsichtlich bereits veröffentlichter Teile der Arbeit verweise ich auf die vorstehend unter lit. a) genannten Veröffentlichungen.

c) Die Arbeit ist unter Einhaltung der Regeln guter wissenschaftlicher Praxis der Deutschen Forschungsgemeinschaft entstanden.

Kiel, 4. Januar 2016, _____

Maria-Luise Erfurth

DAS SCHÖNE PRINZIP

ILLUSION

DIE LAUTLOSEN STERNE

DER FRIEDLICHE PLANET

AUS EXPLOSIONEN GEBOREN

UNSERE ERDE

ILLUSION

DAS SCHÖNE PRINZIP

DAS ALLES DURCHZIEHT

Therese Chromik
"Mit meinen Armen teile ich das Meer " (2013)

Table of contents

Abstract

Axon guidance is the developmental process during which outgrowing neurites of cells travel long distances to reach their proper synaptic targets. Precision in wiring is essential for any function of the nervous system. Therefore, axon guidance is critical to the existence of all animals. The navigation of growing neurites occurs at their tips in a sensory-motor structure known as the ***growth cone***. The cell membranes of growth cones are equipped with ***axon-guidance-receptor-molecules***. These trans-membrane proteins sense the composition of the environment and respond to the information by initiating intracellular signaling cascades. Hence, axon guidance receptors represent the regulatory central elements of neural wiring.

Higher order species distinguish themselves from evolutionary lower species by more complex nervous systems. The formation of complex neuronal networks calls for a specialized sub-class of guidance receptors. The larger extent of the neuronal arborization requires the capacity of the neurites to sense the position of a given extension in relation to other neurites derived from the same cell. This task is assumed by "***self-recognition receptors***". They guarantee that a neuron covers the biggest possible area with a given set of neurites. Unnecessary "self-crosses" are avoided by triggering repulsion between neurites of the same cell. The importance of an organizing principle based on self-recognition is emphasized by the fact that it has evolved more than once. Interestingly vertebrates and invertebrates use different combinatorial systems of surface receptors to unmistakably label a neuronal surface. Among such neuronal self-recognition molecules, ***Drosophila Dscam1*** is the first receptor described. Therefore, Dscam1 mediated neuronal self-recognition is very well understood.

The *Dscam1* gene can be spliced into thousands of different isoforms, providing the basis for ***a cell surface code***: Each cell expresses a distinct subset of 10-50 Dscam1 isoforms, rendering its surface uniquely recognizable. The importance of Dscam1 for axonal and dendritic patterning has been demonstrated in numerous *in vivo* assays. However, surprisingly little is known regarding ***the signaling pathway*** of the Dscam1 receptor. This dissertation describes my efforts into gaining insights into the molecular mechanisms of neuronal self-recognition. My dissertation is divided into ***three chapters***: The first two chapters consist ***of two published papers*** to which I have contributed during my time in the neuronal wiring laboratory (Dascenco and Erfurth et al., 2015; He et al., 2014a). They

demonstrate that the Dscam1 receptor is indispensable for the axonal patterning of mechanosensory neurons (ms-neurons) in the ventral nerve cord (VNC). In contrast to its role in uniform dendritic patterning, it is critical to regulate Dscam1 signaling in some sub-compartments of the outgrowing axons. Such spatial regulation of Dscam1 signaling by the ***novel ligand Slit*** and ***tyrosine-phosphorylation*** allows the formation of complicated neurite patterns, such as the branched arborization of mechanosensory-neurons. Dscam1 tyrosine phosphorylation is positively regulated by ***Src kinases*** and negatively modulated by the receptor tyrosine phosphatase ***RPTP69D***. I identified ***three critical tyrosine residues*** in the intracellular domain of Dscam1 important for the interaction with RPTP69D. We also showed that Dscam1 physically interacts with RPTP69D substrate traps on both of the two RPTP69D phosphatase domains. These interactions modulate Dscam1 phosphorylation, rendering Dscam1 the ***first identified substrate of RPTP69D*** as of today.

In ***the third part*** of my dissertation, I summarize the results of a combination of ***proteomic screens***. They were aimed at unraveling the Dscam1 ***signaling complex*** and at ***identifying tyrosine phosphorylated proteins*** that are regulated by Dscam1 signaling. I identified new downstream targets of the pathway. These results link the Dscam1 receptor directly to the actin and tubulin ***cytoskeleton*** and suggest that the receptor is capable of physically recruiting components of the ***translational machinery*** to the membrane. Furthermore, I found the cytoplasmic domain to be associated with components of the cellular ***endomembrane system***, suggesting that receptor internalization might be an important regulatory mode, fine-tuning the signaling response. Among the confirmed novel Dscam1 binding partners are the receptor ***Pvr***, the scaffolding protein ***α-Spectrin*** and the guanine nucleotide exchange (GEF) ***DOCK4***. Surprisingly, I also detected a link of Dscam1 to the ***transcriptional machinery***, which I confirmed via microarrays in hemocytes. Notably, some of the novel interactors, such as the Dscam1-Pvr complex, might be of special interest, because they can be detected among the vertebrate orthologous receptors as well.

Taken together, this dissertation demonstrates that Dscam1 signaling is tightly regulated at several levels: An intrinsic sensitivity threshold for self-recognition is set by regulating the number of isoforms expressed on the cell surface. In a second layer, distinct ligands activate the receptor and the phosphorylation state of the intracellular domain, affecting thereby local translation, Dscam1 endocytosis and local cytoskeletal dynamics. It will be a challenge in the future to dissect under which circumstances and in which cellular context the different signaling complexes are formed and activated.

Zusammenfassung*

Axonale Wegfindung ist ein Entwicklungsprozess in dessen Verlauf Neuriten aus neuronalen Zellkörpern auswachsen und sich über lange Distanzen bewegen, um ihre jeweiliges synaptisches Ziel zu erreichen. Präzise Vernetzung ist eine essentielle Grundvoraussetzung für jede Funktion des Nervensystems. Axonale Wegfindung stellt folglich eine kritische Voraussetzung für die Existenz aller tierischen Organismen dar. Die Navigation von wachsenden Neuriten findet an deren Spitze in einer sensori-motorischen Struktur statt, die als ***Wachstumskegel*** bezeichnet wird. Die Zellmembranen dieser Strukturen enthalten ***Wegführungs-Rezeptoren.*** Diese Transmembranproteine erspüren die Eigenschaften der Umgebung und reagieren auf diese, indem sie intrazelluläre Signalkaskaden initiieren. Folglich sind axonale Wegführungsrezeptoren das zentrale regulatorische Element der neuronalen Vernetzung.

Evolutionär höher gestellte Organismen unterscheiden sich von niedriger entwickelten Arten insbesondere durch ihre komplexeren Nervensysteme. Diese erhöhte Komplexität erfordert ein höheres Maß an räumlicher Steuerungsfähigkeit. Sie erhöht mithin die Anforderung an die axonalen Wegführungsrezeptoren. Für die Ausbildung erweiterter neuronaler Verzweigungen ist es nämlich unabdingbar, dass ein Neurit seine Position im Verhältnis zu anderen Neuriten derselben Zelle erspüren kann. Diese Funktion erfüllen sogenannte ***Selbsterkennungs-Rezeptoren***. Sie garantieren, dass eine Nervenzelle mit ihren Neuriten die größtmögliche Fläche erfasst. Unnötige „Selbst-Überkreuzungen“ werden dabei dadurch vermieden, dass sich Neuriten derselben Zelle abstoßen. Die besondere Bedeutung eines auf Selbsterkennung basierenden ordnenden Prinzips wird nicht zuletzt dadurch deutlich, dass es im Laufe der Evolution mehrfach entstanden ist. Interessanterweise benutzten Vertebraten und Invertebraten verschiedene Kombinationen von Zelloberflächen-Rezeptoren um neuronale Oberflächen eindeutig zu markieren. Der *Drosophila* ***Dscam1 Rezeptor*** ist das erste neuronale Selbsterkennungs-Molekül, das entdeckt wurde. Deswegen ist Dscam1-vermittelte Selbsterkennung auch sehr gut untersucht.

Das *Dscam1*-Gen kann in Tausende voneinander unterschiedliche Protein-Isoformen translatiert werden. Diese stellen die Grundlage für einen ***Zelloberflächencode*** dar: Jede Zelle exprimiert eine individuelle Kombination von 10-50 Dscam1 Isoformen. Dies verleiht der Zelloberfläche eine einzigartige Identität. Der Belang von Dscam1 für die

Bildung axonaler und dendritischer Verzweigungs-Muster ist in zahlreichen *in vivo* Studien überzeugend demonstriert worden. Allerdings ist überraschend wenig über den Dscam1-Signalweg bekannt. Diese Dissertation dokumentiert meine Bemühungen, die molekularen Mechanismen der neuronalen Selbsterkennung zu verstehen.

Diese Dissertation gliedert sich in ***drei Teile***: Die ersten beiden Teile umfassen zwei bereits publizierte Studien, zu denen ich als Autorin während meiner Zeit im Neuronal-Wiring-Labor beigetragen habe (Dascenco and Erfurth et al., 2015; He et al., 2014a). Diese zeigen, dass der Dscam1 Rezeptor unentbehrlich für die Bildung axonaler Verzweigungen von mechanosensorischen Neuronen in der ventralen Nervenschnur ist. Im Gegensatz zur Bildung gleichmäßiger dendritischer Muster ist es sehr wichtig, das Dscam1-Signal in Unterregionen des auswachsendenden Axons zu regulieren. Nur wenn solch eine lokale Kontrolle des Dscam1 Signalweges durch den neu identifizierten ***Liganden Slit*** und ***Tyrosin-Phosphorylierung*** gewährleistet ist, können sich komplizierte axonale Verzweigungen bilden. Die Tyrosin-Phosphorylierung des Dscam1-Rezeptors wird durch ***Src-Kinasen*** positiv und durch die Rezeptor-Tyrosin-Phosphatase ***RPTP69D*** negativ reguliert. Ich habe ***drei kritische Tyrosine*** in der intrazellulären Domäne des Dscam1-Moleküls identifiziert, die wichtig für die Interaktion mit RPTP69D sind. Des weiteren zeige ich, dass Dscam1 an die RPTP69D Phosphatase-Domänen bindet. Damit ist Dscam1 ***das erste bekannte Substrat von RPTP69D.***

Im ***dritten Teil*** meiner Dissertation befasse ich mich mit den Ergebnissen einer Kombination ***proteomischer Experimente***. Sie waren darauf ausgerichtet Proteine zu identifizieren, die auf ein Dscam1-Signal mit der Veränderung ihres Tyrosin-Phosphorylierungs-Status reagieren. Dabei konnte ich Signaleffektoren der Dscam1-Signalkaskade identifizieren. Aus den Ergebnissen lässt sich eine direkte Verbindung zwischen dem Dscam1 Rezeptor und dem Aktin- und Tubulin-***Zytoskelett*** ableiten. Sie legen des weiteren nahe, dass der Rezeptor auch Komponenten der ***Translationsmaschinerie*** an die Membran rekrutieren kann. Die festgestellte Assoziation der zytoplasmatischen Domäne des Rezeptors mit ***Vesikelkomponenten*** legt auch nahe, dass Endozytose ein wichtiger Modus der feinabgestimmten Signalregulierung sein könnte. Für folgende Proteine ließ sich eine Funktion als Dscam1-Bindungs-Partner bestätigen: Der Rezeptor ***Pvr,*** das Gerüst-Protein ***Alpha-Spektrin***, und der G-Protein-Austauschfaktor ***DOCK4***. Überraschenderweise konnte ich auch eine Verbindung zwischen Dscam1 und ***transkriptioneller Regulation*** feststellen, und diesen Befund mit Microarrays in

Hämozyten untermauern. Interessanterweise sind einige der Komplexe, wie die Interaktion zwischen Dscam1 und Pvr, auch zwischen den orthologen Proteinen in Vertebraten präsent und deshalb potentiell von besonderem Interesse.

Zusammengenommen zeigt diese Dissertation, dass der Dscam1 Signalweg streng und auf mehreren Ebenen reguliert wird: Die Zahl der Isoformen, die auf der Zelloberfläche exprimiert sind, legt die intrinsische Empfindlichkeit fest, mit der Selbsterkennung erspürt und signalisiert wird. Eine zweite Ebene stellen verschiedene Liganden dar, die die Dscam1 Phosphorylierung und Internalisation sowie die lokale Translation und die Dynamik des Zytoskeletts beeinflussen. Es wird eine wichtige Aufgabe für zukünftige Studien sein, zu bestimmen unter welchen Umständen sich die verschiedenen Dscam1-Signalkomplexe bilden.

* Dutch and German abstracts are translated from the original text written in English. I'm am thankful for the advice of Hartwig Erfurth, Derya Ayaz and Tineke Breynaert during translations.

Samenvatting*

Axonale padvinding is een ontwikkelingsproces waarbij uitgroeiende neurieten van cellen lange afstanden afleggen om hun synaptische doelen te bereiken. De precisie in het vormen van neuronale verbindingen is essentieel voor elke functie in het zenuwstelsel. Axonale padvinding is daarom zeer belangrijk voor het bestaan van alle dieren. De navigatie van groeiende neurieten gebeurt ter hoogte van hun uiteinden in een sensorisch-motorische structuur gekend als de ***groeikegel.*** De celmembranen van groeikegels zijn uitgerust met ***axonale padvindingsreceptormoleculen***. Deze transmembranaire proteïnen voelen de compositie van de omgeving aan en beantwoorden aan deze informatie door het initiëren van intracellulaire signalisatiecascades. Hierdoor zijn axonale padvindingsreceptoren de regulatorische, centrale elementen van neuronale netwerkvorming.

Evolutionair hogerstaande organismen onderscheiden zich van evolutionair lagere organismen door een complexer zenuwstelsel. De vorming van complexe neuronale netwerken vereist een gespecialiseerde subklasse van padvindingsreceptoren. De hogere graad van neuronale vertakkingen vereist dat neuriten die behoren tot dezelfde cel hun positie met betrekking tot elkaar kunnen aanvoelen. Deze taak wordt vervuld door ***"zelf-herkenningsreceptoren"***. Ze zorgen ervoor dat een neuron met zijn neurieten de grootst mogelijke oppervlakte bedekt. Onnodige "zelf-kruisingen" worden gemeden door initiatie van afstotingsmechanismen tussen neuriten die behoren tot dezelfde cel. Het belang van een dergelijk ordeningssysteem van neuriten gebaseerd op zelfherkenning wordt onderstreept door het feit dat het meermaals is geëvolueerd. Vertebraten en invertebraten gebruiken echter verschillende combinatoriële systemen van oppervlaktereceptoren om feilloos de oppervlakte van een neuron te kenmerken. Van dergelijke neuronale zelf-herkenningsmoleculen is Drosophila Dscam1 de eerste receptor die beschreven is. Dscam1 gemedieerde neuronale zelf-recognitie is daarom al zeer goed begrepen.

Het *Dscam1*-gen kan vertaald worden in duizenden verschillende isovormen. Deze leggen de grondbasis voor een ***celoppervlakte code***: elke cel brengt een verschillende subset van 10-50 Dscam1 isovormen tot expressie waardoor de celoppervlakte uniek wordt. Het belang van Dscam1 voor axonale en dendritische patroonvorming is aangetoond in verschillende *in vivo* assays. Toch is er verrassend weinig geweten over de ***signalisatieroute*** van de Dscam1 receptor. Deze doctoraatsproef beschrijft mijn

inspanningen om meer inzicht te verwerven in de moleculaire mechanismen van neuronale zelfherkenning.

Deze proefschrift is ingedeeld in ***drie hoofdstukken***: De eerste twee hoofdstukken bestaan uit ***twee gepubliceerde papers*** waarvoor ik heb bijgedragen tijdens mijn tijd in het laboratorium voor neuronale netwerkvorming. Ze tonen aan dat de Dscam1 receptor onmisbaar is voor axonale patroonvorming van mechanosensorische neuronen in de ventrale zenuwstreng. In tegenstelling tot de rol van Dscam1 in uniforme dendritische patroonvorming, is het belangrijk om Dscam1 signalering te reguleren in bepaalde subcompartimenten van groeiende axonen. Een dergelijke spatiale regulatie van Dscam1 signalisatie door het ***nieuw ligand Slit*** en door ***tyrosine-fosforylering*** laat toe complexe neurietenpatronen te vormen. De tyrosine-fosforylering van Dscam1 wordt positief gereguleerd door Src kinasen en negatief gereguleerd door de receptor tyrosine fosfatase ***RPTP69D***. Ik heb drie kritieke tyrosinen in het intracellulair domein van Dscam1 geïdentificeerd die belangrijk zijn voor de interactie met RPTP69D. We tonen ook aan dat Dscam1 bindt en interageert met RPTP69D via alle twee de RPTP69D fosfatase domeinen. Deze interacties moduleren Dscam1 fosforylering en maken van Dscam1 het ***eerst geïdentificeerd substraat van RPTP69D tot heden***.

In het ***derde gedeelte*** van mijn proefschrift vat ik de resultaten samen van een combinatie ***van proteomische screenen***. Deze screens hadden als doel om het Dscam1 ***signalisatiecomplex*** te ontrafelen en ***tyrosine gefosforyleerde proteïnen*** te identificeren die gereguleerd worden door Dscam1 signalisatie. We hebben nieuwe doelwitten van Dscam1 signalisatiecascades ontdekt. Deze resultaten tonen een rechtstreeks verband tussen de Dscam1 receptor en het ***actine- en tubuline-cytoskeleton*** en suggereren dat de receptor in staat is componenten van het ***translationeel complex*** aan het celmembraan aan te werven. Verder tonen wij ook aan dat het cytoplasmatisch gedeelte kan associëren met het cellulair ***endomembraansysteem***. Dit suggereert dat receptorinternalisatie een belangrijke manier van regulatie kan zijn voor het verfijnen van signaalresponsen. Enkele van de nieuw geïdentificeerde en bevestigde bindingspartners van Dscam1 zijn de receptor ***Pvr***, de ‘scaffold’ proteïne ***spectrin-1*** en de guanine-uitwisselingsfactor ***DOCK4***. Ik heb ook een verrassende link ontdekt tussen Dscam1 en het ***transcriptioneel mechanisme*** die we ook bevestigd hebben in hemocyten.

Bij elkaar genomen toont deze proefschrift aan dat Dscam1 signalisatie streng wordt gereguleerd op verschillende niveaus: Een gevoeligsheidsdrempel voor zelfherkenning

wordt gereguleerd door het aantal isovormen dat tot expressie worden gebracht op de celoppervlakte. Bij het tweede niveau van regulatie activeren verschillende liganden de receptor en de fosforyleringsstatus van het intracellulair domein waardoor lokale translatie, Dscam1 endocytose en lokale cytoskeletale dynamica worden beïnvloed. Toekomstige studies zullen uitwijzen onder welke omstandigheden en in welke cellulaire contexten de verschillende signalisatiecomplexen gevormd en geactiveerd worden

* Dutch and German abstracts are translated from the original text written in English. I'm am thankful for the assistance of Hartwig Erfurth, Derya Ayaz and Tineke Breynaert for help with translations.

General Introduction

Principles of signal transduction in cell biology

Maintenance of ***homeostasis*** is an important characteristic of life. The word homeostasis is derived from the Greek words *ὅμοιος* ("homoios"- "same/equal") and *ιστημι/ στάσις* ("stasis"- "standing still/state"). It describes the tendency of a biological system to sustain a steady state within a dynamic environment. The concept was first introduced by physiologists (Bernard, 1974) but is now widely applied to other biological fields and has even found its place in modern psychology and literature (Damasio, 2003).

An important prerequisite for the maintenance of homeostasis is the capacity of the system to sense its surroundings. Cues from the environment need to be translated by the system into an internal response or a systemic adjustment. Hence, every living organism maintains ***communication*** with the environment in order to preserve homeostasis. In addition, homeostasis is also maintained on a smaller sub-organismic scale: Every organ, cell and even each subcellular compartment sustains its own homeostasis and communicates with its surroundings in order to maintain function.

In cellular systems such communication calls for the existence of molecules that mediate the information flow from the extracellular into the intracellular space. In fact, there is a specialized class of proteins usually anchored in the plasma membrane known as ***receptors*** *(from Latin: "recipere"- "to receive").* Receptors facilitate the flow of information between different cellular compartments. They are capable of binding and sensing cues in the extracellular compartment and mediating them to the intracellular space. This process of translating external events into intracellular responses is widely known as ***signal transduction*** *(from Latin: "traducere "- "to lead across or over").*

The nature of cues sensed by receptors is highly variable: There are chemical cues, changes in illumination, molecular cues (hormones or growth factors or components of the extracellular matrix) as well as mechanical cues. Molecular cues that bind to receptors and influence their signaling behavior are designated as "***ligands***" *(from Latin: "ligare"- "to bind")*. Usually, ligands bind with high affinity (with affinity constants of $K_\alpha \geq 10^8$ liters/mole) to their receptor. Therefore, even minimal ligand concentrations (typically $\leq 10^{-8}$ M) are sufficient to evoke a cellular response (Alberts et al., 2014).

Transmembrane receptors mediate the information flow between different cellular compartments

Receptor molecules are a very diverse family of proteins. Therefore, a number of different classification systems are in use. One example is the distinction of six receptor families based on their mode of signaling (Alberts et al., 2014). Under this classification system, we differentiate between: Gated ion channels, receptor enzymes, G-protein coupled receptors, nuclear receptors, receptors without enzymatic activity that attract and activate cytoplasmic enzymes and adhesion receptors that mediate signals between the extracellular matrix and the cytoskeleton. Other classification systems distinguish receptor families based on their cellular expression profile. It is for example common practice to distinguish immune receptors (expressed in cells of the immune system) from neuronal receptors that are expressed by cells of the nervous system. In addition, there are classification systems based on the presence of certain signature domains. The Immunoglobulin (Ig)-receptor subfamily for example, is characterized by the presence of a globular Ig-domain. Members of the Ig-receptor family however, are found in all cellular systems of the body and are often involved in cellular adhesion. Therefore, many Ig-receptors can also be classified as adhesion receptors, immune- or neuronal receptors.

The interaction of a cue with the extracellular domain of a receptor induces conformational modifications in the receptor protein, which translate into altered activation levels of signaling cascades downstream of the receptor. Some receptors contain an intrinsic signaling activity (gated ion channels, receptor enzymes, nuclear receptors), others signal indirectly by activating or recruiting cytoplasmic proteins. These intracellular signaling proteins transduce the signal within the cell. The transduction chain leading the information from molecule to molecule can form a long cascade before the information finally reaches an ***effector protein***. Effector proteins are responsible for altering the behavior or the property of a cell. Sequences consisting of ligand, receptor, signaling molecules and effector proteins are commonly known as "***Signal transduction pathways***" (Introduction-Figure 1).

Signal transduction pathways mediate the informational flow in all biological systems. However, by looking at a simple textbook image of a signal transduction pathway as illustrated in Introduction- Figure 1, one tends to forget that signal transduction of a receptor does not happen in isolation. Instead there is a multitude of different signals reaching the cell surface at a given time. While the cell is equipped with multiple different

receptor classes to accommodate the distinct signals, a sophisticated integration system is needed to communicate the intracellular flow of information and to compute an appropriate response in order to maintain homeostasis. It is also important to realize that each cellular response has an effect on the environment itself, therefore creating novel signal transduction tasks by itself.

Based on these reflections, one could easily predict that a complex biological system, -such as the human body-, requires an extremely large number of receptors in order to create the enormous signaling variability and specificity required to maintain homeostasis. Interestingly however, specificity in signal transduction is created with a rather limited number of receptor molecules. In fact, a database search for genes linked to the term "transmembrane receptor" in the *ENSEMBLE GENOME BROWSER* results in only 722 hits for the human genome and 283 hits for the fruit fly *Drosophila melanogaster*. Nevertheless, these receptor pathways are sufficient to maintain coordinated cell-cell communication and hence homeostasis of complex organisms consisting in the case of the human of an estimated 3-4x10^{13} cells (Bianconi et al., 2013).

Signaling variability is created by the combinatorial use of a limited set of signaling molecules

Variability is created by the presence and combinatorial use of differential components of a pathway in space and time. A given receptor can be activated by different ligands prompting distinct signaling cascades. Alternatively, the signaling molecules downstream of a receptor can differ depending on the cellular context. Finally, we observe that certain signaling cascades are recycled in different cellular or developmental contexts: Many signaling pathways that play an important role during development are later in life recycled and used in other signaling dependent processes. The Notch receptor for example, regulates many aspects of cell fate decision during embryogenesis but is also involved in the innate immune response of adult organisms.

In summary, signal transduction can be understood as communication of a biological system (cell/cellular compartment) with its environment. Receptors transmit information from the extracellular compartment into the intracellular space. The sensory capability of a cell is defined by the receptors expressed on it’s surface and by the signaling molecules

present in the cytoplasm. The combinatorial use of these signaling components leads to a distinct cellular response.

Generally, one can differentiate the following signaling schemes that allow for variability in signal transduction: (1) Trafficking and location (e.g. Presence and absence of distinct ligands, subcellular localization of receptors based on their interaction with PDZ polarity proteins or receptor mediated endocytosis); (2) recruitment of different adaptor proteins and scaffolds; (3) timing (activation switches, feedback loops); (4) affinity and specificity of signaling molecules (e.g.: capability of ligands to bind to different receptors; specificity of posttranslational modifications).

The advantage of using signaling cascades instead of an unlimited number of direct receptor-target interaction is that the output of the signal can be modulated at every level of the pathway: Signals can be amplified or reduced (one receptor signals to multiple signaling molecules (divergence) or multiple signaling molecules signal to only one target protein (convergence)) and signaling pathways of different receptors often merge and interact with each other forming complex interaction networks in a process known as "***signal integration***". The cellular response can therefore be understood as a signaling pattern, such as musical chord or harmony, with the components of a given signaling pathway modulating each a detail of the outcome.

Signaling pathways can be studied by different approaches

Based on the understanding of signal transduction cascades, an investigator can decide to study signaling from two different perspectives: He/she can either start at a given receptor and design a conditionally inducible system in order to identify downstream effectors and the cellular response (top-down approach); or one can start with a well-defined cellular response and try to decipher the pathway from the bottom up. The latter more traditional approach has been most often used in pharmacological and biochemical studies until the 1980s. With the advent of molecular cloning, sequencing and the availability of entire genomes the focus has shifted towards the receptor centered approach. This enabled the discovery of entirely new signaling cascades. Especially the neurosciences -and within the neurosciences the neurodevelopmental study of neurite guidance- have enormously benefited from the receptor based approach. I will describe in the results section of this dissertation my own efforts into deciphering the signaling components of the neural axon

guidance receptor Dscam1 starting with the design of a conditionally inducible receptor system.

Drosophila melanogaster as an important model organism for the systematic dissection of signaling pathways

The fruit fly *Drosophila melanogaster* has been an invaluable model organism to dissect and understand signaling pathways, specifically those involved in the formation of the nervous system (reviewed in Bellen et al., 2010; Hatzihristidis et al., 2015). Many essential genes and protein families are conserved between vertebrates and the fruit fly. The same holds true for the basic mechanisms of establishing cell-cell communication. For example, the ***size of the kinome and phosphatome are comparable*** between *Drosophila* and humans and most *Drosophila* kinases and phosphatases have a human orthologue (Hatzihristidis et al., 2015). Importantly for the understanding of the development of the nervous system, the anatomy of *Drosophila* is well understood and many neurons form stereotypical projections. This allows for the quick and efficient identification and analysis of phenotypes based on short reproductive life cycles and abundant progeny.

Furthermore, once a phenotype has been detected and characterized there is an ***ample genetic tool kit*** of fly lines available allowing for the targeted (over)expression or interruption of almost any known transcript in multiple ways (e.g. UAS/Gal4 based systems, RNAi, transposon insertions and (imprecise)-excision as well as mutants generated by chemical or X-ray induced mutagenesis) in a tissue or even single cell specific manner. Furthermore, hemocyte and neuronal cell culture models are available, allowing for the study of molecular pathways through an efficient combination of *in vivo* and *in vitro* experiments. This approach is relatively ***cost-efficient and fast*** in comparison to any vertebrate model available.

In addition, the collections and knowledge regarding *Drosophila* genes and stocks are widely and openly shared among the fly communities. An enormous amount of information is deposited in an extraordinarily well annotated data base known as "FLYBASE", facilitating stock and information exchange but also extensive data mining experiments.

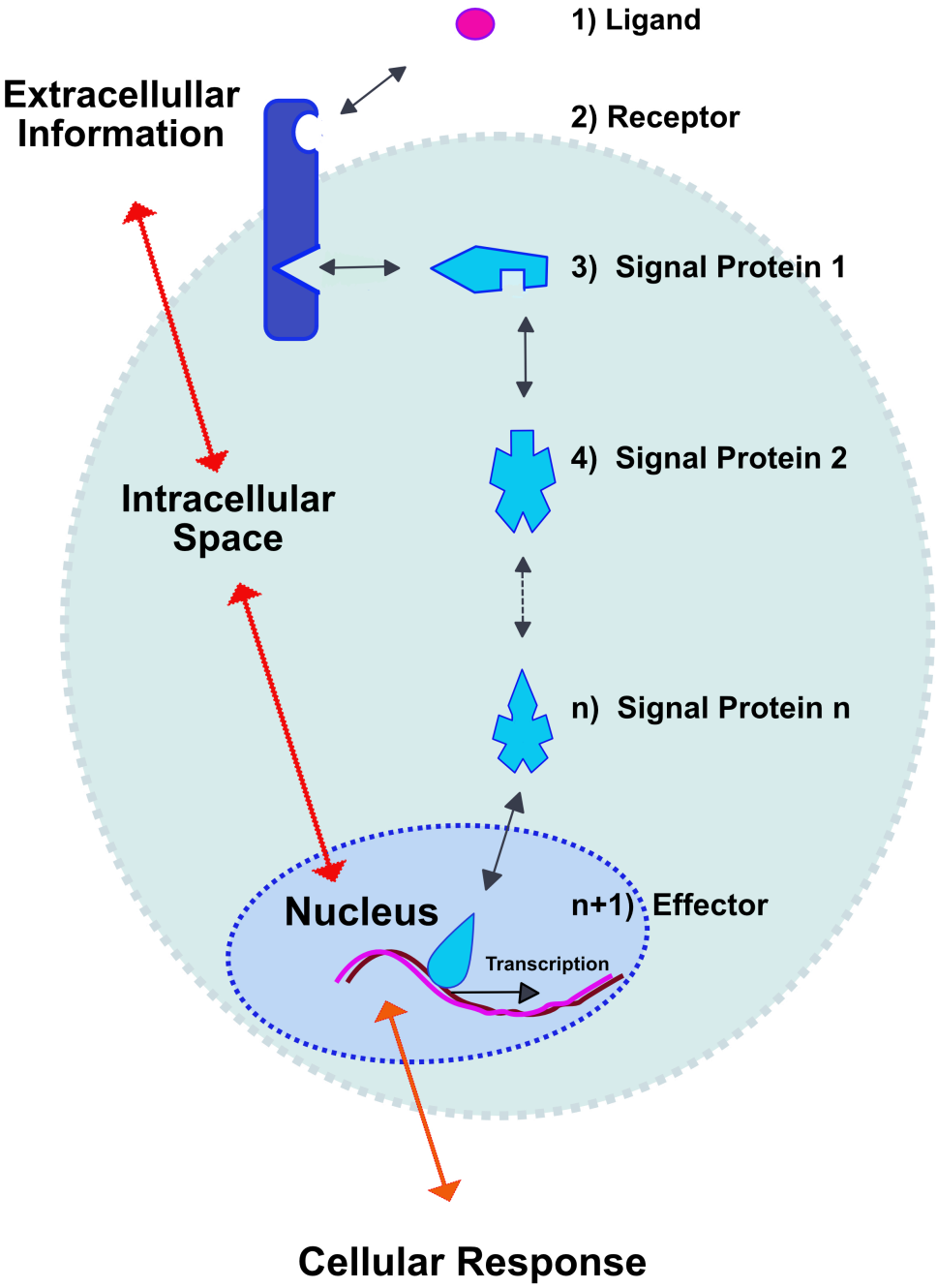

INTRODUCTION- FIGURE 1. **INFORMATION FLOW OF A TYPICAL SIMPLE SIGNAL TRANSDUCTION PATHWAY.**

Extracellular information in form of a ligand-molecule (pink circle) binds to a transmembrane-receptor (Purple). The receptor undergoes a conformational change, thereby transducing the signal from the extracellular into the intracellular compartment. The conformational change of the receptor allows the intracellular domain of the receptor to interact with a signaling molecule (signal protein 1). Subsequently, other signaling molecules (signal protein 2-n) can be recruited to the receptor-complex and transmit the signal to effector molecules. If the effector molecule is a transcriptional regulator as in this hypothetical example, the transcription profile of the cell changes, allowing it to adapt to the external stimulus. The information flow is depicted with red arrows: Information travels from the extracellular space and leads to a cellular response. It is important to realize that the cell in real life is subject to a multitude of different extracellular cues at any given time. Therefore, the information needs to be sensed and processed by multiple signaling systems, requiring signal integration. Importantly, each response of the cell creates changes of the environment and therefore new cues as well.

Neurite Guidance requires Complex Signal Transduction

The common proverb that *"WE ARE THE SUM OF OUR PERCEPTIONS"* is derived from a school of thoughts influenced by Kant and Descartes. Translated into biological terms, it means that the nervous system as the central organ capable of receiving and processing external information is critical to every individuals being. The correct functioning of the nervous system however, depends entirely on the precision of a developmental process commonly known as ***neuronal wiring***.

The initial steps in the formation of the nervous system are based on highly specific, activity independent intrinsic connectivity programs: Neurons extend fibers from the cell body towards other target cells that they are communicating with. The main fiber conducting signals away from the cell body is known as ***axon*** (from Greek: *ἄξων*- axis). The remaining smaller extensions are based on their striking appearance known as ***dendrites*** (from Greek: *δένδρον*- tree). They usually transmit signals towards the cell body and are very variable in terms of size and morphology.

During development, the outgrowing neurites need to navigate - often over very long distances - through a complex environment and maintain motility and direction. In addition, they need to identify correct synaptic targets and establish connections with them. This "self-assembly-program" known as ***neurite guidance*** has fascinated scientist for more than a century. In order to be successful, neurite guidance requires cellular communication with a constantly changing environment and the underlying signal transduction pathways are critical to every animals being. Based on the efforts of many neuroscientists around the world, we understand nowadays many of the molecular mechanisms important for the navigation ***of individual cells or cellular bundles***.

Importantly however, in order to form a fully functional nervous system cells are not navigating in isolation. There are usually many growth cones moving simultaneously through the same environment searching for their individual targets. Furthermore, cells often form complex neurite arborizations connecting them with several target areas. From a signaling perspective, this creates an enormous challenge requiring the signal integration of guidance cues from individual neurites moving into different directions.

Based on these considerations, the field of neural guidance has shifted from understanding the decision making process of an individual isolated neurite to the requirements of forming

complex connectivity patterns. This novel field of ***connectomics*** remains an exciting, fast moving and challenging research topic and is therefore one of the main focus points of my thesis. The perceived impact and socio-economic importance of driving this particular research field is emphasized by the fact that both the US as well as the European Union have established large research initiatives known as the *BRAIN INITIATIVE (US)* and the *HUMAN BRAIN PROJECT (EU)* which both were announced in 2013 during my time in graduate school.

Growth cones: The central elements of neurite guidance

The beginnings of modern neuroscience: The Golgi-method sparks a discussion based on Cajal's neuron doctrine

The Nobel Prize in Physiology and Medicine of 1906 awarded to two scientific "enemies": *"IN RECOGNITION OF THEIR WORK ON THE STRUCTURE OF THE NERVOUS SYSTEM"* the committee honored the Spaniard ***Ramón Y Cajal*** and the Italian ***Camillo Golgi*** (The Nobel Prize in Physiology or Medicine 1906).

The prize was based on studies and observations conducted in the 1890s when the pathologist Santiago Ramón y Cajal illustrated the complexity and beauty of the nervous system by recording the appearance of nerve cells, - the center of his anatomical studies-, in thousands of meticulous manual drawings. This elaborate work captivates the reader with detailed sketches of breathtaking artistic beauty. But it also inspires the mind by the lively and descriptive explanations. The nerve cells and neurites in Cajal's studies travel and navigate over long distances. They sense their environment in such a way, that even a person completely new to neuroscience comprehends easily, how complicated the journey of a neurite towards its target must be. Therefore, Cajal's drawings are even now more than a century later commonly used in presentations introducing neurodevelopmental topics. His choice of language has left an imprint on the vocabulary of all neuroscientists worldwide. These are the reasons why many consider Santiago Ramón y Cajal to be the founding father of modern neuroscience.

His pioneering detailed microscopic studies were based on a novel protocol for the fixation and staining of nerve cells developed by the Italian scientist Camillo Golgi who worked at

the University of Pavia (Golgi, 1873): This procedure based on a silver-chrome staining known as "*LA REAZIONE NERA*" enabled anatomists for the first time to visualize entire neurons in all their complexity, including the finest neurites, ramifications and connections. The observations were meticulously and manually recorded in sketches, each one uniting the observations of several microscopic sections. This little trick of "stacking" was part of the protocol now known as ***"Golgi-method"***. Cajal adopted and refined Golgi's method, and applying it to different animals, developmental stages and tissues was able to visualize neurons and neuronal development in the smallest detail.

His first descriptive "connectomics" study culminated in the formulation of revolutionary and novel conclusions regarding the organization of the nervous system at a cellular level. Cajal arrived at these conclusions by trying to match his anatomical observations with the known function of the brain. He summarized his novel concepts in 1891 as the *NEURON DOCTRINE*, a proposition that sparked an intensive scientific debate. The controversy also reflects in the Nobel speeches given by Golgi and Cajal in Stockholm. Amazingly, it turned out that Cajal had been a true visionary: The interpretation of his data was confirmed by many observations that geneticists and molecular biologists collected in the next 100 years to come.

The growth cone couples sensation with motility

One observation that Cajal made in 1890 on the neurites of a developing brain was the fact that the tips of outgrowing axons were equipped with a fan-like expanded structure. This key decision making axonal sub-compartment is now known as the ***growth cone***. Cajal speculated solely based on the shape and position of the structure that the growth cone (he called it "*CONO DE CRECIMIENTO*") "*IS LIKE A CLUB OR BATTERING RAM ENDOWED WITH EXQUISITE CHEMICAL SENSITIVITY, RAPID AMEBOID MOVEMENTS AND A CERTAIN MOTIVE FORCE ALLOWING IT TO CIRCUMVENT OBSTACLES IN ITS PATH, THUS COURSING BETWEEN VARIOUS CELLS UNTIL REACHING ITS DESTINATION*" (Cajal, 1890). We now know that he was a true visionary when formulating these words. But it took another 100 years to confirm his hypothesis and to fully understand the molecular mechanisms underlying the guidance process.

The growth cone is indeed a dynamic axonal sub-compartment, which bears two functions: It senses the environment which the neurite passes on its journey towards a target, and it translates this sensation into directed movements. This ***dual sensory-motor function*** is enabled by the specific molecular organization of the growth cone which is distinct from

other cellular compartments. In contrast to the ordinary cytoplasm which is filled with a rather uniform gel-like three-dimensional network of microfilaments, the growth cone is divided into separate sub-domains characterized by specific sets of cytoskeletal components (reviewed in Dent et al., 2011).

The cytoskeletal arrangement of the growth cone facilitates mobility

The leading ***edge*** of the growth cone is dominated by ***highly polarized filamentous actin (F-actin) rich structures*** typical for mobile cells and cellular compartments. These regions are central to the creation of mobility and traction. Their cytoplasmic F-actin is organized in bundles of varying thickness (Dent et al., 2011). Some relatively stiff spikes are stabilized by bundles of 15 and more actin filaments. They are known as ***filopodia*** *(from Latin: filium-thread and Greek: πόδι-foot)*. Other F-actin rich projections resemble a broad flat veil known as ***lamellipodia*** *(from Latin: lamella-small plate and Greek: πόδι-foot)*. Their actin cytoskeleton is stabilized by radially arranged meshes of thin actin bundles containing up to 12 filaments. The highly dynamic actin-rich periphery is anchored to a ***microtubule-rich core (base)*** which connects the cone with the axonal shaft. An example of the typical cytoskeletal organization of a growth cone is shown in Introduction- Figure 2.

Growth cones are dynamic and assume many different shapes influenced by the time point at which they are imaged and the nature of their surroundings

The regions described in the paragraph above are depicted in every textbook figure portraying a growth cone. The typical illustration is clearly still influenced by Cajal's initial description of growth cones. Therefore, it often resembles a hand with groping fingers. However, it is important to realize that such illustrations represent an idealized snap-shot. In real life, a growth cone is highly dynamic: The filopodia and lamellipodia constantly change shape and the cone opens and closes in repetitive pulsating movements. Such movements are driven by cycles of actin polymerization in the periphery, competing with a constant non-muscle-myosin driven flow of F-actin away from the leading edge, in a processes known as (tread-milling) (reviewed in Lowery and Van Vactor, 2009). In line with this, we observe under the microscope a variety of different shapes.

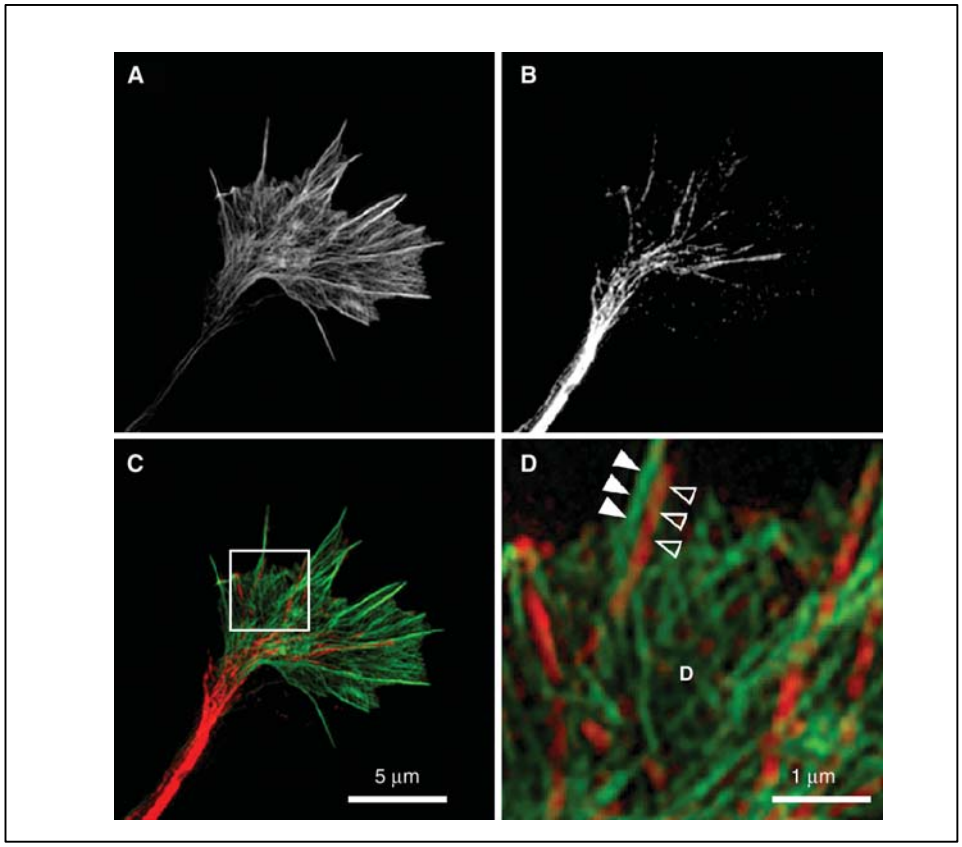

INTRODUCTION- FIGURE 2. **THE CYTOSKELETAL ORGANIZATION OF THE GROWTH CONE.**

(Image taken from Dent et al., 2011). Shown is a fan-shaped typical mouse hippocampal growth cone. (A) Labeling with phalloidin reveals F-actin rich structures organized in bundles (filopodia) or as a mesh (lamellipodia). There is relatively little F-actin in the axonal shaft. (B) Antibody staining with an antibody recognizing tyrosine-phosphorylated tubulin reveals that the base and the axonal shaft are dominated by tubulin. (C) False color overlay of A and B. (D) Magnification of the boxed area and C. At the base of a filopodium, actin bundles (green, closed arrows) and microtubule (red, open arrows) are found in close proximity.

They depend on the space that a growth cone has to expand, on the extracellular matrix that a cone attaches to, on the roughness of the underground and often also on to the type and genetic makeup of the neuron extending the growth cone. Some growth cones appear relatively small and inconspicuous, while others are "*torpedo shaped*" or wildly branched, thereby standing out from the environment with long and numerous neurite extensions. Even though this phenomenon has already been described in the 1990s (Mason and Wang, 1997), it still remains fascinating and surprising how differently shaped growth cone can be, even if derived from neurons of the same model organism. Introduction- Figure 3 illustrates this for growth cones of different *Drosophila* neurons.

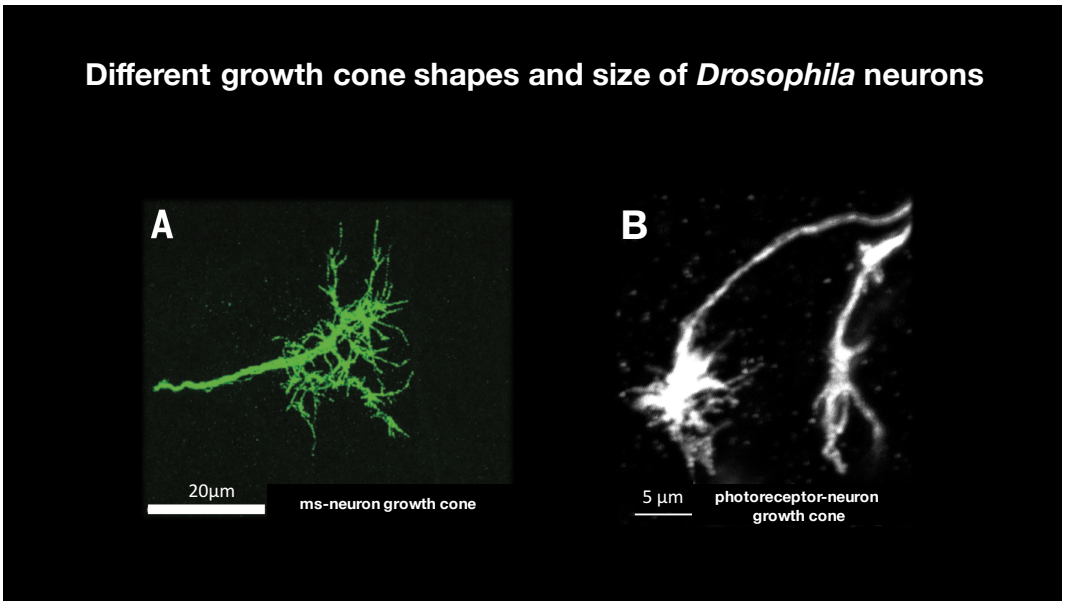

INTRODUCTION- FIGURE 3. **DESPITE THEIR SIMILAR FUNCTION, GROWTH CONES CAN ASSUME VERY DIFFERENT SHAPES AND SIZES EVEN IN NEURONS FROM THE SAME MODEL ORGANISM.**

Panel A was modified from (He et al., 2014a). Panel B is an image received from Dr. Milan Petrovic. (A) growth cone of a Drosophila mechanosensory (ms) neuron entering the ventral nerve cord (VNC). Note the length of the neurites, which exceed in some cases 20µm. (B) Growth cone of an R7 photoreceptor neuron in a 3rd instar Drosophila larva. Note, how despite the similarity in overall shape the neurites are of different length.

Axon guidance receptors: The core components of growth cone sensation

Taken together, it is very well established how the mobility aspect of the growth cone is produced by actin driven re-arrangements of cytoskeletal components in the cytoplasm. However, it wasn't until the dawn of molecular cloning combined with genetics and gene disruption techniques in the 1980s that we started to understand the molecular mechanisms of growth cone sensation and how these perceptions are coupled to the mobility of the cytoskeleton.

A class of transmembrane receptors, now widely known as "***axon guidance receptors***", assumes this central aspect of growth cone function. These sensory signaling molecules cover the cell membranes of growth cone filopodia and lamellipodia. All of them are organized in three ***different functional units***: (1) They possess large "sticky" extracellular domains designed to bind and sense differential environmental cues. (2) They are anchored

to the membrane by a lipophilic transmembrane domain. (3) Their intracellular domains consist of signaling motifs, allowing the interaction with molecular effectors such as kinases, phosphatases, second messengers, GTPases or molecular motors, allowing them to initiate signaling cascades ultimately affecting the cytoskeleton. Structure and function of guidance receptors and the anatomy of the growth cone are evolutionary highly conserved. They can be found in species ranging from the invertebrates *Caenorhabditis elegans (C. elegans)* and *Drosophila melanogaster* to sea slugs (*Aplysia),* frogs, rats, mice, chicken and cells of human origin.

Signal transduction during neural guidance: Ligands, receptors and effectors

One central aspect in understanding neural guidance is the investigation of signaling cascades that trigger distinct guidance and growth decisions. There are many outstanding reviews covering the topic (for example: Corty et al., 2009; Dent et al., 2011; Dickson, 2002; Bashaw and Klein, 2010; Lowery and Van Vactor, 2009). Therefore, I will only focus on the signaling aspects most relevant for this dissertation: Each cascade starts with an ***extracellular guidance cue*** (1), serving as a ligand to the guidance receptor (Corty et al., 2009; Dent et al., 2011; Dickson, 2002; Bashaw and Klein, 2010; Lowery and Van Vactor, 2009). (2) ***The receptor*** translates extracellular stimulation into intracellular signals, thereby influencing effector molecules. (3) The effectors signal to the ***cytoskeleton,*** which leads to changes in growth cone mobility.

Guidance receptors

Many different types of transmembrane proteins can serve as axon guidance receptors (Dickson, 2002; Bashaw and Klein, 2010; Guan and Rao, 2003; Lowery and Van Vactor, 2009). There are different classification systems based on the molecular signature of their extracellular or intracellular domains, by their respective ligands or by the type of response that they evoke in a growth cone (Dickson, 2002; Bashaw and Klein, 2010; Guan and Rao, 2003; Lowery and Van Vactor, 2009).

Historically, ***Ig-CAM receptors*** (Cadherins) have been the first proteins to be attributed with a role in axon guidance (Neugebauer et al., 1988; Hatta et al., 1985; Pierschbacher and Ruoslahti, 1983; Silver and Rutishauser, 1984; Tomaselli et al., 1988). The

extracellular domain of these receptors is characterized by the presence of one or more immunoglobulin (Ig) domains mediating their interactions with different guidance cues (Hatta et al., 1985; Pierschbacher and Ruoslahti, 1983; Silver and Rutishauser, 1984; Tomaselli et al., 1988). The work on Ig-CAMS in axon guidance started to become a "hot topic" in the 1980s. For example, one of the early papers of this newly evolving research-field was featured in the first edition of the journal *Neuron* (Tomaselli et al., 1988). The Ig-domain is an ancient protein family, and Ig-related proteins are already found in bacteria (Bateman et al., 1996). Most Ig-folds are encoded by exons belonging to the same splicing phase. This favored evolutionary diversification, as domains could be gained or lost without disturbing the overall protein reading frame (Trowsdale and Parham, 2004). Therefore, the Ig-superfamily in humans contains almost 1000 distinct members assuming a wide range of different functions. For example, the proteins of the DCC family (Netrin receptors), the Robo receptors (Slit binding) as well as the homophilic cell adhesion molecules, such as NCAM and DSCAM and Cadherins. In addition, there are also receptors with catalytic functions, such as receptor tyrosine kinases (RTKs) and phosphatases (RPTPs), belonging to the superfamily of Ig-receptors. Other classical and well known receptors are the Plexins and Neuropilins (both Semaphorin binding) and the Eph-receptors (Ephrin binding). They contain other extracellular signature motifs typical for guidance receptors, such as FNIII domains, Sema domains, Plexin repeats, IPT (***I***g-like, ***p***lexins, ***t***ranscription factor) domains or ***Eph***rin ***l***igand ***b***inding domains (Eph-LBDs) (Introduction-Figure 4).

One important characteristic that many guidance receptors share, is a ***strictly modular architecture***: The extracellular domain harbors all features necessary to sense a substrate, the transmembrane domain is important for anchoring and localization in the membrane and the intracellular part is encoding specific signaling responses. This peculiar modularity allows for interesting "mix and match" experiments, in which the different domains of guidance receptors are fused by molecular cloning to each other. The resulting ***chimeric receptors*** are surprisingly functional and display distinctive binding and signaling properties based on the modules used in the fusion proteins. A chimeric Robo-DCC receptor (with the extracellular domain of Robo and the intracellular domain of DCC) for example, is responsive to the Robo-ligand Slit, but mediates an attractive growth cone turning response typical for the DCC receptor (Bashaw and Goodman, 1999; Stein and Tessier-Lavigne, 2001).

Ligands (guidance cues)

While the study of the growth cone and its properties advanced rapidly during the 1970s and 80s, it remained for a long time a mystery what the nature of the instructive guidance cues could be. Therefore, the field of molecular axon guidance was shaking with excitement in 1992 and 1994, when Yuling Luo in the lab of Jonathan Raper and Tito Serafini, Timothy Kennedy and Jose de la Torre in the laboratory of Marc Tessier-Lavigne purified and characterized the first guidance cues. The first identified repulsive cue was named ***Collapsin (Sema3A)***, and the first attractive cue received the name ***Netrin***. Both groups demonstrated in cell culture assays that growth cones exposed to a molecular cue turned either away (Collapsin) or towards (Netrin) the respective molecule (Kennedy et al., 1994; Luo et al., 1993; Serafini et al., 1994). The significance of these discoveries lies in the fact that the elements of the signaling cascades of neurite guidance were now understood to such an extent that they could be simulated and induced in a cell culture dish *in vitro*.

Following the discovery of Netrins and Semaphorins, many other guidance cues were rapidly assigned to their respective receptors, leading to the differentiation of active versus repulsive receptor-cue combinations and to the realization that some cues exert their influence over long distances (several hundred micrometers) while other are restrained to the immediate environment or the surface of a secretory cell (reviewed in Bashaw and Klein, 2010 and Guan and Rao, 2003).

In analogy to guidance receptors, it was observed that guidance cues also belong to a wide range of different protein families which can be separated by function, molecular signature or typical growth cone response into different classes: The “canonical’ cues, all of which have been identified in the 1990s, are probably the most well-known molecular representatives. This protein-group comprises the ***Netrin-*** (Hedgecock et al., 1990; Ishii et al., 1992; Kennedy et al., 1994; Serafini et al., 1994), ***Semaphorin-*** (Kolodkin et al., 1993; Luo et al., 1993), ***Slit- family*** (Brose et al., 1999; Kidd et al., 1999; Li et al., 1999) and the ***Ephrin-family*** (Cheng et al., 1995; Drescher et al., 1995). But there are also other classes of guidance cues, such as ***morphogens*** (BMPs, hedgehog and Wnt) as well as ***growth factors.***

Guidance cues are provided by the ***extracellular matrix as well as by cells*** in the vicinity and path of the growth cone. There are direct growth-cone-cell-surface interactions as well

as long-range interactions based on secretion. Currently, it is widely believed that secreted cues form gradients surrounding secretory cells. Such gradients have been studied extensively *in vitro* in so called "***growth cone turning assays"***. They are sufficient to model attractive and repulsive guidance decisions *in vitro,* but their existence *in vivo* still remains a ***hypothesis*** and needs to be demonstrated convincingly. Introduction- Figure 4 depicts the most important neurite guidance receptor and ligand combinations known as of today.

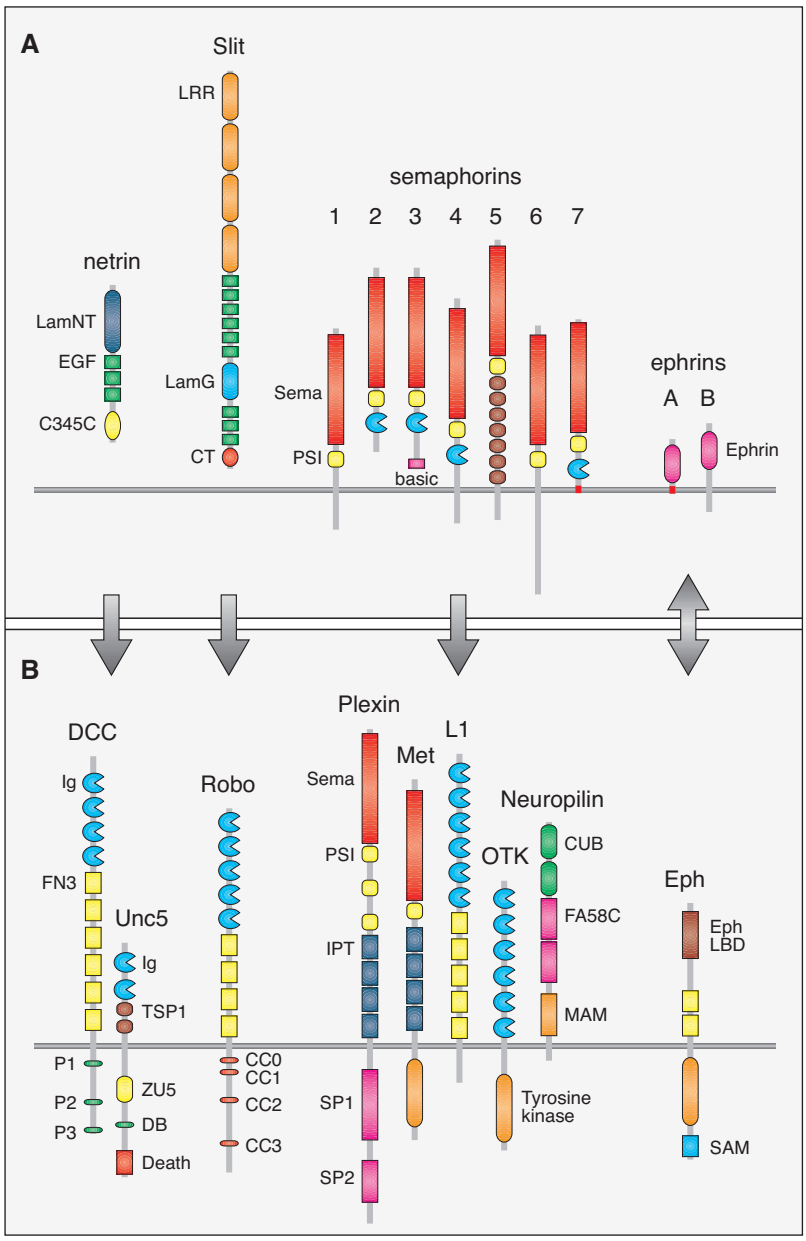

INTRODUCTION- FIGURE 4. **TYPICAL GUIDANCE CUES AND RECEPTORS IMPORTANT FOR NEURITE GUIDANCE.**

This figure was taken from (Dickson, 2002). Both types of molecules, receptors and ligands, are characterized by the presence of distinct protein domains and linear signaling motifs, facilitating the interactions with other molecules of an axon guidance signaling cascade. (A) Classical Guidance cues. (B) Classical guidance receptors. The abbreviations of domain names are used according to the SMART nomenclature (http://smart.embl-heidelberg.de). P1 to P3, DB (DCC-binding), CC0 to CC3, and SP1 and SP2 indicate conserved regions in the cytoplasmic domains of DCC, UNC-5, Robo, and Plexin receptors respectively.

The intracellular domains of guidance receptors display great versatility. They can bear catalytic function, for example kinase or phosphatase activity, or contain regions that are important for the interaction with other intracellular signaling molecules, known as ***"signaling motifs"*** (for example subtypes of src-homology (SH2- and SH3) domains or their respective binding sites, PDZ domains or their binding sites).

The binding of the ligand to a guidance receptor often leads to steric changes, allowing for the recruitment of differential adaptors and signaling effectors. This can lead to ***dimerization or multimerization*** of the receptor with other surface molecules or co-receptors, but also to the recruitment of signaling molecules to the intracellular domain. These clustering events are not only mediated by extracellular-domain interactions, but also by adaptor proteins which serve as molecular linkers between receptors and their effectors. To fully understand axon guidance *in vivo,* it is important to appreciate that no guidance receptor exists isolated within the plasma membrane. Instead, it is part of a larger signaling complex which is in constant cross talk or competition with other signaling complexes, making ***signal integration*** an important aspect of predicting the ultimate response of the growth cone.

Despite the versatility of signaling pathways underlying neural guidance, it has become clear that certain protein families are often involved in typical signal-cascades mediating neurite guidance (reviewed in: Bilimoria and Bonni, 2013; Bashaw and Klein, 2010; Kalil and Dent, 2014; Lowery and Van Vactor, 2009). The four most prominent signaling modes of neurite guidance signaling are (1) cyclic nucleotides (cAMP and CGMP) and calcium, (2) proteins involved in Rho-family GTPase signaling (GTPases, GAPs and GEFs) (reviewed in Hall and Lalli, 2010), (3) reversible phosphorylation and dephosphorylation of Ser, Thr or Tyr (mediated by kinases and phosphatases), (4) as well as proteins binding to or affecting the cytoskeleton (Dent et al., 2011).

The ultimate effectors during axon guidance signaling are the components of the ***cytoskeleton*** (Dent et al., 2011). Neurite guidance receptor signaling is always directed either towards the dynamic actin cytoskeleton or in the direction of the microtubule dominated growth cone core. It can stimulate the polymerization of actin filaments or

enhance retrograde flow, thereby inducing filopodial extension or retraction. Typical signaling targets which affect actin treadmilling are for example the ***Arp2/3 complex or Ena/VASP proteins***, regulating actin nucleation and elongation. ***Myosins*** on the other hand affect the retrograde actin flow. If the signal affects ***microtubule binding proteins (e.g. Mabp1B),*** the stability of the thin filaments at the base of the leading growth cone edge is affected which leads to neurite fortification or instability.

Flexibility in growth cone signaling

A growth cone often travels long distances during the developmental journey from the cell body towards the synaptic target. This navigation of complex and dynamically changing environments requires the capacity of responding to a multitude of different cues (Dickson, 2002). The longest human axons span more than a meter. Axonal projection patterns of the smaller fruit fly *Drosophila melanogaster* still reach several 100 µm in length (e.g. axons of giant fibers around 350µm; mechanosensory axons around 700µm (Olivier Urwyler, personal communication)). The diameter of the typical cell body in the *Drosophila* brain is only 2-6 µm, while a fully expanded typical filopodial growth cone expands from 2-20 µm. Therefore, the journey of the growth cone can be understood as an enormous computational task (Hassan and Hiesinger, 2015). It is initiated from a relatively small cell body and maintained over long distances. This requires not only precision in response but also flexibility and signal integration.

The trip of the growth cone is often divided into a number of different sub-steps passing ***specific landmarks*** in the tissue. Such landmarks are for example pre-existing cells (known as ***guidepost cells***) or cellular structures (such as ***fascicles*** of other neurons). In between, guidance decisions are influenced by secreted cues and extracellular matrix in the vicinity of the growth cone. Importantly however, the guidance principle based on intermediate axon guidance targets means that the growth cone needs to change properties and ***adapt*** to its immediate environment. A tissue landmark for example, initially attracts the growth cone. Once the intermediate target is reached however, the growth cone needs to be able to process the changes of environment, permitting departure from the intermediate target towards the next landmark.

The dynamics of switching from attraction to repulsion upon reaching a landmark require fast and reversible ***dynamic modifications*** of growth cone signaling events. Such signaling

responses need to occur in a timeframe of seconds and minutes. This represents a challenge considering how far away the growth cone moves away from the cell body. Adaption can be achieved by exchange of the receptor combinations expressed at the membrane surface. There are several strategies allowing for modulation of the growth cone receptor makeup in a matter of minutes (reviewed in: Corty et al., 2009; Dent et al., 2011; Bashaw and Klein, 2010; Lowery and Van Vactor, 2009): Guidance receptors can for example be quickly ***endocytosed*** (1), and either be (2) ***proteolytically*** destroyed and processed, or (3) returned in due time to the membrane in a process known as ***trafficking and recycling.*** A fascinating dynamic regulatory principle first described by Christine Holt and colleagues is the fact that growth cones contain the molecular machinery necessary for ***local protein synthesis*** (reviewed in Lin and Holt, 2008). Therefore, the molecular composition of the growth cone can be changed autonomously from the cell body by means of (4) ***translation of locally stored mRNA pools***. In addition, the shape of the growth cone changes often dramatically upon reaching a target, which influences the ***surface area*** presenting guidance receptors but also the ***speed*** with which it moves forward.

Taken together, it is apparent that an individual axon makes its guidance decisions based on the combination of receptors expressed at its surface, the guidance cues presented in the environment and the cytoplasmic signaling effectors expressed at a given place and time. This represents an enormous signal transduction task which needs to respond and quickly adapt to dynamic changes of the environment.

Tyrosine phosphorylation as an important signaling mechanism

Reversible phosphorylation: From Nobel price to most abundant protein modification

In 1992 Edmond Fischer and Edwin Krebs received the Nobel prize *"FOR THEIR DISCOVERIES CONCERNING REVERSIBLE PHOSPHORYLATION AS A BIOLOGICAL REGULATORY MECHANISM"* (The Nobel Prize in Physiology and Medicine, 1992, Press Release) (Introduction- Figure 5). This type of posttranslational modification is based on enzyme-regulated conjugation of a phosphate group to exposed side chains of threonine, serine or tyrosine residues of signaling proteins, hence changing their signaling properties.

The importance of Fishers and Krebs discovery lies in the fact that reversible phosphorylation turned out to be a ***key signaling mechanism,*** affecting almost every known biological process in eukaryotes (reviewed in: Cohen, 2000; Miller, 2012). Years later, Edmond Fischer compared the function of reversible phosphorylation with that of traffic signals: Signaling-"traffic" is allowed to flow based on the phosphorylation state of gatekeeper proteins (Interview with Nobel Prize Laureates at the Lindau Nobel Prize Conference 2003; *http://www.vega.org.uk/video/programme/38*).

Biological processes regulated by reversible phosphorylation range from metabolism over transcription, cell cycle progression, and cytoskeletal rearrangements to cellular movements, apoptosis and differentiation (Manning et al., 2002a; 2002b). Most importantly in the context of this dissertation, it should be noted that reversible phosphorylation is essential for signaling cascades regulating nervous system development and neurite guidance, for the regulation of cellular and synaptic homeostasis, for cell motility and during immune responses (Manning et al., 2002a; 2002b). Furthermore, many diseases are caused by abnormal levels of phosphorylated proteins. Prominent examples are diabetes, an estimated 80% of all forms of cancer as well as rheumatoid arthritis or cardiac diseases (Cohen, 2002a; Hendriks et al., 2013).

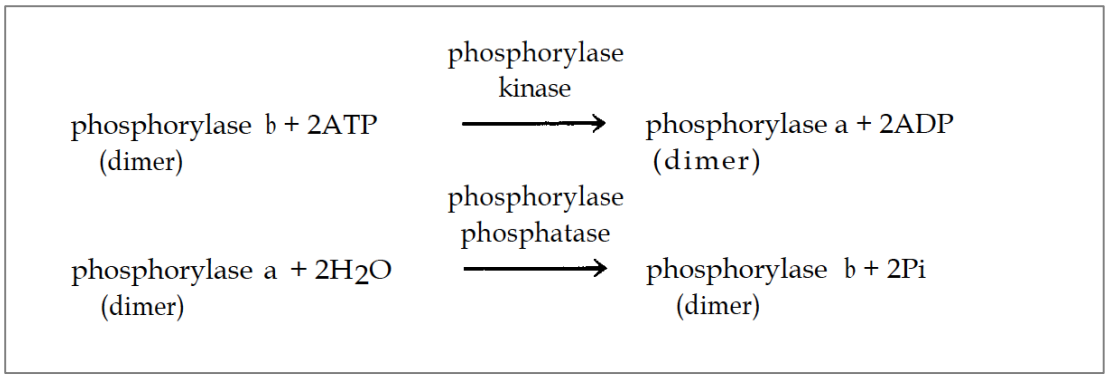

INTRODUCTION- FIGURE 5. **REVERSIBLE PHOSPHORYLATION OF PHOSPHORYLASE AS DESCRIBED BY FISCHER AND KREBS.**

This early figure from the 1993 Nobel Lecture of Edwin Krebs contains already all components known to be important for phosphorylation: Two enzymes (kinase and phosphatase), their substrate (phosphorylase), ATP and water. Fischer and Krebs reported that protein phosphorylase exists in two states: An exposed serine residue is either dephosphorylated (state b) or phosphorylated (state a). The converting enzymes are: (1) A kinase which transfers a phosphate group from the donor ATP to phosphorylase b, and a phosphatase (2) which is responsible for the hydrolysis of phosphorylase-a into phosphorylase-b (figure panel taken from the Nobel lecture of Edwin Krebs).

There are several characteristics that render reversible phosphorylation an important regulatory mechanism in the cell: First and foremost, phosphorylation of the side-chains of structurally exposed amino acid residues of cytoplasmic proteins allows one protein sequence to ***take up two differential physical states***. Such differentiation is a clear prerequisite for the creation of signaling cascades, especially if one considers that most phosphorylated proteins can be modified at more than one amino-acid residue, giving rise to several distinct signaling states differentiated by a ***phosphorylation code*** (Mann et al., 2002). In addition, signaling via reversible phosphorylation is characterized by ***high speed and precision*** of the reaction as well as by ***scalability*** of the signaling response. This renders phosphorylation an ideal signaling mechanism for processes requiring fast and dynamic signaling, such as the communication of cells with their environment, or the maintenance of homeostasis.

Because of its importance, signal regulation by protein phosphorylation is highly evolutionary conserved. Generally, eukaryotic cells are characterized by larger amounts of phosphorylated proteins than prokaryotes. For example, it has been estimated that one third of all proteins in an eukaryotic cell are phosphorylated at any given point in time (Cohen, 2000; 2002a; Mann et al., 2002). Moreover, most - if not all- phosphorylated proteins ***harbor more than one potential phosphorylation site*** (Mann et al., 2002).

While histidine-phosphorylation is already found in prokaryotes, ***serine-, threonine and tyrosine*** phosphorylation are more typical for eukaryotes. These amino acids harbor

hydroxyl (-OH) groups in their side chain. As a nucleophile, this functional group can attack the terminal phosphate group of the universal phosphoryl donor adenosine triphosphate (ATP). This leads to the transfer of the phosphate group from ATP (or sometimes from guanosine triphosphate (GTP)) to the exposed side chain of the amino acid. There exists also phosphorylation of histidine, arginine and lysine (Cieśla et al., 2011). However, these modifications are rare and remain not very well studied. Phosphorylation adds ***negative charge*** to the exposed side chain of the amino acid. This constitutes an indispensable and flexible labeling mechanism. The surrounding area can as a result of phosphorylation be recognized and bound by other proteins initiating signaling cascades. Alternatively, phosphorylation can lead to ***steric changes*** within the protein altering the catalytic activity, opening or closing of potential binding sites or inducing changes in protein stability (Cohen, 2002a).

Strikingly, many signaling cascades that involve protein phosphorylation are chain reactions, adding the same type of protein modification to all involved molecular effectors, a phenomenon known as ***phosphorylation cascades*** (Cohen, 2002a). As a consequence, such cascades can be controlled by structurally and evolutionary related modifier enzymes. A widely known example of such cascades are the mitogen activated protein (MAP) kinases. They transfer phosphoryl groups to each other, thereby mediating signals from the cytoplasm into the nucleus. The resulting terminology in order to distinguish them from each other is striking and mirrors the different steps of the chain reaction: There are MAPKKKs (MAP-kinase-kinase-kinases), MAPKKs (MAP-kinase-kinases) and MAPKs (MAP-kinases) depending on the tier of the cascade. (With a MAPKKK being the kinase phosphorylating the kinase, which phosphorylates a MAP-kinase.)

Kinases and phosphatases: Gatekeepers of cellular homeostasis

The transfer of phosphoryl-groups to the side chains of amino acids is controlled and facilitated by enzymes commonly known as ***phosphatases and kinases***. Their catalytic pockets provide the optimal environment to regulate, enable and facilitate phosphorylation and dephosphorylating-reactions. Therefore, these enzymes assume ***gatekeeper functions*** in many signaling cascades involving phosphorylation.

The ancient kinase family is conserved in all metazoans

The transfer of phosphate groups from ATP or GTP to side chains of serine, threonine or tyrosine requires specialized enzymes. The phosphotransferases catalyzing the transfer of a phosphate to a protein substrate are known as ***kinases*** *(from Greek: κινεῖν- to move)*. Almost all eukaryotic kinases, except the atypical kinases, share ***the same catalytic domain*** (Manning et al., 2002a). This catalytic pocket allows for the proper alignment of all molecular components involved in the reaction, thereby facilitating the transfer of the phosphoryl-group to the substrate.

Kinase activity was first described in the 1950s by Burnett and Kennedy for a liver enzyme, catalyzing the phosphorylation of casein (Burnett and Kennedy, 1954). A little later, Fischer and Krebs, in the course of studying muscle energy supply, reported that the conversion of a protein commonly known as "phosphorylase-b" involves a kinase mediated phosphorylation step (Fischer and Krebs, 1955; Krebs and Fischer, 1956) (see also Introduction- Figure 5).

Following these early reports, many more enzymes of the same function have been described. Kinases raised a strong interest, because they seemed to represent good drug targets. For example, many growth factor receptors harbor intracellular kinase domains (e.g. epidermal growth factor receptor (EGFR) and the insulin receptor (IR)), and many of these receptors undergo auto-phosphorylation during their activation (Cohen, 2002a). Nowadays, we know that the kinase protein family is one of the largest: It covers an estimated ***1,5 – 2.5% of all annotated eukaryotic genes*** (Manning et al., 2002a; 2002b). There is a data base of all kinases at *www.Kinase.com*, curated by Gerard Manning's lab at Genentech which serves as a valuable resource regarding the current kinome (entirety of

all kinases). At the time of writing of this dissertation it contains 498 putative human protein kinases. Depending on their structural and functional properties and their substrate specificity, kinases can be subdivided into 11 subfamilies (Introduction- Table 1). These subfamilies are widely conserved in all metazoans and many of them can also be found in yeast (Manning et al., 2002b).

INTRODUCTION- TABLE 1. **LIST OF KINASE SUBFAMILIES.**

The kinase family is one of the largest protein families known to date. It can be divided into the 11 subfamilies listed in this table. These kinase families are widely conserved in all metazoans, emphasizing their importance for cellular signaling.

#	Kinase subfamily
1.	The ***AGC*** family (serine/threonine modifying) (named after protein kinase ***A***,***G*** and ***C***)
2.	The ***Casein kinase I*** (***CK1***) family (serine/threonine modifying),
3.	The ***CMGC*** family (serine/threonine modifying), (named after initials of some members)
4.	The ***STE*** family
5.	The ***TK*** (***t***yrosine ***k***inase) family (tyrosine modifying)
6.	The ***TKL*** (***t***yrosine ***k***inase ***l***ike) family
7.	The ***OP***K (***o***ther ***p***rotein ***k***inases) group (serine/threonine and dual specificity)
8.	The ***atypical*** kinases
9.	The ***r***eceptor ***g***uanylate ***c***yclases (***RGC***s)
10.	The ***eukaryotic lipid*** kinases.
11.	The ***Ca***$^{2+}$/***ca***l***m***odulin dependent kinases (***CAMK***) family

Notably, there occurred a big diversification of protein kinase families and functions early during eukaryotic and metazoan evolution (Manning et al., 2002a). This diversification went hand in hand with the ***appearance of signaling processes involving inter-cellular communication and coordination of more complex functions***. However, an expanded kinome does not necessarily signify higher organismal complexity. Nematodes for example, present with an extraordinarily expanded family of kinases. In comparison to the nematodes, the kinome of *Drosophila melanogaster* appears relatively ordinary. The fruit fly kinome harbors at least 240 kinase family members (Hatzihristidis et al., 2015). There is no kinase exclusively specific to flies. Importantly for the work with flies, ***all of the 21 Drosophila kinase-subfamilies have human orthologues***. In addition, there are only 13 human kinase families that are not represented in the kinome of fly or worm (Manning et

al., 2002a), demonstrating that both organisms represent good tools for the study of pathways involving phosphorylation.

The phosphatase protein family

The counterparts of kinases are enzymes that remove phosphate groups from the side chains of target proteins. They are known as ***phosphatases.*** This protein family can be divided into three main groups listed in Introduction-Table 2.

INTRODUCTION- TABLE 2. **LIST OF PHOSPHATASE PROTEIN SUBFAMILIES.**

Phosphatases are the counter-players of kinases. They are enzymes with highly regulated substrate specificities. This table lists the three main phosphatase subfamilies.

#	Phosphatase Family Name
1.	The ***s***erine/***t***hreonine protein ***p***hosphatases (***STP***s)
2.	The ***p***rotein ***t***yrosine ***p***hosphatases (***PTP***s)
3.	Lipid phosphatases.

Initially, a lot of research regarding phosphorylation was aimed at the regulation, specificity and substrates of kinases. This was based on the widespread assumption that the size of the kinase family exceeds that of the phosphatase protein family. Therefore, it was believed that the large and variable kinase family could provide distinct signaling pathways with their specificity, while the apparently small phosphatase family was thought to be broadly unselective with a general housekeeping function. However, sequencing and annotation of the human, mouse and fly genomes has shown that the phosphatase family is almost as big as the protein kinase family. Especially the PTP family is large and composed of 109 family members (Hatzihristidis et al., 2015), demonstrating their respective importance. Interestingly however, the similarity of family size does not imply that there are overlapping ‘pairs” of kinases with matching phosphatases. Quite on the contrary, it is now established that kinases and phosphatases are versatile enzymes with very distinct functional and regulatory profiles.

The special role of reversible tyrosine phosphorylation

The ratio of phosphorylated amino acids has been estimated to be ***1800: 200: 1 (pSer: pThr: pTyr)*** (Mann et al., 2002). Only two percent of all cellular proteins are tyrosine phosphorylated. This is due to the fact that tyrosine rarely plays a structural role in proteins. Tyrosine phosphorylation constitutes thus a ***rare but extremely important*** posttranslational signaling event. This might be the reason for its late discovery dating back to experiments conducted by Walter Eckhart, Mary Ann Hutchinson and Tony Hunter in 1979 (Eckhart et al., 1979).

Now, more than 35 years later, we know that tyrosine phosphorylation takes up a special role in signal transduction by serving as a tightly regulated signaling "***gate keeper***" in all eukaryotic cells. As such, tyrosine phosphorylation governs almost all cellular processes involving cellular communication, including cell proliferation, cell cycle progression, metabolic homeostasis, transcriptional activation, aging as well as neural transmission, differentiation and development (reviewed in Hunter, 2009). The importance of tyrosine phosphorylation reflects also in the fact, that tyrosine kinases (with 90 family members) represent almost 1/5 of all annotated kinases in humans (Hunter, 2009).

Evolutionary, tyrosine phosphorylation is ***relatively novel*** as compared to other protein modifications. Eukaryotic tyrosine modifying enzymes appeared about ***600 million years ago, just at the split of unicellular and multicellular eukaryotes*** (Miller, 2012; Hunter, 2014). Tyrosine modifying enzymes are not only found in colonial protozoa but also in most multicellular animal organisms, demonstrating how important this flexible mode of signaling is for complex cell-cell-communication. Furthermore, many transmembrane receptors bear tyrosine kinase or phosphatase activity, demonstrating that tyrosine phosphorylation is extremely important for the communication of a cell with the environment.

It remains subject of speculation, why tyrosine phosphorylation specifically carries such a significance in signal transduction (Hunter, 2009). One important hypothesis is raised by Tony Hunter in his 2009 review on the role of tyrosine phosphorylation: He argues that *" the SH2 domain binding energy for a P-Tyr residue is higher than for a P-Ser or P-Thr, based on the contribution of contacts that can be made with the phenolic ring in addition to interactions with the phosphate"* (Hunter, 2009). Another point might be of steric nature:

The phosphate group in phosphorylated tyrosine is much more exposed than that of serine and threonine (Hunter, 2014), thereby providing a prominent and therefore specific binding surface for interacting kinases, phosphatases and effectors.

In general, tyrosine phosphorylation ***facilitates protein-protein interactions*** between an amino-acid that contains a ***tyrosine based signaling motif,*** and a protein containing a ***matching recognition motif*** (e.g. SH2-domain binding to SH2-binding motif) (Hunter, 2009; 2014). Therefore, tyrosine phosphorylation has been an important target of pharmacological studies, because many diseases can be explained by perturbations of signaling pathways involving tyrosine phosphorylation (Hunter, 2009; 2014), and because the involved protein domains and binding motifs are well understood in terms of amino-acid signature and structure.

One interesting aspect of tyrosine phosphorylation is the fact that it's effects are tightly interwoven with the signaling based on the reversible phosphorylation of serine- and threonine. This might be explainable by the evolutionary context, with the tyrosine modifying enzymes evolving later than enzyme modifying the phosphorylation of other amino acids: Specifically, PTPs and SH2 domains are evolutionary older than TKs (Miller, 2012), suggesting that the phosphorylation landscape was initially regulated by signaling of dual-specificity kinases, and that the acidity of tyrosine binding motifs plays an important role during substrate selection (Miller, 2012).

Every signaling cascade that is regulated by tyrosine (Y)-phosphorylation consists of four main components (summarized in Introduction- Table 3 and Introduction- Figure 5). The following paragraphs will briefly introduce each of the Y-based signaling components.

Tyrosine modifying enzymes

The tyrosine kinase (TK) family

One of the largest and most important subgroup of kinases is the tyrosine kinase family. This is surprising, considering the relative scarcity of tyrosine phosphorylation (Hunter, 2014). There are 90 tyrosine kinases in the human kinome, 90 in nematodes and 32 members in the kinase family of *Drosophila* (Manning et al., 2002a; 2002b). Tyrosine kinases are subdivided into two main families with closely related catalytic domains (Introduction- Table 4). Notably, more than half of the annotated human tyrosine kinases

are RTKs, exemplifying how significant tyrosine phosphorylation for cell-environment interactions is (Hunter, 2014).

Introduction- Table 3. List of molecular components involved in signaling mediated by tyrosine phosphorylation.

Every signaling cascade regulated by posttranslational phosphorylation of tyrosine contains the five elements listed in this table.

#	Component of a pathways involving tyrosine phosphorylation
1.	***Tyrosine kinases*** (TKs)
2.	***Tyrosine phosphatases*** (PTPs)
3.	***Linear tyrosine based signaling motifs*** (10 amino acid signature stretch surrounding the modified tyrosine)
4.	Proteins that contain ***tyrosine recognition domains*** (recognize the modified tyrosine and the adjacent signature motif and pass the signal on to downstream effector molecules)
5.	***Effector signaling proteins*** (create a cellular response)

Receptor tyrosine kinases (RTKs) are Type-I transmembrane receptors. Ligand binding to their extracellular domain leads often to phosphorylation (Cohen, 2002a). They usually induce signaling cascades that involve larger phosphorylation networks. Neurotropic receptors are one important subclass of RTKs. They get activated by ligand binding, which leads to receptor clustering and subsequent auto-transphosphorylation events. Neurotropic receptors regulate many important cellular aspects such as survival and apoptosis as well as proliferation and differentiation. However, tyrosine phosphorylation mediated signaling can also be initiated by interaction of two cytosolic proteins: In this case, one of the two involved proteins needs to contain a Y-based signaling motif and the other a tyrosine recognition motif.

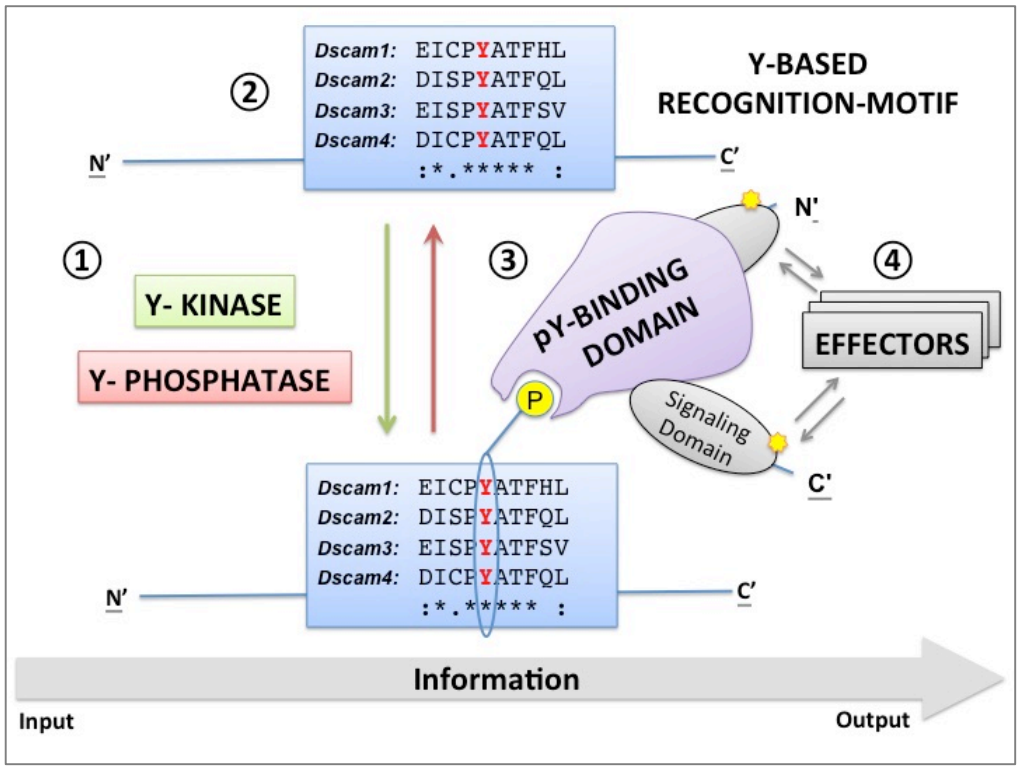

INTRODUCTION- FIGURE 5. **THE COMPONENTS OF A TYROSINE BASED SIGNALING SYSTEMS.**

The posttranslational modification of tyrosine by reversible phosphorylation plays an important role during signal transduction processes in the cell. Tyrosine-phosphorylation based signaling involves four constitutive components that allow the processing of information: (1) Tyrosine-modifying enzymes which are known as kinases and phosphatases. Kinases catalyze the addition of a phosphoryl-group to a tyrosine while phosphatases facilitate the opposing reaction. These tyrosine-modifying enzymes can sense the presence of a cellular signal either because they are transmembrane receptors themselves or by being recruited to a receptor or signaling molecule. (2) A protein that contains a tyrosine-based signaling motif. Signaling motifs are small evolutionary conserved stretches of 10 amino acids or less, that can be identified by simple sequence alignments. In this figure, I depicted the motif known as the "Dscam-box" which is present in all invertebrate Dscam1 paralogues. (3) A protein containing a phosphor-tyrosine binding domain and other signaling domains. These proteins can recognize the presence of the linear tyrosine-phosphorylation motif and will only bind in case of phosphorylation. Often they contain other signaling domains allowing the signal transduction to downstream effector molecules (4) which elicit the ultimate cellular response.

Historically, the work on tyrosine kinases has started ten years earlier than the work on kinases. This has two main reasons: (1) The first enzymes identified as tyrosine modifiers were kinases and not phosphatases. (2) Second, the work with kinases turned out to be technically easier than the work with phosphatases: Kinases are generally ***expressed at higher levels than phosphatases*** and ***mis- or over-expression is mostly unproblematic***. Furthermore, they form ***relatively stable complexes*** with their substrates allowing for ***easy purification*** of their signaling complexes. Additionally, they have raised great interest in the medical community, because many of the human tyrosine kinases could be linked to diseases. This enormously pushed to the progression of drugs regulating kinase functions (Hunter, 2009; 2014), resulting in the discovery of more than 20 protein kinase inhibitors (small molecules or humanized monoclonal antibodies) already approved as medications or currently undergoing clinical trials (Cohen, 2002b; Hunter, 2009). The Abelson-kinase-

inhibitor *Imatinib/Gleevec* which was approved in 2001 for the treatment of CML is probably the most prominent example for this kinase-targeting type of novel drugs (Cohen, 2002b).

INTRODUCTION- TABLE 4. **LIST OF TYROSINE KINASE SUBFAMILIES.**

Note that more than half of all human tyrosine kinases are receptor tyrosine kinases, exemplifying how important tyrosine phosphorylation is for cell-environment interactions.

	Tyrosine kinase subfamily
1.	***Receptor tyrosine kinases*** (RTKs) • 58 human members
2.	***Cytosolic tyrosine kinases*** • 32 human members

The protein tyrosine phosphatase (PTP) family

Protein tyrosine phosphatases (PTPs) represent also a relatively large and evolutionary conserved family of proteins. With the exception of the nematode *C. elegans,* phosphatase encoding genes represent about 0.2% of all encoded genes in eukaryotes (Hatzihristidis et al., 2015). For example, the human PTP-family consists of 109 family-members and the genome of *Drosophila melanogaster* contains 44 *PTP* genes (Hunter, 2009; Hatzihristidis et al., 2015) (Introduction- Figure 6). Based on their catalytic mechanisms and their domains, PTPs are divided into the five main families (Hatzihristidis et al., 2015) listed in Introduction-Table 5.

In analogy to the *Drosophila* kinome, ***all fly PTPs have a human orthologue,*** emphasizing the value of *Drosophila* for the study of tyrosine-phosphorylation mediated signaling. Interestingly, there are tyrosine phosphatase orthologues in yeast, even though these organisms do not possess tyrosine kinases (Hunter, 2009). Therefore, phosphatases can be understood as the ***evolutionary older*** components in phosphorylation dependent signal transduction, suggesting that they might also harbor the ***most essential regulatory mechanisms***.

The first PTP (PTP1B) was purified in 1988 by Nicholas Tonks in the Fischer lab. everybody's surprise it turned out to be a transmembrane receptor already known as

LAR/CD45 (Tonks et al., 1988; Fischer et al., 1989). While the PTP family has for a long time been overshadowed by the more prominent research centered around tyrosine kinases, it has become increasingly clear that *it is often the phosphatase component of a signaling pathway, which dictates the spatio-temporal specificity of the signal* (Nguyen et al., 2013). Therefore, phosphatases are important novel drug targets, especially for cancer and diseases affecting the nervous system (He et al., 2014b; Hendriks et al., 2013; Julien et al., 2011).

All PTP proteins are characterized by a ***typical 240 aa large catalytic*** domains, most often with an ***essential catalytic cysteine*** residue at the core. In most cases the catalytic domain is complemented by some other functional protein domains. Of the 17 phosphatase affiliated domains reported for PTPs in *Drosophila,* the most important four subgroups are: Domains affecting (1) phosphatase localization, (2) protein-protein interactions, (3) catalysis of other target molecules or (4) the binding to some small molecules (Hatzihristidis et al., 2015). An overview of the domain structure of all annotated *Drosophila* PTPs can be found in Introduction-Figure 6.

Receptor PTPs (RPTPs) represent 20% of all known human PTPs and cover a similar fraction of the *Drosophila* phosphatome (Hatzihristidis et al., 2015), emphasizing the importance of tyrosine phosphorylation for cell-cell and cell-environment communication. RPTPs are of special interest for the study of neuronal development: They are expressed in the nervous system, mediate communication of the extracellular space with the neuronal cytoplasm and have been found to majorly affect axon guidance and branching (reviewed in Hatzihristidis et al., 2015).

Substrate traps revolutionized the way of working with PTPs

Despite their importance for axon guidance, the work with tyrosine phosphatases has remained a considerable technical challenge for a long time (Hatzihristidis et al., 2015). This had several reasons: (1) First, many tyrosine phosphatases are ***expressed at relatively low levels*** but are (2) ***highly catalytically active***, which rendered cDNA and overexpression based experiments often toxic to the cell. (3) In addition, it turned out to be ***more difficult to show the absence of a phosphorylated tyrosine*** than to demonstrate its presence. Furthermore, (4) most phosphatase inhibitors identified today are ***very hydrophobic***, rendering them unsuitable for cell culture and *in vivo* experiments. (5) Finally, it is a

commonly reported phenomenon that tyrosine phosphatases interact with their substrates only in a very ***transient manner,*** creating difficulties in capturing the protein complex during catalysis (Hatzihristidis et al., 2015).

These problems were overcome by the thorough structural characterization of the catalytic domain of PTPs enabling the smart design of efficient ***substrate trapping mutations*** pioneered by Nicholas Tonks and colleagues (Introduction-Figure 7). The availability of novel tools sparked an early age of phosphatase biology, leading to the realization that the local and spatial dynamic and strength of protein phosphorylation signaling are critically defined by phosphatases and not as initially assumed by kinases (Hatzihristidis et al., 2015; Nguyen et al., 2013) These results and the recent realization that RPTPs might be significant regulators of synaptic organization, have pushed PTPs into the focus of drug development in order to tackle cancer and autoimmune diseases as well as a range of neurological disorders (reviewed in Julien et al., 2011; Tonks, 2013).

Tyrosine based signaling motifs

The function of intracellular signaling proteins is not only defined by large globular domains but also by ***small linear stretches*** of approximately 10 amino acid lengths. They serve as recognition and anchor points for other proteins. Their presence significantly influences the binding affinities and signaling properties of cytosolic signaling domains: The short nature of linear motifs translates into relative weak affinities to their interactors (0.5-10 μM as opposed to pico-nanomolar affinities between protein domains) (Neduva and Russell, 2005), rendering them ***ideal mediators of transient*** interactions. Often, linear motifs are modified by reversible posttranslational modifications, such as phosphorylation or acetylation. Therefore, linear motifs represent an important class of regulatory signaling elements, differing in their evolutionary origin and binding capacities from protein domains (Neduva and Russell, 2005).

There are several initiatives targeted at cataloging protein-protein interaction motifs. In line with this, online tools have been created allowing fast screening of these databases. Based on these catalogues it is now possible to predict signaling-units solely based on the amino acid sequence of a receptor. Useful is also the capability of estimating the frequency of a given amino acid sequence, allowing to assess the likelihood of a given motif to be of

functional importance. I have used several such online tools during my PhD. Notable and very useful tools are for example listed in Introduction- Table 6.

INTRODUCTION- TABLE 5. **LIST OF MAIN PTP-SUBFAMILIES.**

Note that RPTPs represent 20% of all known PTPs, emphasizing how important tyrosine phosphorylation is for the signal transduction between intra- and extracellular compartments.

#	PTP SUBFAMILY
•	***Class I PTPs*** with a catalytic center surrounding the cysteine based core motif (H/V)-C-X_5-R-(S/T) divided into two subfamilies: *a.* ***Classical Tyrosine PTPs*** i. substrate: Phosphor-tyrosine ii. 38 in humans and 16 in *Drosophila* iii. Cytosolic 17 members in humans b. ***Trans-membrane RPTPs*** (21 members)
•	***Dual specificity PTPs*** (DSPs) (very promiscuous in terms of substrate specificity: Phosphor –tyrosine, -serine, threonine but also mRNA-5'-triphosphate or lipids) (61 in humans and 21 in *Drosophila);* several subfamilies: a. 11 ***MKPs*** b. 16 ***Myotubularins*** c. 4 ***CDC14s*** d. 3 ***Slingshots*** e. 5 ***PTENs*** f. 3 ***PRLs*** g. 19 ***Atypical DSPs***
•	***Class II PTP*** • known as low molecular weight PTP (LMW-PTP) with a cysteine based core motif; structurally related to arsenate reductases; • evolutionary highly conserved • 1 in humans and 4 in *Drosophila*
•	***Class III PTPs*** • known as CDC25A, B and C with a cysteine based core motif (Substrates: Phosphor-tyrosine and –threonine) • (3 in humans and 2 in *Drosophila)*
•	***Class IV PTPs*** • aspartate based core motif

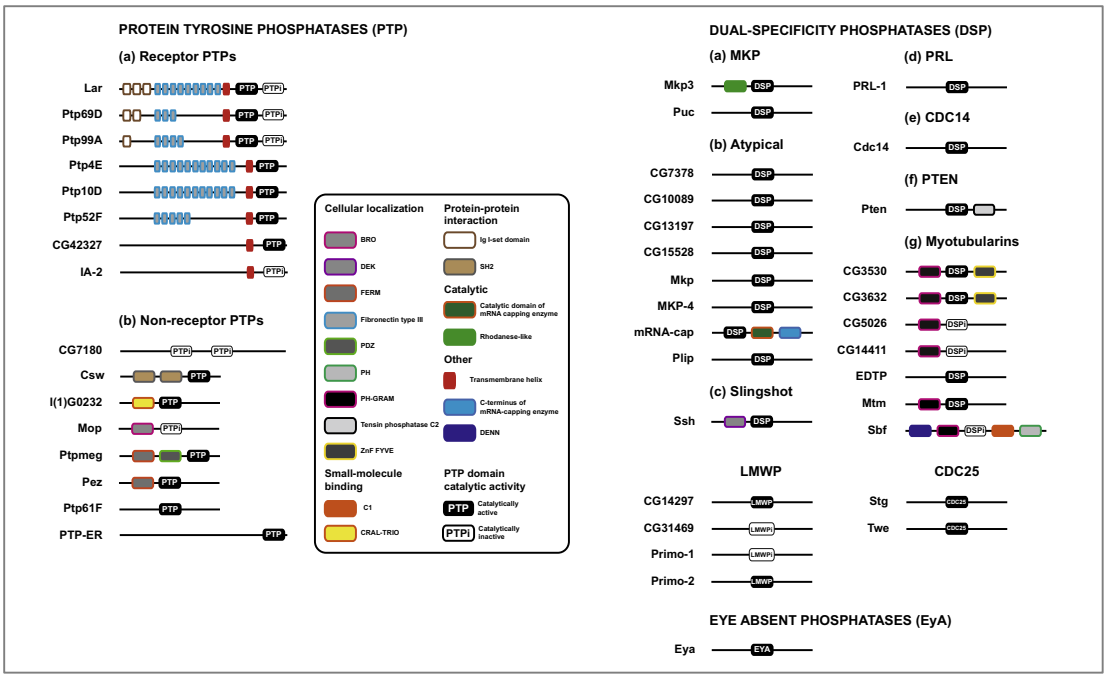

INTRODUCTION- FIGURE 6. **OVERVIEW OF ALL *DROSOPHILA* PTPS AND THEIR ACCESSORY DOMAINS.**

In addition to the phosphatase domains, there are 17 distinct signaling domains found in association with PTP proteins. They affect the signaling function, localization and interaction with other molecules. This image was taken from Hatzihristidis et al., 2015.

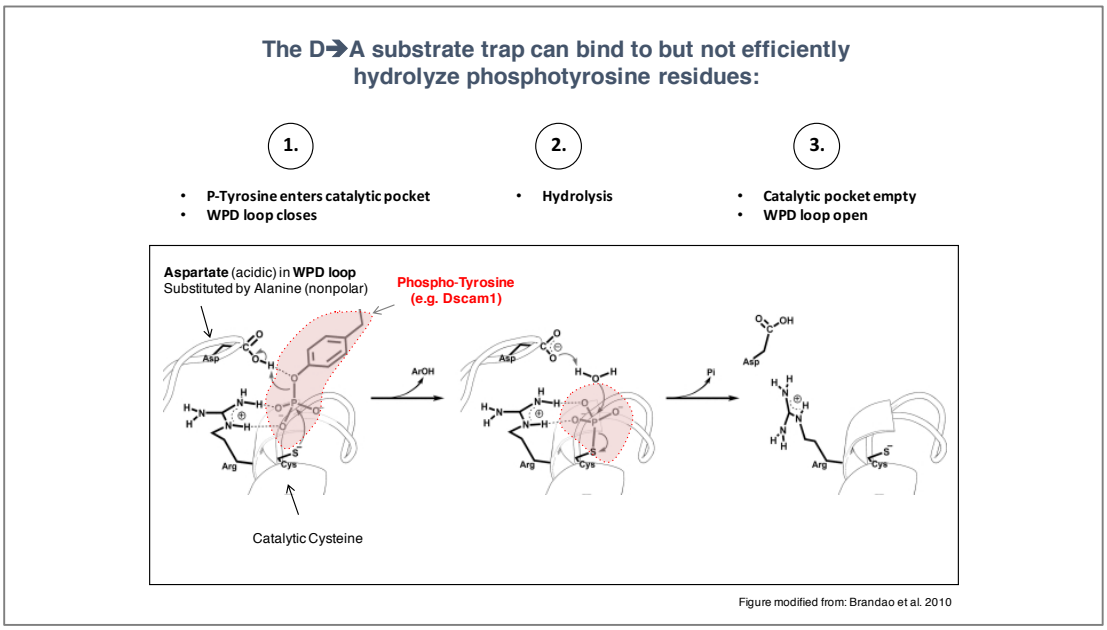

INTRODUCTION- FIGURE 7. **IMAGE ILLUSTRATING THE LOCALIZATION OF THE CRITICAL AMINO ACID RESIDUES MUTATED IN D>A SUBSTRATE TRAPS.**

The D>A substrate trap is the most common molecular modification of PTPs in order to capture enzyme-substrate interactions. Under normal circumstances, the catalytic reaction consists of three main steps: (1) A phosphorylated tyrosine enters the catalytic pocket and the WPD loop closes. (2) Hydrolysis. (3) The WPD loop opens releasing the substrate. The aspartate of the WPD loop assumes a critical position. It serves first as a proton donator and later as an acceptor during hydrolysis. Mutation of the acidic aspartate to alanine therefore inhibits the catalysis, while still allowing for substrate binding. Since the substrate cannot be efficiently catalyzed, it is "stuck" in the catalytic pocket allowing for efficient co-purification of the otherwise transient PTP-substrate complex. The image was modified from (Brando et al., 2010).

INTRODUCTION- TABLE 6. **DATABASES USED DURING MY PHD TO IDENTIFY LINEAR SIGNALING MOTIFS.**

These databases allow for the prediction of signaling interactions based on the amino acid sequence of a protein. Often, it is possible to evaluate the prediction based on a probability score, which is usually calculated based on the frequency of a given sequence in the genome, the subcellular localization and the predicted folding of the protein area in question.

#	Database
✓	***Scansite*** (http://scansite.mit.edu) (Obenauer et al., 2003)
✓	***Motif Scan*** (http://myhits.isb-sib.ch/cgi-bin/motif scan)
✓	***Elm Motif Scan*** (http://elm.eu.org) (Dinkel et al., 2014)

Taken together, linear signaling motifs constitute important building blocks of the cellular signaling machinery (Hunter, 2014; Neduva and Russell, 2005). *They represent the smallest subunits of intracellular signaling pathways.* In the following paragraphs, I will specifically focus on signaling motifs that are centered around exposed tyrosine residues.

Tyrosine based signaling motifs and their recognition domains

The regulatory function of tyrosine phosphorylation lies in the ***controlled transient recruitment of effector proteins*** to a signaling complex (Hunter, 2014). The context of the phosphorylated tyrosine is decisive for the specificity of protein-protein interactions. Together with the tyrosine, these regions form small linear binding motifs for transient protein-protein interactions. The binding surface is accessible or closed based on the phosphorylation-status. The aim of this subchapter is to summarize the information available on protein domains capable of recognizing post-translationally modified tyrosine and their respective binding motifs. Since tyrosine phosphorylation is an event only appearing in the cytoplasm, these domains are strictly found on the intracellular side of the plasma membrane. The two most studied recognition domains for phosphor-tyrosines are known as ***the SH2-domains*** and the ***PTB*** (phosphor-tyrosine binding domain) interacting with SH2-biding sites and ***PTB-binding sites*** respectively.

The SH2 domain as the prototype of tyrosine recognition motifs, was first described in 1986 as a domain selectively interacting with a tyrosine-phosphorylated amino acid stretch (Sadowski et al., 1986). SH2-domains fulfill various functions: They are important for the recruitment of distinct signaling effectors and adaptor proteins but they also can engage in

intramolecular interactions and regulate the activation status of a protein. Proteins that contain SH2 domains often also contain other modular signaling motifs, creating adaptors, which are important for the assembly of multi-protein complexes.

Structurally the SH2-domain is a cassette consisting of a 4-stranded β-sheet and a three-stranded β-sheet connected by a single beta strand. The four-stranded β-sheet is flanked by two alpha-helices on either side. The interaction site for the phospho-tyrosine lies in a pocket, formed by an extended chain perpendicular to the β-sheet. The human genome contains 87 SH2-domain containing-proteins of three different subtypes (Yaffe, 2002): They are known as (1) Phospholipase Cγ1 (PCLγ1)-like, (2) Src-like and (3) Grb2-like SH2-domains.

Evolutionary, SH2-binding sites are as old as PTPs: They are found in yeast even in the absence of tyrosine kinases (Hunter, 2014). Therefore, it is reasonable to assume that the SH2-domain evolved from a recognition motif for acidic moieties (Hunter, 2014), and that some of that preference for acidic residues might still be of importance today. In line with this, SH2-domain binding sites are not only characterized by a phosphorylated tyrosine but also by the C-terminally adjacent amino-acid residues. In addition, SH2-domains and their binding sites can be combined into ***tandem-arrangements***, allowing for protein-protein interactions with ***increased specificity and affinity***. Since the description of the first SH2-domain, many more tyrosine based signaling motifs have been described and annotated, the most prominent of which I have listed in Introduction-Table 7.

Substrate specificity and recruitment of tyrosine kinases and phosphatases

Most of the specificity of tyrosine based signal transduction is encoded by the amino-acid sequence surrounding the tyrosine to be phosphorylated. The composition of this critical area of the protein determines which kinases and phosphatases are capable of catalyzing the transduction of phosphoryl-groups. Furthermore, they affect which signaling effectors/tyrosine recognition domain will be recruited to the protein labeled by tyrosine phosphorylation. The study of kinase function has left us with an extensive list of kinase recognition sites and databases that allow for the prediction of kinase-substrate interaction. Often an “educated guess” can be made based on the amino acids sequence surrounding a given tyrosine (Gafken and Lampe, 2006). Generally, acidic residues surrounding a tyrosine represent good kinase-substrate sites (Turk, 2008). Additionally, target protein

harbor often other recognition motifs that facilitate the recruitment of a specific kinase to its substrate (Hunter, 2009).

Tyrosine phosphatases display an extraordinary substrate specificity. The recruiting signaling motifs are not as conserved as tyrosine kinase recognition motifs. Instead, binding of a tyrosine phosphatase is defined by the charge and size of the amino acids surrounding the tyrosine in question (He et al., 2014b). Therefore, in contrast to the prediction of tyrosine kinase substrate sites, the precise bioinformatics-based prediction of a tyrosine-phosphatase-substrate remains challenging and is most often still conducted manually and experimentally.

Y-based recognition MOTIF	Recognizing protein domain	Description	References
SH2-binding site	***SH2-domain***	First modular signaling motif known to be recognized by a tyrosine-phosphorylation specific domain. The SH2 domain id found in receptor molecules, enzymes, transcription factors adaptor proteins and cytosolic signaling proteins, such as tyrosine kinases. An Sh2 domain binds only to a SH2-binding site upon Y-phosphorylation (except in the case of two Grb-like SH2 domain in the proteins SAP and Grb10). The signaling specificity of the motif is determined by the 3-5 peptides C-terminal of the tyrosine residue. There are at least 87 proteins encoded in the human genome. Based on structural feature one can classify three distinct types of SH2-domain (Phospholipase-C like; Src-like and Grb2-like).	(Pawson et al., 2001; Yaffe, 2002)
ITAM (Immunoreceptor tyrosine-based activating motif)	***SH2-domain***	Tandem SH2-domain binding site found in many multi-subunit immune recognition receptors. Repeat of a *YxxL* sequence with a 6-8 amino acid spacer sequence in between. Important for the formation of homophilic receptor complexes. Tyrosine phosphorylation is linked to receptor clustering and recruitment of SH2 domain containing kinases (usually signaling activation).	(Gergely et al., 1999; Isakov, 1998)
ITIM (Immunoreceptor tyrosine-based inhibiting motif)	***SH2-domain***	Tandem SH2-domain binding site found in many multi-subunit immune recognition receptors. Repeat of a *YxxL* sequence with a 6-8 amino acid spacer sequence. Important for the formation of heterophilic receptor complexes with ITAM containing receptors. Tyrosine phosphorylation is linked to receptor clustering and recruitment of SH2 domain containing phosphatases (usually signaling inhibition).	(Gergely et al., 1999)
Y-based sorting signal	***Mu subunit of AP (Adaptor protein) complex***	*Yxx(LMVIF)* motif of 4-6 amino acid length. This motif is found in membrane proteins and proteins in the endosomal and secretory pathways. It mediated binding top the mu subunit of the Ap-complex and hence determines the vesicular trafficking and the subcellular localization of a protein. If such a tyrosine residue is phosphorylated, binding to the AP-complex is structurally inhibited. Therefore, it is unclear if tyrosine phosphorylation assumes a regulatory function for this interaction.	(Owen and Evans, 1998)
PTB ligand	***PTB/PID (phosphor-tyrosine binding or interacting domain)***	*NxxY* motif recognized by PTB domain in a tyrosine phosphorylation specific manner. However, not all PTB domains require tyrosine phosphorylation. Motif specificity is conferred by the amino-acid residues N-terminally of the phosphorylated tyrosine, which need to form a beta-strand. The ligand binding specificity is much broader than that of the SH2-dmoain. There are 27 PTB-containing proteins in the human genome. Structurally the motif is highly similar to the Ena/Vasp homology domain, recognizing polyproline stretches.	(Yaffe, 2002; Yan et al., 2002)
eIF4E binding motif	***Dorsal surface of eIF4E***	*YxxxxL* motif mediating binding to a tryptophan in the dorsal motif of the cap-binding protein eIF4E. It is important for the recruitment of the ribosome to an mRNA. Tyrosine phosphorylation of the inhibitory 4E binding protein is important for the release of eIF4E and its recruitment to the mRNA.	(Richter and Sonenberg, 2005)

INTRODUCTION- TABLE 7. **LIST OF IMPORTANT SIGNALING MOTIFS CENTERED AROUND TYROSINES.** *Information regarding the motifs was collected from the ELM database.*

Tyrosine phosphorylation during neural guidance

The importance of reversible tyrosine-phosphorylation during axon guidance was discovered in parallel with the development and use of antibodies specific to tyrosine-phosphorylated proteins. Such antibodies were developed within two years of the discovery and description of tyrosine phosphorylation (Hunter, 2014). These novel molecular tools were for example used to stain growth-cones and it was discovered that some sub-compartments of growth cones are enriched with tyrosine phosphorylated proteins. Notably, the distribution of the phosphor-tyrosine signals differed, depending on the type, shape and speed of the respective growth cone (Wu and Goldberg, 1993). By imaging the relatively large and accessible *Aplysia* growth cones, Da-Yu Wu and Daniel Goldberg concluded that the filopodia of slow moving growth cones are characterized by an intense phosphor-tyrosine signal at their filopodial tips. This specific localization however, perished if the cells were plated on growth promoting substrates (hemolymph) or in the presence of F-actin inhibitors, such as Cytochalasin D, suggesting that tyrosine phosphorylation mediated signaling plays an ***important role for the dynamics of the filopodial growth cone compartment*** (Wu and Goldberg, 1993) (see also Introduction-Figure 8).

Further clues towards the importance of kinases and phosphatases in axon guidance, growth and targeting have been obtained through pharmacological studies in cell culture of cell lines and primary neuronal cells. These studies demonstrated, that the phosphatase inhibitor vanadate inhibits formation of neuromuscular junctions and dispersion of acetylcholine-receptors (Dai and Peng, 1998). In addition, the use of phosphatase inhibitors affects axonogenesis and axonal outgrowth in different cell types, such as hippocampal neurons, neuroblastoma or PC12 cells (Mandell and Banker, 1998; Rogers et al., 1994; Wu and Bradshaw, 1993).

Taken together, these early experiments suggested, that tyrosine phosphorylation is an important regulator of neuronal morphogenesis and that altering the relative levels of phosphorylated and dephosphorylated proteins affects neuronal morphogenesis. In addition, it became already then clear that it is important to dissect the effects of tyrosine phosphorylation using tools and techniques specific to a certain phosphatase, kinase as well as cellular contexts.

Therefore, *in vivo* studies of tyrosine phosphorylation became an important tool to complement the molecular characterization of kinases and phosphatases and their substrates. In *Drosophila melanogaster* the phenotypes of the RPTPs *Lar, RPTP69D, RPTP99A, RPTP4E, RPTP10D* and *RPTP52F* raised awareness for the importance of tyrosine phosphorylation during axon guidance and synapse formation (reviewed in Desai et al., 1997; Hatzihristidis et al., 2015; Johnson and Van Vactor, 2003). Furthermore, many kinases and phosphatases have very specific expression profiles in the nervous system, suggesting that regulated tyrosine phosphorylation is of importance there (Desai et al., 1997; Johnson and Van Vactor, 2003) Furthermore, kinases and phosphatases have been implicated in many diseases affecting the nervous system (Hatzihristidis et al., 2015; Hendriks et al., 2013). Finally, many axon guidance receptors are tyrosine phosphorylated, harbor phosphor-catalytic functions or interact with kinases and phosphatases (Dent et al., 2011; Bashaw and Klein, 2010; Guan and Rao, 2003; Hatzihristidis et al., 2015; Hing et al., 1999; Johnson and Van Vactor, 2003; Lowery and Van Vactor, 2009).

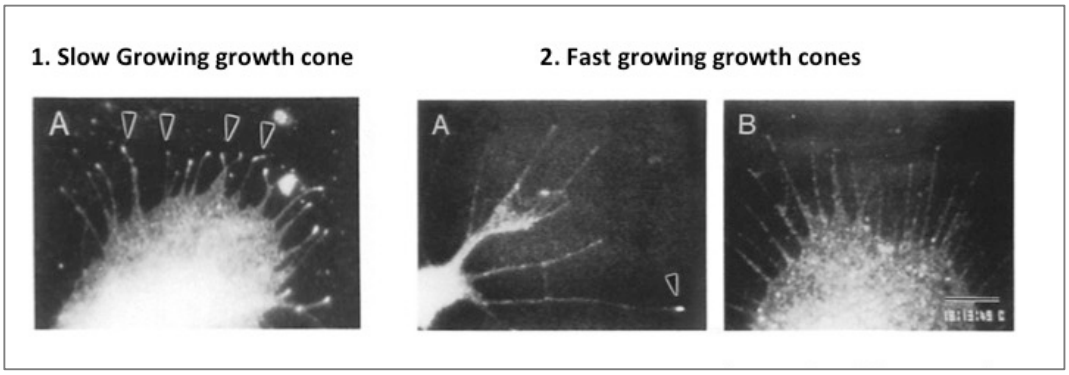

INTRODUCTION- FIGURE 8. **TYROSINE PHOSPHORYLATION IS ENRICHED IN FILOPODIA OF THE GROWTH CONE.**

(Image modified from Wu and Goldberg, 1993) (1) Anti-phosphor-tyrosine staining of an Aplysia neuronal growth cone derived from dissociated ganglia and plated on poly-lysine substrate. Arrowheads are pointing to single filopodia which show a bright signal at their tip. (2) Anti-phosphor-tyrosine staining of the same type of dissociated sample in the presence of growth promoting hemolymph. Note, how most of the filopodia are lacking the intense staining at the tip which was seen in (1). One of the few filopodial tips marked by phosphor-tyrosine is labeled with an arrowhead in panel (A).

Purification of tyrosine phosphorylated proteins

Based on the key-function that tyrosine phosphorylation has during signal transduction in an abundance of biological processes, it is not surprising that many efforts have been made to study the tyrosine-phosphor-proteome. The purification of tyrosine phosphorylated proteins has been largely optimized and simplified during the last fifteen years, making it

more and more feasible to study tyrosine phosphorylation on a proteomic scale. However, it still remains technically challenging to conduct experiments in a setting that differs from the standard experimental. A typical workflow for a phosphor-proteomic experiment is depicted in Introduction-Figure 9.

Most approaches to study phosphor-proteomics start with a purification and enrichment step of phosphorylated proteins/peptides followed by mass spectrometry based peptide fingerprinting. However, the analysis of the phosphor-proteome by mass spectrometry remains ***technically demanding*** for a number of reasons (reviewed in Mann et al., 2002): (1) Phosphorylated peptides are negatively charged (electrospray is performed in positive mode); (2) phosphorylated peptides are hydrophilic (which means that they stick to many of the columns used to enrich and purify the peptides); (3) their peptide peaks are not intense especially in presence of non-phosphorylated peptides (owing to ionic suppression). Furthermore, it is commonly known that phosphorylated proteins are represented with (4) low stoichiometry. Finally, (5) proteins can be phosphorylated at multiple sites or exist in multiple different signaling states and isoforms leading to sample heterogeneity, which cannot be resolved by ordinary proteomic mass spectrometry based approaches.

Purification strategies for phosphorylated proteins

Traditionally, tyrosine phosphorylation sites within candidate proteins were identified ***by two-dimensional gel electrophoresis*** in combination with ***on site-directed mutagenesis mapping***. Nowadays, tyrosine phosphorylated proteins can be purified on large scale if there is enough sample available. The resulting protein-mix is subjected to mass-spectrometry based peptide fingerprinting in order to identify candidate proteins (Introduction- Figure 9). This approach is highly efficient. Generally, the only limiting factor is the initial purification step. Some newer mass-spectrometry based studies suggest that we might underestimate the abundance of tyrosine-phosphorylation as a posttranslational modification by far: In response to the activation of a single RTK, hundreds of phosphorylation sites change, suggesting that tyrosine signaling networks are not only extraordinarily large and flexible but possibly also highly dynamic (Mann et al., 2002; Zhang and Neubert, 2011). Importantly, none of the commonly employed strategies is capable of resolving the entire tyrosine-phosphor-proteome (Mann et al., 2002; Zhang et al., 2015).

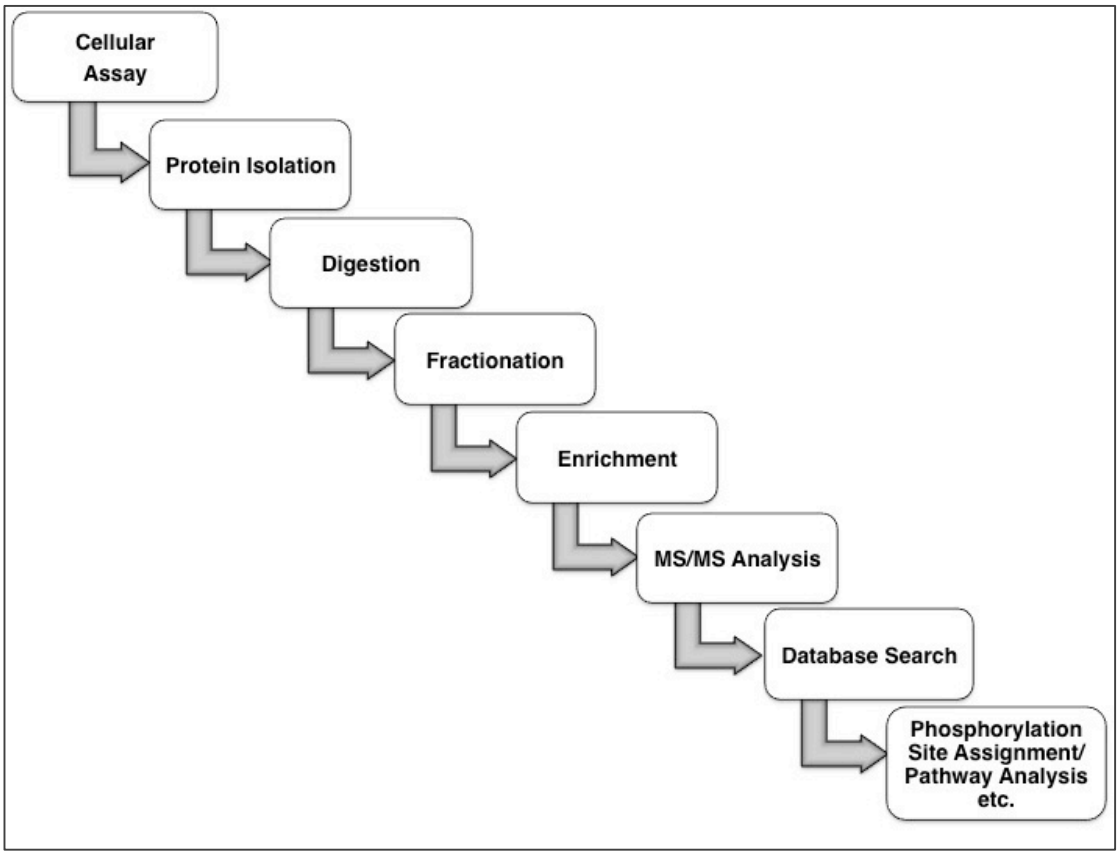

INTRODUCTION- FIGURE 9. **STANDARD WORK FLOW OF A PHOSPHOR-PROTEOMIC EXPERIMENT.**

(Inspired by Yang, Zhong and Li 2014) An inducible cellular assay is used to achieve distinct signaling states. Proteins are harvested, purified, enriched, digested and fractionated in preparation for MS-MS-Analysis. Mass-spectrometry based fingerprinting heavily depends on well annotated databases in order to assign peptides to their cognate proteins. The global view attained by proteomic experiments can be used to detect cellular signatures and pathways affected by the stimulus induced to activate the cellular system.

However, some of these problems can be addressed by ***combining the purification strategies of phosphorylated proteins with novel highly quantitative labeling approaches*** (Gafken and Lampe, 2006). Hence, if one is capable of collecting enough samples, the comparisons of up to eight different experimental conditions is possible, allowing a detailed analysis of the phosphor-proteome. Of these quantitative methodical approaches, the most common two approaches are stable isotope labeling by metabolic incorporation of amino acids (*SILAC*) and chemical labeling by isobaric tags *(*iTRAQ*)* (Gafken and Lampe, 2006; Zhang et al., 2015).

The most commonly employed approaches to purify phosphorylated peptides are based on the high affinity of phosphates towards a metal-chelated stationary phase, such as immobilized metal affinity chromatography (IMAC) or metal oxide affinity

chromatography (MOAC) experiments (Mann et al., 2002). The positively charged metal ions are typically Fe^{3+}, Al^{3+}, Ga^{3+}, Zr^{4+} and Ti^{4+}, which are in IMAC experiments immobilized on a support, such as beads, a chromatographic column or a MALDI plate. The biggest problems with metal affinity based methods arise from ***specificity and efficiency***: The purification is entirely based on affinity towards negative charge. For this reason, one has to adjust the pH of loading and washing buffers in order to avoid binding of peptides characterized by acidic residues. This often leads to massive sample loss. Furthermore, one has to take into account that peptides with multiple phosphorylation sites will be preferably enriched, skewing the experiments towards high abundance proteins and proteins with multiple phosphorylation sites.

The chemical modification of phosphorylated amino acids is perceived as a more sophisticated approach to enrich phosphor-peptides from complex mixtures. The biggest difficulty in these approaches lies in the fact that it requires several chemical reaction and purification steps before one can perform MS. Therefore, ***large amounts of sample are needed and more abundant proteins are preferentially detected.*** Finally, there is the possibility to purify tyrosine phosphorylated proteins by ***antibody purification***. However, concerns have been raised regarding the efficiency of this method (Mann et al., 2002).

Current state of research regarding Dscam1-Receptor mediated signaling transduction

The *Drosophila* cell surface receptor Dscam1 encodes for thousands of different isoforms

Precise navigation requires from the helmsman not only to record the surroundings but also to be aware of the exact position and size of his own vehicle. This principle applies to the steering of moving vehicles but also to mobile cells or cellular compartments, such as growth cones. Neuronal circuit formation calls for the capability of neurons to sense the position of their own neurites. The importance of this ability lies in developmental economy: The sensory field of a neuron needs to cover the largest possible area with a limited set of membrane/neurites. Unnecessary auto-activation/inhibition loops, created by connecting neurites of the same neuron, should be avoided.

But how does a neuron attain a sense of self? In cells of the nervous system, this important task is assumed by so-called ***self-recognition receptors***. In contrast to their counterparts, the classical extrinsic guidance receptors (please refer to the chapter *Signal transduction during neural guidance: Ligands, receptors and effectors* for further details), neuronal self-recognition receptors have been identified relatively late (in the late 1990s-2000). Therefore, the research regarding the molecular mechanisms of neuronal self-awareness is still considered a novel field.

However, the idea that neurons possess a sense of "*self* "or "*identity*" has been around for a long time. It was first proposed by ***Roger Sperry*** in 1963. His ***chemo-affinity hypothesis*** predicts ″THAT THE CELLS AND FIBERS OF THE BRAIN AND THE CORD MUST CARRY SOME KIND OF INDIVIDUAL IDENTIFICATION TAGS, PRESUMABLY CYTOCHEMCIAL IN NATURE, BY WHICH THEY ARE DISTINGUISHED FROM ONE ANOTHER ALMOST, IN MANY REGIONS, TO THE LEVEL OF A SINGLE NEURON″ (Sperry, 1963). While the overall concept was intriguing, because it was capable of explaining a lot of phenomena observed during neuronal wiring, the chemoaffinity hypothesis presented the research community also with a stunning and at that time unresolvable ***"labeling problem"***. After all, Sperry's hypothesis predicted the capability to distinguish *" LITERALLY MILLIONS, AND POSSIBLY BILLIONS, OF CHEMICALLY DIFFERENTIATED NEURON TYPES"* (Sperry, 1963).

How this enormous labeling task could be achieved and what the nature of such labels could be, remained mysterious and controversial for a long time. The dawn of the genomic area and the sequencing of the human genome made it soon clear, that the surface label conferring neuronal identity to a neuron could not simply be encoded by a multitude of different neuronal "identity genes": After all, the human genome consists only of 20,000-25,000 predicted protein coding genes, of which only a fraction is actually expressed in the nervous system. The total number of human neurons however, has been estimated to be in the range of 86.1 billion different neurons (Azevedo and Carvalho, 2009). Therefore, the source of unique neuronal identity must be hidden somewhere else.

In line with this thought, some genes expressed in neurons encode for ***multiple isoforms*** or paralogues, suggesting that they could serve as potential neuronal surface labels. Among these variable proteins proposed to be potential surface labels were the odorant receptors (Malnic et al., 2004; Wang et al., 1998), the different cadherins (classical and cadherin related receptors) (Hulpiau and van Roy, 2009), the polymorph family of MHC proteins (over 500 different alleles) (Huh et al., 2000; Trowsdale and Parham, 2004) as well as the highly diverse family of neurexins with an estimated 1,000 members (Missler and Südhof, 1998a; 1998b; Ullrich et al., 1995). However, ***none of these receptor families was large enough*** to cover the enormously high demand of diversity that would be necessary to confirm the chemoaffinity hypothesis.

Therefore, when several studies originating in the Zipursky lab demonstrated that that the enormous variability of the *Drosophila* axon guidance receptor ***Dscam1*** (*encoding for thousands of different potential isoforms*) is essential for proper neuronal wiring, the answer to the Sperry's labeling problem seemed to be a little closer (Schmucker et al., 2000; Wojtowicz et al., 2007). Since then, hypervariable *Dscam* family genes have been reported in many different species: They exist for example in different *Drosophila* subgenus, *Tribolium castaneum* (red flour beetle), *Apis mellifera* (honeybee), *Bombyx mori* (silk moth), different types of mosquitos *(Anopheles gambiae*, *Aedes aegypti*), pea aphid (*Acyrthosiphon pisum*), head louse (*Pediculus humanus*), different types of shrimp (*Litopeneaus vannamei, Marsupenaeus japonicas*), *Penaeus monodon* (giant tiger prawn), water fleas (*Daphnia pulex, Daphnia magna*), crayfish (*Pacifastacus leniusculus*) and crab (*Eriocheir sinensis*) (Anastassiou et al., 2006; Brites et al., 2008; Chou et al., 2011; 2009; Crayton et al., 2006; Graveley, 2004; 2005; Jin et al., 2013; Watson, 2005; Watthanasurorot et al., 2011).

Neuronal surface identity is conferred by combinatorial expression of different subsets of Dscam1 isoforms

The gene identified by Schmucker et al. is now widely known as ***Dscam1*** (CG17800). It belongs to the Dscam-family of cell adhesion molecules (CAMs). The extracellular domain of these single pass trans-membrane proteins consists of 10 Ig-repeats and six fibronectin (FN) domains. This means that the extracellular domain is not only ***very large*** in comparison with other receptors but also that it contains more Ig-domains than most Ig-CAMs (Ng et al., 2015). *Dscams* are expressed in the CNS and PNS as well as in cells of the invertebrate immune system (Schmucker et al., 2000; Watson, 2005). *Each cell expresses multiple isoforms of Dscam1 on the surface and different cells carry distinct Dscam1 subsets* (Neves et al., 2004; Zhan et al., 2004).

The enormous variability of *Drosophila Dscam1* arises from ***mutually exclusive splicing*** of the *Drosophila Dscam1* gene locus, which spans almost 80 kb (Introduction-Figure 10). It consists of 115 exons, 95 of which are alternatively spliced. The alternatively spliced exons are organized into four clusters known as the exon 4, 6, 9 and 17 cluster. In the mature protein they encode the first half of Ig-domain 2 and 3 (exon 4 and 6), the full Ig-domain 7 (exon 9) and a single pass trans-membrane domain (exon 17) (Introduction-Figure 10).

There are a number of different expression studies addressing the presence and distribution of distinct *Dscam1* isoforms in different cells. Taken together, they suggest that the invertebrate *Dscam1* gene serves as a ***molecular bar code***, providing particular cells with unique identities: Individual cells, even if they are derived from the same tissue or cell line, express ***differential subsets of 14-50 Dscam1 isoforms*** on their surface, ensuring that they are distinct from each other (Neves et al., 2004; Zhan et al., 2004).

Splicing of the Dscam1 genomic locus is "***stochastic yet biased"*** (Neves et al., 2004). This means that during a serious of successive splicing events each exon cluster is inserted in a probabilistic manner (Sun et al., 2013b). The different alternative exon clusters are spliced independently from each other (Sun et al., 2013b). Interestingly however, there is certain spatial and temporal regulation that is not fully understood: For example, a bias has been noted for certain exons to be included into the otherwise stochastically assembled transcript (Sun et al., 2013b; Watson, 2005). This additional layer of bias on top of a stochastic assembly is not fully understood yet, but is most likely mediated by cell type specific

splicing factors (Anastassiou et al., 2006; Miura et al., 2013; Neves et al., 2004; Olson et al., 2007; Park et al., 2004). In addition, the *Dscam1* isoform pool remains flexible, resulting in altered isoform signatures of a given cell at distinct time points throughout life (Miura et al., 2013). The fact that there are 12 alternative versions of exon 4, 48 versions of exon 6, 33 versions of exon 9 and 2 possible variants of exon 17 allows by combinatorial use to create ***19,008 distinct Dscam1 extracellular domains,*** which are linked to 2 different trans-membrane-domains. Moreover, there is further variability generated by exon skipping: Exon 19 and exon 23 can be omitted during splicing, resulting in ***four different potential versions of the intracellular domain*** (Introduction- Figure 10).

Several studies have tried to address the exon signatures of single cells. However, these efforts are hampered by the fact that it is hard to obtain enough high quality material from a single cell. In the case of the nervous system, the problem is further aggravated by the fact that a pool of mRNAs exists far ways from the cell body in the growth cone and that it is most likely this hard to purify such mRNA pool, which after all influences a growth response. The most striking cell type specific differences in *Dscam1* isoform signatures are seen when comparing neuronal and immune derived cells: Hemocytes for example, display an expression pattern very distinct from brain tissue, which is more restricted (e.g. 7317 isoforms in S2 cells). ***Generally, single neurons are estimated to express between 14 and 50 different Dscam1 isoforms*** (Neves et al., 2004; Zhan et al., 2004). Some exons display specific expression patterns in different neuronal tissues (Celotto and Graveley, 2001; He et al., 2014a; Neves et al., 2004; Sun et al., 2013a; Watson, 2005; Zhan et al., 2004). Most importantly, it has been shown that ***except from exon 6.11 every other Dscam1 exon is expressed*** (Sun et al., 2013b).

Two distinct Dscam1 trans-membrane domains regulate Dscam1 localization

There are ***two distinct Dscam1 transmembrane domains*** encoded by alternative versions of exon 17. Their presence in the transcript is decisive for the location of Dscam1 expression: *Dscam1*-isoforms with exon ***17.1 are preferentially located in dendrites***, while the ***17.2 isoform is targeted to axons*** (Shi et al., 2007; Wang et al., 2004; Yang et al., 2008). The targeting mechanism facilitating localization of Dscam1 to the dendrites involves ***dynein-dynactin***. The same molecular interaction might also be involved in the exclusion of the 17.1-isoforms from the axonal compartment (Yang et al., 2008). The targeting to

axons is mediated by interaction with the membrane associated protein ***vap-33*** (Yang et al., 2012).

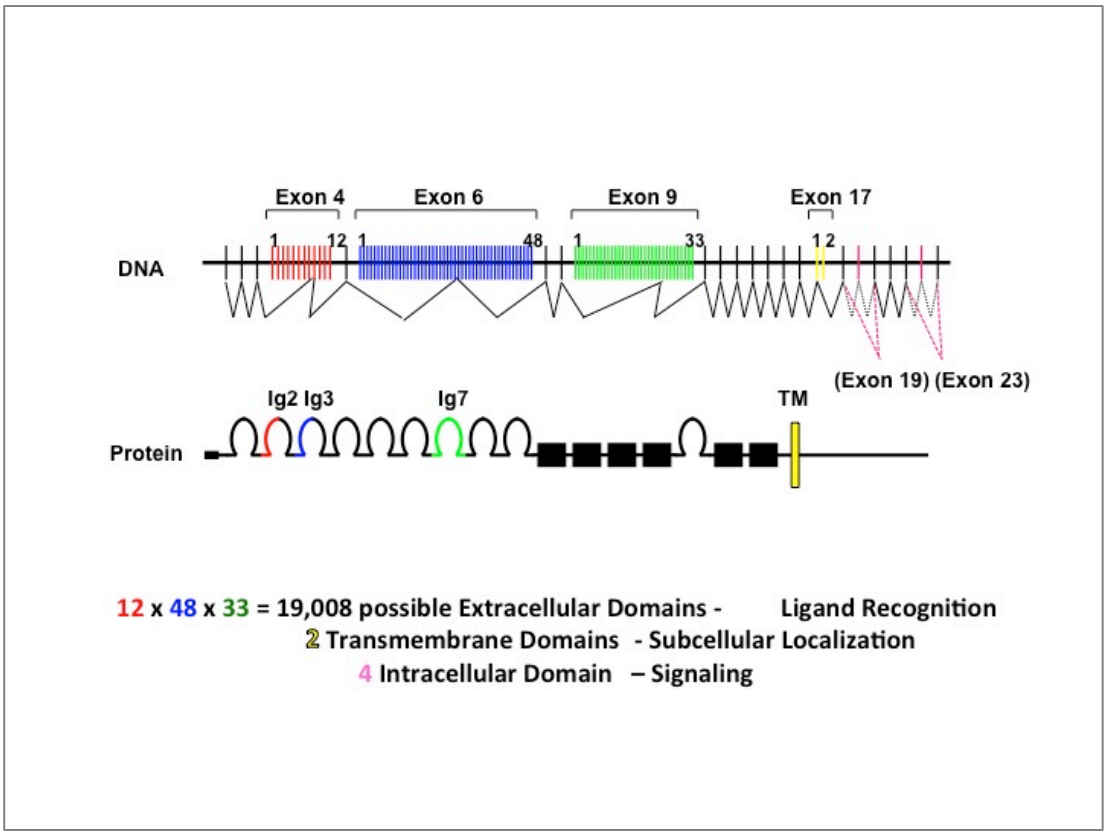

INTRODUCTION- FIGURE 10. **THE DROSOPHILA GENE DSCAM1 IS EXTENSIVELY SPLICED.**

(Adapted from Schmucker et al. 2000.) Three exon clusters (exon 4 in red; exon 6 in blue and exon 9 in green) encode for the variability of Ig-domains in the Dscam1 extracellular domain by virtue of exclusively alternative splicing. The extracellular domains are important for Dscam1-ligand interactions. The fourth alternatively spliced exon cluster (exon 17 in yellow) encodes for two distinct transmembrane domains. Dscam1 is localized to dendrites, if the transcript contains the 17.1 transmembrane domain. If the cDNA of Dscam1 contains exon 17.2, the protein will be located in axons. The exons depicted in pink (exon 19 and 23) can be skipped during the splicing process, leading to four different potential versions of the Dscam1 intracellular domain.

Only equal Dscam1 extracellular domains are capable homophilic binding

The combinatorial use of different isoforms on the neuronal surface provides the nervous system with a molecular Dscam1-barcode sufficient to overcome the labeling problem presented by Sperry's chemoaffinity hypothesis: Even though it is unlikely that each cell in the nervous system expresses a unique Dscam1 isoform-set on the surface, mathematical modeling suggests that two neighboring cells express always distinct sets of Dscam1 isoforms (Hattori et al., 2009). However, in order to make use of such a diverse labeling

system the cell needs ***a matching recognition system*** capable of reading and distinguishing the different bar codes.

In the case of the Dscam1 receptor, we do understand quite well, how such recognition specificity is created: In fact, the Dscam1 extracellular domains harbor remarkably ***selective homophilic binding*** interfaces (Wojtowicz et al., 2004). These exposed protein stretches, known as "***Dscam1-epitope 1"*** (Meijers et al., 2007), are formed by the ***N-terminal eight Ig-domains*** of the extracellular domain around the three variant extracellular Ig-domains (Ig2, Ig3 and Ig7) (Meijers et al., 2007; Sawaya et al., 2008). The extracellular domain folds into an S-shape which is tethered by a long linker to the cell surface (Sawaya et al., 2008). The bends of the S-shape are arranged in such a way, that the three variable Ig-domains forming epitope1 align into one plane thereby creating a binding interface.

Importantly, *in vitro* binding studies have convincingly demonstrated that Dscam1s act as highly exclusive ***homophilic adhesion molecules***: *Two Dscam1 extracellular domains bind solely to each other if they consist of the exact same combination of variable Ig-domains* (Meijers et al., 2007; Sawaya et al., 2008; Wojtowicz et al., 2004; 2007; 2008; Wu et al., 2012). This ***'all or nothing'-binding*** mechanism (Sawaya et al., 2008) forbids interaction, even if only one of the three variable Ig-domain is non-matching. Introduction-Figure 11 summarizes the molecular mechanisms underlying homophilic Dscam1-Dscam1 interactions.

Biological processes requiring *Drosophila* Dscam1 signaling and function

Numerous studies conducted during the past 25 years have provided evidence for a functional requirement of the Dscam1 signatures (reviewed in Grueber and Sagasti, 2010; Zipursky and Grueber, 2013; Neves and Chess, 2004): They are necessary for dendritic patterning, axon-guidance, axon-branch-segregation, axon-targeting, axon-terminal arborization and synaptic targeting (Andrews et al., 2008; Chen et al., 2006; Cvetkovska et al., 2013; He et al., 2014a; Hughes et al., 2007; Hummel et al., 2003; Matthews et al., 2007; Millard et al., 2010; Schmucker et al., 2000; Soba et al., 2007; Wang et al., 2002; Wojtowicz et al., 2004; Zhan et al., 2004; Zhu et al., 2006) (Summarized in Introduction-Table 8). In addition, Dscam1 also has important functions in cells of the invertebrate immune system (Watson, 2005).

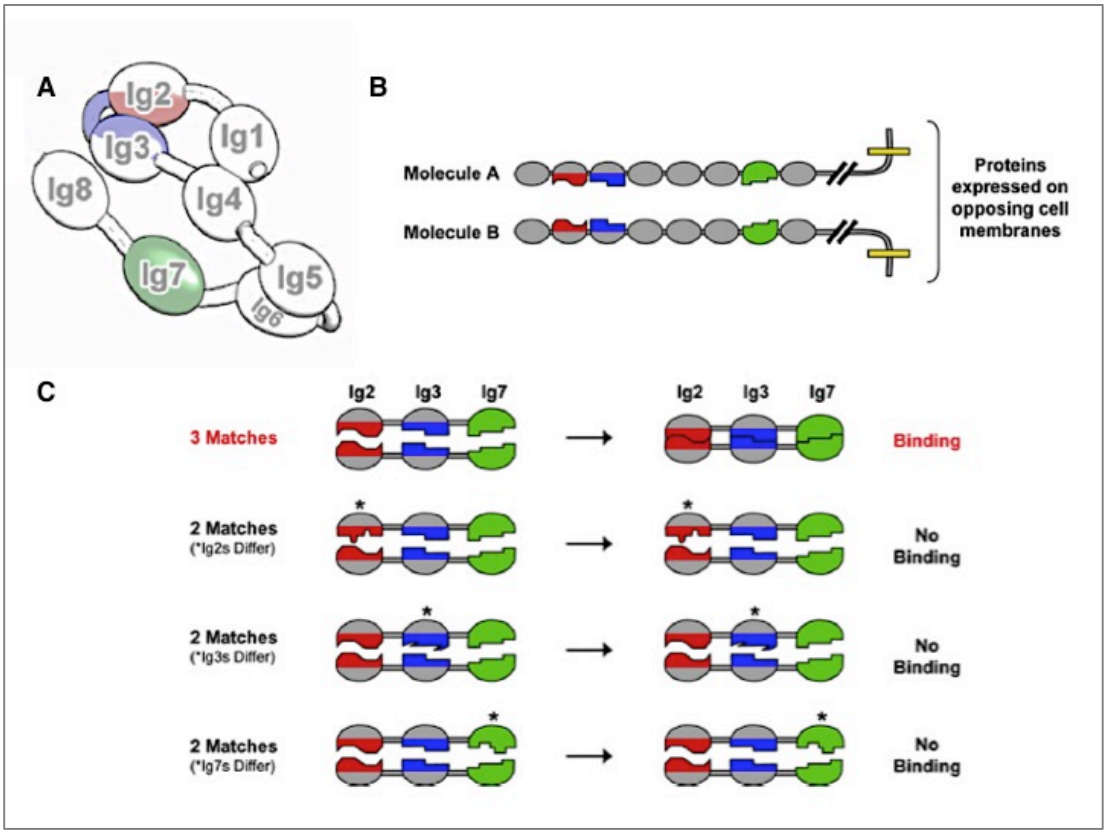

INTRODUCTION- FIGURE 11. **THE EXTRACELLULAR DOMAIN OF DSCAM1 IS AN EXTREMELY SPECIFIC HOMOPHILIC BINDING MOLECULE.**

(Modified from Sawaya and Wojtowic et al. 2008.) (A) S-shape of the N-terminal eight Ig-domains: The three variable Ig-domains are aligned in one plane, forming a binding interface. (B and C) The extracellular domains of two Dscam1 molecules, that encounter each other on two opposing membranes, must contain the exact same variable Ig domains. It has been proposed that the extracellular domain of Dscam1 is relaxed in absence of homophilic binding (B). If two extracellular domains match in all three variable Ig-domains, Dscam1-Dscam1 binding occurs. (C) Homophilic Dscam1-Dscam1 interactions represent an all-or-nothing mechanism: Mismatch in any of the three variable Ig-domains obstructs any detectable homophilic interaction.

INTRODUCTION- TABLE 8. **LIST OF *DROSOPHILA* DSCAM1-RECEPTOR FUNCTIONS *IN VIVO*.**

Cell type/Compartment	Phenotype	Developmental stage	Reference
VNC; Axons stained by BP102 (VUM neurons)	***LOF:*** ✓ ***Disruption of commissures*** and irregularities of ***longitudinal tracts***	***embryo stage 16***	(Schmucker et al., 2000)
VNC; Fas-II positive axons	***LOF:*** ✓ ***Disrupted longitudinal fascicles*** (especially the outer two) and ***abnormal midline crossing***	***embryo stage 16***	(Schmucker et al., 2000)
Bolwig's Nerve	***LOF:*** ✓ ***Mistargeting*** of the entire nerve bundle or a subset of axons (stopping before or after the P2 intermediate target);	***embryo stage 16*** ***embryo stage 17***	(Schmucker et al., 2000) (Andrews et al., 2008)

Cell type/Compartment	Phenotype	Developmental stage	Reference
	✓ ***Abnormally expanded nerve termini*** at P2 in the axons that did not mistarget ✓ ***Defasciculation and looping***		
	GOF*:*		
	✓ Individual ***axons project in abnormal directions*** over the optic lobe		
Mushroom Body Axons	***LOF:***		(Wang et al., 2002) (Zhan et al., 2004)
	✓ ***Sister branches*** of the same neuron ***cannot separate from each other*** along different pathways		
	GOF:		
	✓ Overexpression of a ***single isoform in multiple mushroom body neurons*** severely disrupts the ***organization of the axon bundle*** ✓ Overexpression of a ***single isoform in a single cell*** has ***no effect***		
Axons of Olfactory receptor neurons	***LOF:***		(Hummel et al., 2003)
	✓ ***ORNs terminate in abnormal sites*** even outside of the antennal lobe ✓ ***Altered morphology of axon terminals*** independent of targeting		
Cell bodies and axons of posterior commissure interneurons (PC neurons)	***GOF:***		(Wojtowicz et al., 2004)
	✓ ***Less densely packed PC cell bodies*** ✓ If Dscam1 is overexpressed in both PC neurons and midline cells, ***midline crossing is inhibited***		
Dendrites of olfactory projection neurons and interneurons	***LOF:***		(Zhu et al., 2006)
	✓ ***Clumped de***ndrites and ***reduced*** size of ***dendritic field***		
Axonal projections of mechanosensory (ms) neurons	***LOF:***		(Chen et al., 2006) (Cvetkovska et al., 2013) (He et al., 2014a)
	✓ ***Stalling*** and characteristic ***clumping of filopodia*** in the growth cone upon reaching the VNC		
	GOF:		
	✓ ***Loss of axonal branches*** (reduced isoform diversity) ✓ Synaptic ***targeting errors*** (increased protein levels)		
dendrites of da neurons	***LOF:***		(Hughes et al., 2007) (Matthews et al., 2007) Soba et al., 2007)
	✓ ***Class I, II, III and IV***: Extensive ***crossing and clumping of sister dendrites***; uneven innervation of the overall dendritic field ✓ ***Class II:*** Modest increase in ***dendritic termini*** ✓ ***Class III: Collapsed terminal branches*** near the chordotonal organ ✓ ***Class III:*** Crossing of ***dendritic spikes***		
	GOF:		
	✓ ***No phenotype in class I da neurons***; ✓ Expression of a ***single isoform*** is ***sufficient to rescue the LOF phenotype*** of class I dendrites		
	Misexpression in neighboring cells:		
	✓ Inappropriate ***repulsion between dendrites of normally overlapping cells*** of different classes and of duplicated cells of the same class (This is the only case, where a switch in branching directionality is reported for dendrites of da neurons)		

Cell type/Compartment	Phenotype	Developmental stage	Reference
	✓ Time lapse imaging shows ***stalling and retraction*** if two dendrites come into close proximity.		
Axonal projections of da neurons	***LOF:*** ✓ Changed ***axonal projections of class IV neurons***, which could partially be rescued by a single isoform ✓ ***Reduced presynaptic arbor length*** ***GOF:*** ✓ ***Overgrowth*** of presynaptic arbor (diversity independent) ✓ Problems with axonal ***targeting*** if a ***single isoform*** is expressed at ***endogenous levels*** (diversity dependent)		(Kim et al., 2013) (Soba et al., 2007)
S2 cells	***Misexpression of a single isoform*** ✓ ***Clumping*** of cells; ✓ If two different isoforms are expressed, they separate into distinct clumps ***LOF:*** ✓ Blockage of Dscam1 signaling with ***anti-Dscam1 antibody*** reduces phagocytotic index by 30%	***in vitro; cell culture***	(Matthews et al., 2007) (Watson, 2005)
COS cells	***Misexpression of Drosophila Dscam1****:* ✓ Rounded cells that adhere to each other ✓ Loss of attachment to the dish ***LOF:***	***in vitro; cell culture***	(Andrews et al., 2008) (Watson, 2005)
SP1 pioneer commissural axons	✓ ***No phenotype*** ✓ Dscam1, fra double mutant: Missing commissural axons ✓ Dscam1, Dscam3, fra triple mutant: Missing commissural axons and shifted Sp1 cell bodies	***embryo late stage 15 and early stage 16***	(Andrews et al., 2008)
EG commissural axons	***LOF:*** ✓ ***No phenotype*** ✓ Dscam, fra double mutants: Commissural axons missing		(Andrews et al., 2008)
Salivary gland cells	***LOF:*** ✓ ***Shorter salivary gland*** due to increased curvature ✓ Dscam, fra double mutant: Stalling of migration or kinking of the gland.	***embryo stage 13/14***	(Andrews et al., 2008)
ftz-longitudinal axons	***Misexpression:*** ✓ ***Inappropriate midline crossing*** (Fas2 staining) ✓ Stalled axons (Fas2 staining) ✓ Disrupted separation of anterior and posterior commissure (BP102 staining) ✓ pCC pioneer axons are unaffected	***embryo stage 12/13 (pioneer axons) and stage 16/17***	(Andrews et al., 2008)
Tetrad synapses of photoreceptor neurons in the first optic neuropil (lamina)	***LOF:*** ✓ Dscam1 and Dscam2 LOF leads to formation of ***inappropriate self-synapses***		(Millard et al., 2010)
Hemocytes, fat body, hemolymph	***LOF:*** ✓ Hemocyte-specific RNAi mediated knockdown of Dscam1 impairs ***phagocytosis*** of bacteria		(Watson, 2005)

Dscam1 mediated self-avoidance facilitates uniform patterning of neurites

The most intensely studied function of Dscam1-mediate self-recognition is ***neurite-self avoidance*** (reviewed in Grueber and Sagasti, 2010; Zipursky and Grueber, 2013) (see also Introduction- Figure 12): Two neurites extending from the same cell body recognize each other's surface by homophilic Dscam1-Dscam1 interactions. This triggers the initiation of an as of yet ***unknown signaling cascade*** mediating ***neurite-retraction***. Such a patterning principle based on repulsion allows for the formation of elaborate dendritic trees and axonal arborizations (Hughes et al., 2007; Kim et al., 2013; Matthews et al., 2007; Soba et al., 2007; Wang et al., 2002; Zhan et al., 2004; Zhu et al., 2006).

As a uniting theme one can conclude, that Dscam1 is used to ensure maximal space between all involved neurites. Such ***uniformly spaced neurite pattern*** ensures optimal coverage of a sensory field area. Typical for this function is that loss of Dscam1 causes striking ***"self-crossing"-phenotypes,*** characterized by ***entangled neurites*** (Hughes et al., 2007; Kim et al., 2013; Matthews et al., 2007; Soba et al., 2007; Wang et al., 2002; Zhan et al., 2004; Zhu et al., 2006). While the signaling cascade mediating Dscam1-inititated repulsion remains unknown, it is generally possible to rescue the typical neurite segregation phenotypes by expression of a single Dscam1 isoform (Hughes et al., 2007; Matthews et al., 2007; Soba et al., 2007; Wang et al., 2012; Zhan et al., 2004; Zhu et al., 2006).

Dscam1 mediates opsonization and phagocytosis in the immune system

Similar to self-avoidance of sister neurites in the nervous system, it is relatively easy to describe the proposed function of Dscam1 in the immune system (Boehm, 2007; Rimer et al., 2014). Dscam1 is expressed by cells of the fat body and in hemocytes (Watson, 2005). A cleaved form of Dscam1 (extracellular domain) is also found in the hemolymph (Watson, 2005). The extracellular domain of Dscam is capable of ***binding pathogens*** with distinct preferences of specific isoforms for different pathogens (Dong et al., 2006; Watson, 2005; Watthanasurorot et al., 2011). Based on these binding properties and the fact that loss of invertebrate Dscam leads to impaired ***phagocytosis*** and ***wound healing***, it has been proposed that secreted Dscam ***floating in the hemolymph*** could ***opsonize*** pathogens (Boehm, 2007; Dong et al., 2006; Watson, 2005). Phagocytosis competent cells expressing matching Dscam isoforms, such as specialized hemocytes (plasmatocytes), would be

attracted to the Dscam labeled pathogens and initiate phagocytosis by coupling the hemocyte to the pathogen, either via homophilic Dscam1-Dscam1 or via heterophilic Dscam1-integrin interactions (Boehm, 2007; Dong et al., 2006; Ng et al., 2015; Watson, 2005; Watthanasurorot et al., 2011) (see also Introduction- Figure 14). In line with this, it has been reported that invertebrate Dscam-receptors localizes to the attachment site of bacteria on phagocytosing *Anopheles* hemocytes (Dong et al., 2006; Jin et al., 2013), and that *Drosophila and Anopheles* Dscam-proteins bind to bacteria *in vitro* (Dong et al., 2006; Watson, 2005). Alternatively, the activation of Dscam1 signaling could lead to the expression of other immune competent molecules, thereby boosting the innate immune response.

While Dscam1's function in pathogen binding and phagocytosis remain indisputable, it is not entirely clear, if Dscam1 mediated pathogen recognition also could initiate ***an adaptive immune response*** by stimulating the expression of Dscam1-isoforms with high affinity to the respective pathogen (memory). Nowadays, it is well established that insects possess an innate immune response. However, there exists also the potential for adaptive immunity in invertebrates, a process described with the term "***priming"*** (Chambers and Schneider, 2012; Ng et al., 2015; Pham and Schneider, 2008; Sadd and Schmid-Hempel, 2006). *Priming of the immune system allows a faster and more efficient response when an organism encounters the same pathogen a second time.* The concept has been first introduced to the scientific community in 1979 during the study of phagocytosis in lobster hemocytes (reviewed in Brehélin and Roch, 2008; Kurtz and Franz, 2003; Paterson and Stewart, 1979; Sadd and Schmid-Hempel, 2006). Priming has been described for a wide range of arthropod species challenged with bacteria and viruses. This immune response is of special economic interest, because of its potential to protect valuable animal cultures by "*vaccination*", preserving for example beehives (Sadd and Schmid-Hempel, 2006) or shrimp colonies (Johnson et al., 2008; Powell et al., 2011). Priming responses last for several weeks (e.g. 22 days in the bumble bee (Sadd and Schmid-Hempel, 2006)) and might be more important the longer the life of a given animal species lasts (Ng et al., 2015).

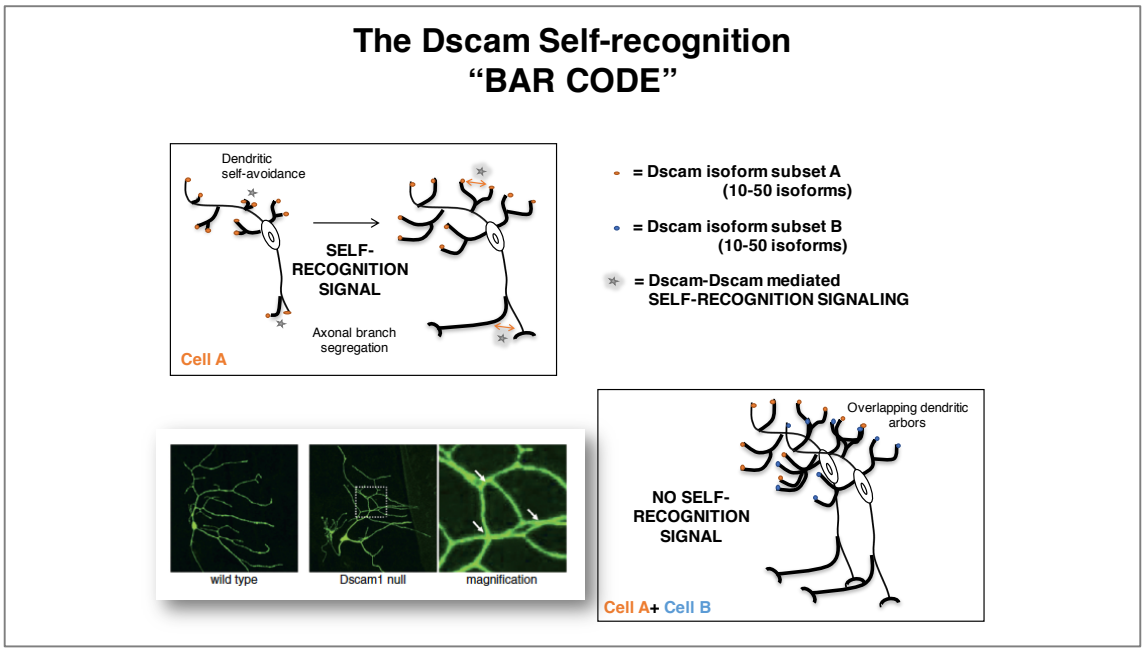

INTRODUCTION- FIGURE 12. **DSCAM1 MEDIATES SELF-AVOIDANCE BETWEEN SISTER NEURITES.**

Every neuron is labeled by a distinct subset of Dscam1 isoforms (red or green dots). If during patterning two neurites come too close to each other, their neurites recognize each other via homophilic Dscam1-Dscam1 interactions leading to neurite repulsion (sketch on the top). Neurite-self-recognition allows for maximal spacing of neuronal arborizations. The confocal image shows the dendritic arborizations of Da-neurons which are uniformly spaced. Lack of Dscam1 leads to a reduced sensory field, characterized by unnecessary neurite self-crosses (Dscam1 null and magnification). At the same time, two different cells not sharing the same Dscam1 set of isoforms (red and blue cell), can have widely overlapping neurite arbors, allowing them to sample overlapping sensory fields (bottom right sketch).

Initial findings suggest that challenge with bacteria ***primes the Dscam isoform set*** in the mosquito (Dong et al., 2006) and the fruit fly (Watson, 2005). While these results were based on quantitative RT-PCRs, a recent approach employing RNAseq could not recapitulate the same findings in flies (Armitage et al., 2014). However, upregulation of total *Dscam*-RNA and -protein levels in response to immune challenges have been reported for a number of different arthropod species (Chiang et al., 2013; Hung et al., 2013; Jin et al., 2013; Khongphinitbunjong et al., 2015; Ng et al., 2014; Riddell et al., 2014; Wang et al., 2013; Watthanasurorot et al., 2011), sometimes with differential temporal expression profiles regarding membrane bound (long term response) and secreted isoforms (short term response) (Chiang et al., 2013). Even more exciting are preliminary observations that *CERTAIN DSCAM1 ISOFORMS MIGHT BE TOXIC TO BACTERIA* (Franziska Thomas and Dietmar Schmucker, personal communication). However, further and in depth analysis of these findings is still needed.

Taken together, it remains undisputable that Dscam1 plays a role in the innate immune defense of flies. These observations are strengthened by the reported Dscam-receptor involvement in the immunity of other invertebrates species, such as the honeybees response

to mite infection (Khongphinitbunjong et al., 2015) or the bumblebees reaction to the parasite *Crithidia* (Riddell et al., 2014) as well as the crayfish's, shrimps and crabs responses to viruses and bacteria (Chiang et al., 2013; Hung et al., 2013; Jin et al., 2013; Ng et al., 2014; Wang et al., 2013; Watthanasurorot et al., 2011). If and how the *Dscam* isoform set adapts based on an immune challenge, remains still controversial but opens exciting new avenues in understanding invertebrate immunity. Overall, it can be concluded that according to the most widely favored working model Dscam1 mediates ***adhesion and/or attractive guidance*** in cells of the immune system. The signaling cascades downstream of the receptor remain unknown, including the question if Dscam1 activation regulates the transcription and expression of immune specific effector molecules.

Other Dscam1 guidance and targeting phenotypes

A last group of phenotypes covers such biological functions of Dscam1, which cannot fully be explained by Dscam1 mediated attraction of repulsion alone. Importantly, these phenotypes are usually characterized by strong dosage dependency: These functions display distinct and severe Dscam1 loss and gain of function phenotypes.

For example in the embryonic nervous system, Dscam1 promotes interactions between Bolwig's nerve growth cones and ***an intermediate target*** (Schmucker et al., 2000). *Dscam1* loss of function (LOF) phenotypes are highly similar to LOF phenotypes observed for *dock* and *Pak* in this cellular environment (Schmucker et al., 2000). In a similar manner, ***targeting*** of a subset of *Drosophila* olfactory neurons (ORNs) (Hummel et al., 2003), ***synaptogenesis*** of photoreceptor neurons (Millard et al., 2010), ***localization and packing*** of cell bodies of PC interneurons (Wojtowicz et al., 2004) and the ***terminal axonal arborizations*** of da-sensory neurons (Kim et al., 2013) depend on the correct dosage of Dscam1. Interestingly, Dscam1 is also required during the ***migration of salivary gland cells.*** Furthermore, *Dscam1* overexpression causes ***bristle phenotypes*** as well as ***rough eyes*** suggesting that *Dscam1* might be expressed and important for the development of other non-neuronal cell types. In the case of salivary glands Dscam1-Netrin interactions are responsible for guidance response, while it is not entirely clear which epitope of the two Dscam1 interfaces elicits which guidance response. Finally, Dscam1 molecular diversity is indispensable for the fidelity and precision during formation of the ***axonal arborizations of mechanosensory neurons*** (Cvetkovska et al., 2013; Chen et al., 2006;

Dascenco and Erfurth et al., 2015; He et al., 2014a), a function that I will be focusing on in the results section of this dissertation.

The molecular mechanisms mediating Dscam1 signaling

While the number of phenotypic studies on Dscam1 functions keep increasing, very little is known regarding signaling effectors and proteins of the Dscam1 signaling complex. Initially, genetic and biochemical studies suggested that during axonal targeting of Bolwig's nerve *Drosophila* Dscam1 activates the ***serine/threonine kinase Pak*** (p21-activated kinase; CG10295) by using ***dock*** (dreadlocks; Nck; CG3727) as an adaptor molecule (Schmucker et al., 2000). However, later analysis in other systems revealed that these results are ***context dependent***: For example, *dock* and *Pak1* are dispensable for dendritic patterning of da-neurons and axonal arborization of ms-neurons. Overexpression of membrane-linked (myristilated) Dock on the other hand, causes *Dscam1*-LOF like phenotypes in the arborizations of ms-neurons (Dan Dascenco, personal communication) and during pathfinding of pdf-neurons (Marta Koch, personal communication).

But how is it possible that Dscam1 has potentially context specific differential signaling functions? To explain this phenomenon it might be helpful to recall the characteristic features of the Dscam1 protein which are depicted in Introduction- Figure 10 and Introduction- Figure 11: First, it is important to note that the Dscam1 receptor harbors ***two distinct binding epitopes*** in its extracellular domain (epitope 1 and epitope 2) (Meijers et al., 2007). Lying on two opposing sides of the S-shaped extracellular domain (like head and tail of a coin), they permit independent interactions with different ligands: Epitope 1 engages in homophilic Dscam1-Dscam1 interactions (Meijers et al., 2007; Sawaya et al., 2008), and epitope 2 is thought to mediate interactions with heterophilic ligands, such as the guidance factor Netrin or pathogens.

Second, it is often overlooked that ***there are four distinct versions of the intracellular domain,*** created by exon skipping of exon 19 and exon 23 (Yu et al., 2009) (Introduction-Figure 10). This creates four different types of cytoplasmic domains, harboring distinct sets of signaling motifs. One can easily imagine, how different signaling molecules would interact with these different intracellular domains, delivering a possible explanation for variability in Dscam1 signaling.

More faces than Janus:

The Dscam1 extracellular domain is capable of interacting with thousands of potential ligands

The extraordinary capacity of the Dscam1 extracellular domain to bind and distinguish thousands of different isoforms from each other is a hallmark of Dscam1 signaling that distinguishes the receptor from most other signaling systems. The extracellular domain of the protein is S-shaped and harbors two distinct binding epitopes ***(epitope 1 and epitope 2)***. They lie on opposite sides of the molecular surface and mediate independently from each other binding to ***different types of ligands*** (Introduction- Figure 13). In the following paragraphs, I will describe the different three characterized types of Dscam1 ligands and their functions in three chapters focusing on: (1) Strong Dscam1-Dscam1 homophilic interactions, (2) Dscam1-Netrin interactions, (3) Dscam1-pathogen interactions.

1. Strong Dscam1-Dscam1 homophilic interactions

The interactions between equal extracellular domains of Dscam1 have been most intensively studied. These interactions are thought to be the ***main mode of signal transduction***. Homophilic Dscam1-Dscam1 interactions have first been reported and extensively studied *in vitro* by Woj Wojtowizc, James Clemens and colleagues in the laboratory of Larry Zipursky (Wojtowicz et al., 2004). They utilized a high throughput Elisa-assay to systematically demonstrate that ***only equal Dscam1 extracellular domains bind to each other.*** Further biochemical (Wojtowicz et al., 2004; 2007; 2008; Wu et al., 2012) and structural characterization of the binding properties (Meijers et al., 2007; Sawaya et al., 2008) revealed that homophilic Dscam1-Dscam1 binding is tremendously specific. Isoforms that differ in only one of the three extracellular variable Ig-domains do no bind to each other or show only very weak interactions. The binding of two homophilic Dscam1 domains requires tight bending of the S-shape at two critical points (between Ig2+3 and between Ig5+6) to allow for the antiparallel matching of the variable domains.

The combination of the initial experiments with bead aggregation and bead-cell as well as pull-down assays demonstrated that ***equal Dscam1 extracellular domains bind tightly to each other*** *in vivo* and *in vitro*. In terms of signaling homophilic Dscam1-Dscam1

interactions correspond to ligand-receptor interactions, characterized by an enormous variability of both ligand and receptor.

Interestingly, it has been observed that there are different binding rates and properties of the Dscam1 mediated aggregation reaction, suggesting that ***distinct isoforms mediate different adhesion strengths and rates.*** The details of the differential binding affinities have not been studied any further. There are reports on ultracentrifugation based experiments to establish a K_D value for homophilic Dscam1-Dscam1 binding. The reported values for different isoforms lie in the range of ***1-14µM*** depending on the isoform tested (Grueber et al., 2003; Wu et al., 2012). While this points to relatively low affinity, it is notable that the values lie in the range typically reported for other cell adhesion molecules (Grueber et al., 2003). Importantly, such low affinities allow for ***transient interactions*** and are therefore predestined for the signal transduction of dynamic processes, such as axon guidance. Many questions regarding the binding characteristics remain still open. For example, it is unknown if binding to epitope 2 would inhibit binding to epitope 1 and vice versa. Furthermore, there are multiple reports of the tendency of Dscam1 to dimerize or multimerize. However, the *in vivo* significance of Dscam1 multimers has never been demonstrated.

While homophilic Dscam1-Dscam1 interactions have been studied extensively, it has never been formally excluded that heterophilic isoforms can also weakly bind to each other. Such interactions could be mediated by epitope1 or 2. The total adhesive capacity between two Dscam extracellular domains is the sum of the weak interactions between all three variable Ig-domains. Therefore, heterophilic interactions between two highly similar isoforms (differing in only 10 amino acids like 7.25.25 and 7.27.26) - if they do exist - might just be below the detection threshold of any assay used this far. In line with this idea, it has been suggested that *Dscam1 signaling can qualitatively and quantitatively be regulated by the number of isoforms present on the cell membrane, the type of isoforms and the binding affinity and avidity of the expressed isoforms* (Wojtowicz et al., 2004). Importantly, it remains unknown how these differences translate into signaling: For example, one could imagine that different signaling cascades are activated based on the isoform/ligand binding.

Dscam1 mediated self-avoidance requires signaling, however the signaling pathway induced by homophilic Dscam1-Dscam1 interactions remains unknown

It is widely accepted that Dscam1-Dscam1 mediated ***homophilic self-recognition*** (mediated by ***adhesive forces***) evokes a ***repulsive growth response***. This process is widely known as ***neurite self-avoidance*** (reviewed in Zipursky and Grueber, 2013). It has been intensively studied during the extensive patterning of somatosensory dendrites in the larval bodywall of *D.melanogaster* (Hughes et al., 2007; Matthews et al., 2007; Soba et al., 2007). However, the effect has also been observed in other cellular compartments, such as axonal arborizations (Neves et al., 2004; Wang et al., 2002; Zhan et al., 2004). Based on these observations, the uniting functional theme of homophilic Dscam1-Dscam1 mediated interactions is a neurite turning response pushing the involved neurites as far apart as possible from each other. This growth principle leads to uniformly spaced arborizations.

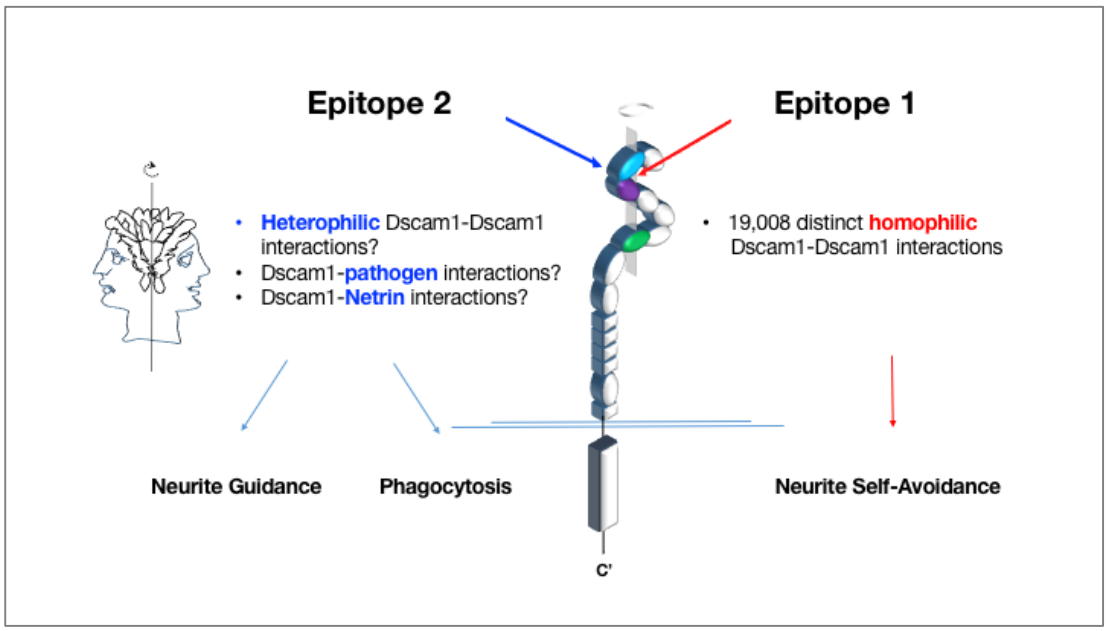

INTRODUCTION- FIGURE 13. **THE EXTRACELLULAR DOMAIN OF DSCAM1 HARBORS AT LEAST TWO BINDING INTERFACES, ALLOWING FOR INTERACTIONS WITH THOUSANDS OF DIFFERENT LIGANDS.**

The two binding interfaces are known as epitope 1 and epitope 2. They lie in one plane on the two opposing sides of the S-shaped extracellular domain. There are thousands of distinct interfaces derived through variability in three Ig-domains (Ig2,3 and 7). Epitope 1 (red) has been studied most intensively, because it has an important role during neuronal self-avoidance. It mediates homophilic-Dscam1-Dscam1 interactions. Epitope2 (blue) is less well studied. It is potentially the interaction site for Dscam1 with heterophilic ligands during axon guidance and with pathogens in the immune system. (Ovals: Ig-domains; cubes: FN domains; box: Dscam1 intracellular domain). Known heterophilic Dscam1 ligands are pathogens in immune cells and the canonical guidance cue Netrin in the nervous system. However, other as of yet unidentified factors might exist.

In terms of signaling many questions remain open: For example, it remains unclear how close two cells have to come to each other to initiate Dscam1-Dscam1 mediated signaling. Does the interaction require direct cell-surface contact? Or is it mediated by Dscam1shedding? In addition, it also remains mysterious how the initially adhesive homophilic Dscam1 interactions are ultimately translated into neurite retraction or turning. It has been proposed that intracellular signaling events transform the initially adhesive interactions at the cell surface and trigger repulsion (Wang et al., 2002; Wojtowicz et al., 2004): One could imagine for example a contact dependent initial neurite-neurite contact, followed by a cleavage step: The two neurites could snap back, upon release by a protease mediated Dscam1 cleavage-step. While Dscam1 cleavage and shedding have been reported in cells of the immune system (Watson, 2005), it remains unclear if the same is true for the nervous system and specifically if it happens at the growth cone.

The notion that *Dscam1 is more than just a co-receptor* is supported by the fact that a Dscam-construct lacking the intracellular domain (but containing the 17.1 transmembrane domain) is not able to mediate repulsion in da neurons (Hughes et al., 2007). The importance of Dscam1-signaling is further emphasized by experiments conducted by Matthews et al., who used a *Dscam1* allele with an in-frame deletion of exon 18 (Dscam^{47}) and showed that the intracellular domain is necessary for repulsion between sister dendrites (Matthews et al., 2007).

2. Dscam-Netrin interactions elicit positive guidance responses

The repulsive (negative) guidance responses implicated in neurite self-recognition are not the only cellular processes affected by Dscam1 signaling. Both vertebrate and invertebrate Dscams are capable of binding to the canonical guidance cue ***Netrin***, an interaction that induces ***attraction*** of the involved neurites towards the Netrin source (Andrews et al., 2008; Liu et al., 2009; Ly et al., 2008). The dissociation constant of the Netrin/Dscam1 complex lies approximately at ***30nM***, which is comparable to the values reported for Netrin/DCC. The contact point of the Netrin-Dscam1 interaction has not been mapped yet, but is assumed to be positioned in epitope 2 (Introduction- Figure 13). Similar to homophilic Dscam1-Dscam1 interactions, the nature of the molecular pathways mediating the attractive guidance response remains elusive.

3. Dscam1 binds to bacteria and mediates phagocytosis in hemocytes

A third class of Dscam ligands is restricted to tissues mediating the invertebrate immune response: *Dscam* is expressed in ***cells of the innate immune system***, namely ***hemocytes*** and cells of ***the fat body*** (Chou et al., 2009; 2011; Dong et al., 2006; Jin et al., 2013; Watson, 2005; Watthanasurorot et al., 2011) (Introduction- Figure 14). Hemocytes are considered to be the invertebrate equivalent of ***blood cells,*** with functions comparable to macrophages in vertebrates (Meister, 2004). They float in the hemolymph and patrol the body by migrating out into the tissue. If hemocytes encounter any foreign material during their journey (e.g. a pathogen), they attach to and phagocytize it. Dscam is important for this pathogen clearance (Dong et al., 2006; Watson, 2005). Hence, *Drosophila* and *Anopheles* cells lacking Dscam protein are incapable of efficient ***phagocytosis*** (Dong et al., 2006; Watson, 2005).

The exact molecular mechanisms of Dscam-mediated phagocytosis remain in the dark. Dscam could simply act as an immune (co)-receptor. However, the more favored model is, that shed Dscam extracellular domain acts as a ***pathogen recognizing opsonin*** (Dong et al., 2006; Watson, 2005). Other hemocytes expressing the same Dscam isoform would then be attracted and initiate destruction (Chou et al., 2011; Dong et al., 2006; Ng et al., 2015) (Introduction- Figure 14 and Introduction- Figure 15).

In line with this, invertebrate Dscam is found in hemocytes and fat body cells as well as in the hemolymph (Chou et al., 2009; 2011; Dong et al., 2006; Hung et al., 2013; Jin et al., 2013; Wang et al., 2013; Watson, 2005; Watthanasurorot et al., 2011). Furthermore, proteolytic cleavage and shedding of the extracellular domain has been reported (Watson, 2005) and a FACS based binding assay revealed that the 10 N-terminal domains (Ig 1-9 + FN 1) are sufficient for binding to live *E. coli* (Watson, 2005). Shrimps and crabs even possess some *Dscam*-genes entirely lacking the transmembrane- and cytoplasmic-parts (Chou et al., 2009; 2011; Hung et al., 2013), suggesting that in some species the immune function predominates. Finally, mosquito and crab Dscams accumulate at the spot of physical interaction of hemocytes challenged with bacteria (Dong et al., 2006; Jin et al., 2013). Furthermore, Dscam could be isolated from the surface of bacteria incubated with protein extracts from *Anopheles* immune cells (Dong et al., 2006).

Interestingly, it seems that distinct Dscam isoforms have different affinities for pathogens (Dong et al., 2006; Hung et al., 2013; Watson, 2005; Watthanasurorot et al., 2011). In flies for example, isoforms 7.27.25 and 7.27.13 readily bind to *E. coli,* while isoform *1.30.30.* does not (Watson, 2005).

Taken together, the Dscam1-extracellular domain is capable of binding to pathogens. This interaction is important for pathogen clearance and potentially leads to initiation of an immune priming response. In terms of signaling this adds, at least in the immune system, ***an unknown number of pathogens*** to the thousands of canonical Dscam1 signaling ligands (Boehm, 2007). If all of these pathogen Dscam1-interactions elicit a signaling response remains to be established in the future. There are however reports of Dscam isoforms lacking the transmembrane and signaling competent intracellular domain (e.g. shrimp Dscam) (Chiang et al., 2013; Chou et al., 2009; Hung et al., 2013).

Outlook: Are there any other Dscam1 ligands?

To conclude this chapter, I would like to point out, that the list of potential Dscam1 ligands ***might not be complete***. There have been rumors about other molecular cues being capable of binding to Dscam1 ever since I started my PhD. More concretely, Andrews et al. suggest that there might be other as of yet unknown ligands. They base their hypothesis on the *Dscam1, fra* and *Dscam1, Dscam3, fra* double- and triple-mutant effects on midline crossing (Andrews et al., 2008). Typical for an Ig-CAM however, Dscam1 protein is an extremely "sticky" protein to work with. Therefore, it needs to be carefully evaluated if any of these potential interactions are meaningful *in vivo.*

In summary we can conclude that the Dscam1 ***extracellular domain acts as a versatile signaling module:*** It acts as receptor for thousands of distinct ligands, some of which bind to the exquisitely selective homophilic epitope 1 and others that probably bind to the counter side of the extracellular domain in a region known as epitope 2 (Introduction-Figure 15).

Dscam1 signaling: Effectors

Very little and even controversial data is available regarding Dscam1 signaling. I have tried to sort the different signaling themes and I will present them in the following five subchapters presenting (1) the potential effects of distinct Dscam1 cytoplasmic domains, (2) Dscam1 signaling to the actin cytoskeleton via dock and Pak, (3) Dscam1 signaling and tyrosine phosphorylation, (4) Dscam1 interaction with sorting nexins, (5) Dscam1 interaction with vap-33 protein and ubiquitin and (6) Dcam1 signaling and tubulin.

Four different versions of the Dscam1 intracellular domain allow for diverse signaling

The diverse number of Dscam1 functions and ligands suggest that there also must be diversity in cytoplasmic Dscam1 signaling capacity. Therefore, it is not surprising that there exist ***four different versions*** of the Dscam1 intracellular domain (Yu et al., 2009) (Introduction- Figure 10). They arise by optional skipping of the cytoplasmic exons 19 and 23. While the skipping event omitting exon 19 simply shrinks the intracellular domain (and adds 4 extra amino acids), it is notable that skipping of exon 23 leads to a frameshift, and therefore encodes for an alternative C-terminal tail of the protein. This might have important consequences for Dscam1 signaling, since the C-terminal potential PDZ-binding domain is not present in isoforms lacking exon 23.

Initial studies suggest, that there might be important functional differences between the different Dscam1-cytoplasmic domains: ***Dscam1 isoforms, carrying distinct intracellular domains, lead to different Dscam1-localization patterns*** (Yu et al., 2009). For example, Dscam1 lacking exon 19 is preferentially located in neurites and the short isoform lacking exon 19 and exon 23 is critically involved in axon bifurcation during mushroom body development (Yu et al., 2009). Indeed, the longest version of the intracellular domain (including exon 19 and 23) is only expressed during embryogenesis and the shortest version (lacking exon 19 and 23) is the most abundant cytoplasmic postembryonic isoform (Yu et al., 2009). Regardless of these facts, almost all *Dscam1* studies involving cDNA have been using the longest version of the intracellular domain (including exon 19 and 23) (Yu et al., 2009). Therefore, we still poorly understand the exact roles and differences regarding signaling mediated by the different Dscam1 cytoplasmic domains.

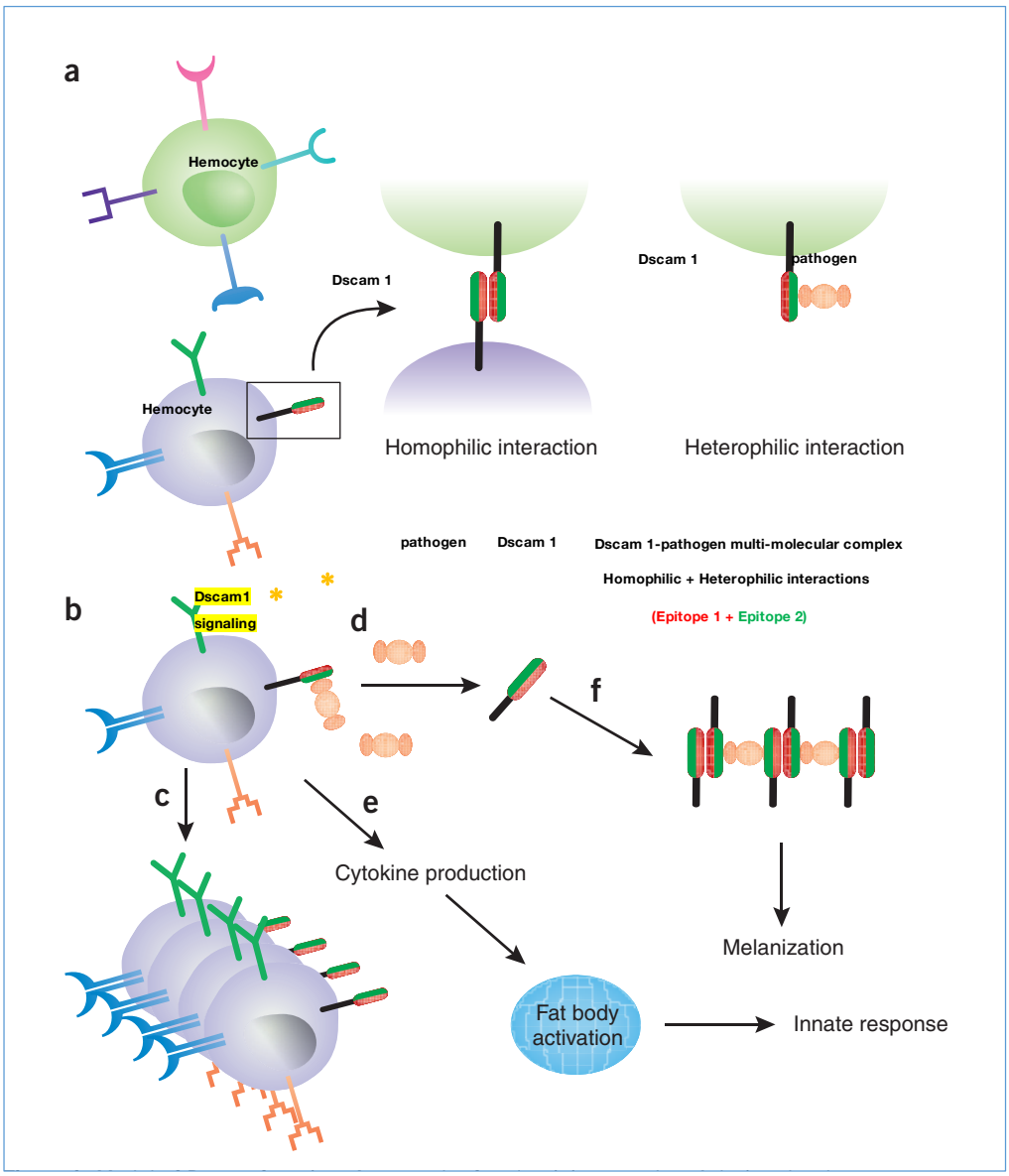

INTRODUCTION- FIGURE 14. **THE EXTRACELLULAR DOMAIN OF DSCAM1 ON THE SURFACE OF IMMUNE COMPETENT CELLS CONTAINS TWO DISTINCT BINDING SITES.**

Hemocytes (purple and green) express different cell surface receptors (e.g. pattern recognition receptors PRRs) (pink, blue, purple and green symbols on cell surface). Dscam1 (boxed, black, red and green) harbors special properties as it encodes for highly variable extracellular domains with two independent binding surfaces: Epitope 1 (red) is involved in homophilic Dscam1-Dscam1 interactions (left side of panel a) between two cell surfaces, while epitope 2 (green) is involved in heterophilic Dscam1-pathogen interactions (right side of panel a). Importantly, ligand-receptor interactions occupying one epitope do not hamper the accessibility of the other epitope. Activation of Dscam1 signaling (b) leads to upregulation of the innate immune response: Either by inducing the expansion of cells with the same Dscam1 isoform set (c,) or by opsonizing the pathogen, coupling heterophilic and homophilic interactions in a large multi-molecule complex and inducing a melanization response (f), or alternatively by inducing the secretion of immune competent molecules, such as cytokines (e). (Image adapted from Boehm, 2007.)

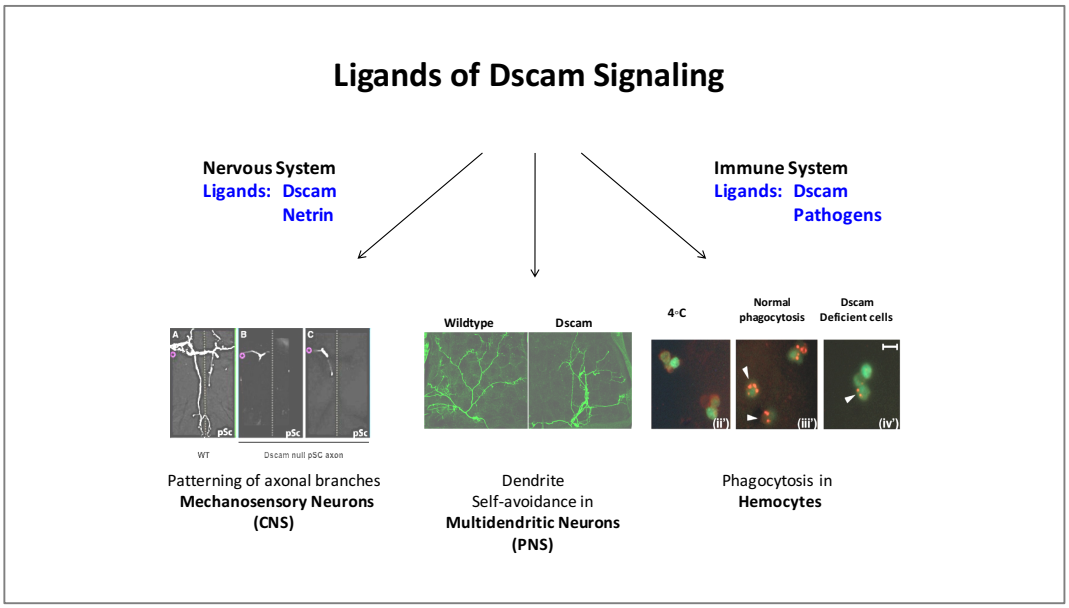

INTRODUCTION- FIGURE 15.**THE DSCAM1 RECEPTOR CAN BE ACTIVATED BY THOUSANDS OF DIFFERENT LIGANDS.**

In the nervous system, there are potentially 19,008 distinct homophilic Dscam1 ligands. In addition, Dscam1 can be activated by Netrin. This is important for axonal and dendritic patterning during development. Furthermore, Dscam1 is also expressed in cells of the immune system, namely hemocytes and the fat body. Here it is thought, that Dscam1 mediates binding via epitope 2 to pathogens. This interaction is important for phagocytosis mediated clearance of foreign material.

Importantly, the diversification of the intracellular domain is a conserved trait, emphasizing its functional relevance: Indeed, differential Dscam cytoplasmic domains have also been observed in *D. magna*, *L. vannamei, P. monodon, P. leniusculus* and *E. sinensis* (Brites et al., 2008; Chou et al., 2009; 2011; Wang et al., 2013; Watthanasurorot et al., 2011), with some cytoplasmic isoforms (including an endocytosis motif) being preferentially expressed following an immune challenge (Hung et al., 2013). In addition, there are distinct isoforms of the 3'-UTR created by different polyadenylation signals (Chou et al., 2011) similar to vertebrate DSCAM 3'-UTR isoforms. Further work in *Drosophila melanogaster* is needed to understand the functional roles of the distinct Dscam1 cytoplasmic domains and of the 3'-UTR isoforms in fruit flies.

1. *Dscam Signaling mediated by dock and Pak*

In *Drosophila,* Dscam1 was originally identified as one out of five tyrosine phosphorylated proteins co-purified with the epitope tagged ***SH2-domain*** of the adapter protein ***dock*** (CG3727; dreadlocks) (Schmucker et al., 2000; Worby et al., 2001) (see also Chapter 3-Figure 4). *Dock* is the *Drosophila* orthologue of the human proto-oncogenes *NCK1* and *NCK2* and consists of three tandem SH3 domains and a single SH2 domains. There is one *dock* paralogue known as downstream of receptor kinase (***drk***; CG6033). Dock interacts with Dscam1 via a ***SH2- and SH3-binding sites*** in the Dscam1 intracellular domain (Schmucker et al., 2000) (Introduction- Figure 16).

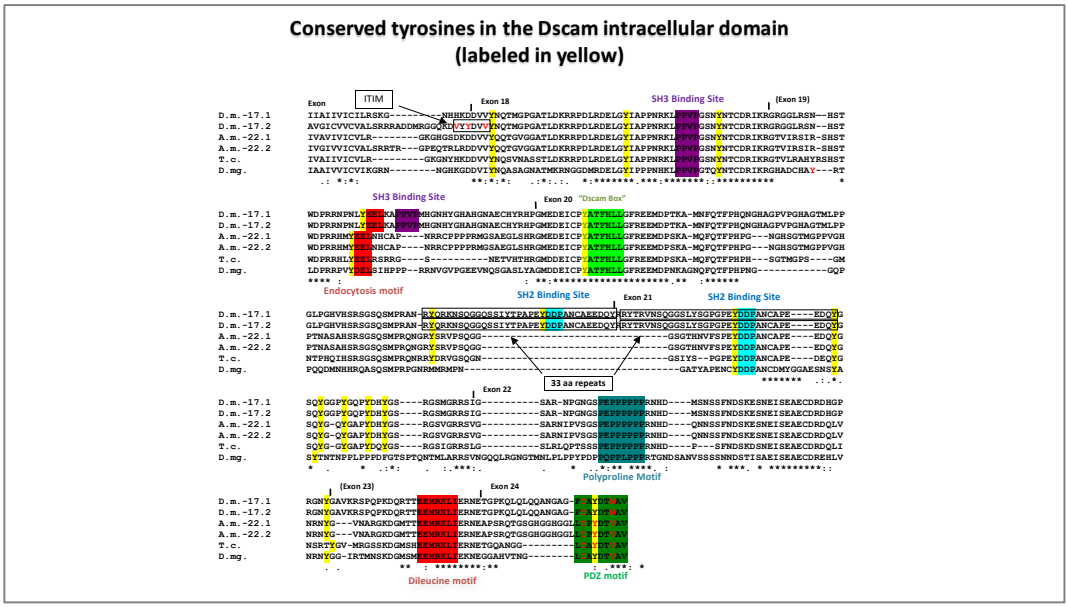

INTRODUCTION- FIGURE 16. **THE INTRACELLULAR DOMAIN OF *DROSOPHILA DSCAMS* CONTAINS MULTIPLE SIGNALING MOTIFS.**

Alignment of the intracellular domains of Dscam of Drosophila melanogaster (D.m.) Apis mellifera (A.P.) (honey bee), Tribolium castaneum (T.m.) (Flour Beatle), and Daphnia magna (D.mg.) (water flea). The exon containing the transmembrane domain has been included (17.1 and 17.2 for D.m. and 22.1 and 22.2 for A.m.). Signaling motifs are labeled in color. Conserved tyrosines are labeled in yellow. Signaling motifs were derived from current literature and predicted with the Elm prediction tool. Note, that some conserved tyrosines are contained in potential signaling motifs, and that exon 21 contains a multitude of tyrosines creating a signature which could be described as a multi-tyrosine motif. The green Dscam-box motif is proposed to be the interactions site with Abl-kinase and is found in all Drosophila Dscam1 paralogues. The SH-3 binding sites (purple) and the poly-proline motif (green) are involved in the interaction with the sorting nexin SH3PX1.

The Nck/dock adaptor protein family links signaling from cell surface receptors to the ***actin cytoskeleton*** (Kaipa et al., 2013; Li et al., 2001). ***Tyrosine phosphorylation*** plays an important role, since SH2-binding sites consist typically of an amino-acid sequence

surrounding a phosphorylated tyrosine. In line with the notion that Dock translates signals from the cell surface to the cytoplasm, it is signaling downstream of the following cell surface proteins: Dscam1 (Schmucker et al., 2000; Worby et al., 2001; Yang et al., 2012), EgfR, Pvr (Bianco et al., 2007), InR (Wu et al., 2011), hibris, kirre, rst and sns (Kaipa et al., 2013; Tutor et al., 2014) as well as robo1 (Fan et al., 2003).

Downstream of dock the signaling pathway can ***vary in a context dependent manner***: Signaling can be mediated ***via Rho-GTPases to the cytoskeleton*** or translated ***into MAPK kinase signaling*** by recruiting different types of kinases to the signaling complex: Interaction with the ***Ste-20 kinases Pak*** (CG10295) (Schmucker et al., 2000) and ***misshapen*** (msn, CG16973) (Ruan et al., 1999; Su et al., 2000) activate the MAP kinase cascade. However, Pak can also directly recruit Rho-GTPases, such as Rac or cdc42, and thereby affect the polymerization state of the actin cytoskeleton (Manser et al., 1994). In addition, dock has been found to bind and co-localize with the tyrosine kinase Ack (CG14992), an interaction that leads to direct recruitment of the Rho-GTPase cdc42 (Abdallah et al., 2013). This is critical for localizing dock to ***clathrin-positive endocytotic vesicles***. Genetic interaction has furthermore been reported with the GTPase RAS85D (Schnorr et al., 2001).

Dock is also found at focal adhesion sites (Kaipa et al., 2013) and regulates ***actin polymerization*** by interacting with ARP2/3 activators, such as the Wiskott-Aldrich syndrome protein (WASp, CG1520), SCAR (DWave, CG4636), Vrp1 (Verprolin 1, CG13503) (Kaipa et al., 2013) and the sorting nexin ***SH3PX1*** (CG6757), which in turn can directly bind to Dscam1 (Worby et al., 2001).

Drosophila Dscam1 activates the serine/threonine kinase ***Pak*** (CG10295) via dock-adaptor during axonal targeting of Bolwig's nerve (Schmucker et al., 2000). This mediates the signal most likely to Rho-GTPases, in a mechanisms similar to signaling events downstream of the robo1 receptor (Fan et al., 2003) or during photoreceptor guidance (Hing et al., 1999). Therefore, it has been proposed that Dscam1 recognizes guidance signals and translates them into changes of the actin-based cytoskeleton through interaction with Dock and Pak. However, this mode of signal transduction appears to be ***context specific,*** as Dock and Pak are dispensable for Dscam1 mediated dendritic repulsion and determination of the presynaptic arborization-size in Drosophila da-neurons (Hughes et al., 2007; Kim et al., 2013). Furthermore, loss of dock-function affects axonal patterning of ms-neurons in the VNC only mildly (Derya Ayaz and Dan Dascenco, personal communication), while

targeting it to the membrane leads to unexpected phenotypes resembling loss of Dscam1 function (clumping of neurites) (Dan Dascenco, personal communication). A similar trend is observed for the axon pathfinding of pdf-neurons (Marta Koch, personal communication). The molecular basis of the described cell type specific signaling differences are currently unknown.

2. Dscam1 signaling and tyrosine phosphorylation

Overall ***tyrosine-phosphorylation*** plays an important role in the regulation of Dscam1 signaling, as both Dscam1 and dock are ***heavily tyrosine phosphorylated*** (Schmucker et al., 2000) (see also Chapter 3- Figure 4). The intracellular domain of Dscam1 contains ***multiple tyrosines***, some of which are centers of signaling signature motifs (SH2-binding sites, PDZ domain, endocytosis motif, ITIM) (Introduction- Figure 16). Notably, there is a ***multi-tyrosine motif*** in exon 21 which jumps immediately to the eye but has no assigned function as of today (Introduction- Figure 16).

The ***kinases Src42A*** (CG44128) and ***Src64B*** (CG7524) are primarily responsible for the tyrosine phosphorylation of Dscam1 ***in hemocytes*** (Muda et al., 2002) (Chapter 3- Figure 4). These kinases belong to the SRC family of tyrosine kinases, represented by FGR, FYN, HCK, BLK YES1, LCK, SRC and LYN in vertebrates. The third *Drosophila* paralogue known as ***Abl tyrosine kinase*** (CG4032) has no effect on Dscam1 tyrosine phosphorylation in hemocytes (Muda et al., 2002), but ***interacts genetically*** with Dscam1 signaling during axon guidance of Bp102 positive axons in the embryonic ventral nerve cord (VNC) (Andrews et al., 2008) and during presynaptic arbor formation of da-neurons (Sterne et al., 2015). Furthermore, Abl and Dscam1 ***interact physically*** (Sterne et al., 2015) and presynaptic defects caused by elevated Dscam1 signaling can be rescued pharmacologically by Abl-tyrosine-kinase inhibitors (Sterne et al., 2015). It has been proposed that the interaction is mediated through the ***Dscam-box*** motif (*PYAT)* (Introduction- Figure 16), found in all four *Drosophila Dscam1* paralogues (Andrews et al., 2008).

Dock interacts with the tyrosine-kinase ***Ack*** (Worby et al., 2001; 2002; Abdallah et al., 2013;) and is a substrate of the protein tyrosine phosphatase ***dPTP61F*** (Clemens et al., 1996; Guruharsha et al., 2014; Muda et al., 2002). In addition, I find it notable, that during my own experiments I could detect the physical interaction between dock and Dscam1 ***only***

in the presence of tyrosine-phosphatase inhibitors, suggesting that tyrosine phosphorylation is a critical component of the Dscam1 signaling complex.

Taken together, reversible tyrosine phosphorylation appears to be an important and conserved mode of Dscam1 signal transduction. However, the cellular context and sequence of these phosphorylation events remains largely unknown.

3. Dscam1 interaction with the sorting nexin SH3PX1

The sorting nexin ***SH3PX1*** (CG6757) was one out of five ***tyrosine-phosphorylated*** proteins purified with the SH2 domain of Dock (Worby et al., 2001). The tyrosine phosphorylation of SH3PX1 is critical for the interaction with dock (Worby et al., 2001). It binds to Dscam1 in immunoprecipitations of S2 cell extracts and in yeast two-hybrid assays (Worby et al., 2001). The interaction between SH3PX1 and Dscam1 occurs between the SH3-domain in SH3PX1 and the ***poly-proline motif*** of Dscam1 (Introduction- Figure 16). SH3PX1 contains, like its vertebrate orthologues (***SNX9, SNX33, SNX18***), one SH3 domain coupled to two types of phospholipid binding domains: A Bar dimerization-domain and a Phox homology (PX) phospholipid binding-domain. SH3PX1 might link the Dscam1 signaling complex directly to regulators of the cytoskeleton as it interacts with the ***ARP2/3 activator Wasp*** (Worby et al., 2001). However, it might also link the receptor to ***endocytosis*** via the ***AP2 complex*** (Worby et al., 2001).

4. Dscam interaction with Vap-33 protein and ubiquitin

A recent study conducted in the Clemens lab employed TAP-purification of the Dscam1-receptor complex with mass-spectrometry based fingerprinting in order to identify Dscam1 interacting proteins (Yang et al., 2012). They report physical interaction with two novel candidates ***vap-33*** (CG5014) and ***Ubiquitin-63E*** (CG11624).

Vap-33, a vesicle-membrane-associated protein, binds to microtubules (Pennetta et al., 2002). The cytoplasmic *m*ajor-*s*perm *p*rotein domain (MSP) can be cleaved and secreted into the extracellular space, where it acts on axon guidance receptors, such as EphR, Robo or Lar-like receptor tyrosine phosphatases (Han et al., 2012; Tsuda et al., 2008). There is one *Drosophila* paralogue annotated under the name *farinelli* (fan).

Little is known regarding the signaling of *Drosophila* vap-33. A mass-spectrometry based interactions screen places it between several signaling proteins (CG13220, CG1513, CG2064, CG4792 (Dicer), CG5742, CG8765, CG9205, CG9732, Cct2, MRG15, Reep1) (Guruharsha et al., 2014) of mostly uncharacterized function but containing signaling motifs, such as Ankyrin domains, Pleckstrin-homology (PH) domains, Phosphotyrosine-binding (PTB) domain, ubiquitin domain and MRG domains. This suggests that vap-33 might be a signaling hub linking protein and RNA trafficking.

The vertebrate orthologues are known as ***VAPA and VAPB***. These single pass type IV membrane proteins are also found in the plasma membrane and in intracellular vesicles together with SNARE proteins and the cytoskeleton. They are involved in multiple cellular functions, such as lipid and mitochondrial trafficking and formation of synaptic boutons at the neuromuscular junction (Loewen et al., 2003; Pennetta et al., 2002). Mutations in the VAPB gene are linked to a dominantly inherited form ALS (Mitne-Neto et al., 2004). ***Vap-33 binds selectively to Dscam1- proteins with the transmembrane domain encoded by exon 17.2*** (Yang et al., 2012). It is furthermore required for the localization of the axonal Dscam1 isoform but does not influence Dscam1 expression in dendrites (Yang et al., 2012). The exact molecular details of this regulation remain unclear.

5. Dscam1 interaction with TBCD

The core function of axon guidance receptors is to transduce extracellular signals to the cytoskeleton. For Dscam1 signaling the research focus has long been on defining such interaction with the cytoskeleton. This was based on the initial observation that Dscam1 genetically interacts with the Ste20 kinase Pak, suggesting a direct link to the actin cytoskeleton via small GTPases (Schmucker et al., 2000). A recent study by the Chihara lab in Tokyo demonstrated that Dscam1 interacts with ***tubulin folding cofactor D*** (TBCD, CG7261) in S2 cells and in yeast-two hybrid experiments (Okumura et al., 2015). This interaction is necessary for the formation of the dendritic projections of olfactory neuros and for axonal branch segregation of mushroom body neurons (Okumura et al., 2015). Immunohistochemistry suggests that *overexpression of Dscam1 leads to depolymerization of tubulin* (Okumura et al., 2015). Vertebrate DSCAM on the other hand, is found in association with polymerized tubulin (Huang et al., 2015). The interaction with tubulin is

especially interesting in relation with Dscam1 as an important factor for the maturation of neurites (e.g. branch stabilization in ms-neurons).

Regulation of Dscam signaling

Despite the demonstrated importance of Dscam1-signaling, very little is known as to how it is modulated. While the phenotypes of null mutants are clearly characterized, the interpretation of Dscam1 gain of function phenotypes remains challenging. The reason for this difficulty lies in the fact that we need to distinguish between ***two gain of function scenarios***: (1) Gain of function as consequence ***of raised protein levels*** (2) Gain of function based on ***alterations in the number of Dscam1 isoforms*** expressed in a given cell.

Some Dscam1 functions are ***insensitive*** to both changes in isoform diversity and protein levels (for example, dendrites of ms-neurons in the larval body wall) (Hughes et al., 2007). Such Dscam1 null-phenotypes can fully be rescued by the overexpression of any single Dscam1 isoform.

However, other cellular compartments are ***highly sensitive to Dscam1 dosage***: The mere expression of a single isoform is not sufficient to fully rescue the null phenotype. Such Dscam1 dosage-sensitive functions are also characterized by dosage dependent hypomorph phenotypes distinct from null mutants. The axonal pattern formation of ms-neurons in the VNC for example, is highly sensitive to Dscam1 dosage: Manipulation of *Dscam1* isoform diversity leads to prominent lack-of-branching phenotypes, while raised protein levels affect the terminal arborizations (Chen et al., 2006; Dascenco and Erfurth et al., 2015; He et al., 2014a) (see also the results chapter of this dissertation and the dissertation of Dan Dascenco, KU Leuven 2015).

In summary, it is important to note that ***not only Dscam1 protein levels but also the number of expressed isoforms per cell*** and even within a subcellular compartment have important and ***distinct instructive functions***. This raises the question, how these subcellular differences are achieved and how the distinct signals are integrated. In the following paragraphs I am summarizing the facts known regarding regulation of Dscam1 expression levels in two subchapters describing (1) Dscam1 regulation by wallenda/DLK kinase and (2) Dscam1 regulation by FMR1 protein.

1. Regulation of Dscam1 protein expression by highwire/wallenda

The terminal axonal arborizations of larval multidendritic neurons (da-neurons) in the VNC are a prominent example of a developmental cellular compartment that is extremely sensitive to different types of Dscam1 dosage. While axonal targeting towards the terminal arborization zones critically depends on *Dscam1-isoform-diversity*, it appears that the final size of the arborization critically depends on Dscam1 *protein levels* (Kim et al., 2013). Loss of *Dscam1* leads to short clumped arbors, while overexpression of Dscam1 induces overgrowth and consequently elongation of arborizations.

Dscam1 ***protein levels*** in the axons of da-neurons are adjusted by the PHR-family E3-ubiquitin ligase ***highwire*** (hiw; CG32592). Highwire regulates the protein levels of the effector MAP-kinase ***wallenda/DLK*** (wnd; CG8789) ***at the synapse***. There are 7 *Drosophila* paralogues of wallenda (slpr, ksr, Tak1, Ilk, Takl1, phl, Takl2) and two vertebrate orthologues (MAP3K12 and MAP3K13). DLK has not only been implicated in axon outgrowth and synaptogenesis but also in synapse maintenance and axon regeneration after injury (Watkins et al., 2013; Yan et al., 2009).

Wnd interacts with the ***3'-UTR*** of Dscam1, thereby ***stabilizing*** the Dscam1 transcript (Kim et al., 2013) (Introduction- Figure 17). However, the exact mechanism of this regulation remains unclear as there are two potential downstream effectors: One pathway is mediated by ***MAPK-Ak2*** (MAP kinase activated protein-kinase-2, CG3086) while the other option might be signaling through the cytoplasmic polyadenylation element binding protein ***CPEB1*** (*Drosophila* orthologues: ***orb***/CG10868 and ***orb2***/CG43782) (Watkins et al., 2013; Yan et al., 2009). Interestingly, the 3'-UTR of dendritic vertebrate DSCAM associates with CPEB (Alves-Sampaio et al., 2010), rendering it the most likely candidate mode of signaling.

2. Regulation of Dscam1 protein expression by FMR1-Protein

Another protein known to regulate the abundance of transcripts is the fragile X mental retardation protein ***FMRP***. The only fly orthologue of this polyribosome-associated neuronal RNA binding protein is known as ***Fmr1*** (CG6203). This regulatory protein binds to the coding region of mRNAs, thereby inhibiting their translation, which affects transcript stability and processing.

Dscam1-mRNA immunoprecipitates together with Fmr1-protein in brain-lysates of third instar *Drosophila* larvae (Cvetkovska et al., 2013; Kim et al., 2013). This interaction inhibits translation of *Dscam1* transcripts (Cvetkovska et al., 2013; Kim et al., 2013). Functionally, the down-regulation of Dscam1-translation by FMR1 is critical for the ***Dscam1 axonal growth and targeting***. If it is impaired, the terminal axonal arborizations of da-neurons display a typical Dscam1 GOF phenotype, characterized by enlarged presynaptic termini (Kim et al., 2013). A similar phenotype has been reported for the ***axonal arborizations of ms-neurons*** in the VNC, where increased Dscam1 protein levels lead to ectopic formation, misrouting and guidance of higher order branches at potential pre-synaptic arborization sites (Cvetkovska et al., 2013). The importance of this wiring phenotype is underscored by the fact that it translates into behavior, characterized by an altered grooming reflex (Cvetkovska et al., 2013).

Taken together, it can be concluded that Dscam1 protein-expression in some cellular compartments is tightly regulated by two parallel pathways: The DLK-pathway, interacting with the 3'-UTR of the transcript, and the FMRP pathway regulating the expression of the protein by interacting with the coding region of Dscam1 mRNA (Introduction- Figure 17). The regulation by two independent regulatory pathways suggests, that ***the modulation of Dscam1 might be of extreme importance*** for neuronal wiring, and that evolution has equipped the fruit fly with a backup-system to ensure, that nothing goes wrong during the process.

Outlook: What is the functional *Dscam1* equivalent in vertebrates?

One question puzzling the experts for a long time is the identity of the neuronal self-recognition code in vertebrates. There are two *Dscam* family orthologues in vertebrates, known as ***DSCAM*** and ***DSCAML1***. The overall domain structure and total size of vertebrate Dscam proteins are very similar to invertebrate Dscams, however the genes are ***not excessively spliced***. Indeed, there exist only two isoforms of each *Dscam1* vertebrate orthologue (plus at least five distinctly polyadenylated 3'UTRs (Alves-Sampaio et al., 2010)). The amino-acid sequences of the intracellular domains do not align to invertebrate Dscam1 and exhibit no similarity at first sight. Despite the different intracellular domains, there are some remarkable overlaps between vertebrate and invertebrate Dscam signaling and function, which I will describe in the next paragraphs. Vertebrate and invertebrate share

similar function (1), (2) expression patterns, (3) extracellular domains and ligands (4) tyrosine phosphorylation, (5) molecular regulators and even (6) signaling motifs.

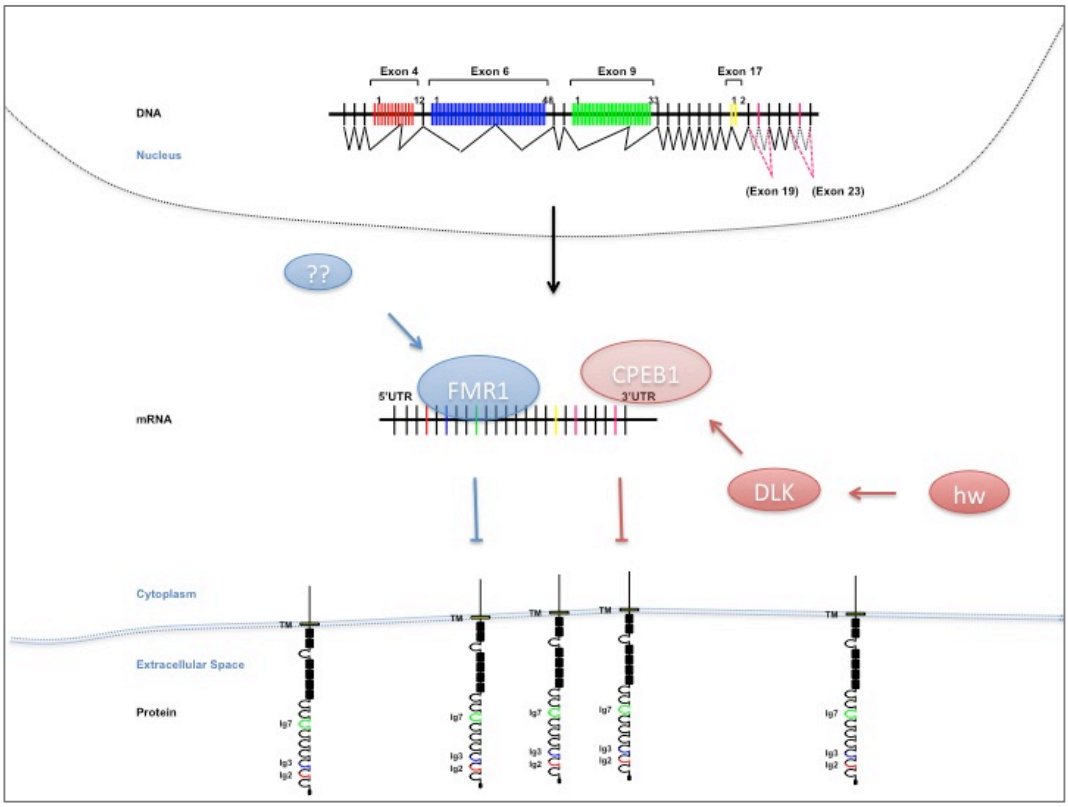

INTRODUCTION- FIGURE 17. **TWO INDEPENDENT REGULATORY PATHWAYS MODULATE DSCAM1 SIGNALING STRENGTH.**

Spliced Dscam1 mRNA is transported away from the nuclear compartment (top) towards the cell surface (e.g. neurite tip) (bottom). The local translation of Dscam1 mRNA is regulated via with Fmr1 protein and the DLK/wallenda regulatory complex. The DLK pathway targets the 3'-UTR, while FMRP has been found to bind to the coding region of the transcript. This regulation is decisive for the amount or isoform subset presented at the surface and hence for the strength of the Dscam1 signaling capacity. The exact mechanism of the highwire-wallenda/DLK pathway is not resolved yet. However, since vertebrate DSCAM is known to be associated with CPEB1 protein, it is very likely that the same regulatory cascade is also responsible for mediating translational control at the 3'UTR.

1. DSCAM, DSCAML1 and Dscam1 mediate similar functions

First and foremost, vertebrate DSCAM and DSCAML1 are in analogy to their invertebrate counterparts ***important for dendritic self-recognition, spacing and arborization*** (Blank et al., 2011; Cui et al., 2013; Fuerst et al., 2008; 2009; 2012; Huang et al., 2015; Yamagata and Sanes, 2008; Alves-Sampaio et al., 2010). The exact molecular mechanism of DSCAM mediated repulsion remains still in the dark. One hypothesis is that the large vertebrate DSCAM receptors mediate repulsion only ***indirectly*** by ***interfering with adhesion*** elicited by other cell surface molecules (reviewed in Montesinos, 2014). In line with this, simple

overexpression of *DSCAM* cDNA is neither sufficient to rescue the loss of function (Li et al., 2015) nor capable of inducing ectopic neurite repulsion. This could however also suggest that the exact time point of expression is critical (and not accurately mimicked by the overexpression), or that other potentially secreted isoforms might play an as of yet unidentified role. In line with this speculations, it has been reported that DSCAM and DSCAML1 have distinct functions during neurite initiation and maintenance (Huang et al., 2015). Furthermore, there exists a shorter potentially secreted isoform of *DSCAM*, lacking the transmembrane- and cytoplasmic domain (*Uniprot* identifier *long isoform* : O60469; *short isoform:* O060469-2) (Yamakawa et al., 1998), and a splice variant of *DCAML1*, which differs in one Ig-domain.

2. DSCAM and DSCAML1 are expressed in the nervous system

Vertebrate *DSCAM* and *DSCAML1* are expressed in the nervous system of *Aplysia* (Li et al., 2009), zebrafish (Yimlamai et al., 2005), mouse (Agarwala et al., 2001a; Agarwala et al., 2001b; Barlow et al., 2001; de Andrade et al., 2014; Huang et al., 2015; Liu et al., 2009), chicken (Yamagata and Sanes, 2008) and frog (Morales Diaz, 2014). Besides dendritic patterning, they are also involved in synapse formation (Li et al., 2009), terminal arborization (Alves-Sampaio et al., 2010), cell migration (Huang et al., 2015; Morales Diaz, 2014; Yimlamai et al., 2005), cell spacing (Fuerst et al., 2012; Blank et al., 2011), axon pathfinding (Ly et al., 2008; Liu et al., 2009), axon growth (Huang et al., 2015; Liu et al., 2009; Purohit et al., 2012) and -targeting (Yamagata and Sanes, 2008; Li et al., 2015). This suggests significant functional overlap with invertebrate *Dscam1* in the nervous system (Introduction- Figure 19). While *DSCAM* has also roles outside the nervous system (e.g. in heart development), there is no report suggesting an implication of *DSCAM* or *DSCAML1* in innate immunity as of today.

3. The extracellular domains of Dscam-family orthologues are highly similar

The ***extracellular domains*** of the vertebrate Dscam1 orthologues do not only have a ***comparable protein-structure,*** consisting of Ig and FNIII domains (Agarwala et al., 2001a; Agarwala et al., 2001b; Yamakawa et al., 1998), but they are also capable of mediating

homophilic DSCAM-DSCAM interactions (Agarwala et al., 2000; 2001b), affecting ***neurite outgrowth*** (Amano et al., 2009; Montesinos, 2014). Additionally, ***Netrin-1*** binding to the extracellular domain is possible, representing another similarity with invertebrate Dscam1 (Huang et al., 2015; Liu et al., 2009; Ly et al., 2008). This interaction influences ***axon pathfinding*** (Liu et al., 2009; Ly et al., 2008) by interfering with DCC mediated axon guidance mechanisms (Huang et al., 2015; Ly et al., 2008).

Another potential heterophilic DSCAM-ligand is called "***draxin"*** (Ahmed et al., 2011). This repulsive guidance cue binds to all Netrin receptors. It does not have a fly orthologue. Other DSCAM ligands have not been characterized as of today, even though it remains possible that DSCAM interacts with other extracellular components, such as COL6A2 (Grossman et al., 2011).

4. DSCAM and DSCAML1 are also tyrosine phosphorylated

Similar to invertebrate Dscam1, both vertebrate orthologues (DSCAM and DSCAML1) are ***tyrosine phosphorylated*** (Cui et al., 2013; Liu et al., 2009; Purohit et al., 2012). ***Src kinases*** are the main mediators of tyrosine-phosphorylation (Purohit et al., 2012). The counteracting phosphatases remain unknown. The Src-substrate within the DSCAML1-protein is a *YEEL*-motif (Cui et al., 2013). This amino-acid motif is found in invertebrate Dscam1 as well (Introduction-Table 9 and Introduction- Figure 18)

Even though vertebrate DSCAM does not interact with Nck, a potential ***link to Pak kinase*** has been reported (Liu et al., 2009; Purohit et al., 2012), as Netrin-1 induced activation of DSCAM signaling induces phosphorylation of Fyn and Pak kinases (Liu et al., 2009; Purohit et al., 2012) and recruitment of TUBB3 in primary cortical neurons (Huang et al., 2015). This interaction with polymerized tubulin influences axonal branching (Huang et al., 2015) and can be pharmacologically inhibited via the Src family kinase (SFK) inhibitor *PP2*. The *Drosophila* orthologues of TUBB3 are betaTub56D, betaTub60D, betaTub85D and betaTub97EF.

5. *The importance of regulating vertebrate DSCAM signaling*

In a disease context, the regulation of DSCAM expression and signaling levels is of special relevance: During development, DSCAM protein levels are dynamically regulated (Agarwala et al., 2001a; de Andrade et al., 2014; Maynard and Stein, 2012). At postnatal days 7-10, a period characterized by extensive axonal branching, their expression levels peak in the murine cerebral cortex (Maynard and Stein, 2012). *DSCAM* expression levels are altered in the context of Down's syndrome (Alves-Sampaio et al., 2010; Saito et al., 2000; Yamakawa et al., 1998), epilepsy (Shen et al., 2011), respiratory disorders (Amano et al., 2009) sudden infant death (Amano et al., 2009), bipolar disorder (Amano et al., 2008) and posttraumatic stress disorder (PTSD) (Ashley-Koch et al., 2015; Logue et al., 2015). *DSCAML1* has been associated with Jacobson's syndrome (Agarwala et al., 2001b).

Similar to its *Drosophila* counterpart, the transcript of mouse *DSCAM* was found to be associated with the FMRP in two independent studies (Brown et al., 2001; Darnell et al., 2011), suggesting that FMRP translational regulation of DSCAM levels is conserved. This hypothesis is strengthened by the observation that Loss of *FMRP* leads to increased Dscam1 expression levels.

6. *The intracellular domains of vertebrate and invertebrate Dscams contain similar signaling motifs*

Finally, my own sequence analysis of the amino acid sequences of the cytoplasmic domains of vertebrate DSCAM and DSCAML1 with the ELM linear motif search tool (http://elm.eu.org) reveals that the *Dscam1* orthologues ***share a lot of signaling motifs*** with their invertebrate counterparts. These are *"scrambled"* and not arranged in the same order as in invertebrates. However, their presence suggests that similar downstream signaling pathways mediate Dscam1, DSCAM and DSCAML1 function (Introduction- Table 9).

INTRODUCTION- TABLE 9. **COMPARISON OF SIGNALING MOTIFS PRESENT IN VERTEBRATE DSCAM AND DSCAML1 WITH *DROSOPHILA* DSCAM1.**

62 available vertebrate DSCAM family protein sequences were downloaded from public resources (NCBI, Uniprot and Ensemble), the Ig and FNIII identified and aligned using the ClustalW tool (EBI). For the alignment of the intracellular domains only the sequences after the last FNIII domain were used. The sequences were also analyzed with the ELM Linear Motif resource tool (http://elm.eu.org) to pinpoint potential signaling Motifs. Of the motifs identified by ELM I only added those to the table above, which fell into a highly conserved region of the CLUSTALW alignment. The probability score suggests how likely it is that this amino acid sequence would occur purely by chance without any functional significance

Motif	Vertebrate DSCAM	Invertebrate Dscam1	Vertebrate DSCAM L1	Class	Sequence	Motif Probability
Endocytosis Motif	***4***	***3***	***3***	Tyrosine based ***sorting signal*** responsible for the interaction with mu subunit of AP (Adaptor Protein) complex	***Y..[LMVIF]***	0.0025875
SH2-binding site (STAT 3)	***1***	***1***	***1***	***Binding site*** found in cytokine receptors	***(Y)..Q***	0.0007975
14-3-3 Binding Motif	***1***	***1***	***1***	***Binding site***	***RxxSxP***	0.0008077
SH2 Binding Site (Src)	***1***	***1***	***1***	***Binding Site***	***(Y)[QDEVAIL][DENPYHI][IPVGAHS]***	0.0008729
SH2 STAT5 Binding site	***4***	***1***	***3***	***STAT5*** Src Homology 2 (SH2) domain ***binding motif***.	***(Y)[VLTFIC]***	0.0032959
SH3 Binding Site	***1***	***2***	***8***	***Binding site***	***[RKY]..P..P/...[PV]..P***	0.0012370/0.0131729
TRAF2 Binding motif	***1***	***2***	***1***	T***RAF2 binding site***	***[PSAT].[QE]EE***	0.0042998
PDZ type 1 motif	***1***	***1***	***1***		***[PSAT].[QE]E***	
Dscam Box	***1***	***1***	***1***		***YxxA***	
Polyproline Motif	***0***	***1***	***1***			

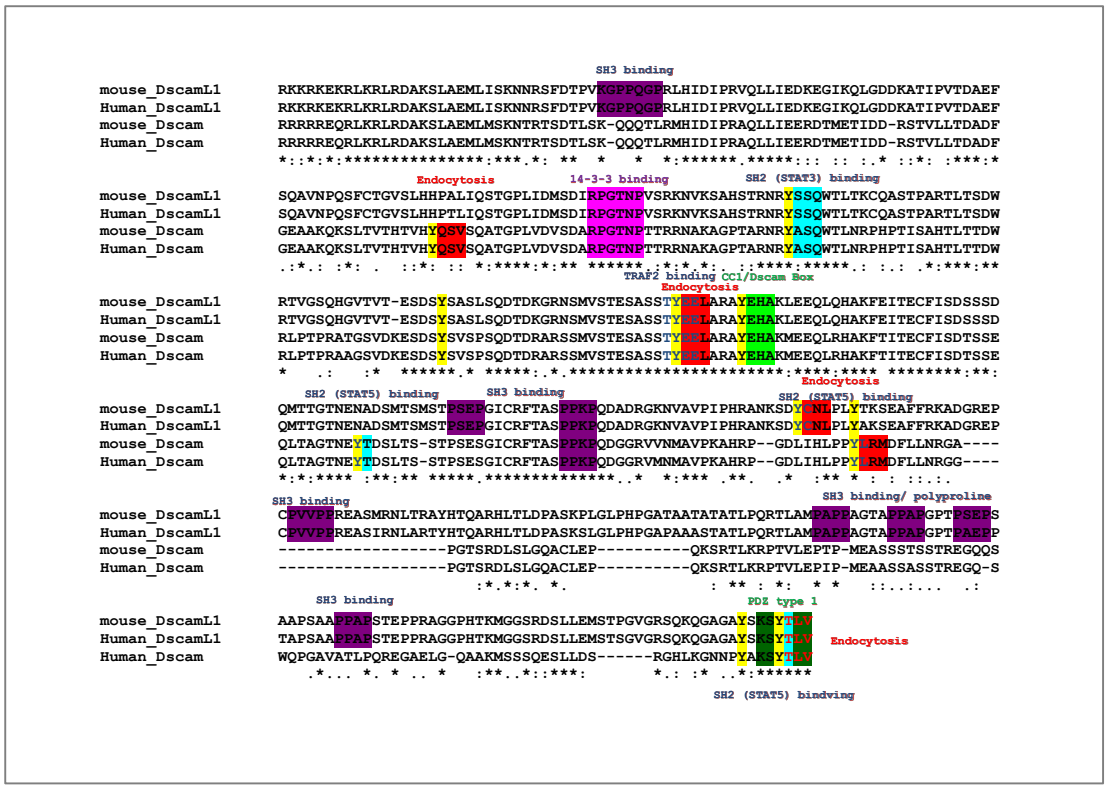

INTRODUCTION- FIGURE 18. **ALIGNMENT OF THE INTRACELLULAR DOMAINS OF HUMAN AND MOUSE DSCAM AND DSCAML1.**

There are many signaling motifs in the vertebrate Dscam receptors which are also found in invertebrate Dscam1, suggesting that the overall signaling properties might be conserved. I have labeled the position of the signaling motifs mentioned in Introduction-Table 9 in different colors. Note for example the YEEL motif (red) which is also found in all invertebrate Dscams.

But what about diversity?

The vertebrate Dscam1 orthologues belong to a large and diverse family of neuronal self-recognition molecules

DSCAM and DSCAML1 are not the only receptors involved in neurite self-recognition and repulsion. Instead, there are other (non DSCAM-family) proteins with similar function, such as ***γ-Pcdhs*** (Lefebvre et al., 2012) (Introduction- Figure 19). Especially the γ-Pcdhs have raised a lot of attention in recent years, since they can be spliced into many different isoforms (Kohmura et al., 1998; Wu and Maniatis, 1999). Therefore, it has been proposed that *γ-Pcdhs* could represent the *functional Dscam1 vertebrate homologues* in creating distinctive neuronal surfaces (Lefebvre et al., 2012; Sanes and Zipursky, 2010). Alternatively one could imagine , that diversity in invertebrates might be replaced by the ***combinatorial use of differential Ig-receptors*** in vertebrates, since none of the mentioned

protein families is large enough to overcome the labeling problem arising from Sperry's chemoaffinity hypothesis (e.g. proposed in Schmucker and Chen, 2009).

Why did evolution take such different roads in vertebrates to create cell surface identity in vertebrates and in invertebrates? This question cannot satisfyingly be answered as of today. However, one possible hint might be the fact that Dscam1 diversity is not only used for neuronal self-recognition but has also a role in the innate immune response, leading to selective pressure in favor of Dscam1 diversity in invertebrates.

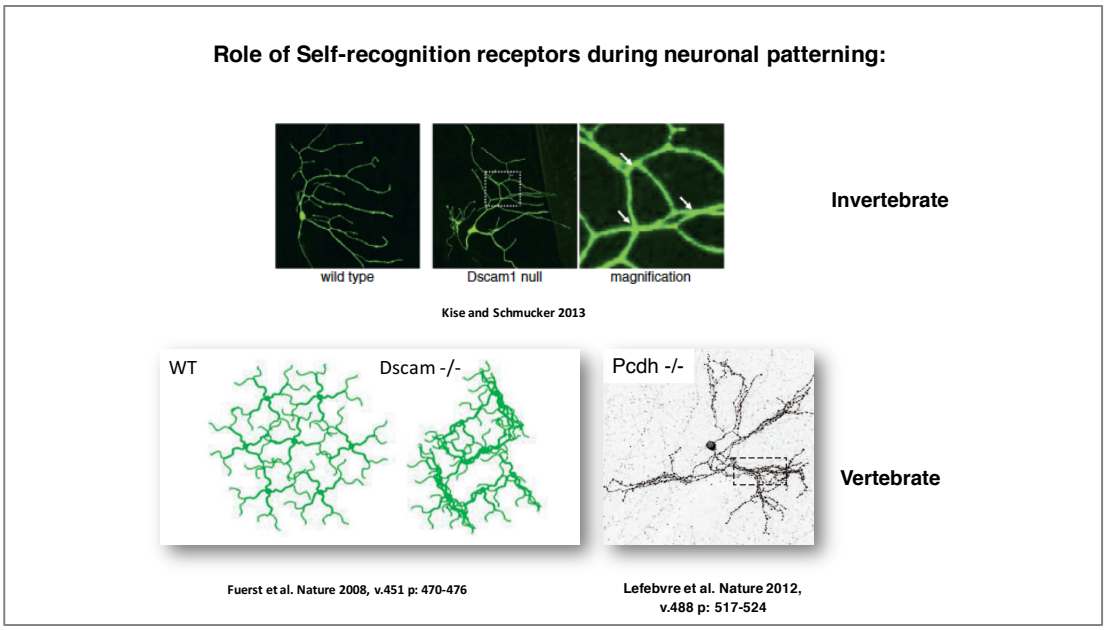

INTRODUCTION- FIGURE 19. **THERE IS SIGNIFICANT FUNCTIONAL OVERLAP BETWEEN VERTEBRATE AND INVERTEBRATE DSCAM FAMILY RECEPTORS.**

Self-recognition receptors ensure uniform spacing of neurites derived from the same cell. This function is assumed by invertebrate Dscam1 (top panels). Shown are multi-dendritic neurons of the Drosophila larval body wall. Loss of Dscam1 leads to entangling and self-crossing of neurites derived from the same cell. In vertebrates the same function is assumed by a number of different receptors. The panel on the bottom left shows, how DSCAM ensures even spacing of neurites from vertebrate amacrine cells. The same function is executed by Pcdhs in other subsets of amacrine cells (bottom right), suggesting that the cell surface code for neuronal self-recognition is mediated by a receptor signature composed from several homophilic Ig-CAM protein families.

Surface receptor diversity has been created by different expansion strategies several times throughout evolution

Interestingly, there are other invertebrate arthropod species genomes (*myriapoda* and *chelicerata*), that do not display the excessive alternative splicing to diversify *Dscam1*. Instead, they harbor ***a multitude of gene duplications***, leading to many distinct *Dscam* paralogues (Chipman et al., 2014; Kenny et al., 2015). For example, the centipede *S. maritima* has 60-80 *Dscam* paralogues (Chipman et al., 2014) and the millipede still 43 (Kenny et al., 2015). In addition to gene duplications, the *Dscam* genes of *S. maritime* and the tick *Ixodes* encompass also exons subjected to alternative splicing, creating an even bigger *Dscam* repertoire (Brites et al., 2013).

Taken together, Dscam mediated functions are ***conserved*** traits. Strikingly however, ***the manner in which diversity is being created, seems to differ from species to species.*** *Dscam* family genes are present in all species with neurites patterning derived from neuronal self-recognition underlining the importance of the receptor to the mechanism. Surface receptor diversity is created by expansion strategies as different as gene duplication, alternative splicing and recruitment of other (co-)receptor families. Hence, it seems likely that through a convergent evolution mechanism different types of neuronal surface barcodes developed based on a common selection criterion (e.g. higher neuronal circuit complexity).

Objective of this dissertation

The highly ordered connection of axons and dendrites (wiring) during development requires the establishment of trillions of connections. This process is based on an immensely complex developmental program that is still only partially understood. Gaining insight into the molecular mechanisms involved in neuronal wiring bears great promise for modern neurobiology: It potentially could lead to a better understanding of brain functions and the background of many disorders of the nervous system, such as epilepsy, schizophrenia, autism and mental retardation.

The aim of this dissertation is to dissect the signaling mechanisms of the hypervariable *Drosophila* self-recognition receptor Dscam1. *Dscam1* is expressed in cells of the nervous system as well as in cells belonging to the *Drosophila* innate immune system. It is involved in axon guidance, targeting and branching, the formation of dendritic fields as well as in the recognition of pathogens. The importance of *Dscam1* for axonal and dendritic patterning has been demonstrated in numerous *in vivo* assays. However, surprisingly little is known regarding the signaling pathway downstream of the receptor. This dissertation describes my efforts into gaining insights into the molecular mechanisms of neuronal self-recognition by combining ***proteomic screens***, with ***cell culture*** and ***biochemistry*** in order to identify Dscam1 signaling regulators and effectors and to characterize their interaction with the Dscam1 signaling complex.

Chapter 1

Cell-intrinsic requirement of Dscam1 isoform diversity for axon collateral formation

Haihuai He,1,2,3* Yoshiaki Kise,1,2* Azadeh Izadifar,1,2 Olivier Urwyler,1,2 Derya Ayaz,1,2† Akhila Parthasarthy,3 Bing Yan,1,2 ***Maria-Luise Erfurth,1,2,4*** Dan Dascenco,1,2 Dietmar Schmucker1,2‡

This chapter is an adapted version of the article published in ***Science*** (6 JUNE 2014 • VOL 344 ISSUE 6188). All references, figure numbers and legends are assigned to and listed separately for this chapter.

Maria-Luise Erfurth contributed to the publication in the following aspects:

1. By ***optimizing the protocol for bacterial recombineering*** of the Dscam1 genomic locus based on a preliminary procedure proposed by Dr. Akhila Parthasarthy. This allowed for reliable routine use of bacterial recombineering in the Schmucker laboratory (see also the dedicated section in Material and Methods), and was instrumental to the **cloning of some *genomic Dscam1 constructs*** and the ***establishment of the respective transgenic fly lines*** used in this paper.
2. She contributed to the ***development of a model for the role of Dscam1 signaling*** during patterning of mechanosensory growth cones in the VNC of *Drosophila melanogaster* presented in the discussion section of this chapter.
3. Importantly, she did the ***neurite tracings shown in Figure 3*** to visualize the different growth cones.
4. She contributed to the ***writing of the manuscript***.

[1]Neuronal Wiring Laboratory, Vlaams Instituut voor Biotechnologie (VIB) Vesalius Research Center, 3000 Leuven, Belgium. [2]Department of Oncology, School of Medicine, University of Leuven, 3000 Leuven, Belgium. [3]Department of Cancer Biology, Dana-Farber Cancer Institute, Boston, MA 02215, USA. [4]Institute of Biochemistry, Christian-Albrechts-University of Kiel, 24118 Kiel, Germany. *These authors **contributed equally to this work**. †Present address: Laboratory of Ion Channel Research, University of Leuven, 3000 Leuven, Belgium. ‡Corresponding author. E-mail: dietmar. schmucker@vib-kuleuven.be

The isoform diversity of the Drosophila Dscam1 receptor is important for neuronal self-recognition and self-avoidance. A canonical model suggests that homophilic binding of identical Dscam1 receptor isoforms on sister dendrites ensures self-avoidance even when only a single isoform is expressed. We detected a cell-intrinsic function of Dscam1 that requires the coexpression of multiple isoforms. Manipulation of the Dscam1 isoform pool in single neurons caused severe disruption of collateral formation of mechanosensory axons. Changes in isoform abundance led to dominant dosage-sensitive inhibition of branching. We propose that the ratio of matching to nonmatching isoforms within a cell influences the Dscam1-mediated signaling strength, which in turn controls axon growth and growth cone sprouting. Cell-intrinsic use of surface receptor diversity may be of general importance in regulating axonal branching during brain wiring.

Several classes of neuronal cell surface receptors exhibit an exceptional degree of protein diversity and have been implicated in important aspects of neuronal differentiation (1–5). Evidence for the importance of isoform diversity during development has been provided for the Drosophila Down syndrome cell adhesion molecule (Dscam1) and the mouse clustered protocadherins (PCDHs) (6–14). The Dscam1 gene uses combinatorial alternative splicing to generate tens of thousands of different receptor isoforms, whereas the clustered PCDHs rely on combinatorial oligomerization to provide a huge diversification of their binding specificities (2, 7, 9, 11). The isoform diversity is thought to provide neurons with distinct "surface tags," thereby endowing them with unique molecular identities. Such complex molecular recognition mechanisms are particularly important for the development of highly branched neurite compartments.

Many neuronal circuits depend on the presence of highly branched axons or dendrites which serve to increase either the wiring complexity or the size of the input/output fields. The development of branched dendritic fields requires a dedicated mechanism, often referred to as self-avoidance, that ensures correct spacing between sister neurites and prevents hypo- or hyper innervation (7). For Dscam1 it has been shown that isoform-specific homophilic binding on the surface of sister dendrites provides the molecular recognition mechanism that underlies neurite repulsion and self-avoidance (12–14). This molecular model of self-avoidance has also been proposed for the vertebrate PCDH gamma receptors (10).

This model, which we refer to as the canonical model of Dscam1/PCDH function, states that isoform-specific homophilic receptor binding on the surface of sister dendrites initiates neurite repulsion, and that the expression of a single Dscam1 isoform per neuron is sufficient for Dscam1 function (12–15). The question of whether this canonical role provides the mechanistic basis of all Dscam1 functions is still open to debate (3, 7, 9). Addressing this point, we found evidence for a strictly cell-intrinsic requirement of multiple diverse Dscam1 isoforms and describe a function of isoform diversity specifically required for the patterning of complex axonal arborizations.

To examine the role of Dscam1 diversity, we generated bacterial artificial chromosome (BAC)– based conditional alleles (16) that express Dscam1 protein at endogenous levels and allow for the manipulation of Dscam1 diversity in a spatially and temporally specific manner (Fig. 1A) (17). We found that the [Dscam1] EX6.1-FRT allele recapitulates all known neuronal wiring functions of Dscam1 and is functionally equivalent to the endogenous Dscam1 (Fig. 1, Fig. S1, and Table S1). We analyzed thoracic mechanosensory (MS) neurons, which innervate the macrochaetae of adult flies and show a stereotypic axonal branching pattern in the ventral nerve cord (VNC) (3) (Fig. 1B). The loss of Dscam1 in MS neurons causes severe MS axon growth and branch patterning defects (3) (Fig. 1C). However, replacing the endogenous Dscam1 locus with the BAC-based [Dscam1] EX6.1-FRT allele rescued all mutant defects (Fig. S1).

In sharp contrast to the [Dscam1] EX6.1-FRT allele, the [Dscam1] EX6.1-Flpd allele lacking all but one of the exon 6 variants (Fig. 1A) did not restore the axon collateral formation (Fig. 1, D and E). Often only an ipsilateral primary axon shaft was formed (Fig. 1E), but collateral branches were missing (78%, n = 37). In some cases, primary branches were formed but lacked higher order branches and varicosities (Fig. S2) (22%, n = 37). Because similar branching defects have been observed in experiments where exon 9 diversity was lacking in whole flies (8), we conclude that any substantial and global reduction in Dscam1 isoform diversity causes a loss of MS axon collaterals.

The use of BAC-based Dscam1 alleles allowed us to combine multiple engineered and endogenous Dscam1 alleles and revealed a striking dominant and dosage-dependent influence of Dscam1 diversity on axonal branching (Fig. 1, F to I). A single copy of [Dscam1] EX6.1-Flpd in a wild-type background dominantly caused a specific lack of a primary anterior ipsilateral branch (86%) (Fig. 1H). When two copies of [Dscam1] EX6.1-Flpd were added, the dominant phenotype was enhanced such that additional primary branches were missing in 45% of the flies (n = 29) (Fig. 1F). Overall, higher severity and penetrance of the branching phenotype were observed by increasing the ratio of [Dscam1] EX6.1-Flpd to endogenous Dscam1. Conversely, the dominant effect was partially suppressed by adding a normal Dscam1 allele (i.e., [Dscam1] EX6.1-FRT) and was completely suppressed by having three copies of wild-type Dscam1 alleles (Fig. 1I).

Similar branching defects were observed when using the analogous [Dscam1] EX6.7-Flpd and [Dscam1] EX6.21-Flpd alleles in which exon 6 variants have been swapped (Fig. S2). Profiling the Dscam1 mRNA in flies bearing [Dscam1] EX6.n-Flpd alleles revealed that alternative exons 4 and 9 of transgenic and endogenous Dscam1 can still be normally spliced and their protein expression is not impaired (Fig. S1 and Tables S2 and S3). Taken together, the dominant nature of the branching defects makes it unlikely that the lack of axonal branches resulted from potentially reduced levels of Dscam1 protein.

On the basis of the role of Dscam1 in self versus nonself discrimination (4–9), one might assume that global reduction of the Dscam1 diversity in [Dscam1] EX6.1-Flpd flies results in an increased frequency of "same-isoform" encounters between neurons contacting each other. To investigate this possibility, we used the [Dscam1] EX6.1-FRT allele to reduce the Dscam1 diversity by Flp recombinase expression in a cell-specific fashion (Fig. 2, A and B, and Figs. S3 and S4) (17). We found that the selective elimination of exon 6 diversity in a subset of peripheral sensory neurons also caused strong axon branching defects at high penetrance (80 to 90%), despite spatial and temporal differences in Flp recombinase expression (Fig. 2B, Table 1, and Figs. S3 and S4) (17). Frequently, only the main axon shaft was formed (Fig. 2B and Fig. S3C), or only distal branches (Figs. S3D and S4G), or only short stubs or varicosities were detected (Fig. S3E and Fig. S4, C, E, and H).

We also used double dye fills to compare the axon branching pattern of two MS neurons in- innervating the same VNC target area. We found, without exception, that only MS neurons expressing Flp recombinase exhibited branch patterning defects (Fig. 2B and Figs. S3G and S4); their neighboring MS neurons were unaffected (Fig. 2B′ and Figs. S3G′ and S4).

In contrast to the strong branching defects observed in MS neurons, we did not observe any defect in dendritic branch formation of class I dendritic arborization (DA) neurons (Fig. S5). Therefore, consistent with previous reports (12–15), we found no indication for a cell-intrinsic requirement of Dscam1 isoform diversity for dendrite morphogenesis of DA neurons.

To investigate further why a potential repertoire of 396 Dscam1 isoforms in MS neurons is not sufficient for proper MS axon branching, we directly examined Dscam1 isoform expression in single posterior scutellar (pSc) neurons (Fig. S6). In single wild-type pSc

neurons, many isoforms are expressed with no clear preference of exon 6 variants. However, in agreement with previous multicellular profiling experiments (18–21), we found that expression of exon 4 and exon 9 was highly biased and that exon 4.2 and exon 4.8 were the most frequently identified exon 4 variants (>65%) in pSc neurons.

In single pSc neurons of Dscam1-null; [Dscam1] EX6.1-Flpd flies, we found a similar strong bias in exon 4 and exon 9 variants, but all variants contained exon 6.1. We found no evidence that the excision of exon 6.2–6.48 would indirectly or aberrantly influence splicing of isoforms (Tables S2 and S3).

Taken together, these results indicate that a much smaller set of isoforms than the hypothetically available repertoire of up to 396 isoforms is used in mutant MS neurons. Because of strong quantitative differences in expression levels (19), we conclude that very few Dscam1 isoform variants are predominantly expressed in MS neurons of [Dscam1] EX6.1-Flpd flies.

This increase of identical isoforms in neurons with reduced exon 6 diversity supports the hypothesis that too many "same-isoform" interactions within MS neurons are causing an over activation of Dscam1 function cell-intrinsically, but does not strictly exclude other possibilities. To exclude a potential role of axon-axon interactions, we used several approaches to restrict the isoform reduction to single neurons (Fig. 2, C and E, and Figs. S7, S8, S9, and S11). Even if the reduction of exon 6 diversity was limited to only one MS neuron, pronounced axon branching defects were frequently detected (80 to 85%; Fig. 2D, Table 1, and Fig. S7). The phenotypic spectra were similar to those observed in flies in which Dscam1 diversity was reduced in broad tissue domains (Fig. 2B and Figs. S3 and S4). Performing double dye-fill experiments, we found that the branching pattern of the neighboring anterior scutellar neuron (aSc) was normal despite strong defective branch patterning of the pSc neuron (Fig. 2D′ and Fig. S7), which is in direct contact with the aSc axon (Fig. S7). The penetrance of the phenotypes was high (80 to 85%), although the expressivity differed depending on the respective GAL4 transactivator used (Table 1 and Figs. S7 to S10) (17).

In a complementary approach, we used heat shock–mediated induction of sparse stochastic Flp recombinase expression (Fig. S11 and S12) (17) to generate flies in which single MS neurons had reduced Dscam1 diversity (Fig. 2, E and F, and Fig. S11). We found that a significant number of green fluorescent protein (GFP)– positive cells with reduced Dscam1

diversity (47%) exhibited strong or moderate axon branching defects (Fig. 2F, Table 1, and Fig. S11).

To further test the cell-autonomous function of Dscam1 diversity in MS axons, we overexpressed a Dscam1 isoform selectively in single MS neurons (Fig. S13). Consistent with our single-cell Flp-out experiments, we observed strong defects in axonal branching of posterior dorsocentral (pDc) neurons (Fig. S13 and Fig. S17, G and H). We also examined wether Dscam1 isoform interactions between axons of MS neurons and processes and neurites of potential target neurons contribute to branch patterning, and found that Dscam1 diversity in the VNC is dispensable for the overall mechanism of axon collateral formation of MS axons (Fig. S14 to S16) (17).

These results indicate that the presence of too many identical isoforms within MS axons is detrimental to axon growth and branching. This suggests that in contrast to self-avoidance in DA neuron dendrites, the Dscam1 isoform diversity in MS axons is required cell-intrinsically.

Finally, we asked how reduction of Dscam1 isoform diversity impairs the ability of axons to elaborate collateral branches during development. We examined single growth cones of MS axons, comparing pDc axon growth of neurons from wild type flies, flies with Dscam1 knockdown through RNA interference (RNAi), and flies with Dscam1 isoform reduction (Fig. 3) (17). In wild-type neurons, a characteristic sprouting phase could initially be identified, with a plethora of long filopodia-like extensions starting to project in many different directions (Fig. 3A). This was followed by a more ordered redistribution of filopodia-like extensions along the anterior-posterior axis as well as toward the midline (Fig. 3B). In the next phase, the consolidated axon collaterals and the main axon shaft were growing in length (Fig. S17A).

In MS axons with reduced Dscam1 protein levels, the early growth cones exhibited a defective morphology with abnormally dense and short filopodia-like extensions (Fig. 3, C and D, and Fig. S17B). In contrast, growth cones with a reduced Dscam1 diversity appeared to have fewer filopodia-like extensions (Fig. 3, E and F, and Fig. S17C). Note that for mutant pDc neurons, the earliest onset of growth cone sprouting occurs with an 8- to 10-hour delay, suggesting the possibility of an impairment of axon growth *per se*. However, although Dscam1 has a role in axon growth, several observations suggest that Dscam1 diversity may also contribute directly to growth cone sprouting and branching (Figs. S18

and S19). For example, a moderate increase in Dscam1-Dscam1 homophilic interactions does not cause any axon growth delay but causes branching defects (Fig. S17I and S18). Similarly, single isoform expression does not lead to a delay but nonetheless leads to dominant axon branching defects (Fig. S13 and Fig. S17, G and H). In summary, the developmental analysis suggests that changes in the abundance and diversity of Dscam1 isoforms influence axon growth and growth cone sprouting, resulting in disrupted growth cone morphologies.

Why does cell-intrinsic isoform reduction cause axonal branching defects in single MS neurons? Given that our single-cell isoform profiling revealed that the reduction of isoform diversity leads to the presence of more identical Dscam1 isoforms in MS neurons, it seems prudent to assume that this results in more homophilic Dscam1-Dscam1 binding in mutant growth cones and causes a gain of Dscam1 function. The dominant dosage sensitive effects of [Dscam1] EX6.1-Flpd (Fig. 1, G to I, and Fig. S17I) and the cell-autonomous single isoform overexpression (Fig. S13), as well as the sensory neuron–specific Flp-out experiments (Fig. 2), are all consistent with the interpretation that the observed axon branching defects result from Dscam1 gain-of-function signaling. In molecular terms, we propose a model in which growth cones of MS axons are exquisitely responsive to quantitative differences in Dscam1 signaling. Specifically, we propose that when more identical-type isoforms are present in growth cones, more Dscam1 signaling occurs, and as a consequence, axon growth as well as growth cone dynamics (e.g., regulation of filopodia-like extensions) are strongly impaired (model in Fig. S20).

Chapter 1- REFERENCES AND NOTES

1. Q. Wu, T. Maniatis, Cell 97, 779–790 (1999).
2. D. Schmucker et al., Cell 101, 671–684 (2000).
3. B. E. Chen et al., Cell 125, 607–620 (2006).
4. D. Schmucker, Nat. Rev. Neurosci. 8, 915–920 (2007).
5. D. Hattori et al., Nature 449, 223–227 (2007).
6. D. Hattori, S. S. Millard, W. M. Wojtowicz, S. L. Zipursky, Annu. Rev. Cell Dev. Biol. 24, 597–620 (2008).
7. Y. Kise, D. Schmucker, Curr. Opin. Neurobiol. 23, 983–989 (2013).
8. D. Hattori et al., Nature 461, 644–648 (2009).
9. S. L. Zipursky, J. R. Sanes, Cell 143, 343–353 (2010).
10. J. L. Lefebvre, D. Kostadinov, W. V. Chen, T. Maniatis, J. R. Sanes, Nature 488, 517–521 (2012).
11. D. Schreiner, J. A. Weiner, Proc. Natl. Acad. Sci. U.S.A. 107,14893–14898 (2010).
12. M. E. Hughes et al., Neuron 54, 417–427 (2007).
13. B. J. Matthews et al., Cell 129, 593–604 (2007).
14. P. Soba et al., Neuron 54, 403–416 (2007).
15. W. Wu, G. Ahlsen, D. Baker, L. Shapiro, S. L. Zipursky, Neuron 74, 261–268 (2012).
16. K. J. Venken, Y. He, R. A. Hoskins, H. J. Bellen, Science 314, 1747–1751 (2006).
17. See supplementary materials on Science Online.
18. X. L. Zhan et al., Neuron 43, 673–686 (2004).
19. W. Sun et al., EMBO J. 32, 2029–2038 (2013).
20. A. M. Celotto, B. R. Graveley, Genetics 159, 599–608 (2001).
21. G. Neves, J. Zucker, M. Daly, A. Chess, Nat. Genet. 36, 240–246 (2004).

Chapter 1- ACKNOWLEDGMENTS

Supported by NIH grant 2RO1NS046747-05A1 (D.S.); Fonds Wetenschappelijk Onderzoek (FWO) grants G059611N, G078913N, and G077013N (D.S.); BELSPO IUAP VII-20 “WIBRAIN project” (D.S.); VIB funding; a JSPS postdoctoral fellowship and a Human Frontier Science Program long-term fellowship (Y.K.); an FWO Ph.D. fellowship (D.D.); a Swiss National Science Foundation postdoctoral fellowship (O.U.); and ***a Boehringer Ingelheim Fonds Ph.D. fellowship (M.-L.E.).*** We thank members of the lab and especially B. Hassan (VIB, Center for the Biology of Disease) for critical reading of the manuscript, discussions, and insightful comments.

Chapter 1- SUPPLEMENTARY MATERIALS

Supplemental information can be found online under:

www.sciencemag.org/content/344/6188/1182/suppl/DC1

- ✓ Materials and Methods
- ✓ Supplementary Text
- ✓ Figs. S1 to S20
- ✓ Tables S1 to S3 References (22–35)

6 February 2014;
accepted 8 May 2014
Published online 15 May 2014;
10.1126/science.1251852

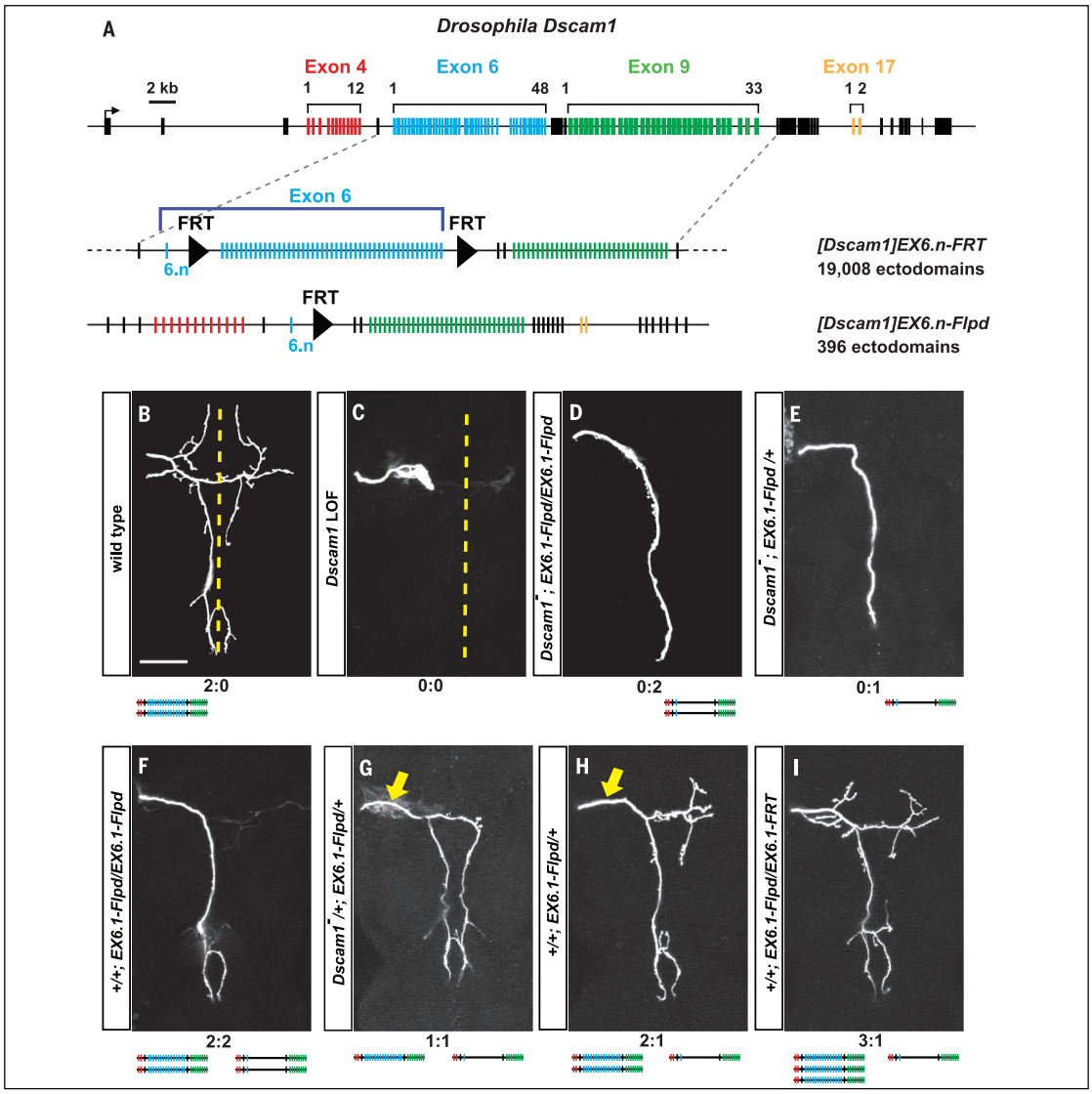

CHAPTER 1- FIGURE 1. **REDUCTION OF DSCAM1 DIVERSITY CAUSES DOMINANT AND DOSAGE-DEPENDENT IMPAIRMENT OF AXONAL BRANCHING.**

(A) Schematic representation of the genomic structure of the Dscam1 gene and Dscam1 BAC alleles, used for manipulation of Dscam1 diversity. (B to I) Axonal branching patterns of MS neurons resulting from different combinations of endogenous Dscam1 (left) and the [Dscam1] EX6.1-Flpd allele (right) as indicated below panels. Phenotypic defects have been quantified (Chapter 1- Table 1). The dashed line indicates the midline of the central nervous system; arrows indicate missing primary branches. Scale bar, 50 µm.

Genotype	*n*	Strong	Moderate	Normal branching
Wild type	171	0%	2.9%	97.1%
Reduced diversity in all neurons, wild type versus EX6.n-Flpd				
0:1 (6.1)	37	78%	22%	0%
0:2 (6.1)	33	73%	27%	0%
0:1 (6.7)	41	73%	27%	0%
0:1 (6.21)	39	79%	21%	0%
Dominant effects, wild type versus EX6.1-Flpd				
2:2	29	45%	55%	0%
1:1	37	11%	89%	0%
2:1	35	0%	86%	14%
3:1	32	0%	3.1%	96.9%
Reduced diversity in sensory field				
455-Gal4	201	62%	18%	20%
pnr-Gal4	34	62%	29%	9%
Reduced diversity in single MS neurons				
R36D01-Gal4	40	67%	18%	15%
R15E08-Gal4	39	31%	49%	20%
Heat shock single clones	45	38%	9%	53%
Reduced diversity in target area				
worniu-Gal4	37	0%	2.7%	97.3%

CHAPTER 1- TABLE 1. **QUANTIFICATION OF BRANCHING PHENOTYPES OF PSC NEURONS.**

Branching phenotypes were classified into two groups: In strong phenotypes, the midline crossing branch is not formed (i.e. Fig.1, D to F; Fig.2, B, D and F; fig. S2, B, D and F; fig. S3, C, D and G; fig. S4, C, D, G and H; fig. S7, C, C', D, D', F and G; fig. S11, E, E', and G). In moderate phenotypes, the midline-crossing branch or a stub is formed but is missing other primary and higher-order branches (i.e. Fig. 1, G and H; fig. S2, C and E; fig. S3E; fig. S4E; fig. S7, C'' and D''; fig. S11E'').

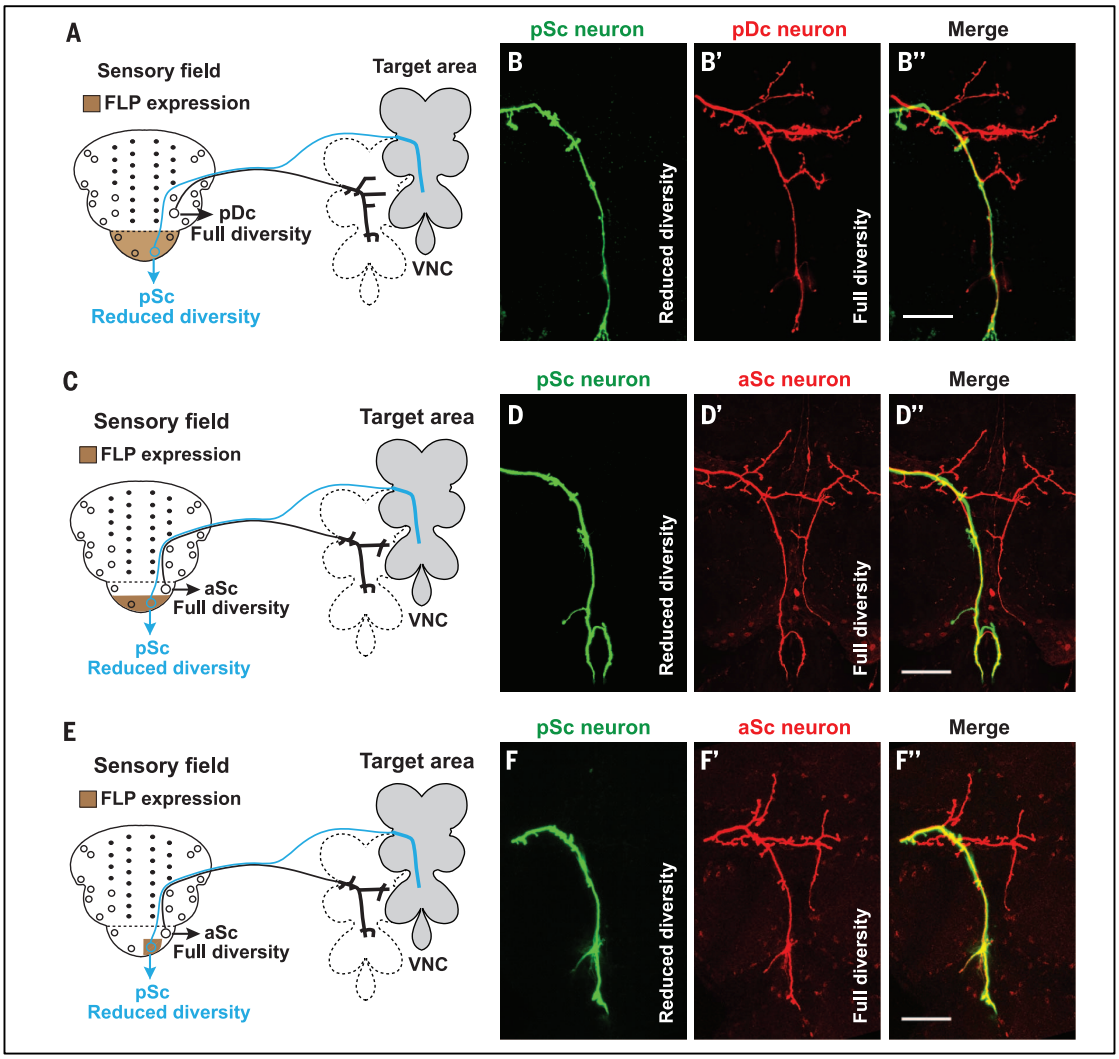

CHAPTER 1- FIGURE 2. **CELL-INTRINSIC REQUIREMENT OF DSCAM1 ISOFORM DIVERSITY FOR AXONAL BRANCHING PATTERN OF MS NEURONS.**

(A, C, and E) Schematic representation of reducing Dscam1 diversity in two pairs of neurons (pSc, aSc) (A), in both pSc neurons (C), or in a single pSc neuron (E) by using 455-Gal4, R36D01- Gal4, or mild heat shock, respectively, to induce Flp recombinase expression (17). For illustration purposes, the axon branching patterns are sketched separately. (B, D, and F) Despite strong branching defects in the mutant pSc neuron, the pDc neuron (B) and aSc neuron with full Dscam1 diversity [(D) and (F)] both show a normal branching pattern (see also figs. S3, S7, and S11). Branching patterns of pSc and neighboring pDc or aSc neurons were visualized by double dye labeling (17). Quantification of phenotypic defects is summarized in Table 1. Scale bars, 50 μm.

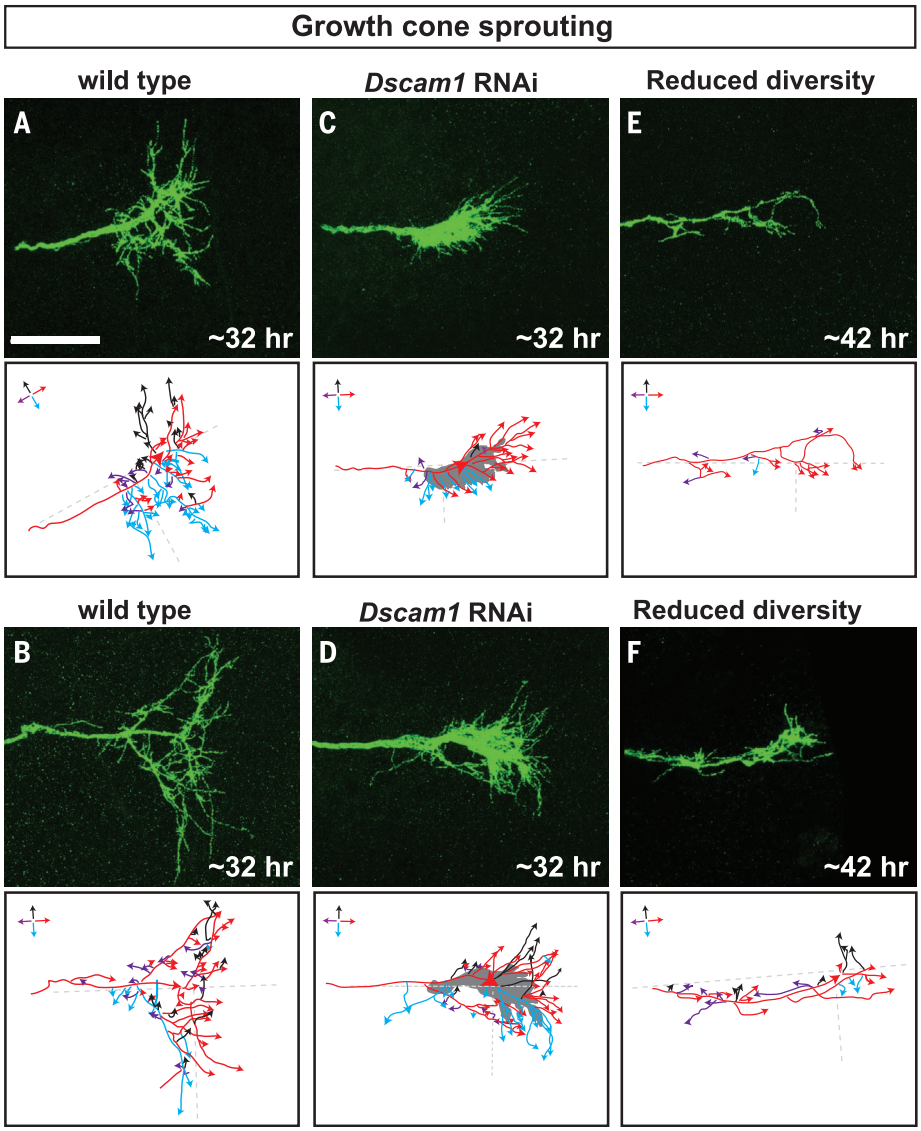

CHAPTER 1- FIGURE 3. **MANIPULATION OF DSCAM1 ACTIVITY AFFECTS GROWTH CONE SPROUTING.**

Images show growth cone morphology of single pDc neurons at the sprouting stage. Tracings of filopodia-like extensions are color- coded; arrowheads indicate growth direction of single filopodia-like extensions. (A and B) Growth cones of wild-type pDc at ~32 hours APF (after puparium formation) show a complex morphology with many long filopodia-like extensions projecting into all directions. (C and D) Growth cones of pDc neurons with Dscam1 RNAi knockdown at ~32 hours APF. The abnormally dense filopodia-like extensions do not separate well and within the center (gray area) are too dense to be traced individually. Filopodia-like extensions "escaping" from the central domain often project in the same direction. (E and F) Growth cones of pDc neurons with reduced Dscam1 diversity at ~42 hours APF. Axon growth is delayed by ~10 hours and the growth cones are highly abnormal, exhibiting a reduced number of filopodia-like extensions. Scale bar, 20 µm.

Chapter 2

Slit and Receptor Tyrosine Phosphatase 69D Confer Spatial Specificity to Axon Branching via Dscam1

Dan Dascenco,[1,2,7] ***Maria-Luise Erfurth,***[1,2,3,7] Azadeh Izadifar,[1,2] Minmin Song,[4] Sonja Sachse,[1,2,5] Rachel Bortnick,[6] Olivier Urwyler,[1,2] Milan Petrovic,[1,2] Derya Ayaz,[1] Haihuai He,[1] Yoshiaki Kise,[1,2] Franziska Thomas,[6] Thomas Kidd,[4] and Dietmar Schmucker[1,2,*]

[1]Neuronal Wiring Laboratory, VIB, Herestraat 49, 3000 Leuven, Belgium [2]Department of Oncology, School of Medicine, University of Leuven, Herestraat 49, 3000 Leuven, Belgium [3]Institute of Biochemistry, Christian-Albrechts-University of Kiel, Olshausenstr. 40, 24098 Kiel, Germany [4]Biology/MS 314, University of Nevada, Reno, NV 89557, USA [5]Department of Biology, Chemistry & Pharmacy, Free University Berlin, Takustr. 3, 14195 Berlin, Germany [6]Department of Cancer Biology, Dana-Farber Cancer Institute, 450 Brookline Avenue, Boston, MA 02215, USA [7]*Co-first author*

This chapter is an adapted version of the article published in ***Cell*** 162, 1140–1154 August 27, 2015; http://dx.doi.org/10.1016/j.cell.2015.08.003

All references, figure numbers and legends are assigned to and listed separately for this chapter.

Maria-Luise Erfurth contributed to the publication in the following aspects:

(1) ***Design and planning of experiments*** together with Dan Dascenco and Dietmar Schmucker
(2) M-L Erfurth was critically involved in ***all aspects of the biochemical and molecular biology data*** presented (planning, organization, cloning, experimental execution, data analysis) except the binding data obtained by the Kidd lab. She had technical help from Tineke Breynaert (cell culture, protein biochemistry). Sonja Sachse and Dan Dascenco contributed Figure 6-Panel M based on cell culture and Slit purification protocols developed by Maria-Luise Erfurth.
(3) She contributed to the ***development of a model for the regulation of Dscam1 signaling*** function in the developing growth cones of mechanosensory neurons in the VNC of *Drosophila melanogaster* presented in the discussion section.
(4) M-L Erfurth, D. Dascenco and D. Schmucker ***wrote the manuscript*** *and* ***designed the figures.***

*Correspondence: dietmar.schmucker@vib-kuleuven.be

Article

Cell

Slit and Receptor Tyrosine Phosphatase 69D Confer Spatial Specificity to Axon Branching via Dscam1

Graphical Abstract

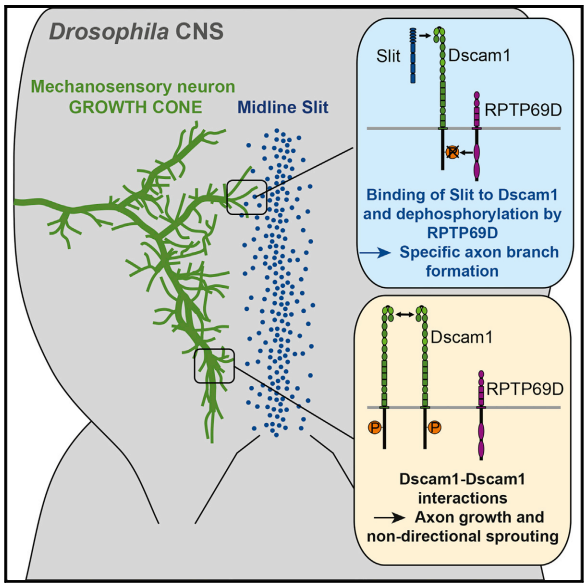

Highlights

- Modulation of Dscam1 activity in growth cones regulates axonal branching
- RPTP69D dephosphorylates Dscam1 to promote midline-crossing axon collaterals
- Local binding of Slit to Dscam1 drives spatial specificity of axon collateral formation

Authors

Dan Dascenco, Maria-Luise Erfurth, Azadeh Izadifar, ..., Franziska Thomas, Thomas Kidd, Dietmar Schmucker

Correspondence

dietmar.schmucker@vib-kuleuven.be

In Brief

The neuronal receptor Dscam1 in *Drosophila* can be regulated through direct binding of the extrinsic ligand Slit and through dephosphorylation. This mode of regulation of Dscam1 signaling enables localized control of axon branch outgrowth in circuit formation.

Chapter 2- SUMMARY

Axonal branching contributes substantially to neuronal circuit complexity. Studies in Drosophila have shown that loss of Dscam1 receptor diversity can fully block axon branching in mechanosensory neurons. Here we report that cell-autonomous loss of the receptor tyrosine phosphatase 69D (RPTP69D) and loss of midline-localized Slit inhibit formation of specific axon collaterals through modulation of Dscam1 activity. Genetic and biochemical data support a model in which direct binding of Slit to Dscam1 enhances the interaction of Dscam1 with RPTP69D, stimulating Dscam1 dephosphorylation. Single-growth-cone imaging reveals that Slit/RPTP69D are not required for general branch initiation but instead promote the extension of specific axon collaterals. Hence, although regulation of intrinsic Dscam1-Dscam1 isoform interactions is essential for formation of all mechanosensory-axon branches, the local ligand-induced alterations of Dscam1 phosphorylation in distinct growth-cone compartments enable the spatial specificity of axon collateral formation.

Chapter 2- INTRODUCTION

The *Drosophila* Dscam1 receptor belongs to the immunoglobulin-superfamily (Ig-SF) of transmembrane proteins and is known to function as a homophilic surface receptor important for neuronal wiring (reviewed in Kise and Schmucker, 2013). Dscam1 is unique due to its extraordinary molecular diversity. Through alternative splicing thousands of structurally diverse receptor isoforms with different binding properties are generated (Schmucker et al., 2000; Wojtowicz et al., 2004), and up to 18,496 of those isoforms are expressed *in vivo* (Sun et al., 2013). Loss of *Dscam1* disrupts the proper development of many different neurons and affects in particular growth and patterning of neurite arborizations (Chen et al., 2006; Hughes et al., 2007; Hummel et al., 2003; Kim et al., 2013; Matthews et al., 2007; Soba et al., 2007; Wang et al., 2002).

An analysis of single mechanosensory neurons (ms-neurons) has revealed that Dscam1 diversity is essential for growth cones undergoing axonal sprouting as well as for axon growth and branch formation (Chen et al., 2006; He et al., 2014). Dscam1 activity is highly sensitive to the level of Dscam1-Dscam1 isoform interactions in a growth cone. For example, a cell-intrinsic alteration of the number of matching isoforms expressed in ms-neurons can lead to the loss of a subset or even all axon collaterals. The mechanistic basis, however, of how enhanced Dscam1 isoform interactions can block formation of axon collaterals is currently unknown. Moreover, it seems highly likely that axon branching of ms-neurons requires additional instructions by local extracellular signals, which may play an important role in controlling the specific targeting of each axon arbor. What these signals are, or how they influence branching, has not been determined.

In general, the question of how branches of the same neuronal compartment (e.g. axon collaterals) can achieve growth toward different targets is still poorly understood, and few *in vivo* studies have addressed this question (Hao et al., 2010; Liu and Halloran, 2005; McLaughlin et al., 2003). Moreover, some signals controlling branching, such as Semaphorins, Ephrins or Slit have been found to be multifunctional and can exert diverse or opposing effects on neurite branching (Liu and Halloran, 2005; Ma and Tessier-Lavigne, 2007; McLaughlin et al., 2003; Polleux et al., 2000). For example, the guidance cue Slit can function as a potent axon repellent by binding to Robo receptors present on growth cones (Brose et al., 1999; Chedotal, 2007; Kidd et al., 1999) and can also contribute to axon

branching, where it is thought to function as a ‘‘positive’’ factor stimulating axon branching. This was demonstrated by in vitro assays (Wang et al., 1999) wherein Slit2-N strongly enhanced the number of axonal branchpoints and total neurite length of sensory neurons. However, subsequent genetic studies revealed that the role of Slit in axon branching is more complex and multifunctional (Campbell et al., 2007; Ma and Tessier-Lavigne, 2007; Yeo et al., 2004). For example, loss-of-function of Slit in mice does not lead to less axon branching of sensory neurons of the dorsal root ganglion but results in a disruption of branch guidance consistent with a lack of repulsion. On the other hand, Slit mutants do show a reduction of the sensory field arborization of ophthalmic trigeminal neurons, indicating a positive growth-promoting activity during neurite arborization (Ma and Tessier-Lavigne, 2007). Taken together, it remains an intriguing question how Slit and other factors contribute to axon branching and exert such diverse roles in different neurons.

Here we present a genetic and biochemical characterization of how Dscam1 activity in growth cones can be regulated by differential phosphorylation through direct *cis*-interactions with the receptor tyrosine phosphatase RPTP69D. This modulation of Dscam1 signaling activity can be spatially restricted to a subset of axonal branches by the extracellular signal Slit, which functions as a ligand of Dscam1. This function of Slit is independent of Robo1–3 receptors and selectively promotes the consolidation and extension of midline-crossing axon collaterals. Overall, we propose a molecular and cellular model of how compartmentalized regulation of Dscam1 phosphorylation in growth cones contributes to divergent growth decisions underlying the formation of specific axon collateral projections.

RPTP69D promotes formation of specific axon collaterals

The afferent projections of adult ms-neurons, such as posterior scutellar (pSC) neurons, connect with multiple post-synaptic targets in the CNS through the formation of axon collaterals (Ghysen, 1978; Urwyler et al., 2015). Although the main axon shaft and several axonal branches only establish ipsilateral connections, other axon collaterals also project across the midline (Figures 1A–1C). Previous work has shown that the neuronal receptor Dscam1 is essential for the formation of the elaborate axon branch pattern of ms-neurons (Chen et al., 2006) (Figure 1D). Importantly, ms-neuron-specific increase of Dscam1 expression (Experimental Procedures; Figures S1A and S1B) and reduction of isoform diversity result in a loss of some or all axon collaterals, whereas growth of the main axon shaft is unaffected (Figures 1E and S1C–S1F). For example, specific *Dscam1* alleles with decreased isoform diversity show a dominant interference with axon collateral formation, often resulting in a loss of some axon collaterals (Hattori et al., 2009; He et al., 2014) (Figure 1E). It is important to note that a decrease in isoform diversity concomitantly leads to an increase in the frequency of homotypic isoform interactions, and we therefore refer to it as Dscam1 gain of function (GOF). Consistent with this notion, we find that ms-neuron-specific overexpression of single Dscam1 isoforms in otherwise wild-type (WT) ms-neurons also leads to a reduction of collateral formation (Figures S1C–S1F).

In a reverse genetic screen, we discovered that selective loss of axon collaterals also occurs in ms-neurons with reduced RPTP69D function. RPTP69D has previously been shown to be important for guidance and targeting of motor as well as sensory neurons (Berger et al., 2008; Garrity et al., 1999; Hofmeyer and Treisman, 2009; Kurusu and Zinn, 2008). We found that RNAi- mediated knockdown (KD) of the receptor tyrosine phosphatase RPTP69D results in a selective loss of a distinct subset of axon collaterals (Figures S1G–S1J). To confirm this, we further analyzed ms-neuron projections in mosaic analysis with a repressible cell marker (MARCM) null clones and homozygous hypomorphic adults. In all loss-of-function (LOF) genotypes examined, we found that reduction or complete loss of RPTP69D led to a frequent and specific lack of axon collaterals, which normally grow across the midline (Figures 1F–1H0 and S1G–S1O). The main axon shaft and other axon branches were not aberrant, with the exception of an infrequent (17%) shortening of the anterior ipsilateral branch (Figure S1I). Moreover, by examining MARCM clones or

homozygous mutant animals of other receptor tyrosine phosphatases encoded in the fly genome (*LAR, RPTP99A, RPTP4E, and RPTP10D*) (Johnson and Van Vactor, 2003), we found no phenotypic defects of axon collateral formation (Figures S1P–S1S), suggesting that RPTP69D serves a unique role in the axonal branching of ms-neurons.

We conclude that RPTP69D functions cell-autonomously in ms-neurons and is specifically required for formation of a subset of axon collaterals that cross the central nervous system (CNS) midline.

RPTP69D is an inhibitor of Dscam1 function in vivo

Given the similarity of RPTP69D LOF and Dscam1 GOF phenotypes, we set out to determine potentially direct interactions of these receptors. In order to utilize genetic interaction studies, we first characterized several hypomorphic non-lethal *RPTP69D* alleles that were described previously (Figures S1K–S1O and S1T) (Desai and Purdy, 2003). Combining hypomorphic and null (*RPTP69D1*) alleles, we found that the anterior midline-crossing branch of pSC neurons was absent or truncated in over 70% of mutant flies. (Figures 1F, S1N, S1O, S1T, and S1U). As expected, the frequency of phenotypic defects correlated with the strength of hypomorph combinations (Figures S1M, S1N, and S1T). Strikingly, removal of only one copy of *Dscam1* was sufficient to dominantly suppress these defects in *RPTP69D* mutants. Specifically, we found that the anterior midline-crossing collaterals were intact in the majority of these samples (Figures 1I and 1J) and that the extent of suppression correlated with the *Dscam1* allele strength (Figures 1I and 1J). As a control, removal of one copy of *Robo1* did not affect the penetrance of the *RPTP69D* hypomorph phenotype (Figure 1J), suggesting that this suppression is specific to *Dscam1*.

We also tested reciprocal genetic combinations. Although all known hypomorphic allele combinations of *Dscam1* already cause severe early axonal growth defects (Figures S2A–S2A') (Zhan et al., 2004), we nevertheless found that reducing RPTP69D levels in a *Dscam1* mutant background resulted in weak dominant suppression of Dscam1 defects (Figures S2A– S2E). In addition, the viability of either *RPTP69D* or *Dscam1* homozygous mutant animals is strongly increased upon removal of one copy of *Dscam1* or *RPTP69D*, respectively (Figures 1K and S2F). Furthermore, strong genetic interactions of *Dscam1* and *RPTP69D* are also evident when mushroom body development is examined (Figures S2G–S2L).

Taken together we show in multiple cellular and functional assays that *Dscam1* and *RPTP69D* genetically interact. The apparent antagonistic functional relations suggest the possibility that RPTP69D is an important negative regulator of Dscam1 function.

RPTP69D phosphatase physically interacts with and directly dephosphorylates Dscam1

We next tested whether RPTP69D directly dephosphorylates Dscam1. We assayed Dscam1 phosphorylation in a cell culture system by engineering a chimeric Dscam1 receptor, ‘‘Met-Dscam’’, which can be activated by addition of a non-*Drosophila* ligand. We fused the Dscam1 transmembrane and cytoplasmic tail (CT) (exons 17–24) with the extracellular domain of the mouse Met receptor (Figure 2A). This chimeric receptor can be activated by soluble hepatocyte growth factor (HGF) and provides an on/off trigger for assaying cytoplasmic Dscam1 signaling without interference from endogenous Dscam1.

We found baseline Met-Dscam1 tyrosine phosphorylation (Y-phosphorylation) in S2 (hemocyte-like) and BG3C2 (neuronal) cell lines in the absence of HGF and a rapid increase of Y-phosphorylation following HGF addition (Figures 2B–2D). Activation reached a peak after a few minutes in S2 cells, whereas the signal increased steadily for more than 30 min in BG3C2 cells (Figures 2B, 2C, and S3A–S3A’). Moreover, consistent with previous cell culture studies (Muda et al., 2002; Purohit et al., 2012), we found that the Met-Dscam1 chimeric receptor is Y-phosphorylated by Src-family kinases (SFKs) (Figures S3B–S3B’) and leads to efficient recruitment of the SH2-domain-containing adaptor Dock (Figures S3C–S3C’).

In order to examine which RPTP contributes to Dscam1 dephosphorylation, we combined chimeric receptor expression with RNAi-mediated KD of RPTPs. Strikingly, we found that of the five tested *Drosophila* RPTPs only RPTP69D reduced Met-Dscam1 baseline phosphorylation (Figure 2E).

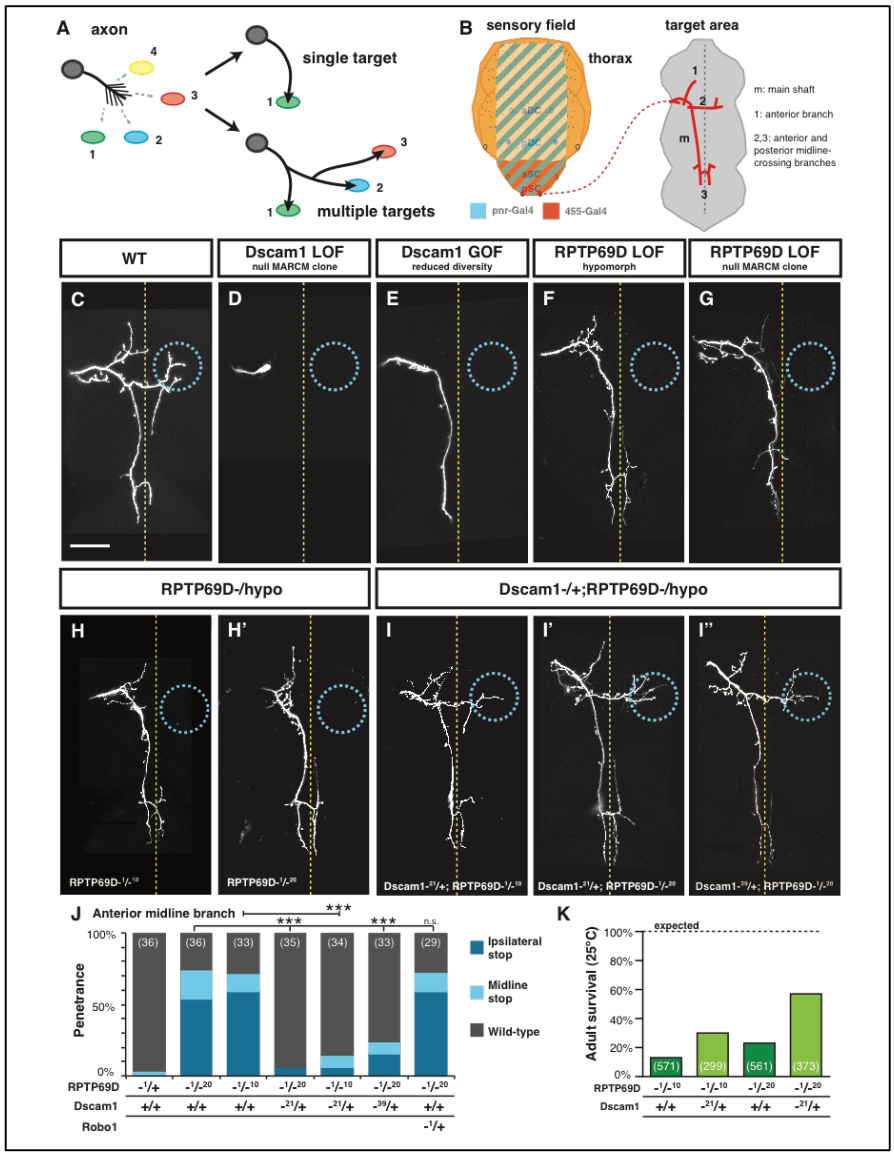

CHAPTER 2- FIGURE 1. **RPTP69D AND DSCAM1 PLAY OPPOSITE ROLES IN MIDLINE-DIRECTED COLLATERAL FORMATION**

*(A) Axonal branching of ms-neurons leads to an increase in network complexity by allowing a neuron to connect to different post-synaptic targets. (B) Stereotyped branching pattern of Drosophila ms-neurons. (C–I) Representative pSC neurons dye-filled with carbocyanine dyes. (C) WT pSC ms-neurons displaying the stereotyped branching pattern. (D) Dscam1 LOF in pSC neurons (generated by MARCM technique) leads to the formation of a ''clump'' of entangled processes. (E) Dscam1 GOF phenotypes resulting from a loss of isoform diversity. (F and G) RPTP69D LOF partially phenocopies Dscam GOF (G) RPTP69D strong hypomorph combinations (F) For allele designations and additional quantifications, see Figures S1K, S1T, and S1U. (H and H') RPTP69D1/RPTP69D10 and RPTP69D1/RPTP69D20 mutants display a characteristic absence of the anterior midline-crossing collateral. (I–I'') Heterozygosity of Dscam1 in RPTP69D mutants suppresses RPTP69D branching defects. Dscam121/+; RPTP69D1/RPTP69D10 (I), Dscam121/+; RPTP69D1/RPTP69D20 (I'), and Dscam139/+; RPTP69D1/RPTP69D20 (I''). (J) Quantification of ms-neuron defects (chi-square test, ****p % 0.0001). (K) Dscam1 heterozygosity in RPTP69D hypomorphic background also improves adult survival. For all figures, numbers between parentheses represent the numbers of neurons scored. Normal target areas of anterior midline-crossing collaterals are indicated by blue circles. Dotted yellow line indicates the midline. Scale bars are 50 mm unless specified otherwise. See also Figures S1 and S2.*

Next we examined whether Dscam1 is a direct substrate of RPTP69D. It is known that RPTPs often interact very transiently with their substrates and that enzyme-substrate binding is strongly stabilized by mutating specific residues of the so-called ''WPD'' loop

in the catalytic domains. This approach is referred to as ‘‘substrate trapping’’ (Blanchetot et al., 2005; Flint et al., 1997). RPTP69D has two phosphatase domains (D1, D2), and we therefore engineered HA-tagged RPTP69D D > A substrate-trap constructs with mutations in either one or both phosphatase domains (DA1, DA2, DA12) (Figures 2F and S3D). Transient expression and immunoprecipitations (IPs) in BG3C2 cells showed that substrate-trapping mutants but not WT RPTP69D bound to endogenous Dscam1 (Figure 2F).

If RPTP69D inhibits Dscam1 signaling through dephosphorylation, then overexpression of RPTP69D should lead to reduction of Y-phosphorylation of Dscam1. We confirmed this by examining Y-phosphorylation of endogenous Dscam1 in BG3C2 cells transiently overexpressing V5-tagged RPTP69D. We found that overexpression of RPTP69D caused a strong reduction of phosphorylation of endogenous Dscam1 (Figure 2G).

These results suggest that RPTP69D can directly dephosphorylate Dscam1 and that endogenous RPTP69D-Dscam1 interactions are normally transient.

Constitutive binding of RPTP69D substrate-trap mutant to Dscam1 phenocopies Dscam1 LOF

For RPTPs bearing two phosphatase domains, it is thought that only one domain is catalytically active, whereas the second domain contributes to substrate specificity (Tonks, 2006). Consistent with this, we found that mutations in D1 and D2 of RPTP69D have strikingly different effects. The RPTP69D-DA1 mutant failed to reduce Dscam1 CT phosphorylation levels, suggesting that D1 is the main catalytically active domain (Figure 2G). In contrast, the expression of the RPTP69D-DA2 mutant resulted in a pronounced reduction of Dscam1 phosphorylation levels (stronger than WT-RPTP69D) and appears to be toxic for cells. This hyper-dephosphorylation was eliminated when both catalytic domains (RPTP69D-DA12) were mutated (Figure 2G). These results suggest that the RPTP69D-DA2 mutant blocks the dissociation from Dscam1, thereby enhancing dephosphorylation by the catalytically intact D1 domain.

We reasoned that the RPTP69D-DA12 double-mutant protein might interfere dominantly with Dscam1 function *in vivo*. Therefore, we expressed RPTP69D-DA12 in pSC neurons

and examined for direct comparison ms-neuron-specific KD of Dscam1 expression (Figures 3C–3C'). We indeed found that expression of the RPTP69D-DA12 mutant protein caused strong dominant defects in ms-axon projections almost identical to Dscam1 LOF defects (Figure 3). In contrast, expression of a WT form of RPTP69D had no effect on the branching pattern of ms-neurons (Figure 3D). These results strongly suggest that the D1 domain of RPTP69D is essential for Dscam1 dephosphorylation and that Dscam1 can serve as a direct substrate of RPTP69D, both *in vitro* and *in vivo*.

RPTP69D dephosphorylates specific tyrosines of the cytoplasmic domain of Dscam1

We set out to identify which of the 22 tyrosines of the cytoplasmic domain of Dscam1 are RPTP69D substrates (Figures 4A and S4A). We tested tyrosine to phenylalanine mutations (Y > F mutations) in the chimeric Met-Dscam1 receptor assay and found that five tyrosine mutations (Y1707F, Y1857F, Y1890F, Y1911F, and Y1981F) significantly reduced Met-Dscam1 baseline phosphorylation (Figures 4B, 4C, and S4B), whereas the Y1857F and Y1890F mutations also showed strong reduction of ligand-induced Met-Dscam1 activation (Figures 4B and 4C). Further sequence motif analysis suggests that Y1857, Y1890, and Y1911, are potential RPTP substrate sites (Figures 4D and S4D) (Ren et al., 2011; Selner et al., 2014; Tonks, 2013).

We also examined Y > F mutations in the context of a full-length HA-tagged Dscam1 isoform (Figures 4E, 4F, and S4C). We reasoned that the dephosphorylation of Dscam1 proteins caused by RPTP69D co-expression should at least be partially diminished in mutant Dscam1 proteins lacking substrate tyrosines. Co-transfection of RPTP69D with a WT full-length Dscam1 cDNA reduced the Dscam1 Y-phosphorylation levels by approximately 70% (Figures 4E, 4F, and S4C). In contrast, RPTP69D-dependent dephosphorylation of Dscam1 was fully blocked as a result of the Y1890F and Y1981F mutations and partly blocked for the Y1857F mutation (Figures 4E and 4F). Taken together, we identified three tyrosines (Y1857, Y1890, and Y1981) in the Dscam1 cytoplasmic domain that can serve as substrates for RPTP69D-mediated dephosphorylation. In the following we refer to these sites as ''RPTP69D target sites.''

RPTP69D target sites can regulate Dscam1 activity in vivo

We sought to determine whether these potential RPTP69D target sites also play a role for Dscam1 function *in vivo*. Previous studies have shown that cell-intrinsic UAS-based overexpression of WT Dscam1 can dominantly interfere with branching of ms-neurons (He et al. 2014). We therefore reasoned that these GOF phenotypes might provide a sensitive readout to assay the influence of regulatory mutations on Dscam1 activity *in vivo* (Figure 5).

For each of the three RPTP69D target sites, we generated Y > F substitutions in the context of full-length Dscam1 UAS- controlled transgenes and expressed them in ms-neurons (Figure 5F). Expression of WT Dscam1 in ms-neurons neurons leads to frequent aberrant ipsilateral or midline stop of the anterior axon collaterals (Figures 5B–5B' and 5G; for genotypes, see Supplemental Experimental Procedures). The Dscam1 GOF defects were strongly suppressed by the Y1857F mutation (Figures 5C–5C') and weakly by the Y1890F mutation (Figures 5D–5D' and 5G). In contrast, expression of the Y1981F mutant protein resulted in dominant branching defects significantly stronger than expression of the WT Dscam1 protein (Figures 5E–5E' and 5G). We observed complete absence of anterior midline collaterals in approximately 40% and absence of all branches in over 30% of ms-axons, suggesting a strongly enhanced Dscam1 activity. It is intriguing that the expression of a Dscam1-Y1981F mutant results in a phenotype qualitatively indistinguishable from that of Dscam1 alleles where isoform diversity is reduced (Figure 1E) (He et al., 2014). In summary, these results suggest that the Y1857F and less so the Y1890F mutations reduce Dscam1 GOF, whereas the Y1981F mutation strongly enhances Dscam1 GOF activity.

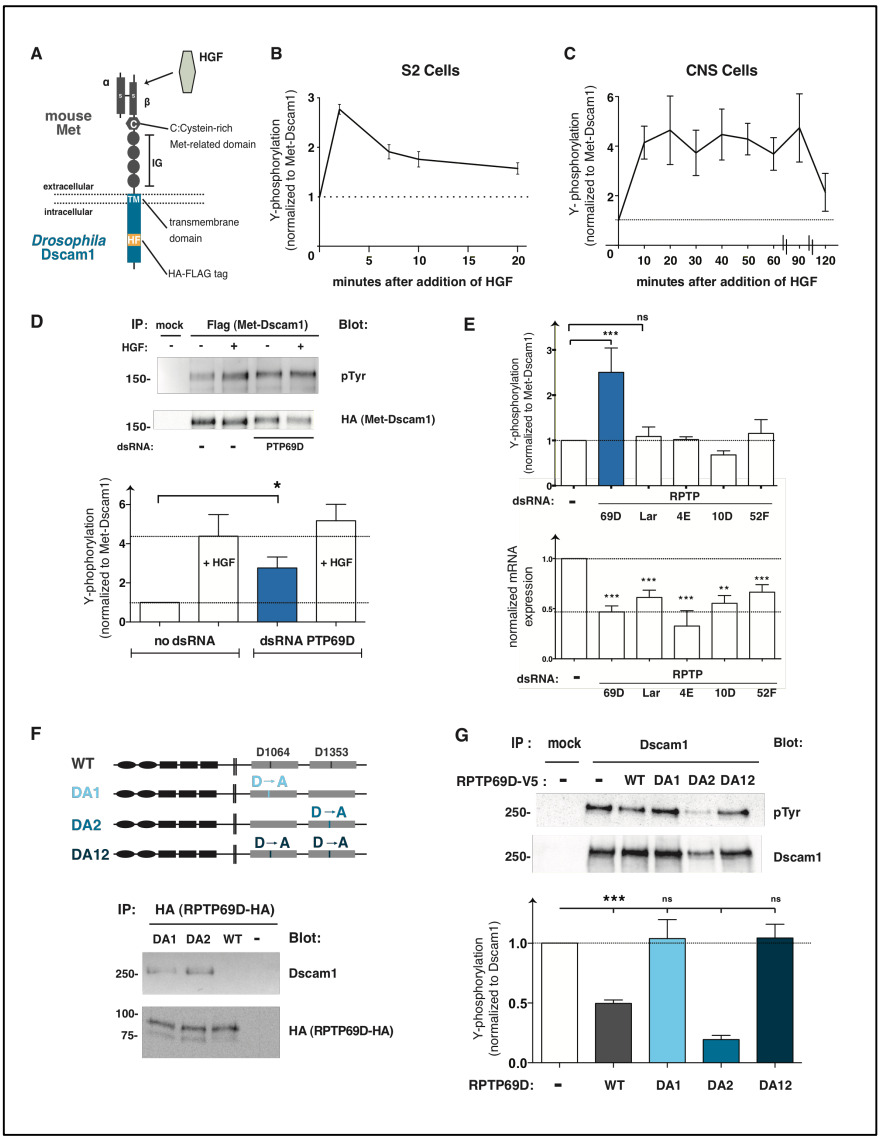

CHAPTER 2- FIGURE 2. **DSCAM1 IS AN *IN VITRO* SUBSTRATE FOR RPTP69D**

*(A) Design of the chimeric Met-Dscam1 receptor. (B and C) HGF-mediated activation of Met-Dscam1 leads to an increase of its Y-phosphorylation in S2 or BG3C2 cells. (B) Met-Dscam1 expressed in S2 cells was immunoprecipitated and phosphorylation assessed by semi-quantitative western blot (WB) analysis. All measurements normalized to baseline phosphorylation (summary of six experiments). (C) HGF-mediated activation of Met-Dscam1 is stronger and lasts longer in BG3C2 cells than in S2 cells (n = 6 for 10 min, n = 4 for 20, 60, 90, and 120 min, n = 5 for 30 min, n = 3 for 40 min). (D) Met-Dscam1 IP from BG3C2 cells before and 30 min after HGF addition in the presence or absence of RPTP69D shows that RPTP69D KD leads to increased baseline phosphorylation of Met-Dscam1. Top: Representative WB of one experiment. Bottom: Quantification of multiple experiments. (n = 6; paired t test, *p % 0.05.) (E) RNAi tests show that RPTP69D is the only neuronal RPTP affecting Met-Dscam1 baseline phosphorylation (see also Figures S1L–S1S). Top: Summary of multiple experiments for each dsRNA (n = 7 for RPTP69D and Lar, n = 2 for RPTP 4E, 10D, and 52F). ANOVA/Dunnett, ***p % 0.001. Bottom: KD efficiency assessed by quantitative RT-PCR (n = 6 for PTP69D, n = 3 for Lar, RPTP10D, 4E, and 52F. ANOVA/Dunnett, **p % 0.01; ***p % 0.001). (F) Endogenous Dscam1 binds to substrate-trapping mutants in BG3C2 cells. Top: Mutations introduced in the WPD loop of domain 1 (DA1), or 2 (DA2), or both (DA12). Bottom: Co-IP of Dscam1 from S2 cells transiently expressing HA-tagged RPTP69D. Only DA1 and DA2 mutants are able to co-IP Dscam1. (G) Mutational analysis of RPTP69D phosphatase domains. Dscam1 IPs from S2 cells expressing V5-tagged RPTP69D WT and Y > F mutant proteins. Y-phosphorylation status evaluated by semi-quantitative WB analysis. Top: WB of one representative experiment. Bottom: Summary of multiple experiments (n = 6 for WT, n = 4 for DA1 and DA2, n = 2 for DA12; ANOVA/Dunnett, **p % 0.01; ***p % 0.001). Error bars: SEM. See also Figure S3.*

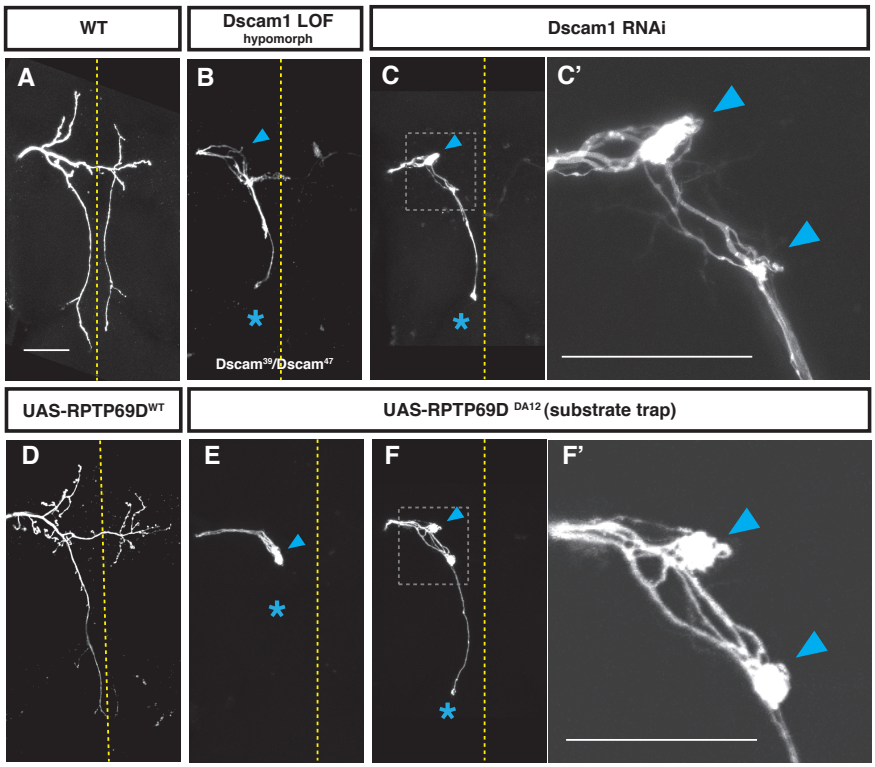

CHAPTER 2- FIGURE 3. **EXPRESSION OF A RPTP69D SUBSTRATE-TRAP MUTANT PHENOCOPIES DSCAM1 LOF**

(A–F') Representative dye-fills of pSC neurons. (A) WT pSC neuron. (B) Defects in Dscam39/Dscam47 reveal ''clump'' formation (arrowheads) and longitudinal axon growth defects (asterisks). (C–C') RNAi KD of Dscam1 results in ''clumps'' (arrowheads) and longitudinal axon growth defects (asterisks); higher magnification in (C'). (D–F') Expression of RPTP69DA12 mutant in ms-neurons phenocopies Dscam1 LOF defects. Expression of UAS-RPTP69D-WT (D) and UAS-RPTP69D-DA12 (E–F') in ms-neurons using pnr- Gal4 is shown; higher magnification in (F').

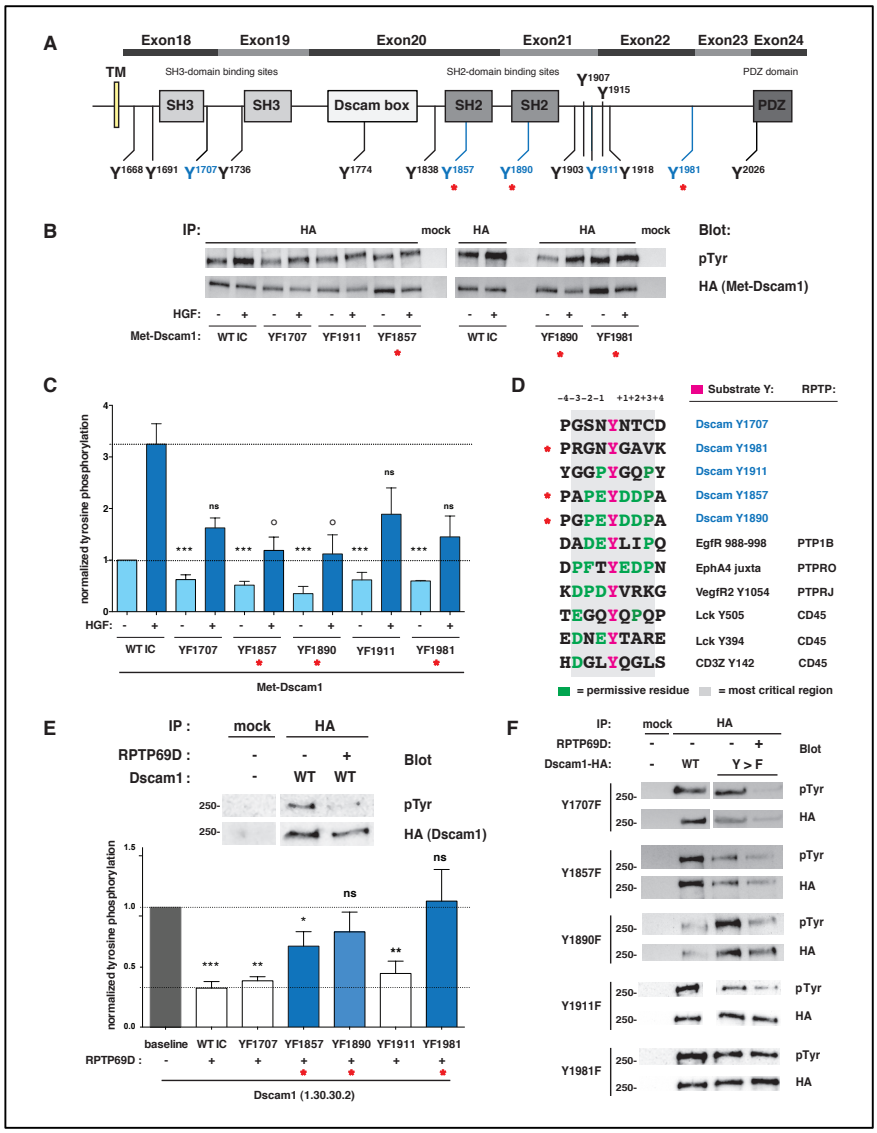

CHAPTER 2- FIGURE 4. **RPTP69D TARGETS SEVERAL TYROSINE RESIDUES OF DSCAM1 CT**

*(A) Position of 15 conserved tyrosines in Dscam1 CT (in invertebrates). PDZ domain refers to PDZ-binding site. (B–C) Five Y>F mutations lead to significant decrease of baseline Y-phosphorylation. (B) IP of WT and Met-Dscam1 Y>F mutants before and after HGF addition. (C) Semi-quantitative WB analysis of multiple experiments. Mean values compared to the baseline phosphorylation of WT Met-Dscam1. Baseline phosphorylation is reduced in all five Y > F mutants, but significant reduction in response to HGF is only observed for mutants in SH2-binding sites (Y1857 and Y1890). (n = 5 for YF1707 and YF1911; n = 4 for YF1857; n = 3 for YF1890 and YF1981; ANOVA/Dunnett to compare the phosphorylation states of Met-Dscam1 in presence and absence of HGF: * or p % 0.05; **p % 0.01; ***p % 0.001.) (D) Sequence alignment of the five candidate RPTP69D target sites and known PTP tyrosine substrate residues (Selner et al., 2014). Substrate tyrosines are shown in magenta; acidic or large hydrophobic residues in green. (E and F) RPTP69D interacts with at least two tyrosines of Dscam1 IC. (E) An overexpression-based phosphatase assay to examine RPTP69D-mediated dephosphorylation of Dscam1. Top: Representative WB of the IP of WT Dscam1-HA from S2 cells in the presence and absence of WT RPTP69D-V5. Bottom: Quantification of phosphorylation of mutant Dscam1-HA proteins. Co-expression of RPTP69D significantly reduces the Y-phosphorylation of WT Dscam1-HA as well as Y1707, Y1857, and Y1911 Dscam1-HA mutants. Y-phosphorylation is abolished in YF1890 and YF1981 mutants. Bars represent the mean of several experiments normalized to the baseline phosphorylation of a given construct (in absence of RPTP69D). (n = 3 for YF1707; n = 11 for YF1857; n = 7 for YF1890 and YF1981; n = 4 for YF1911; n = 6 for WT; paired t tests: *p % 0.05; **p % 0.01; ***p % 0.001.) (F) Representative WBs showing single experiments of the over- expression-based phosphatase assay described in (E). Each lane represents data from one gel with lanes from other YF mutations omitted. Error bars: SEM. See also Figure S4.*

Slit enhances Dscam1-RPTP69D interactions and is important for axon collateral formation

Although LOF and GOF alleles of *Dscam1* can affect the formation of all branches of ms-neurons (He et al., 2014), the loss of RPTP69D primarily affects the formation of contra-lateral axon branches. We hypothesized that the apparent spatial specificity of the RPTP69D phenotype is due to either differential subcellular localization of the RPTP69D receptor itself or a compartmentalized control of RPTP69D-Dscam1 interactions. However, overexpression of RPTP69D throughout the growth cone and axon did not result in GOF defects (Figure 3D). The localization of an overexpressed HA-tagged RPTP69D was examined by anti-HA staining and was found to be uniformly distributed and present in growth cones as well as all axon branches (data not shown). These findings suggest that the subcellular restriction of RPTP69D protein is unlikely to account for the mechanism of promoting specific axon collateral formation. Alternatively, the branch-specific functions could arise from local interactions with extracellular cues and ligands activating or recruiting RPTP69D. A previous genetic analysis has uncovered that the secreted guidance cue Slit influences RPTP69D function in the embryonic nervous system (Sun et al., 2000). Consistent with this, we found that mutations in *Slit* cause a frequent truncation or lack of the midline-crossing axon collateral of pSC neurons (Figures 6B, 6C, 6F, and S5A). As *Slit* null mutations are lethal, we used viable transallelic combinations (Tayler et al., 2004). We found that in Sli^{dui}/Sli^{dui} and Sli^{2}/Sli^{dui}, midline-crossing axon branches are absent in 35% to 60% of adults, respectively, and closely phenocopy RPTP69D defects (Figures 6B, 6C, 6F, S5A, and S5D). Moreover, *Slit* mutants show dominant genetic interactions with both *RPTP69D* and *Dscam1* in ms-neurons (Figures 6D–6F and S5B–S5D). In addition, increasing and broadening the expression of Slit in the ventral nerve cord (VNC) using the pan-glial Gal4-transactivator repo-Gal4 resulted in a GOF phenotype with an increase of ectopic midline-crossing axonal branches (Figures S5G and S5H).

Slit is a well-known ligand for the Robo family of axon guidance receptors (Brose et al., 1999; Evans and Bashaw, 2010; Kidd et al., 1999; Spitzweck et al., 2010) and is expressed at the pupal VNC midline (Figures 6G, S5E, and S5F). However, clonal analysis of null alleles of *Robo1* and *Robo2* (Figures 6H, 6I, S6A, and S6C), as well as *Robo3* (Figure S6F), did not reveal any defects of ms-neuron projections. Moreover, ms-neuron-specific KD of each Robo family member or Robo1 and Robo2 together did not reveal defects in ms-

neurons (Figures S6B, S6D, S6E, and S6G). Furthermore, anti-Robo1 and anti-Robo3 antibody stainings suggest that these receptors are not expressed in ms-neurons (Figures S6H–S6K). These results confirm a role of Slit for the formation of specific axon collaterals and suggest that this function of Slit is Robo independent.

Slit enhances RPTP69D-Dscam1 interactions and can directly bind Dscam1

We next examined whether Slit might be directly modulating RPTP69D-dependent regulation of Dscam1 signaling. We found that Slit-conditioned medium enhanced the complex formation of Dscam1 with RPTP69D (Figure 6L). An enhanced Dscam1-RPTP69D interaction was also observed with purified Slit protein (n = 3, Figure S5I). In order to determine whether the observed increase of Dscam1-RPTP69D complex formation had an effect on Dscam1 phosphorylation, we incubated S2 cells with Slit-conditioned supernatant and found that this led to a significant decrease in Dscam1 phosphorylation levels (37% on average, peak value 65% reduction; n = 5, Figure 6M).

Importantly, recent studies on Slit processing and receptor binding suggested that an N-terminal fragment of Slit (Slit-N) might directly bind to the N-terminal Ig domains of Dscam1 (M.S. and T.K., data not shown). We therefore directly measured the binding affinity of a purified N-terminal fragment of Dscam1 and Slit-N by using a standard alkaline phosphatase-based enzymatic assay (Experimental Procedures). We used purified protein of the first four Ig domains of Dscam1 (Dscam-EC4) fused to the antibody constant region (Fc) domain (Wojtowicz et al., 2004) and Slit-N fused to alkaline phosphatase (AP-Slit-N) (Figures 6J and 6K). From five independent experiments, we determined an average dissociation constant K_D of 22.2 ± 2.85 nM for Slit-N/Dscam-EC4 binding. In addition, co-IP experiments from S2 cell supernatant expressing a secreted form of Dscam1 (Dscam-EC10; Wojtowicz et al., 2004) revealed that full-length Slit protein was also able to physically interact with the extracellular domain of Dscam1 (Figure 6N).

In summary, the biochemical data suggest that Slit can directly bind Dscam1 and enhance RPTP69D-Dscam1 interactions as well as Dscam1 dephosphorylation.

RPTP69D and Slit are specifically required for axon collateral selection and extension

In order to investigate the developmental mechanism by which RPTP69D and Slit regulate axon collateral formation, we employed a genetic labeling strategy (see Supplemental Experimental Procedures) (He et al., 2014) to visualize single pSC growth cones during development (Figure 7). During early pupal development, pSC growth cones undergo a highly dynamic sequence of morphological transitions lasting about 12–15 hr. During an early phase (‘‘sprouting phase’’), many different processes extend from a highly complex growth cone into all directions (Figure 7A). Whereas some processes are very thin filopodia-like, others are thicker and exhibit their own side branches (e.g., dotted circles in Figures 7A, 7E, and 7I). In analogy to what has been described for sprouting sensory neurites in amphibian embryos (Roberts and Taylor, 1983), we refer to these processes as ‘‘micropodia’’. Comparing WT with *RPTP69D* or *Slit* mutant growth cones, we were unable to find any morphological differences between sprouting growth cones, neither in overall shape, nor extent of sprouting, nor presence of filopodia or micropodia (Figures 7A, 7E, and 7I).

During an intermediate phase (Figures 7B, 7C, 7F, 7G, 7J, and 7K), two primary axon branches become apparent, segregating in opposite (anterior-posterior) directions. At this stage some micropodia appear to have small distinct growth cone-like tips, which we refer to as ‘‘satellite growth cones’’ (e.g., arrows and arrow- heads in Figures 7B, 7C, 7F, 7G, 7J, and 7K). Satellite growth cones are present in WT as well as mutant samples. Importantly, however, in WT, micropodia projecting toward the midline can be detected in most samples (e.g., arrows in Figures 7B and 7C). In contrast, in *RPTP69D* or *Slit* mutant animals, distinct midline- directed micropodia are rare and only very short (Figures 7G and 7K). Quantifications of midline-directed micropodia and total number of processes confirm that mutant pSC axons reveal a specific inhibition of midline-directed collaterals (Figures 7M–7’).

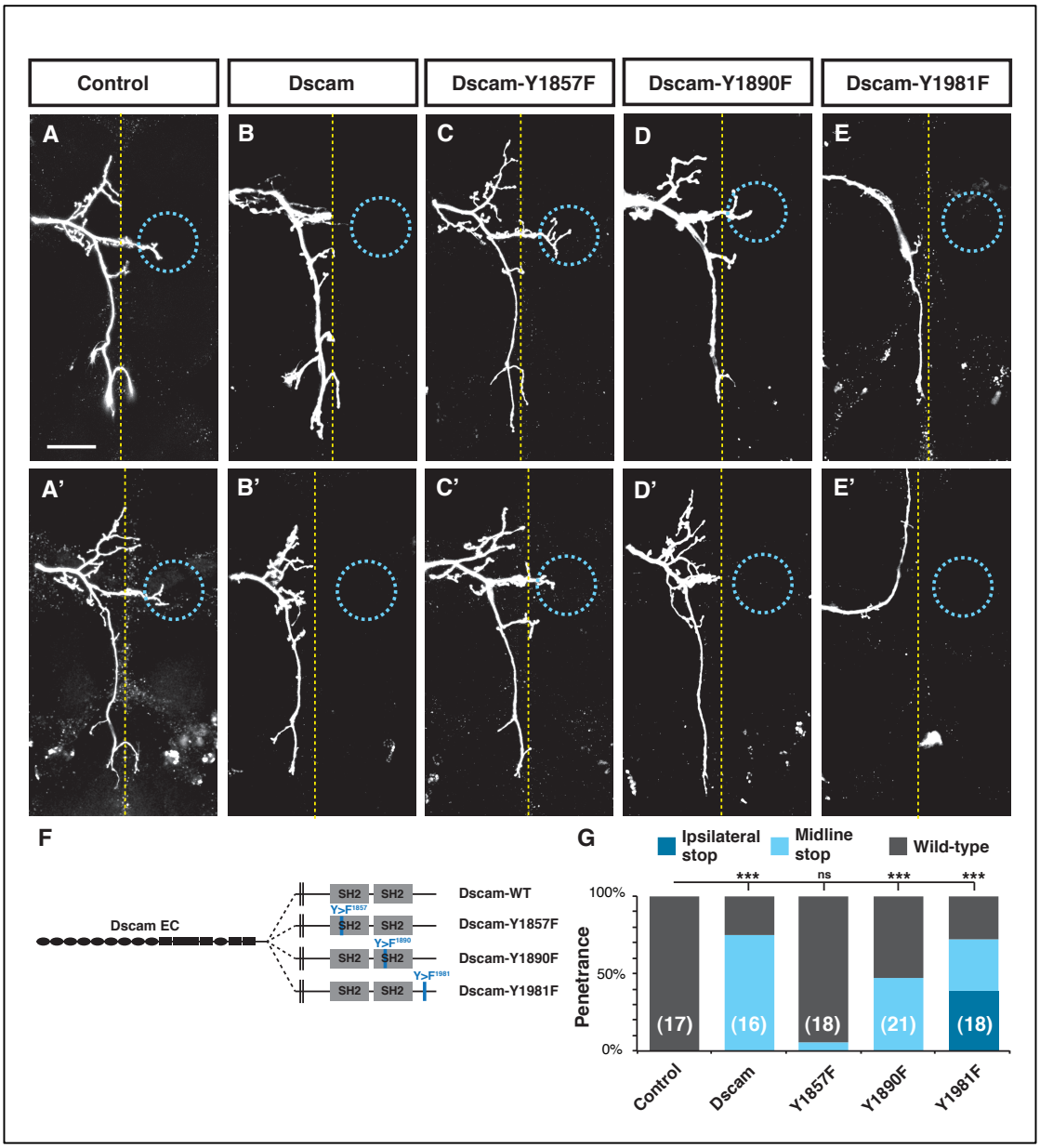

CHAPTER 2- FIGURE 5. **THE RPTP69D-TARGET SITES ARE IMPORTANT FOR DSCAM1 FUNCTION *IN VIVO***

*(A–E) Representative confocal images of pDC dye-fills. (A and A') WT pDC neurons have a stereotypical branching pattern similar to that of pSC neurons. (B–E) Overexpression of WT or mutated Dscam1 isoforms in single pDC neurons (see Figure S1A) results in branching defects. Whereas expression of WT Dscam1 leads to truncation or shortening of the anterior midline-crossing collateral (B and B'), expression of the Y > F1857 Dscam1 mutant does not (C) or only weakly (C'). Expression of the Y > F1890 Dscam1 mutant (D and D') results in weak defects (D'). Expression of the Y > F1981 Dscam1 mutant leads to dominant defects that affect all axon collaterals (E and E'). (F) Schematics of the different Dscam1 mutants. (G) Quantification of the phenotypic defects. Statistics: chi-square, ***p < 0.001.*

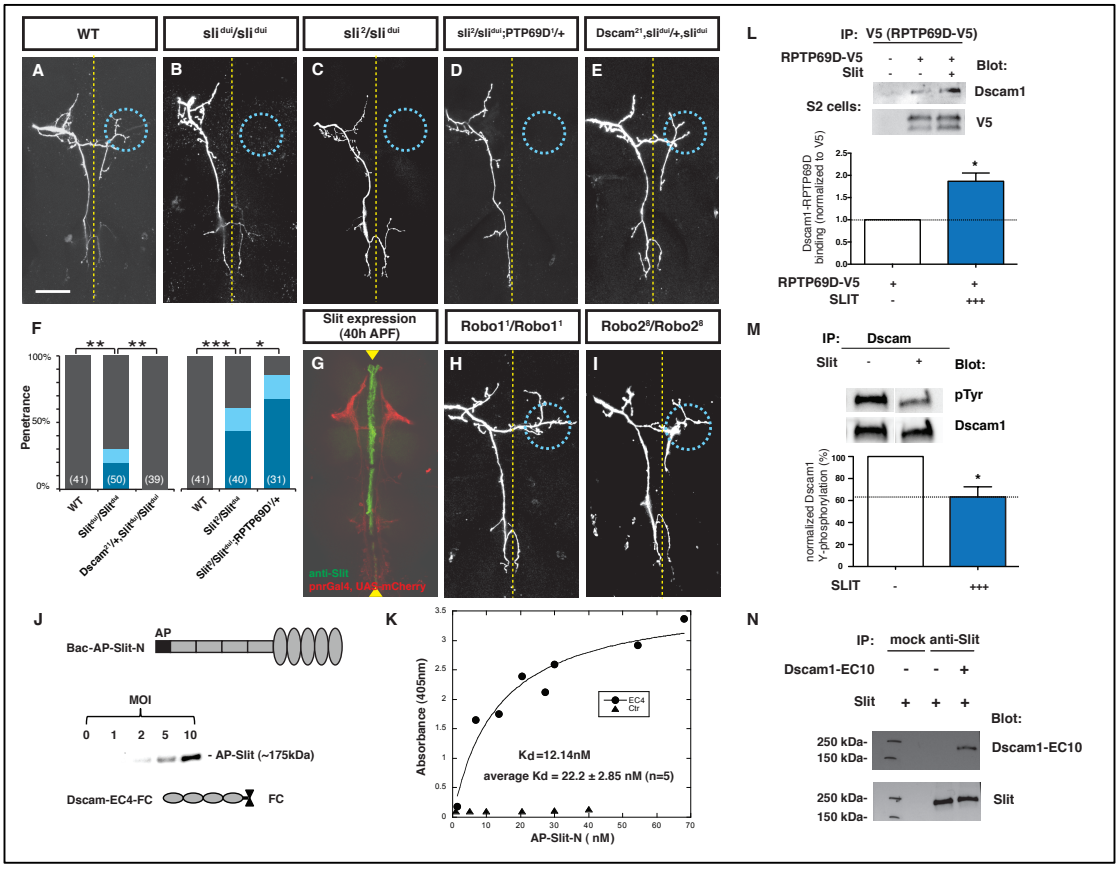

CHAPTER 2- FIGURE 6. **SLIT IS REQUIRED FOR MIDLINE COLLATERAL FORMATION AND ENHANCES RPTP69D-DSCAM COMPLEX FORMATION BY BINDING TO DSCAM1.**

*(A–E) Representative confocal images of pSC dye-fills. (B and C) Reduction of Slit expression in Sli^{dui}/Sli^{dui} (B) or Sli^{2}/Sli^{dui} (C) mutants results in defects similar to those observed in RPTP69D mutants. Removal of one copy or RPTP69D enhances the penetrance of midline collateral defects in Sli2/Slidui flies (D). Removal of one copy of Dscam1 reduces the defects seen in Slidui/Slidui flies (E). (F) Quantifications of the genetic interactions. Statistics: chi-square test, *p % 0.05; **p % 0.01; ***p < 0.001. (G) Slit is expressed at the VNC midline during pupal development. Expression is strongly reduced in Slidui/Slidui flies (see Figure S5F). (H and I) MARCM clones for Robo1 and Robo2 in ms-neurons show that neither Robo1 nor Robo2 LOF affects branching of ms-neurons (for Robo3, see Figure S6F). (J) Schematic representation of the protein expression constructs. Top: Alkaline phosphatase (AP) was fused to the Slit-N fragment consisting of the N-terminal 4 LRR-repeats (boxes) and the 5 EGF-like domains (circles) and expressed by baculovirus-mediated infection of high five cells (see Experimental Procedures). The optimal MOI (pfu/cell) was found to be 10. Bottom: A Dscam1-EC4 construct consisting of the N-terminal 4 Dscam1-IG domains fused to Fc tag. (K) Representative binding curve for AP-Slit-N and EC4. Five independent experiments with an average KD for Slit-N/Dscam1-EC4 binding of 22.2 ± 2.85 nM. (L) Slit promotes the formation of a Dscam1-RPTP69D complex. Co-IP of Dscam1 and RPTP69D from a stable cell line shows small amounts of Dscam1- RPTP69D complex, which is significantly increased when cells were incubated with Slit-conditioned medium (Experimental Procedures). Complexes were assessed by semi-quantitative WB analysis. Top: Representative WB of one experiment. Bottom: Quantification of multiple independent experiments (n = 3 experiments; paired t test, *p % 0.05). (M) Slit incubation leads to Dscam1 dephosphorylation in S2 cells. Endogenous Dscam1 was immunoprecipitated from S2 cells incubated with or without Slit. Phosphorylation levels were evaluated by semi-quantitative WB analysis. Top: representative WB from one experiment. Bottom: Quantification of multiple independent experiments (n = 5 experiments; paired t test, *p % 0.05). (N) Slit and the extracellular domain of Dscam1 can physically interact in vitro. IP of Slit and Dscam1 extracellular domain (EC10) from conditioned S2 cell media (Experimental Procedures). Error bars: SEM. See also Figures S5 and S6.*

In later stages, the midline-projecting axon collateral become more prominent and grow contralaterally. During this phase micropodia start disappearing, whereas filopodia remain concentrated at branching points and distal parts of extending axon branches (Figure 7D). At this stage most mutant axons exhibit only short processes or stubs (Figures 7H and 7L) that are present at axon segments, whereas in WT a prominent commissural axon collateral has formed (Figures 7D).

In summary, the single-growth-cone analysis suggests that Slit and RPTP69D are unlikely to influence axon sprouting, or branch initiation of ms-neurons, but rather control the selective consolidation and directed extension of midline-crossing axon branches.

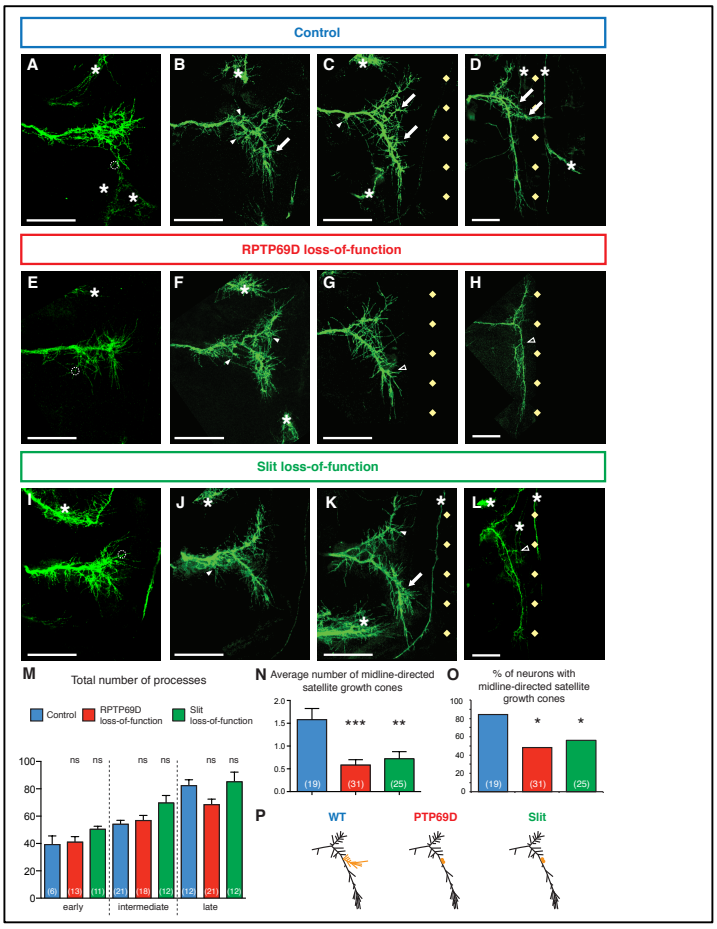

CHAPTER 2- FIGURE 7. **RPTP69D AND SLIT ARE REQUIRED FOR SPECIFIC AXON-BRANCH CONSOLIDATION AND EXTENSION BUT NOT BRANCH INITIATION.**

*(A–L) Single-growth-cone analysis. Representative confocal images of single pSC axons expressing GFP under a pSC-specific Gal4 driver, at early (first column), intermediate (second and third columns), and later stages (last column). All samples were collected between 23 hr and 30 hr after puparium formation (APF). Midline position is indicated by yellow diamonds. Stochastic ectopic GFP expression in unrelated neurons/axons occurs occasionally and is indicated by asterisks. WT pSC axons (A) as well as RPTP69D (E) and Slit (I) mutant growth cones are highly complex, displaying a great number of filopodia and micropodia processes (dotted circles) during early stages when the growth cones start to expand and sprout (B and C). In intermediate stages, a separation into a posterior and anterior axon branch compartment is recognizable (B, C, F, G, J, and K). Numerous micropodia can be observed, some of which show small globular tips (satellite growth cones) and secondary short filopodia (arrowheads in B, C, F, and K). A subset of micropodia are midline directed (arrows, B, C, and D) and form stable axon branches (white arrows, C and D). In WT, sometimes two anterior midline-directed collateral branches are present (arrows in C and D), but only one is stabilized subsequently. The axons of RPTP69D (E–H) and Slit (I–L) mutants are still able to form many processes early (E and I), but at intermediate stages, midline-directed projections of micropodia with satellite growth cones are shorter and stunted (arrows in G and K). An impairment of the ability to extend toward the midline persists into later stages (H and L, open arrowheads). In most cases, mis-directed (H) or stunted (L) micropodia fail to mature into an anterior midline-directed collateral projection. (M) Quantification of the total number of processes (filopodia and micropodia) at different developmental stages in control, RPTP69D, and Slit mutants. There are no significant differences in total process numbers between control and RPTP69D or Slit mutant axons (M). (N and O) Quantifications of midline-directed micropodia with satellite growth cones (intermediate and late stages). There are reduced numbers of midline-directed collateral growth cones in RPTP69D and Slit mutant axons. Maximum length of the main shaft was used to assign samples to one of three stage groups: early: < 30 µm, intermediate: 30 and 60 µm, and late: > 90 µm. (P) Schematic of the defects observed in RPTP69D and Slit mutant growth cones: although processes are still formed, their midline-directed extension and consolidation are impaired. Statistics: one-way ANOVA followed by Dunnett multiple comparisons, **p % 0.005; ***p % 0.001 (M and N); Fisher's exact test, *p % 0.05 (O). Scale bars represent 25 µm. Error bars: SEM. See also Figure S7.*

Chapter 2- DISCUSSION

This study reports on a molecular mechanism regulating Dscam1 activity in growth cones and provides insight in the regulation and spatial specificity of axon collateral formation. Biochemical and genetic results are consistent with the molecular model that the specificity of ms-axon branching arises from a spatially restricted change of Dscam1 phosphorylation in growth cones.

Dscam1-Dscam1 interactions can be modulated by extracellular cues

Previous studies on the function of Dscam1 have established the model that isoform-specific homophilic Dscam1-Dscam1 inter- actions trigger repulsion between sister dendrites (Hughes et al., 2007; Matthews et al., 2007; Soba et al., 2007). This controls for regular spacing of sister dendrites in a process termed neurite self-avoidance. In addition, cell-intrinsic and isoform-specific interactions have also been shown to be important in sensory axons for growth-cone sprouting and branching (He et al., 2014). Importantly, for both of these functions, it is thought that Dscam1 signaling is primarily dependent on and initiated by homophilic binding of matching isoforms present on sister neurites (Hattori et al., 2009; He et al., 2014; Wojtowicz et al., 2007). The results reported here provide evidence that Dscam1-Dscam1 interactions in axonal growth cones are subject to branch-specific modulation by extrinsic cues. Binding of the ligand Slit to Dscam1 can locally enhance *cis*-interactions with the receptor tyrosine phosphatase RPTP69D as well as the dephosphorylation of Dscam1. Although homophilic Dscam1 interactions can be considered to play an initial permissive role in all neurite-neurite interactions in a sprouting growth cone, the spatial restriction of an extrinsic Dscam1 ligand likely initiates functional disparity of Dscam1 signaling across different growth-cone compartments.

Dscam1 Is a RPTP69D Substrate, and Specific Phosphorylation Events Regulate Dscam1 Activity In Vivo

The biochemical data support the notion that RPTP69D directly dephosphorylates Dscam1

at specific cytoplasmic tyrosines. We identified three candidate tyrosines for the regulation of Dscam1 phosphorylation: Y1857, Y1890, and Y1981. Two of the tyrosine residues, Y1857 and Y1890, are part of consensus SH2-binding sites and therefore are likely involved in regulating recruitment of SH2-domain-containing adaptor molecules. Given that these mutations diminish the Dscam1 GOF effects, it seems reasonable to speculate that they are required for downstream signaling and/or receptor turn-over or trafficking. Surprisingly, the single Y1981F mutation causes strong dominant interference with axon branching where the phenotypic effects are qualitatively indistinguishable from a loss of Dscam1 isoform diversity (He et al., 2014), which is thought to increase the probability of matching isoform interactions (i.e., GOF activity). The primary amino acid sequence surrounding Y1981 does not reveal any distinct signaling motif. However, in silico 3D protein modeling based on structural predictions suggests that phosphorylation of Y1981 could directly result in structural changes of the Dscam1 cytoplasmic domain and thereby influence Dscam1 activity (M-L. E. and D.S., data not shown; see also Chapter 3-Discusssion).

Slit is a ligand for Dscam1 in a Robo1–3-independent pathway

Biochemical results suggest that Slit can enhance Dscam1- RPTP69D complex formation and Dscam1 dephosphorylation. Furthermore, Slit-N can directly bind to the N-terminal Ig do- mains of Dscam1 (Ig1–4) with an affinity comparable to that of other guidance cue/receptor interactions, suggesting that Slit-N can function as a *bona fide* Dscam1 ligand. Numerous studies have shown that the repellent as well as the branch-promoting function of vertebrate Slit require the function of Robo receptors (Brose et al., 1999; Ma and Tessier-Lavigne, 2007; Wang et al., 1999). Our results show that for the formation of specific axon collaterals of *Drosophila* ms-neurons, Slit functions via Dscam1 in a Robo1–3-independent pathway. Slit is one of the best characterized ‘‘axon-repellent’’ cues and also contributes to axon branching (Chedotal, 2007). Imaging single ms-axons and growth-cone branching, we find that in Slit mutant animals, only filopodia or micropodia with a midline-directed growth direction are reduced, consistent with a positive role of Slit in promoting the extension of specific branches. In contrast, branch-point initiation in ms-neurons is likely independent of Slit or RPTP69D.

Slit drives spatial specificity of Dscam1-RPTP69D interactions

Given that high Slit protein concentrations are likely only encountered by filopodia- or micropodia-like extensions that reach the midline proximity, the Slit-Dscam1-RPTP69D interactions are likely only occurring in a spatially restricted sub-compartment of the branching growth cone. We envision that the Dscam1-RPTP69D interactions in ms-axons constitute a molecular selection process, which depends on Dscam1-RPTP69D complex formation in a subset of axonal processes that encounter sufficient Slit protein (Figure S7). As a result, Dscam1 dephosphorylation by RPTP69D is increased locally and triggers a response by either promoting axon-branch extension or blocking repulsion.

The loss of only a subset of axon branches in RPTP69D/Slit mutants suggests that there are multiple molecular control pathways accounting for the selection of different axon collaterals or the extension of the main axon shaft. Although this study has focused on RPTP69D and Slit, it is most likely that other co-receptors and extracellular cues control the activity of Dscam1 in growth cones.

Chapter 2- EXPERIMENTAL PROCEDURES

Cell Culture

S2 cells, Slit-expressing cells, and BG3C2 cells were obtained from DGRC. S2 cells were grown in SF-900 Insect Medium (*Life Technologies*), and BG3C2 cells in Schneider's medium (*Life Technologies*) (10% FBS (*Life Technologies*), BPYE (*Difco*), and insulin [10 mg/ml (*Sigma)*]. Stable cell lines were grown in the presence of Blasticidin (*Life Technologies*) or Hygromycin (*Sigma-Aldrich*). Expression was induced using CuSO4 (Sigma- Aldrich) (750 mM final concentration). The Met-Dscam1 receptor was activated by addition of HGF (*ebioscience*) to the culture medium supplemented with FBS. Conditioned media were harvested after 2 days. For experiments testing the effect of Slit on Dscam1 complex formation or phosphorylation, we added concentrated Slit-conditioned medium at a Slit concentration > 10 mg/ml. For controls, cells were incubated with conditioned medium from WT S2 cells.

Cells were transfected using the Amaxa Nucleofector II device (*Lonza*) with 1 to 2 mg of a given plasmid/double-stranded RNA (dsRNA) (solution V, program D023).

For AP-Slit production, PCR-amplified Slit-N fragment was used to generate a recombinant bacmid in the Bac to Bac HBM expression system (*Life Technologies*). Viral particles were produced in *Sf9 cells* for infection of *high five cells*. Protein concentrations were determined using AP Assay Reagent A (*GenHunter*).

IPs

Cells were harvested post-transfection (day 2 for *S2 cells*; day 5 for *BG3C2 cells*) and lysed in *RIPA* buffer containing protease inhibitors (*Pierce*) and if necessary phosphatase inhibitors (*Sigma-Aldrich*). Lysates were incubated with beads coated with IP-antibody. Antibodies used in this study are described in the Supplemental Experimental Procedures. Proteins were detected using *Pierce* ECL Substrate and analyzed with Chemi-Doc-IT imager with Vision-Works-LS software (*UVP*).

Reagents

Buffers, constructs, Taqman probes, qPCR reagents, dsRNA, and protocols are described in the *"GENERAL MATERIAL AND METHODS"* section of this dissertation and are also available upon request.

Kinetic Binding Studies

Media containing the Dscam-EC4-FC fusion protein (Wojtowicz et al., 2004) were incubated with protein G Dynabeads for 1 hr at room temperature (RT) and then washed with high-salt binding buffer (100 mM phosphate buffer with 1M NaCl, 10 U/ml heparin, 1 mM DTT, 0.2 mM PMSF, and 1/1000 proteinase inhibitor cocktail). AP-Slit was added to the Dscam-EC4 beads, incubated for 1 hr, and washed with high-salt binding buffer. Amount of bound AP-Slit-N was determined using AP Assay Reagent A. Absorbance was measured at 405 nm using a microplate spectrophotometer. For negative controls, supernatant from high five cells only or human anti-IgG Fc fragment were used. Data were plotted with KaleidaGraph (*Synergy software*) and fitted to a Michaelis Menton curve to generate the K_D value.

Genetics

Alleles and transgenes are provided in the Supplemental Experimental Procedures. RNAi lines were obtained from the *VDRC* and *TriP* collections. P-element and fC31-directed integration was performed by *Genetic Services* (MA) and *Rainbow Transgenics* (CA).

All crosses were performed at 25°C, except for RPTP69D hypomorphs, for which a shift to 18°C at mid-pupal stage was used (Desai and Purdy, 2003). Single-cell labeling and transgene expression were performed as described (Urwyler et al.,2015).

Immunohistochemistry

Immunostaining of adult brains and VNCs was done as described (Pfeiffer et al., 2008). Antibodies/concentrations used in this study are listed in the Supplemental Experimental Procedures.

Image Acquisition/Analysis

Images were taken using a Zeiss LSM 710 confocal microscope and processed using *FIJI* and *Adobe PhotoShop* software. z-stack confocal images were flattened and despeckled. Intensity levels and orientation of images were adjusted for better comparisons.

Statistical analysis was performed using *Prism 6* software.

Chapter 2- ACKNOWLEDGMENTS

This work was supported by NIH (2RO1NS046747-05A1) (D.S.); FWO (G059611N) (D.S.); FWO (G078913N) (D.S.); FWO (G077013N) (D.S.); BELSPO IUAP VII-20 ‘‘WIBRAIN’’ (D.S.); VIB funding; and fellowships of FWO (D.D.), ***Boehringer Ingelheim Fonds (M.-L.E.*** and S.S.), EMBO (M.P.), JSPS & HFSP (Y.K.), and SNSF (O.U.). The work of T.K. and M.S. was supported by NSF (IOS-1052555), the National Center for Research Resources (P20RR016464, 5P20RR024210), and the NIGM (8 P20 GM103554) from the NIH. We thank Tineke Breynaert for technical help (cell culture). We thank members of the lab, Paul Garrity (Brandeis University), Fritz Rathjen (MDC, Berlin), Bassem Hassan, Matthew Holt, and Georg Halder (VIB) for critical reading, discussions, and insightful comments. We would like to thank the Clemens, Bashaw, Dickson, Zinn, Suzuki, Treisman, Lee, Hassan, Kidd, and Bogdan labs for fly stocks, antibodies, and plasmids. For cell lines and antibodies, we thank the DGRC, supported by NIH grant 2P40OD010949-10A1, and the DSHB, created by the NICHD of the NIH and maintained by the university of Iowa.

Chapter 2- REFERENCES

Berger, J., Senti, K.-A., Senti, G., Newsome, T.P., Asling, B., Dickson, B.J., and Suzuki, T. (2008). Systematic identification of genes that regulate neuronal wiring in the Drosophila visual system. PLoS Genet. 4, e1000085.

Blanchetot, C., Chagnon, M., Dube, N., Halle, M., and Tremblay, M.L. (2005). Substrate-trapping techniques in the identification of cellular PTP targets. Methods 35, 44–53.

Brose, K., Bland, K.S., Wang, K.H., Arnott, D., Henzel, W., Goodman, C.S., Tessier-Lavigne, M., and Kidd, T. (1999). Slit proteins bind Robo receptors and have an evolutionarily conserved role in repulsive axon guidance. Cell 96, 795–806.

Campbell, D.S., Stringham, S.A., Timm, A., Xiao, T., Law, M.-Y., Baier, H., Nonet, M.L., and Chien, C.-B. (2007). Slit1a inhibits retinal ganglion cell arborization and synaptogenesis via Robo2-dependent and -independent path- ways. Neuron 55, 231–245.

Chedotal, A. (2007). Slits and their receptors. Adv. Exp. Med. Biol. 621, 65–80.

Chen, B.E., Kondo, M., Garnier, A., Watson, F.L., Puettmann-Holgado, R., Lamar, D.R., and Schmucker, D. (2006). The molecular diversity of Dscam is functionally required for neuronal wiring specificity in *Drosophila*. Cell *125*, 607–620.

Desai, C., and Purdy, J. (2003). The neural receptor protein tyrosine phosphatase DPTP69D is required during periods of axon outgrowth in Drosophila. Genetics *164*, 575–588.

Evans, T.A., and Bashaw, G.J. (2010). Axon guidance at the midline: of mice and flies. Curr. Opin. Neurobiol. *20*, 79–85.

Flint, A.J., Tiganis, T., Barford, D., and Tonks, N.K. (1997). Development of ''substrate-trapping'' mutants to identify physiological substrates of protein tyrosine phosphatases. Proc. Natl. Acad. Sci. USA *94*, 1680–1685.

Garrity, P.A., Lee, C.H., Salecker, I., Robertson, H.C., Desai, C.J., Zinn, K., and Zipursky, S.L. (1999). Retinal axon target selection in Drosophila is regulated by a receptor protein tyrosine phosphatase. Neuron *22*, 707–717.

Ghysen, A. (1978). Sensory neurons recognize defined pathways in Drosophila central nervous system. Nature *274*, 864–872.

Hao, J.C., Adler, C.E., Mebane, L., Gertler, F.B., Bargmann, C.I., and Tessier- Lavigne, M. (2010). The tripartite motif protein MADD-2 functions with the receptor UNC-40 (DCC) in Netrin-mediated axon attraction and branching. Dev. Cell *18*, 950–960.

Hattori, D., Millard, S.S., Wojtowicz, W.M., and Zipursky, S.L. (2008). Dscam- mediated cell recognition regulates neural circuit formation. Annu. Rev. Cell Dev. Biol. *24*, 597–620.

Hattori, D., Chen, Y., Matthews, B.J., Salwinski, L., Sabatti, C., Grueber, W.B., and Zipursky, S.L. (2009). Robust discrimination between self and non-self neurites requires thousands of Dscam1 isoforms. Nature *461*, 644–648.

He, H., Kise, Y., Izadifar, A., Urwyler, O., Ayaz, D., Parthasarthy, A., Yan, B., Erfurth, M.L., Dascenco, D., and Schmucker, D. (2014). Cell-intrinsic requirement of Dscam1 isoform diversity for axon collateral formation. Science *344*, 1182–1186.

Hofmeyer, K., and Treisman, J.E. (2009). The receptor protein tyrosine phosphatase LAR promotes R7 photoreceptor axon targeting by a phosphatase-independent signaling mechanism. Proc. Natl. Acad. Sci. USA *106*, 19399–19404.

Hughes, M.E., Bortnick, R., Tsubouchi, A., Bäumer, P., Kondo, M., Uemura, T., and Schmucker, D. (2007). Homophilic Dscam interactions control complex dendrite morphogenesis. Neuron *54*, 417–427.

Hummel, T., Vasconcelos, M.L., Clemens, J.C., Fishilevich, Y., Vosshall, L.B., and Zipursky, S.L. (2003). Axonal targeting of olfactory receptor neurons in Drosophila. Neuron *37*, 221–231.

Johnson, K.G., and Van Vactor, D. (2003). Receptor protein tyrosine phosphatases in nervous system development. Physiol. Rev. *83*, 1–24.

Kidd, T., Bland, K.S., and Goodman, C.S. (1999). Slit is the midline repellent for the robo receptor in *Drosophila*. Cell *96*, 785–794.

Kim, J.H., Wang, X., Coolon, R., and Ye, B. (2013). Dscam expression levels determine presynaptic arbor sizes in *Drosophila* sensory neurons. Neuron *78*, 827–838.

Kise, Y. and Schmucker, D. (2013). Role of self-avoidance in neuronal wiring. Curr. Opin. Neurobiol. *23*, 983–989.

Kurusu, M., and Zinn, K. (2008). Receptor tyrosine phosphatases regulate birth order-dependent axonal fasciculation and midline repulsion during development of the Drosophila mushroom body. Mol. Cell. Neurosci. *38*, 53–65.

Liu, Y. and Halloran, M.C. (2005). Central and peripheral axon branches from one neuron are guided differentially by Semaphorin3D and transient axonal glycoprotein-1. J. Neurosci. *25*, 10556–10563.

Ma, L., and Tessier-Lavigne, M. (2007). Dual branch-promoting and branch- repelling actions of Slit/Robo signaling on peripheral and central branches of developing sensory axons. J. Neurosci. *27*, 6843–6851.

Matthews, B.J., Kim, M.E., Flanagan, J.J., Hattori, D., Clemens, J.C., Zipursky, S.L., and Grueber, W.B. (2007). Dendrite self-avoidance is controlled by Dscam. Cell *129*, 593–604.

McLaughlin, T., Hindges, R., Yates, P.A., and O'Leary, D.D. (2003). Bifunctional action of ephrin-B1 as a repellent and attractant to control bidirectional branch extension in dorsal-ventral retinotopic mapping. Development *130*, 2407–2418.

Muda, M., Worby, C.A., Simonson-Leff, N., Clemens, J.C., and Dixon, J.E. (2002). Use of double-stranded RNA-mediated interference to determine the substrates of protein tyrosine kinases and phosphatases. Biochem. J. *366*, 73–77.

Pfeiffer, B.D., Jenett, A., Hammonds, A.S., Ngo, T.-T.B., Misra, S., Murphy, C., Scully, A., Carlson, J.W., Wan, K.H., Laverty, T.R., et al. (2008). Tools for neuro- anatomy and neurogenetics in Drosophila. Proc. Natl. Acad. Sci. USA *105*, 9715–9720.

Polleux, F., Morrow, T., and Ghosh, A. (2000). Semaphorin 3A is a chemoattractant for cortical apical dendrites. Nature *404*, 567–573.

Purohit, A.A., Li, W., Qu, C., Dwyer, T., Shao, Q., Guan, K.-L., and Liu, G. (2012). Down syndrome cell adhesion molecule (DSCAM) associates with un- coordinated-5C (UNC5C) in netrin-1-mediated growth cone collapse. J. Biol. Chem. *287*, 27126–27138.

Ren, L., Chen, X., Luechapanichkul, R., Selner, N.G., Meyer, T.M., Wavreille, A.-S., Chan, R., Iorio, C., Zhou, X., Neel, B.G., and Pei, D. (2011). Substrate specificity of protein tyrosine phosphatases 1B, RPTPa, SHP-1, and SHP-2. Biochemistry *50*, 2339–2356.

Roberts, A., and Taylor, J.S. (1983). A study of the growth cones of developing embryonic sensory neurites. J. Embryol. Exp. Morphol. *75*, 31–47.

Schmucker, D., Clemens, J.C., Shu, H., Worby, C.A., Xiao, J., Muda, M., Dixon, J.E., and Zipursky, S.L. (2000). Drosophila Dscam is an axon guidance receptor exhibiting extraordinary molecular diversity. Cell *101*, 671–684.

Selner, N.G., Luechapanichkul, R., Chen, X., Neel, B.G., Zhang, Z.-Y., Knapp, S., Bell, C.E., and Pei, D. (2014). Diverse levels of sequence selectivity and catalytic efficiency of protein-tyrosine phosphatases. Biochemistry *53*, 397–412.

Soba, P., Zhu, S., Emoto, K., Younger, S., Yang, S.-J., Yu, H.-H., Lee, T., Jan, L.Y., and Jan, Y.-N. (2007). Drosophila sensory neurons require Dscam for dendritic self-avoidance and proper dendritic field organization. Neuron *54*, 403–416.

Spitzweck, B., Brankatschk, M., and Dickson, B.J. (2010). Distinct protein domains and expression patterns confer divergent axon guidance functions for *Drosophila* Robo receptors. Cell *140*, 409–420.

Sun, Q., Bahri, S., Schmid, A., Chia, W., and Zinn, K. (2000). Receptor tyrosine phosphatases regulate axon guidance across the midline of the Drosophila embryo. Development *127*, 801–812.

Sun, W., You, X., Gogol-Döring, A., He, H., Kise, Y., Sohn, M., Chen, T., Klebes, A., Schmucker, D., and Chen, W. (2013). Ultra-deep profiling of alternatively spliced Drosophila Dscam isoforms by circularization-assisted multi-segment sequencing. EMBO J. *32*, 2029–2038.

Tayler, T.D., Robichaux, M.B., and Garrity, P.A. (2004). Compartmentalization of visual centers in the Drosophila brain requires Slit and Robo proteins. Development *131*, 5935–5945.

Tonks, N.K. (2006). Protein tyrosine phosphatases: from genes, to function, to disease. Nat. Rev. Mol. Cell Biol. *7*, 833–846.

Tonks, N.K. (2013). Protein tyrosine phosphatases—from housekeeping enzymes to master regulators of signal transduction. FEBS J. *280*, 346–378.

Urwyler, O., Izadifar, A., Dascenco, D., Petrovic, M., He, H., Ayaz, D., Kremer, A., Lippens, S., Baatsen, P., Guérin, C.J., and Schmucker, D. (2015). Investigating CNS synaptogenesis at single-synapse resolution by combining reverse genetics with correlative light and electron microscopy. Development *142*, 394–405.

Wang, J., Zugates, C.T., Liang, I.H., Lee, C.-H.J., and Lee, T. (2002). *Drosophila* Dscam is required for divergent segregation of sister branches and suppresses ectopic bifurcation of axons. Neuron *33*, 559–571.

Wang, K.H., Brose, K., Arnott, D., Kidd, T., Goodman, C.S., Henzel, W., and Tessier-Lavigne, M. (1999). Biochemical purification of a mammalian slit protein as a positive regulator of sensory axon elongation and branching. Cell *96*, 771–784.

Wojtowicz, W.M., Flanagan, J.J., Millard, S.S., Zipursky, S.L., and Clemens, J.C. (2004). Alternative splicing of *Drosophila* Dscam generates axon guidance receptors that exhibit isoform-specific homophilic binding. Cell *118*, 619–633.

Wojtowicz, W.M., Wu, W., Andre, I., Qian, B., Baker, D., and Zipursky, S.L. (2007). A vast repertoire of Dscam binding specificities arises from modular interactions of variable Ig domains. Cell *130*, 1134–1145.

Yeo, S.-Y., Miyashita, T., Fricke, C., Little, M.H., Yamada, T., Kuwada, J.Y., Huh, T.-L., Chien, C.-B., and Okamoto, H. (2004). Involvement of Islet-2 in the Slit signaling for axonal branching and defasciculation of the sensory neurons in embryonic zebrafish. Mech. Dev. *121*, 315–324.

Zhan, X.-L., Clemens, J.C., Neves, G., Hattori, D., Flanagan, J.J., Hummel, T., Vasconcelos, M.L., Chess, A., and Zipursky, S.L. (2004). Analysis of Dscam diversity in regulating axon guidance in Drosophila mushroom bodies. Neuron *43*, 673–686.

Chapter 2- SUPPLEMENTAL INFORMATION

Supplemental Figures

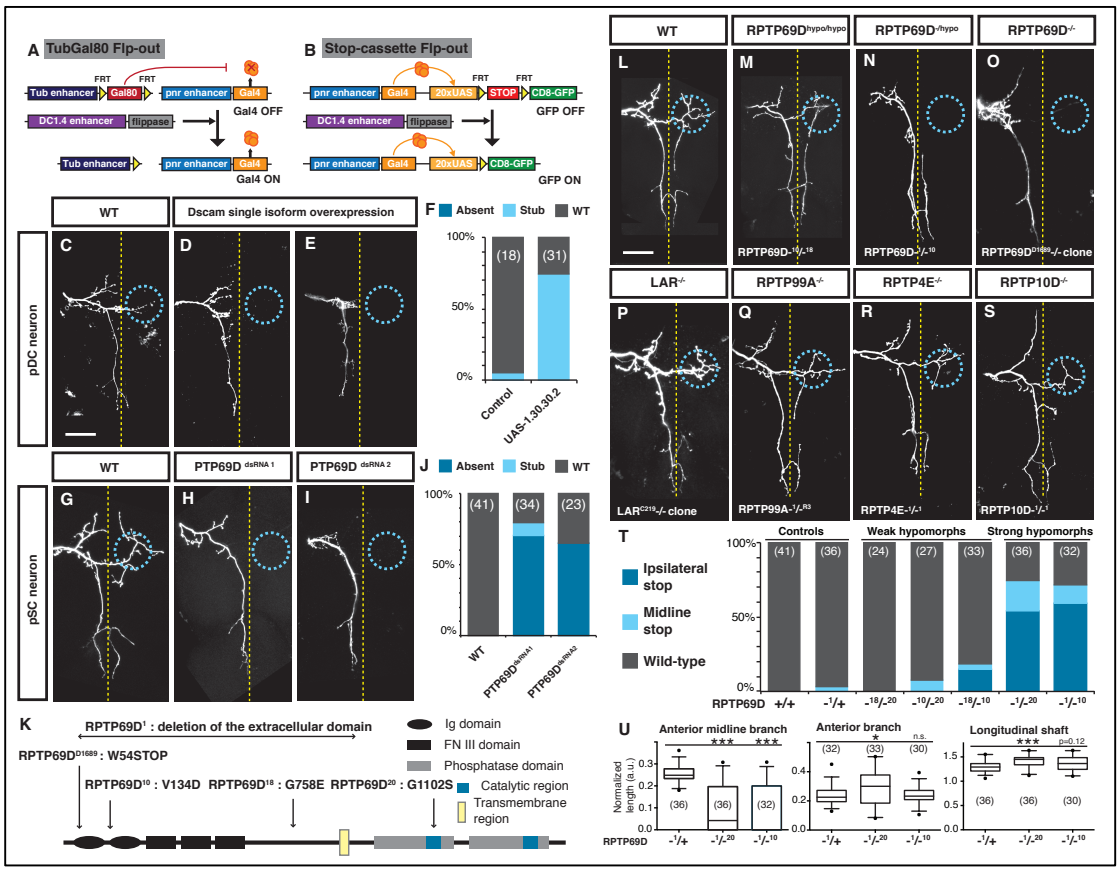

FIGURE S 1. **RPTP69D IS THE ONLY RPTP INVOLVED IN MS-NEURON COLLATERAL FORMATION (RELATED TO FIGURE 1).**

*(A, B) Different Flip-recombinase-based genetic strategies were used in this study to confine expression of the Gal4-transactivator to single ms-neurons (A) or to selectively label single ms-neurons using CD8-GFP (B). (C-F) Over-expression of a single Dscam1 isoform in single pDC neurons leads to a specific defect in the formation of the anterior midline-directed collateral (D, E). Expression of a Dscam1 1.30.30.2 isoform using the method described in panel (A) leads to strong defects in the formation of the anterior midline collateral (D, E) compared to control (C), quantified in panel F. (G-J) Knock-down of RPTP69D in pSC neurons using two different RNAi lines phenocopies Dscam single isoform over-expression and leads to a specific defect in the formation of the anterior midline-directed collateral (H, I) compared to WT (G). Defects are quantified as mild (midline stop/stub) or strong (absent/ipsilateral stub) in panel (J). (K) Schematic of the RPTP69D protein organization describing the important structural and functional domains as well as the nature of the alleles used in this study. (L-O) RPTP69D has a dose-dependent effect on ms-neuron midline collateral formation. Strong RPTP69D allele combinations recapitulate the defects seen in ms-neuron specific RNAi (N, O), whereas weaker hypomorphic combinations (M) appear mostly WT (compare to L). Defects are quantified in panels (T) and (U). (P-S) Other RPTPs have no effect on ms-neuron branching. LAR LOF using the MARCM technique (P), and whole animal nulls for RPTP99A (Q), RPTP4E (R) and RPTP10D (S) all show normal ms-neuron branching patterns. (T) Quantifications of phenotypic penetrance in the genotypes described in (L-O). (U) RPTP69D LOF leads to defects specific to the anterior midline collateral and has minor effects on the length of the anterior branch or the main ipsilateral shaft. Length of the quantified processes was normalized to the width of the VNC. (Box and Whiskers plot 5-95 percentile, Statistical analysis: One-way ordinary ANOVA followed by Tukey's multiple comparisons test, * P ≤ 0.05; ** P ≤ 0.01; *** P ≤ 0.001).*

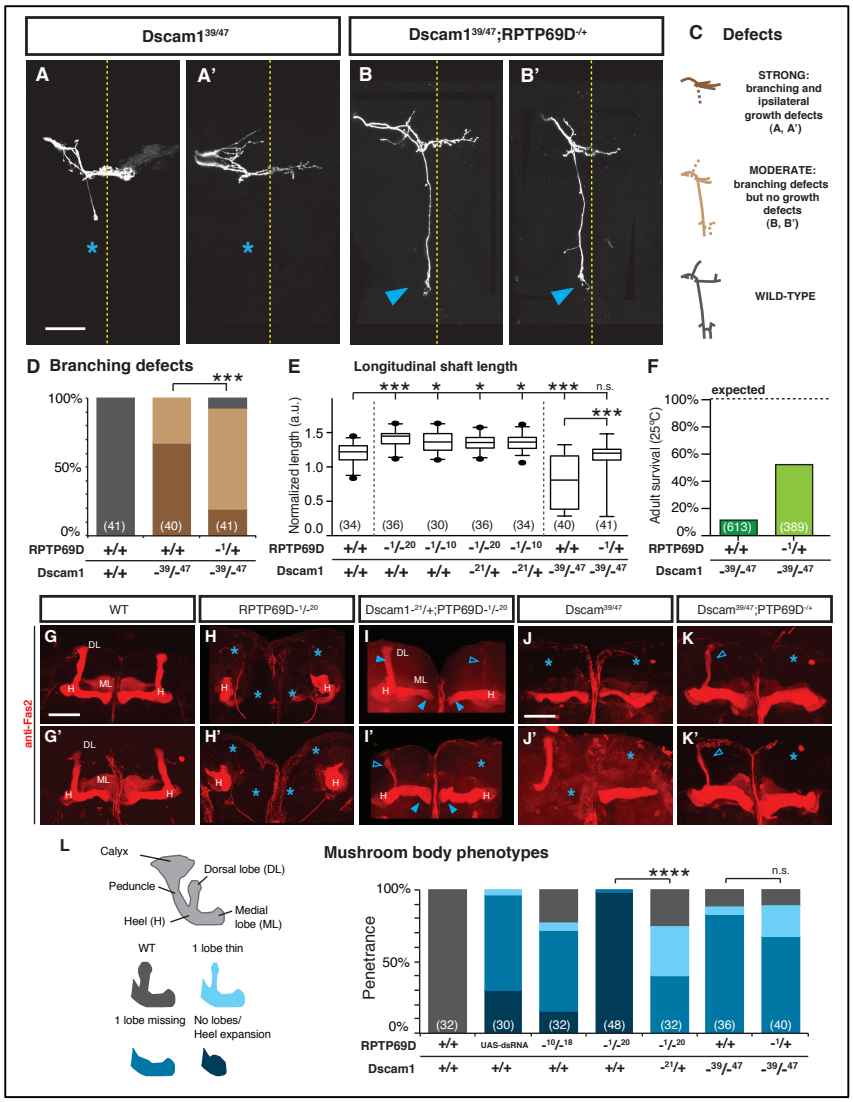

FIGURE S 2. **RPTP69 IS AN IMPORTANT REGULATOR OF DSCAM1 (RELATED TO FIGURE 1)**

*(A-B) Removing one copy of RPTP69D in a strong Dscam1 hypomorph background does partially suppress the Dscam1 phenotypes (A, A') Dscam1^{39}/Dscam1^{47} allele combinations recapitulate characteristic features of Dscam1 LOF, mainly defects in ipsilateral growth (asterisks) and clump formation (B, B') Removal of one copy of RPTP69D in a Dscam1 hypomorphic background partially suppresses ipsilateral growth defects. Dscam1^{39}/Dscam1^{47}; RPTP69D^{1}/+ flies display clearly extended ipsilateral branches (arrowheads) but still exhibit defects in branch formation. (C-E) Quantification of ms-neurons defects penetrance in the genotypes described above. (C) Description of ms-neurons phenotype classification in the genotypes described above (D): Statistical analysis: Chi-square test, *** P ≤ 0.0001. (E): Box and Whiskers plot 5-95 percentile. Length was normalized to VNC width. Statistical analysis: One-way ordinary ANOVA followed by Tukey's multiple comparisons test, * P ≤ 0.05; ** P ≤ 0.01; *** P ≤ 0.001. (F) Removal of one copy of RPTP69D in a Dscam1 hypomorphic background also partially suppresses lethality. (G-K) Representative confocal images of adult brains stained with anti-Fas2 antibody labeling the mushroom bodies (MBs). (G, G') WT MBs are a branched structure, comprised of axonal bundles that branch into two core lobes (α-lobe or dorsal lobe, DL and β-lobe or medial lobe, ML). These axons branch in a specific region called the heel, H. (H, H') RPTP69D mutants display strong defects, including heel expansion and failure of lobe separation and formation (asterisks). (I, I') Removal of one copy of Dscam1 in an RPTP69D hypomorphic background partially suppresses RPTP69D defects, as the majority of MBs in this genetic background have at least one lobe (full arrows). In some cases, these MBs have normal lobe morphology (I left) or display thinner lobes (hollow arrows). (J, J') Dscam^{39}/Dscam^{47} hypomorph mushroom bodies display strong defects, including missing lobes and lobe fusion. (K, K') Removal of one copy of RPTP69D in a Dscam1 hypomorphic background is not sufficient to suppress Dscam1 defects. (L) Schematics and quantification of MB phenotypes in the genotypes described above (Chi-square test, *** P ≤ 0.0001).*

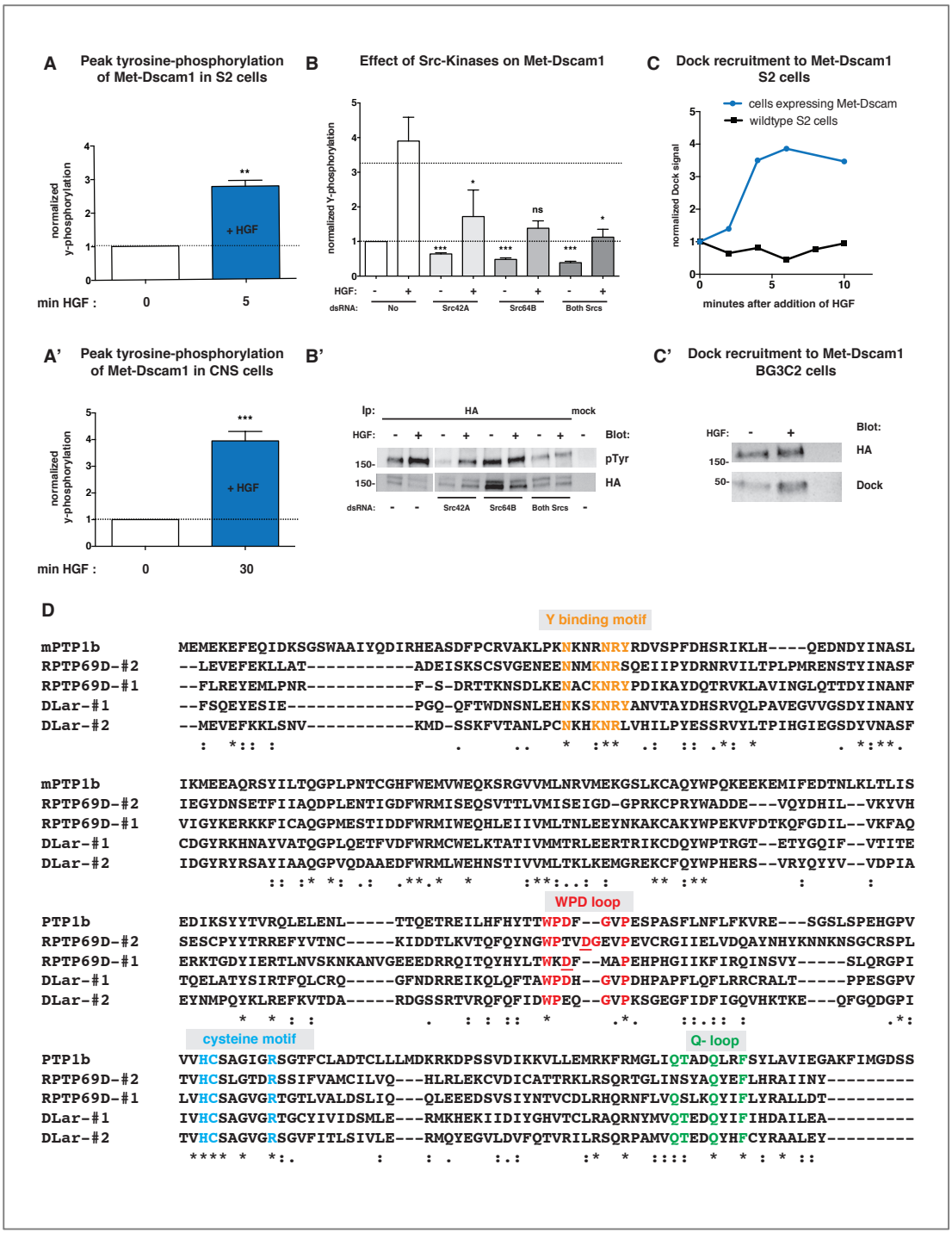

FIGURE S 3. **FIGURE LEGEND ON THE NEXT PAGE.**

FIGURE S3. **EFFECT OF MET-DSCAM1 ACTIVATION ON TYROSINE PHOSPHORYLATION BY SRC KINASES AND DOCK RECRUITMENT. LOCALIZATION OF THE WPD LOOP IN THE RPTP69D CATALYTIC DOMAINS (RELATED TO FIGURE 2).**

*(A,A') Tyrosine phosphorylation of Met-Dscam1 in response to HGF treatment in S2 cells (A) and BG3C2 cells (A'). Stable cell lines expressing Met-Dscam1 were treated with HGF for the indicated time. Met-Dscam1 was immunoprecipitated and the phosphorylation state assessed by semiquantitative Western Blot. Each bar represents the mean of multiple experiments. n=3 for S2 cells; n=23 for CNS cells; error bars= SEM; statistical analysis: paired t-test; p-values: P ≤ 0.05; ** P ≤ 0.01; *** P ≤ 0.001. (B and B') Knockdown of Src kinases 42A and 64B reduces Met-Dscam1 phosphorylation. The stable BG3C2 cell line expressing Met-Dscam1 was treated with dsRNA against Src42, Src64B or against both kinases. Met-Dscam1 was activated by addition of HGF to the medium for 30 minutes. Cells were harvested and the phosphorylation state of Met-Dscam1 was assessed for each condition as described under A. (B) Each bar represents the mean of multiple experiments. n= 8 for WT, n= 4 for Src42A and Src64B, n= 3 for knockdown of both kinases; error bar= SEM; ordinary one-way-Anovas were performed to compare the samples in absence of HGF (p < 0,001) and the samples after ligand addition (p= 0,0153). Multiplicity adjusted p-values (Dunnett): * P ≤ 0.05; ** P ≤ 0.01; *** P ≤ 0.001. (B') Representative WB of one experiment. All lanes from the same gel, but order was changed to show WT first. (C and C') The adaptor protein Dock is recruited to Met-Dscam1 in S2 cells (C) and BG3C2 cells (C'). Met-Dscam1 in stable expressing cell lines was activated with HGF for the times indicated. Cells were harvested and Met-Dscam1 was immunoprecipitated. Dock binding was assessed by Western blot and quantified by area density measurements. (C) Quantification of one representative time-course experiment in S2 cells. (C') Western blot of one representative experiment. (D) ClustalΩ alignment of the phosphatase domains of Drosophila RPTP69D and Lar (DLar) with mouse PTP1B (mPTP1b) in order to localize the most important regions of the catalytic domains. #1= membrane proximal domain; #2= membrane distal domain; Y-binding motif (orange): This motif determines the depth of the catalytic pocket and the specificity for tyrosine; WPD loop (red): This motif serves as a general acid during the catalytic reaction. The aspartate of the motif is crucial for the closure of the catalytic pocket upon substrate binding. Underlined: The two aspartates, which were mutated in the substrate trapping mutants DA1, DA2 and DA12 (Fig. 4F). Cysteine motif: This motif is critical for the phosphatase-substrate interaction. It forms a cysteinyl-phosphate intermediate with the substrate and is sensitive to oxidation. Q-loop: Important for hydrolysis of the cysteinyl-phosphate intermediate.*

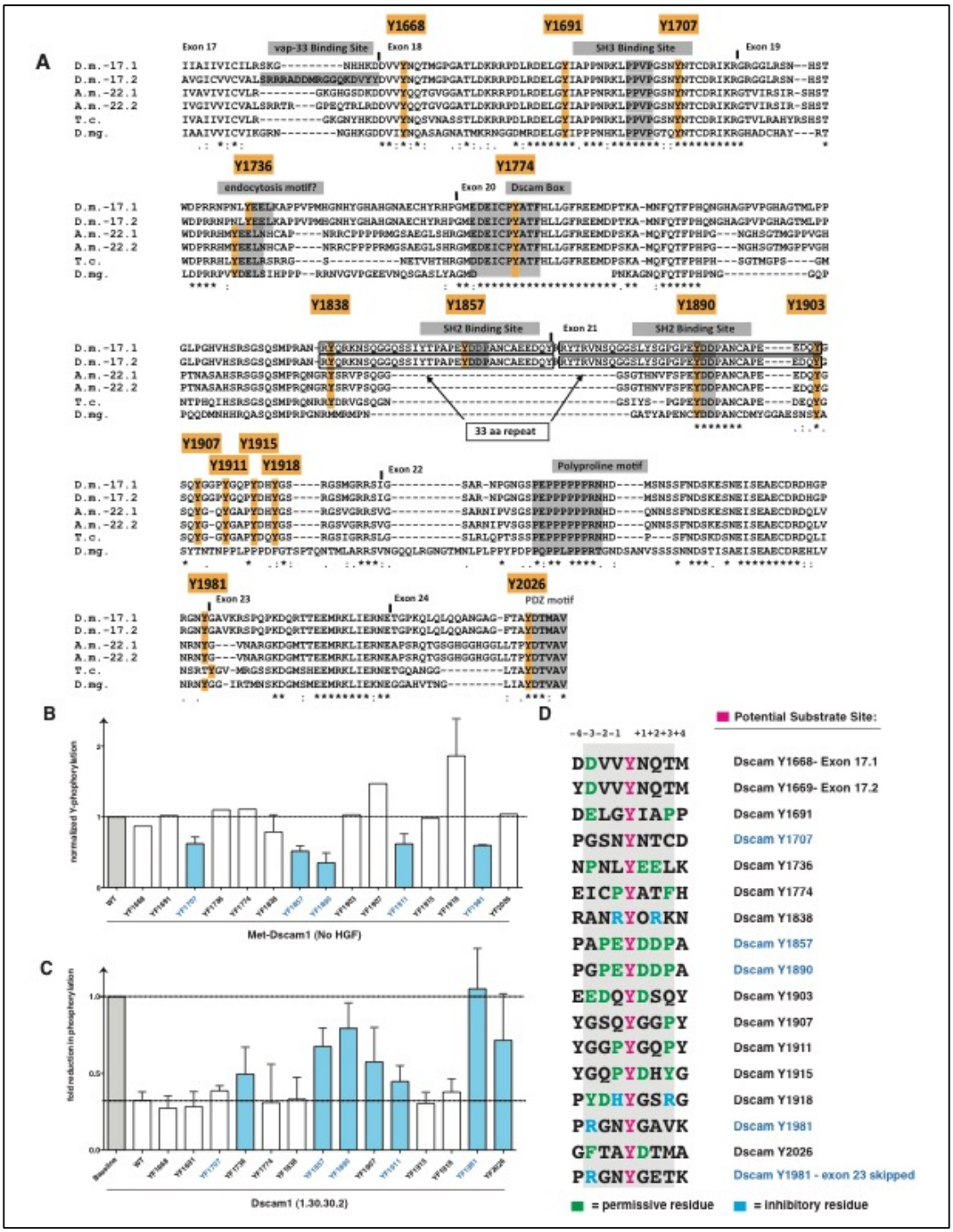

FIGURE S 4. PLEASE FIND THE LEGEND ON THE NEXT PAGE.

FIGURE S4. **SCREENING THE DSCAM1 INTRACELLULAR DOMAIN FOR POTENTIAL RPTP69D SUBSTRATE TYROSINES (RELATED TO FIGURE 4).**

(A) Alignment of different Dscam1 intracellular domains to identify conserved tyrosines. The amino acid sequences C-terminal of the transmembrane domain of the fruit fly Drosophila melanogaster (D.m.), the Western honey bee Apis mellifera (A.m.), the red flour beetle Tribolium castaneum (T.m) and the water flea Daphnia magna (D.m.) were aligned using ClustalW2. We selected 14 tyrosines based on their conservation and one tyrosine in the center of the first SH2-binding site (Y1857) for further analysis. Grey: Signaling motifs; orange: Tyrosines selected for analysis; the Dscam1 genes of D. m. and A.m contain two alternative exons for the transmembrane domains (exon 17 and 22 respectively), which give rise to slightly different amino acid sequences at the beginning of the intracellular domain (D.m.-17.1; D.m.-17.2; A.m.-22.1; A.m.-22.2). (B) Screening experiment utilizing the chimeric Met-Dscam1 receptor to pinpoint tyrosines critical for Dscam1 phosphorylation. HA-tagged Met-Dscam1 constructs containing single Y>F point mutations in each of the 15 conserved tyrosines were expressed in S2 cells and immunoprecipitated with anti-HA antibody. The tyrosine phosphorylation of all chimeric receptor versions was evaluated by semi-quantitative westernblot analysis and compared to Met-Dscam1 containing a wildtype Dscam1 intracellular domain. Experiments were multiple times to confirm results. Blue: Tyrosines with reduced baseline phosphorylation in the screening experiment. (C) Summary of an overexpression based phosphatase assay to test the sensitivity of single phospho-tyrosines to RPTP69D. S2 cells were co-transfected with an HA tagged single isoform of Dscam1 (isoform 1.30.30.2) in the presence and absence of RPTP69D. Tagged Dscam1 was purified by means of HA-immunoprecipitation and the phosphorylation status was evaluated by semi-quantitative western blot analysis. Although the baseline phosphorylation differs from experiment to experiment, we found that the tyrosine phosphorylation of the over-expressed single Dscam1 isoform is significantly reduced in the presence of RPTP69D. We tested Dscam1 single isoform constructs with Y>F mutations in each of the 15 conserved tyrosines and found that the RPTP69D effect is reduced when the tyrosines Y1857, Y1890, Y1981 are mutated. The effect on Y2026 was hard to interpret because of large differences between individual experiments, which is likely caused by increased sensitivity to cell density. The construct harboring a point mutation in Y1903 could not be expressed at high enough levels to conduct meaningful experiments. Bars represent the mean of several experiments normalized to the baseline phosphorylation of a given construct (in absence of RPTP69D). Error bars: SEM; n=2 for Y1774 and Y1907; n= 3 for YF1668, YF1707, YF1911 n=4 for YF1691, YF1736, YF1838, YF1918; n=5 for YF1915; n=6 for YF2026; n=7 for YF1890 and YF1981; n=11 for YF1857. (D) Analysis of amino acids surrounding the 15 conserved tyrosines (magenta) in the Dscam1 intracellular domain. Most RPTP substrate tyrosines are embedded in stretches of acidic or large hydrophobic residues (green) in an area ranging from amino acids -3 to +3 (labeled in grey). Almost all of the 15 conserved tyrosines of the Dscam1 intracellular domain contain at least one permissive residue in their critical region. Especially the two tyrosines at the center of the SH2-binding sites (Y1857 and Y1890) are surrounded by several acidic residues, which could enhance potential phosphatase-substrate interactions. However, Y1707, Y1838 and Y1981 contain no such permissive residue. Y1838 and Y1921 contain even a basic residue (blue) in the region directly N-terminal of the tyrosine, which could lead to difficulties forming a potential substrate-phosphatase interphase.

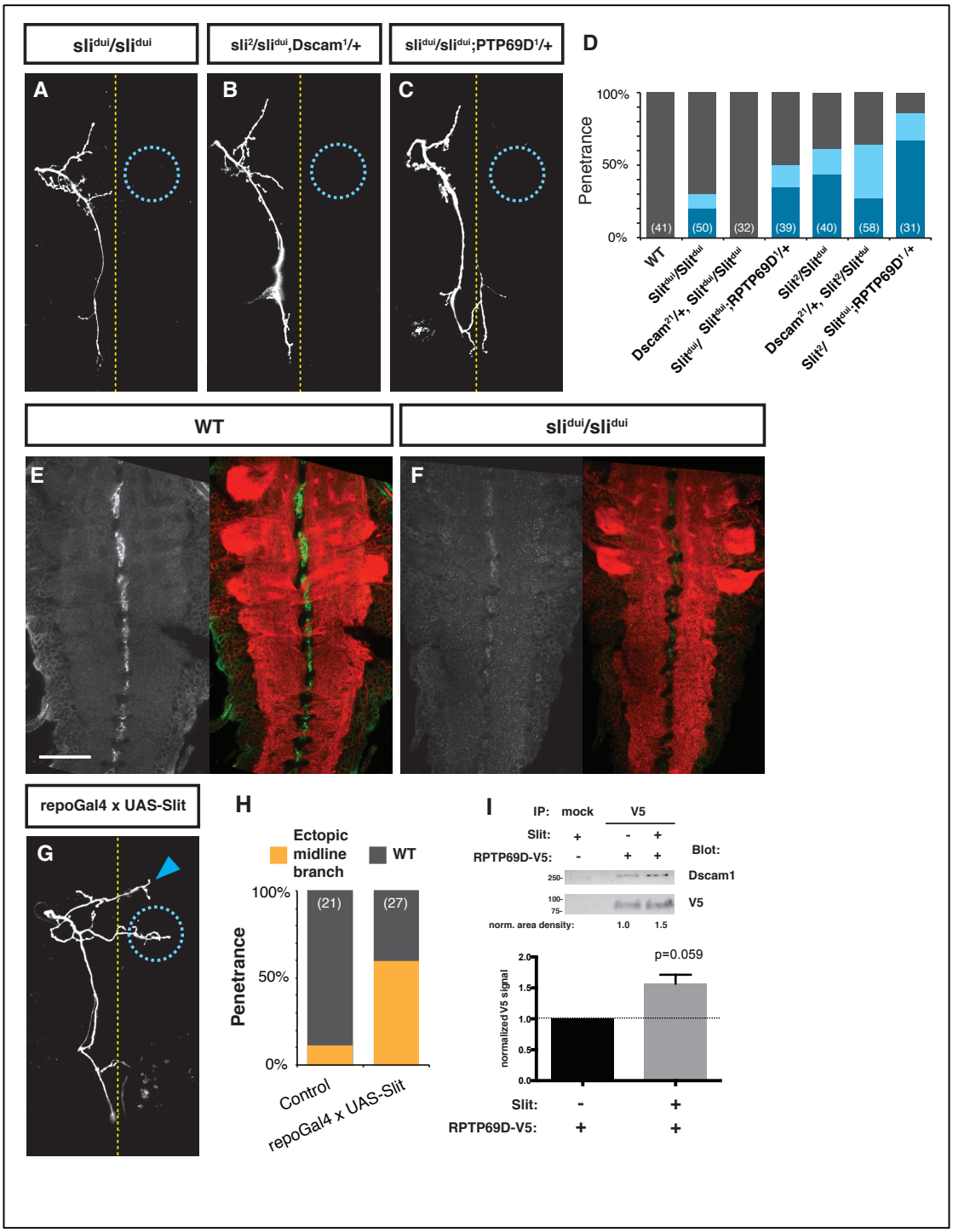

FIGURE S 5. **SLIT IS A MIDLINE-LOCALIZED FACTOR INVOLVED IN MS-NEURONS BRANCHING (RELATED TO FIGURE 6).**

(A-C, G) Representative confocal images of pSC dye-fills. Slit is required for ms-neurons anterior midline collateral formation (A). (B-D) Slit interacts genetically with Dscam1 and RPTP69D, as quantified in D. (E, F) Slit is expressed at the midline of the VNC and its expression is severely reduced in a Slit hypomorph background. Pupae were dissected mid-pupal stage and stained with anti-Slit and anti-Ncad antibodies in a WT (E) and Slit dui hypomorph background (F). Note the residual midline expression in the mutant. (G, H) Ectopic pan-glial expression of Slit results in ectopic midline crossing of the anterior midline-crossing branch (arrowhead, quantified in H). (I) Slit promotes the formation of a Dscam1-RPTP69D complex. Coimmunoprecipitation of Dscam1 and RPTP69D from a stable cell line expressing V5 tagged RPTP69D was increased when cells were incubated for 6h with purified Slit. Dscam1 binding was assessed by semiquantitative Western blot analysis. Representative Western blot of one experiment.

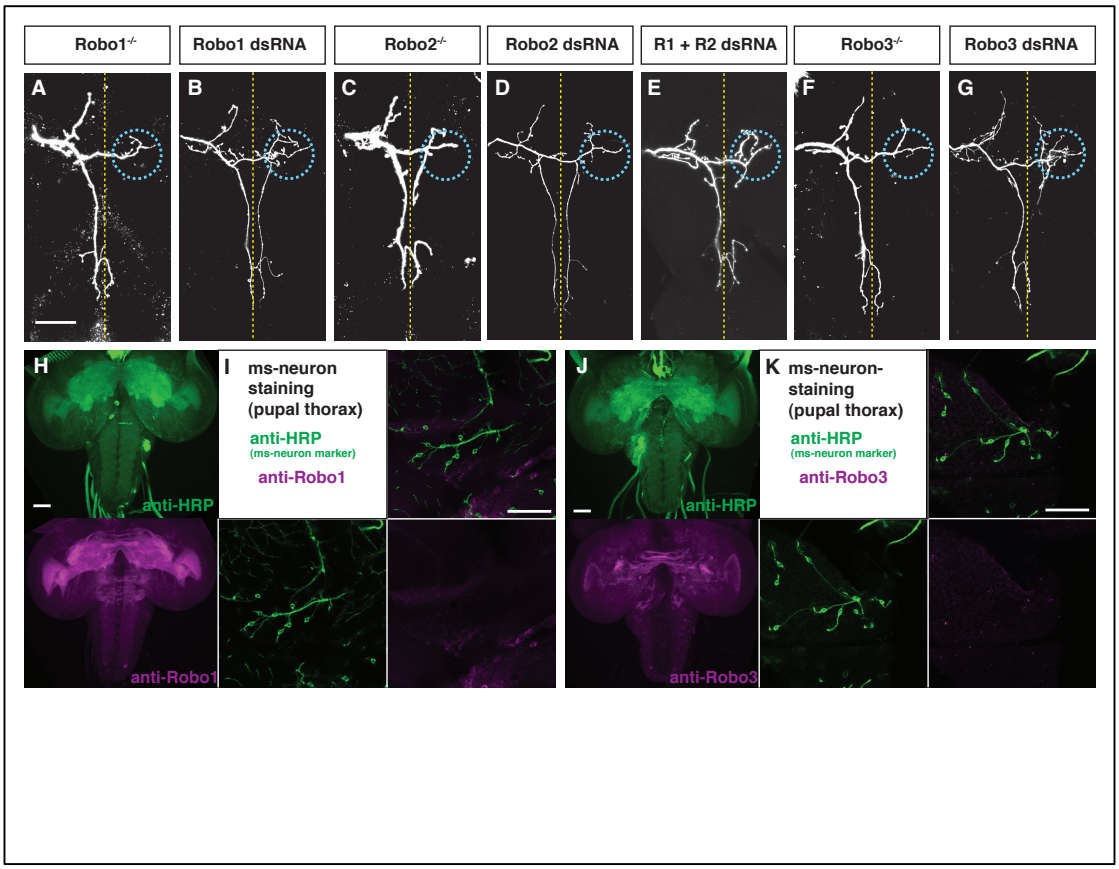

FIGURE S 6. **THE ROBO RECEPTOR FAMILY IS NOT REQUIRED FOR THE FORMATION OF MS-NEURON ANTERIOR MIDLINE COLLATERALS (RELATED TO FIGURE 6).**

(A-G) Slit receptors Robo1, Robo2 and Robo3 are not individually required for ms-neuron collateral formation. (A,B) Dye-fills of Robo1 LOF ms-neuron MARCM clones (Robo11/Robo11, A) or ms-neurons in which Robo1 was knocked-down using RNAi driven by the 455-Gal4 driver (B). (C, D) Dye-fills of Robo2 LOF ms-neuron MARCM clones (Robo28/Robo28, C) or ms-neurons in which Robo2 was knocked-down using RNAi driven by the 455-Gal4 driver (D). (E) Simultaneous KD of Robo1 and Robo2 using the same RNAi technique shows no phenotypes. (F, G) Robo3 LOF ms-neuron MARCM clones (Robo31/Robo31, F) or ms-neurons in which Robo3 was knocked-down using RNAi driven by the 455-Gal4 driver (G). (H-K) Stainings for Robo1 and Robo3 show no expression of these receptors in ms-neurons of the thorax at early pupal stages (co-stained with anti-HRP, I and K), while stainings for Robo1 and Robo3 show prominent expression in the brain and VNC neuropils (H, J).

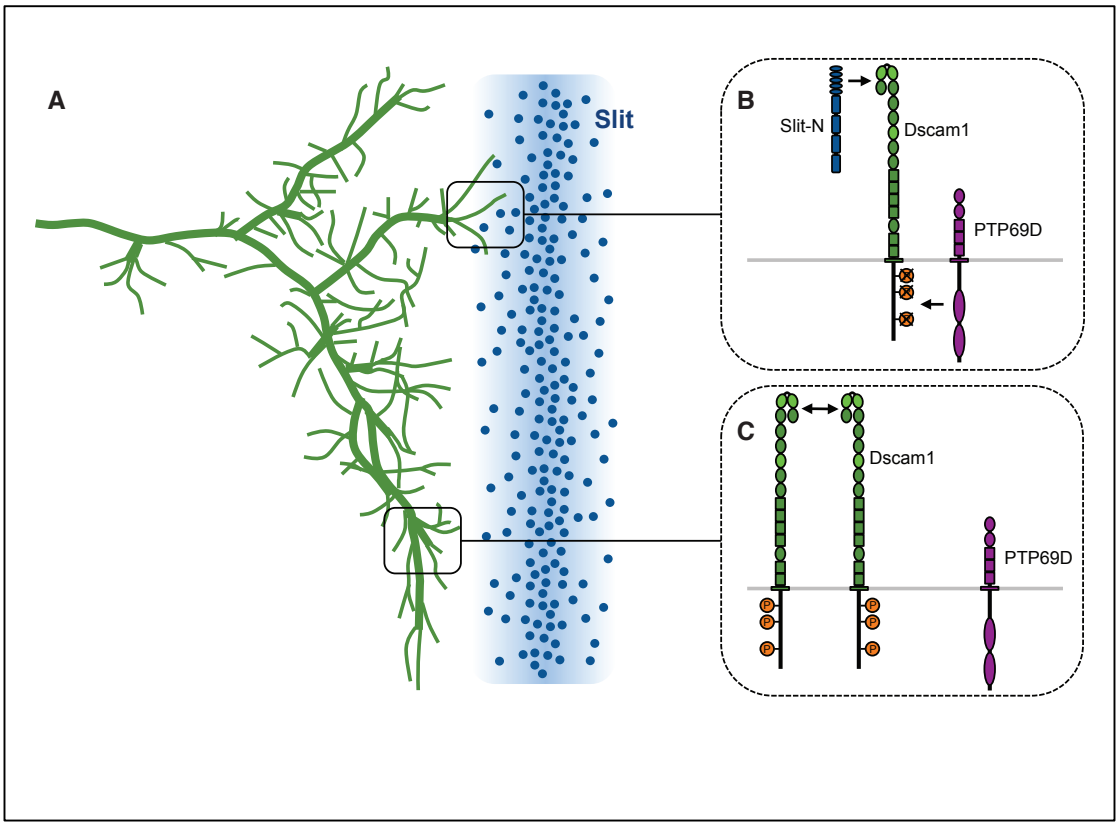

FIGURE S 7. **A MODEL OF MS-NEURON COLLATERAL FORMATION (RELATED TO FIGURE 8).**

Axons of ms-neurons enter the VNC and undergo an initial Dscam1 dependent "sprouting" phase during which they form a plethora of extensions, which probe the local environment (See Figure 8 and He et al. 2014). Some processes are very thin (filopodia) while others are thicker and exhibit their own branched filopodial extensions. (micropodia). (A) Schematic of a WT ms-neuron in an intermediate developmental phase critical for collateral branch formation. Note the two separate primary axon branches, which segregate in anterior-posterior direction. (B) Collateral formation occurs when filopodia and satellite growth cones encounter midline secreted Slit. Slit binding to the extracellular domain of Dscam1 leads to recruitment of RPTP69D and de-phosphorylation of the Dscam1 intracellular domain at three critical tyrosines (orange). Slit and possibly other signals promote midline directed growth and consolidation of an axonal branch. (C) Satellite growth cones further away from the midline are characterized by processes growing in all directions and likely remain dynamic and "in search mode" by means of intrinsic Dscam1-Dscam1 interactions.

Supplemental Experimental Procedures:

Fly alleles and transgenes:

The following mutant alleles were used in this study: *Dscam121* (Hummel et al., 2003), *Dscam139, Dscam147* (Zhan et al., 2004), *RPTP69D1* (Desai et al., 1996), *RPTP69D10, RPTP69D18, RPTP69D20* (Desai and Purdy, 2003), *RPTP69DD1689, LARC219* (Berger et al., 2008), *RPTP4E1, RPTP10D1* (Jeon et al., 2008), *RPTP99A1* (Desai et al., 1996), *Slit2* (Mayer and Nüsslein-Volhard, 1988), *P{lacW}Slitk04807b (Slitdui)* (Tayler et al., 2004), *Robo11, Robo28, Robo31* (Spitzweck et al., 2010).The following transgenes were used: *P{GawB}455.2 (455-Gal4)* (Hinz et al., 1994), *P{GawB}pnrMD237 (pnr-Gal4)* (Heitzler et al., 1996), *P{GAL4}repo (repo-Gal4)* (Sepp et al., 2001), *P{GawB}eyOK107 (OK107-Gal4)* (Connolly et al., 1996), *P{DC1.4::FLP}, P{R15E08-Gal4}* (Pfeiffer et al., 2008), *P{UAS-Dscam 1.30.30.2}* (Chen et al., 2006), *P{UAS-Dscam 1.30.30.2}attP2, P{UAS-Dscam 1.30.30.2-Y1857F}attP2, P{UAS-Dscam 1.30.30.2-Y1890F}attP2, P{UAS-Dscam 1.30.30.2-Y1981F}attP2, P{UAS-RPTP69D.HA}attP2, P{UAS-Slit}* (Battye et al., 2001), *BAC{[Dscam1]EX6.1-Flpd}86B* (He et al., 2014), *P{20xUAS-FRT- STOP-FRT-CD8GFP-2A-syt-mCherry}attP2, P{20xUAS-FRT-STOP-FRT- CD8GFP}attP40, P{alphaTub84B(FRT.GAL80)}1, P{UAS-Ptp69D.DA1DA2}* (Garrity et al., 1999), *P{GD2577}v4789 (UAS-RPTP69D.dsRNA line1), P{KK105220}VIE-260B (UAS-RPTP69D.dsRNA line2), P{KK100296}VIE-260B (UAS-Dscam1.dsRNA), P{w[+mC]=UAS-robo.RNAi}3 (UAS-Robo.dsRNA9285BL), P{KK108817}VIE-260B (UAS-Robo.dsRNA100624KK), P{TRiP.HMS01517}attP2 (UAS- Robo.dsRNA35768TriP), P{UAS-lea.RNAi}3 (UAS-Robo2.dsRNA9286BL), P{TRiP.HMS01063}attP2 (UAS-Robo2.TriP34589), P{TRiP.JF03331}attP2 (UAS- Robo3.dsRNA29398TriP).* The alleles and transgenes used in this study are provided in Supplemental Information. RNAi lines were obtained from the VDRC and TriP collections (Dietzl et al., 2007; Ni et al., 2009).

Software:

Sequences were aligned using Clustal W (http://www.ebi.ac.uk/Tools/msa/clustalw2/) for Dscam1 alignments and Clustal Omega (http://www.ebi.ac.uk/Tools/msa/clustalo/) for RPTP alignments. FIJI is a modified ImageJ distribution (Schindelin et al. 2012).

List of genotypes used in figure panels:

Figure	Panel	Genotype
Figure 1	C, H	WT
	D	elav-Gal4, UAS-GFP, hsFLP/+; FRT42D Dscam^{21}/ FRT42D Tub-Gal80
	E	Dscam1^{21}/Dscam1^{6055}; [Dscam1]Ex6-flpd/+
	F, K, L	RPTP69D^{1}/RPTP69D^{20}
	G	elav-Gal4, UAS-GFP, hsFLP/+;; RPTP69D^{D1689} FRT80B/FRT80B Tub-Gal80
	I	UAS-Dscam1dsRNA108835KK/+; pnr-Gal4/+
	J	Tub-FRT-Gal80-FRT/+; DC1.4-FLP/+; pnr-Gal4, UASmCherry/UAS-Dscam1-1.30.30.2
Figure 2	A	WT
	B	RPTP69D^{1}/RPTP69D^{10}
	B'	RPTP69D^{1}/RPTP69D^{20}
	C	Dscam1^{21}/+; RPTP69D^{1}/RPTP69D^{10}
	C'	Dscam1^{21}/+; RPTP69D^{1}/RPTP69D^{20}
	C''	Dscam1^{39}/+; RPTP69D^{1}/RPTP69D^{20}
Figure 4	A	WT
	B	Dscam1^{39}/Dscam1^{47}
	C, C'	UAS-Dscam1dsRNA108835KK/+; pnr-Gal4/+
	D	UAS-RPTP69D-WT/+; pnr-Gal4/+
	E-F'	pnr-Gal4/UAS-RPTP69D-DA12
Figure 6	A, A'	Tub-FRT-Gal80-FRT/+; DC1.4-FLP/+; pnr-Gal4, UAS-mCherry/+
	B, B'	Tub-FRT-Gal80-FRT/+; DC1.4-FLP/+; pnr-Gal4, UAS-mCherry/UAS-Dscam1-1.30.30.2-WT(attp2)
	C, C'	Tub-FRT-Gal80-FRT/+; DC1.4-FLP/+; pnr-Gal4, UAS-mCherry/UAS-Dscam1-1.30.30.2-Y1857F(attp2)
	D, D'	Tub-FRT-Gal80-FRT/+; DC1.4-FLP/+; pnr-Gal4, UAS-mCherry/UAS-Dscam1-1.30.30.2-Y1890F(attp2)
	E, E'	Tub-FRT-Gal80-FRT/+; DC1.4-FLP/+; pnr-Gal4, UAS-mCherry/UAS-Dscam1-1.30.30.2-Y1981F(attp2)
Figure 7	A, G	WT
	B	Slit^{dui}/Slit^{dui}
	C	Slit^{2}/Slit^{dui}
	D	Slit^{2}/Slit^{dui};PTP69D^{1}/+
	E	Dscam^{21},Slit^{dui}/+,Slit^{dui}
	H	Tub-Gal4, UAS-nGFP, Ubx-FLP/+; FRT42D Robo1^{1}/ FRT42D Tub-Gal80
	I	Tub-Gal4, UAS-nGFP, Ubx-FLP/+; FRT40A Robo2^{8}/ FRT40A Tub-Gal80
Figure 8	A-D	20xUAS-GFP/+;R15E08-Gal4/20xUAS-GFP
	E-H	20xUAS-GFP/+;R15E08-Gal4, RPTP69D^{1}/20xUAS-GFP, RPTP69D^{20}
	I-L	20xUAS-GFP, Sli^{dui}/Sli^{2};R15E08-Gal4/20xUAS-GFP
Figure S1	C	Tub-FRT-Gal80-FRT/+; DC1.4-FLP/+; pnr-Gal4, UAS-mCherry/+

	D, E	Tub-FRT-Gal80-FRT/+; DC1.4-FLP/+; pnr-Gal4, UAS-mCherry/UAS-Dscam1-1.30.30.2
	G, L	WT
	H	455-Gal4/+; UAS-RPTP69DdsRNA4789GD/+
	I	UAS-RPTP69DdsRNA104761KK/455-Gal4
	M	$RPTP69D^{10}/RPTP69D^{18}$
	N	$RPTP69D^{1}/RPTP69D^{10}$
	O	$RPTP69D^{1}/RPTP69D^{20}$
	P	elav-Gal4, UAS-GFP, hsFLP/+; LAR^{C219} FRT40A/ FRT40A
	Q	$RPTP99A^{1}/RPTP99A^{R3}$
	R	$RPTP4E^{1}/RPTP4E^{1}$
	S	$RPTP10D^{1}/RPTP10D^{1}$
Figure S2	A, A', J, J'	$Dscam1^{39}/Dscam1^{47}$
	B, B', K' K'	$Dscam1^{39}/Dscam1^{47}$; $RPTP69D^{1}/+$
	G, G'	WT
	H, H'	$RPTP69D^{1}/ RPTP69D^{20}$
	I, I'	$Dscam1^{21}/+$; $RPTP69D^{1}/ RPTP69D^{20}$
Figure S6	A, F	$Slit^{dui} /Slit^{dui}$
	B	$Dscam^{21}$,$Slit^{dui}/+$,$Slit^{2}$
	C	$Slit^{dui}/Slit^{dui}$;$PTP69D^{1}/+$
	E	WT
	G	Repo-Gal4, UAS-GFP/+ ; UAS-Slit/+
Figure S7	A	Tub-Gal4, UAS-nGFP, Ubx-FLP/+; FRT42D $Robo^{1}$/ FRT42D Tub-Gal80
	B	455Gal4/UAS-Robo1dsRNA.9285BL
	C	Tub-Gal4, UAS-nGFP, Ubx-FLP/+; FRT40A $Robo2^{8}$/ FRT40A Tub-Gal80
	D	455Gal4/+ ; UAS-Robo2dsRNA.34059.TriP/+
	E	455Gal4/UAS-Robo1dsRNA.9285BL ; UAS-Robo2dsRNA.9286BL/+
	F	Tub-Gal4, UAS-nGFP, Ubx-FLP/+; FRT40A $Robo3^{1}$/ FRT40A Tub-Gal80
	G	455Gal4/+ ; UAS-Robo3dsRNA.29398.TriP/+
	H, I	WT

TABLE S 1. **LIST OF GENOTYPES USED IN FIGURE PANELS**.

List of antibodies:

Name	Distributor	Working Concentration	Epitope	species of origin
Alexa Fluor® 488 Goat Anti-Rat IgG	Life Technologies	1:300-1:1000 IHC	Rat IgG (H+L)	goat
Alexa Fluor® 488 Goat Anti-Rabbit IgG	Life Technologies	1:300-1:1000 IHC	Rabbit IgG (H+L)	goat
anti GFP Polyclonal Antibody	Life Technologies	1:500 IHC	GFP	rabbit
Alexa Fluor® 633 Goat Anti-Rat IgG (H+L)	Life Technologies	1:300-1:1000 IHC	Anti-Rat IgG (H+L)	goat
Alexa Fluor® 555 Goat Anti-Mouse IgG	Life Technologies	1:300-1:1000 IHC	Anti-Mouse IgG (H+L)	goat
Dscam IC (357)	Schmucker Lab	1:1000 WB 1:100 IP 1:450 IHC	*Drosophila* Dscam1 full length intracellular domain	rabbit
Dscam IC (358)	Schmucker Lab	1:1000 WB 1:100 IP	*Drosophila* Dscam1 full length intracellular domain	rabbit
Dscam EC (19545)	Schmucker Lab	1:1000 WB 1:100 IP	*Drosophila* Dscam1 Ig 1-4	rabbit
Dscam EC (19546)	Schmucker Lab	1:1000 WB 1:100 IP	*Drosophila* Dscam1 Ig 1-4	rabbit
4G10 Platinum	Millipore	1:1000 WB 30µl crosslinked agarose beads for IP	phosphotyrosine	mouse
Phospho-Tyrosine 100	Cell Signaling	1:1000 WB	phosphortyrosine	mouse
anti pTyr HRP (pY20) monoclonal	Pierce	1:2000 WB	phosphortyrosine	mouse
anti-Dock	Zipursky Lab	1:2000 WB	*Drosophila* Dock	rabbit
anti-Dock	Bogdan Lab	1:1000 WB	*Drosophila* Dock	rabbit
anti actin ACTN05	abcam	1:5000 WB	actin	mouse
anti mouse-HRP	Jackson Laboratories	1:10000 WB	mouse IgG (H+L)	goat
anti rabbit-HRP	Jackson Laboratories	1:10000 WB	rabbit IgG (H+L)	goat
anti guinea-pig HRP	Jackson Laboratories	1:10000 WB	guinea pig IgG (H+L)	goat
monoclonal anti HA agarose conjugate HA-7	Sigma-Aldrich	30µl/IP	HA Epitope Tag	mouse
3F10	Roche	1:1000 WB	HA Epitope Tag	rat
HA-Antibody-HRP	Pierce	1:1000 WB	HA Epitope Tag	
Anti-Ha magnetic Beads	Pierce	30µl/IP	HA Epitope Tag	mouse
M2 or M2 affinity gel	Flag	1:1000 WB IP with 30µl affinity gel	Flag epitope Tag	mouse
V5 Tag Mouse Monoclonal Antibody	Life Technologies	1:2000 WB IP 1:250	V5 Epitope Tag	mouse
anti-Slit C555	Hybridoma Bank (DSHB)	1:40 WB 1:10 IP 1:20 IHC	Slit protein	mouse
anti RPTP69D (3F11)	Hybridoma Bank (DSHB)	1:10 WB	RPTP69D	mouse
Dynabeads® M-280 Sheep Anti-Mouse IgG	Life Technologies	30µl/100µl lysate	mouse IgG	sheep
Dynabeads Sheep Anti-Rat IgG	Life Technologies	30µl/100µl lysate	rat IgG	sheep
anti-Fasciclin II 1D4	Hybridoma Bank (DSHB)	1:20 IHC	Fasciclin II	mouse
anti-Robo1	Hybridoma Bank (DSHB)	1:20 IHC	Robo1	mouse
anti –Robo3	Hybridoma Bank (DSHB)	1:20 IHC	Robo3	mouse
anti HRP			HRP	rat
anti-DsRed	Clontech	1:300 IHC	DsRed	rabbit

TABLE S 2. **LIST OF ANTIBODIES USED IN THIS STUDY.**

Supplemental references

Battye, R., Stevens, A., Perry, R.L., and Jacobs, J.R. (2001). Repellent signaling by Slit requires the leucine-rich repeats. J. Neurosci. 21, 4290–4298.

Berger, J., Senti, K.-A., Senti, G., Newsome, T.P., Åsling, B., Dickson, B.J., and Suzuki, T. (2008). Systematic Identification of Genes that Regulate Neuronal Wiring in the Drosophila Visual System. PLoS Genetics 4, e1000085.

Chen, B.E., Kondo, M., Garnier, A., Watson, F.L., Püttmann-Holgado, R., Lamar, D.R., and Schmucker, D. (2006). The Molecular Diversity of Dscam Is Functionally Required for Neuronal Wiring Specificity in Drosophila. Cell 125, 607–620.

Connolly, J.B., Roberts, I.J., Armstrong, J.D., Kaiser, K., Forte, M., Tully, T., and O'Kane, C.J. (1996). Associative learning disrupted by impaired Gs signaling in Drosophila mushroom bodies. Science 274, 2104–2107.

Desai, C.C., and Purdy, J.J. (2003). The neural receptor protein tyrosine phosphatase DPTP69D is required during periods of axon outgrowth in Drosophila. Genetics 164, 575–588.

Desai, C.J., Gindhart, J.G., Jr., Goldstein, L.S.B., and Zinn, K. (1996). Receptor Tyrosine Phosphatases Are Required for Motor Axon Guidance in the Drosophila Embryo. Cell 84, 599–609.

Dietzl, G., Chen, D., Schnorrer, F., Su, K.-C., Barinova, Y., Fellner, M., Gasser, B., Kinsey, K., Oppel, S., Scheiblauer, S., et al. (2007). A genome-wide transgenic RNAi library for conditional gene inactivation in Drosophila. Nature 448, 151–156.

Garrity, P.A., Lee, C.-H., Salecker, I., Robertson, H.C., Desai, C.J., Zinn, K., and Zipursky, S.L. (1999). Retinal Axon Target Selection in Drosophila Is Regulated by a Receptor Protein Tyrosine Phosphatase. Neuron 22, 707–717.

He, H., Kise, Y., Izadifar, A., Urwyler, O., Ayaz, D., Parthasarthy, A., Yan, B., Erfurth, M.L., Dascenco, D., and Schmucker, D. (2014). Cell-Intrinsic Requirement of Dscam1 Isoform Diversity for Axon Collateral Formation. Science 344, 1182–1186.

Heitzler, P., Haenlin, M., Ramain, P., Calleja, M., and Simpson, P. (1996). A genetic analysis of pannier, a gene necessary for viability of dorsal tissues and bristle positioning in Drosophila. Genetics 143, 1271–1286.

Hinz, U., Giebel, B., and Campos-Ortega, J. (1994). The basic-helix-loop-helix domain of Drosophila lethal of scute protein is sufficient for proneural function and activates neurogenic genes. Cell 76, 77–87.

Hummel, T., Vasconcelos, M.L., Clemens, J.C., Fishilevich, Y., Vosshall, L.B., and Zipursky, S.L. (2003). Axonal targeting of olfactory receptor neurons in Drosophila is controlled by Dscam. Neuron 37, 221–231.

Jeon, M., Nguyen, H., Bahri, S., and Zinn, K. (2008). Redundancy and compensation in axon guidance: genetic analysis of the Drosophila Ptp10D/Ptp4E receptor tyrosine phosphatase subfamily. Neural Development 3, 3.

Mayer, U., and Nüsslein-Volhard, C. (1988). A group of genes required for pattern formation in the ventral ectoderm of the Drosophila embryo. Genes & Development 2, 1496–1511.

Ni, J.-Q., Liu, L.-P., Binari, R., Hardy, R., Shim, H.-S., Cavallaro, A., Booker, M., Pfeiffer, B.D., Markstein, M., Wang, H., et al. (2009). A Drosophila resource of transgenic RNAi lines for neurogenetics. Genetics 182, 1089–1100.

Pfeiffer, B.D., Jenett, A., Hammonds, A.S., Ngo, T.-T.B., Misra, S., Murphy, C., Scully, A., Carlson, J.W., Wan, K.H., Laverty, T.R., et al. (2008). Tools for neuroanatomy and neurogenetics in Drosophila. Proceedings of the National Academy of Sciences 105, 9715–9720.

Schindelin, J., Arganda-Carreras, I., Frise, E., Kaynig, V., Longair, M., Pietzsch, T., Preibisch, S., Rueden, C., Saalfeld, S., Schmid, B., et al. (2012). Fiji: an open- source platform for biological-image analysis. Nat Meth 9, 676–682.

Sepp, K.J., Schulte, J., and Auld, V.J. (2001). Peripheral glia direct axon guidance across the CNS/PNS transition zone. Developmental Biology 238, 47– 63.

Spitzweck, B., Brankatschk, M., and Dickson, B.J. (2010). Distinct Protein Domains and Expression Patterns Confer Divergent Axon Guidance Functions for Drosophila Robo Receptors. Cell 140, 409–420.

Tayler, T.D., Robichaux, M.B., and Garrity, P.A. (2004). Compartmentalization of visual centers in the Drosophila brain requires Slit and Robo proteins. Development 131, 5935–5945.

Zhan, X.-L., Clemens, J.C., Neves, G., Hattori, D., Flanagan, J.J., Hummel, T., Vasconcelos, M.L., Chess, A., and Zipursky, S.L. (2004). Analysis of Dscam diversity in regulating axon guidance in Drosophila mushroom bodies. Neuron 43, 673–686.

Chapter3

A proteomic screen to identify tyrosine phosphorylated protein complexes involved in Dscam1 signaling

Chapter 3- SUMMARY

The transmembrane protein Dscam1 is a self-recognition receptor of the immunoglobulin (Ig) superfamily of cell adhesion molecules (Schmucker et al., 2000). To date two *DSCAMs* have been identified in humans, two in mouse and four in *Drosophila*. An extraordinary feature of *Drosophila Dscam1* is that it potentially encodes more than 100,000 possible isoforms with distinct extracellular domains by virtue of mutually exclusive alternative splicing (Schmucker et al., 2000). *Drosophila Dscam1* is expressed in neuronal cells of both the CNS and PNS as well as in cells of the innate immune system (Hummel et al., 2003; Schmucker et al., 2000; Watson, 2005). Over the past years, phenotypic and functional studies emphasized that *Drosophila* Dscam1 mediated self-recognition is necessary for several aspects of axon guidance, targeting, axon branch specification and dendrite patterning (Chen et al., 2006; Dascenco and Erfurth et al., 2015; He et al., 2014a; Hughes et al., 2007; Hummel et al., 2003; Schmucker et al., 2000; Wang et al., 2002; 2004; Zhan et al., 2004; Zhu et al., 2006).

Recent work conducted in our laboratory underlines the notion that Dscam1 signaling can be controlled in multiple ways: An intrinsic cellular signaling threshold is set by regulating the number of isoforms expressed on the cell surface (He et al., 2014). In addition, different ligands can lead to activation, mediated through tyrosine phosphorylation of the intracellular domain (Dascenco and Erfurth et al., 2015). Such tight signaling control is indispensable for the formation of highly branched axonal patterns.

Despite the essential function of Dscam1 during neuronal development, surprisingly little is known about Dscam signal transduction. In fact, the only proposed pathway downstream of the Dscam1 receptor appears to be context specific. The ability of Dscam1 to participate not only in homophilic but also in heterophilic interactions (Andrews et al., 2008; Watson,

2005; Wojtowicz et al., 2004; 2007) leaves thousands of potential ligands to the receptor, thereby hindering the study of Dscam1 signaling.

In this chapter, I am describing several approaches to dissect the Dscam1 signaling pathway. I purified the Dscam1 cytoplasmic domain in BG3C2 cells to better understand the Dscam1 signaling complex in neurons. Furthermore, I employed a conditionally inducible Met-Dscam1 receptor to investigate proteins that change their tyrosine-phosphorylation status in response to Dscam1 signaling.

I identified several novel functional groups of proteins as being involved in Dscam1 signaling. Some of them interact in a tissue specific manner, such as the receptor-tyrosine kinase ***Pvr*** or the actin scaffolding protein ***alpha-spectrin.*** The interaction of Pvr with Dscam1 is even conserved for the vertebrate orthologues, suggesting that it affects an important general function of the Dscam receptor family.

In addition, I identified ***regulators of translation*** to be important signaling targets of the Dscam1 receptor. One of these candidates, namely ***Fmr1***-protein has in the meantime been reported to regulate Dscam1-protein translation during formation of axonal terminal arbors (Cvetkovska et al., 2013). My data suggests that Dscam1 activation might be capable of regulating Fmr1 regulated translation locally at sites of receptor activation, creating an auto regulatory feedback mechanisms. Other important signaling units downstream of the Dscam1 receptor are the ***actin cytoskeleton*** and the ***endomembrane-system***. This suggests that besides phosphorylation there are additional modes of fine-tuning the strength of a Dscam1 signal.

Surprisingly, I also identified ***transcriptional regulators*** as potential Dscam1 interactors. A pilot microarray study suggests that Dscam1 signaling indeed has a long-term transcriptional component. This observation was made in hemocyte like S2 cells. If the result is only relevant for immune cell priming or if it can also be translated into cells of neuronal origin needs to be evaluated in the future. However, my results clearly show that Dscam1 signaling might not only affect global tyrosine phosphorylation but also influence local translation and the endocytotic machinery as well as the transcriptional signature of a cell. This multifaceted signaling reaction opens room for speculation as to how these molecular mechanisms are utilized in different (sub)cellular contexts.

Chapter 3- INTRODUCTION

The Dscam1 transmembrane-receptor is a neuronal self-recognition molecule of the Ig-superfamily (Schmucker et al., 2000), required for dendrite patterning, axon guidance, branching and terminal arborization (reviewed in Grueber and Sagasti, 2010; Jan and Jan, 2010; Kolodkin and Tessier-Lavigne, 2011; Zipursky and Grueber, 2013). The regulation of Dscam signaling is extremely important. For example, the level of vertebrate *DSCAM* expression is high during neuronal development and neurite outgrowth and decreases with adulthood. This regulation is impaired in patients with Down's syndrome, indicating that *DSCAM* contributes to the development and maintenance of mental capacities (Saito et al., 2000). Interestingly, hyper-activation of *Drosophila* Dscam1 leads to strong axon guidance phenotypes, suggesting that neuronal wiring may be particularly sensitive to *Dscam1* dosage (Chen et al., 2006; Dascenco and Erfurth et al., 2015; He et al., 2014a; Schmucker et al., 2000).

In *Drosophila,* Dscam1 is expressed in neuronal cells of both the CNS and PNS (Hummel et al., 2003; Schmucker et al., 2000). Furthermore, *Dscam1* is also expressed and required in cells of the innate immune system of flies, the hemocytes and fat body (Watson, 2005). *Dscam1* null mutations are either late embryonic or early larval lethal. An extraordinary feature of *Drosophila Dscam1* is that it potentially encodes thousands of isoforms with 19,008 distinct extracellular domains by virtue of mutually exclusive alternative splicing (Schmucker et al., 2000) (Introduction- Figure 10). Systematic *in vitro* binding studies have shown that Dscam isoforms can interact in a highly selective homophilic manner (Wojtowicz et al., 2007). Homophilic Dscam1-Dscam1 interactions induce neurite-neurite repulsion. However, such interaction occurs exclusively between neurites stemming from the same cell because they share the same *Dscam1* isoform set. A patterning principle based on homophilic Dscam1-Dscam1 repulsive interactions is critical for the expansion of uniformly spaced neurite arborizations. This is not only important during dendritic patterning but plays also a critical role for axonal branching (Dascenco and Erfurth et al., 2015; He et al., 2014a; Hughes et al., 2007).

Despite the importance of Dscam1 signaling for neuronal patterning surprisingly little is known regarding the signaling pathway. All known molecular interactors of the Dscam1 cytoplasmic domain exert their function only in a subset of cellular contexts. Interestingly, we recently demonstrated that Dscam1 activation involves a highly regulated local tyrosine

phosphorylation step (Dascenco and Erfurth et al., 2015). However, the downstream effector molecules activated by the phosphorylation events remain in the dark.

Reversible tyrosine phosphorylation is a very common and rapid way of modifying protein function. It usually affects the function or stability of a protein or its interactions with other molecules, thereby influencing the outcome of many signaling pathways (Gafken and Lampe, 2006). While many proteins are modified by reversible phosphorylation of serine and threonine, only a small but significant fraction of the proteome is tyrosine phosphorylated (Mann et al., 2002). The study of tyrosine phosphorylation has largely been facilitated by the development of phosphor-specific antibodies (Gafken and Lampe, 2006; Mann et al., 2002). Such antibodies recognize a protein only if it is phosphorylated. For example, the widely used antibody 4G10 allows for the purification of tyrosine-phosphorylated protein complexes. However, the fraction of tyrosine phosphorylated proteins in cells is very small and experience shows that antibody based strategies perform poorly during the enrichment of phosphor-peptides (Mann et al., 2002). Therefore, it has become common practice to purify such proteins by enriching negatively charged phosphorylated peptides over positively charged metal columns (IMAC) (Mann et al., 2002; Gafken and Lampe, 2006). While this approach has been widely used, it also has limited the view of the "tyrosine-phosphor-proteome" to such proteins, that readily give rise to tyrosine phosphorylated peptides. Proteins with several phosphorylation sites might be overrepresented, and protein complexes centered around tyrosine phosphorylated proteins are not resolved at all.

In this chapter, I am describing how I combined antibody based purification of tyrosine-phosphorylated protein complexes with quantitative mass-spectrometry based fingerprinting to identify signaling complexes that change their phosphorylation status upon Dscam1 activation. I identified a number of different proteins, many of which belong to protein families involved in regulating the translation of mRNA into proteins. I compared the data obtained by tyrosine-phosphor-proteomics with the results that I obtained by analyzing the Dscam1-signaling complex in neuronal BG3C2 cells.

My results suggest that ***many components of the translational machinery*** are present in the Dscam1 signaling complex. This indicates that Dscam1 is capable of directly recruiting components of the translational machinery to the cytoplasmic domain. This would allow the Dscam1 receptor to locally control the translation of mRNAs in sub-compartments of an outgrowing growth cone. While further experiments are needed to test the *in vivo*

significance of these results, we also exploited a possible link of our proteomic data to ***transcriptional regulation***. Thus far, it remains unknown if Dscam1 has any effect on the nuclear transcription of DNA. Based on the results of a pilot-microarray experiments in S2 cells, I can report that Dscam1 indeed affects transcription. The most notable group of candidate genes are ***G-protein coupled receptors***. If this result represents solely an immune response or if it also translates into neurons remains an open question.

Taken together my results suggest that Dscam1 signaling has a ***long-term and a short-term component***. Activation of Dscam1 signaling leads to phosphorylation events and the recruitment of translational machinery to the receptor. While this event happens in a matter of minutes, I also observed changes in the transcriptional signature of cells after induction of the chimeric Met-Dscam1 receptor. This suggests that Dscam1 has also longer terms effects on the transcription of target genes, which could change the properties of a cell, for example by altering the presence of surface receptors at the membrane. This might not only be relevant for the detection and phagocytosis of pathogens but also for effective axon guidance or later in life during memory formation and for the maintenance of synaptic homeostasis.

The Dscam1 intracellular domain contains many conserved tyrosines of unknown function including a poly-tyrosine motif

Both invertebrate Dscam1 and vertebrate DSCAM are tyrosine phosphorylated. The intracellular domain of *Drosophila* Dscam1 for example, contains 21 tyrosines (Chapter 3- Figure 1). Functionally, only three of the tyrosines have a confirmed function *in vivo* function: *Y1857* and *Y1890* are part of SH2 binding sites important for the interaction with the adaptor protein Dock (Schmucker et al., 2000). Furthermore, we have shown that both SH2-binding sites as well as a tyrosine in exon 23 (*Y1981*) interact with the receptor tyrosine phosphatase RPTP69D (Chapter 3 and Dascenco and Erfurth et al., 2015). However, the functional consequence of dephosphorylating the SH2 binding sites are fundamentally different from dephosphorylating *Y1981* and therefore not fully understood. While dephosphorylating of *Y1857* and *Y1890* leads to reduction of Dscam1 signaling, we observed and enhancement of function upon mutating *Y1981* to phenylalanine (Dascenco and Erfurth et al., 2015). In addition, it has been suggested that a fourth tyrosine in the center of the so-called "*Dscam-box*" (*Y1774*) is a target for the interaction with Abl-kinase (Andrews et al., 2008).

In order to better understand which of the tyrosines in the Dscam1 intracellular domain might be of functional importance, I used the ClustalΩ algorithm to align the sequences of Dscam family members of different species (*Drosophila melanogaster, Tribolium castaneum, Daphnia magna and Apis mellifera)* to identify highly conserved tyrosines. I reasoned that such tyrosines are more likely to be important mediators of cellular signals. We found ***14 highly conserved tyrosines***, one of which is part of a *Drosophila* specific 33-amino-acid-repeat region (Chapter 3- Figure 1).

Strikingly, there is a ***poly-tyrosine motif*** at the center of the intracellular domain in exon 21. It is characterized by the sequence *YXXYXX(X)YXXXYXXY*. Tyrosine-rich stretches have been observed in other ***aggregating proteins***, such as in alpha- and beta synucleins (Negro et al., 2002). The sheer number of tyrosines as well as the length of the motif however, are unusual. Therefore, it might be very interesting to investigate in the future if this accumulation of tyrosine has a role in Dscam1-Dscam1 multimerization.

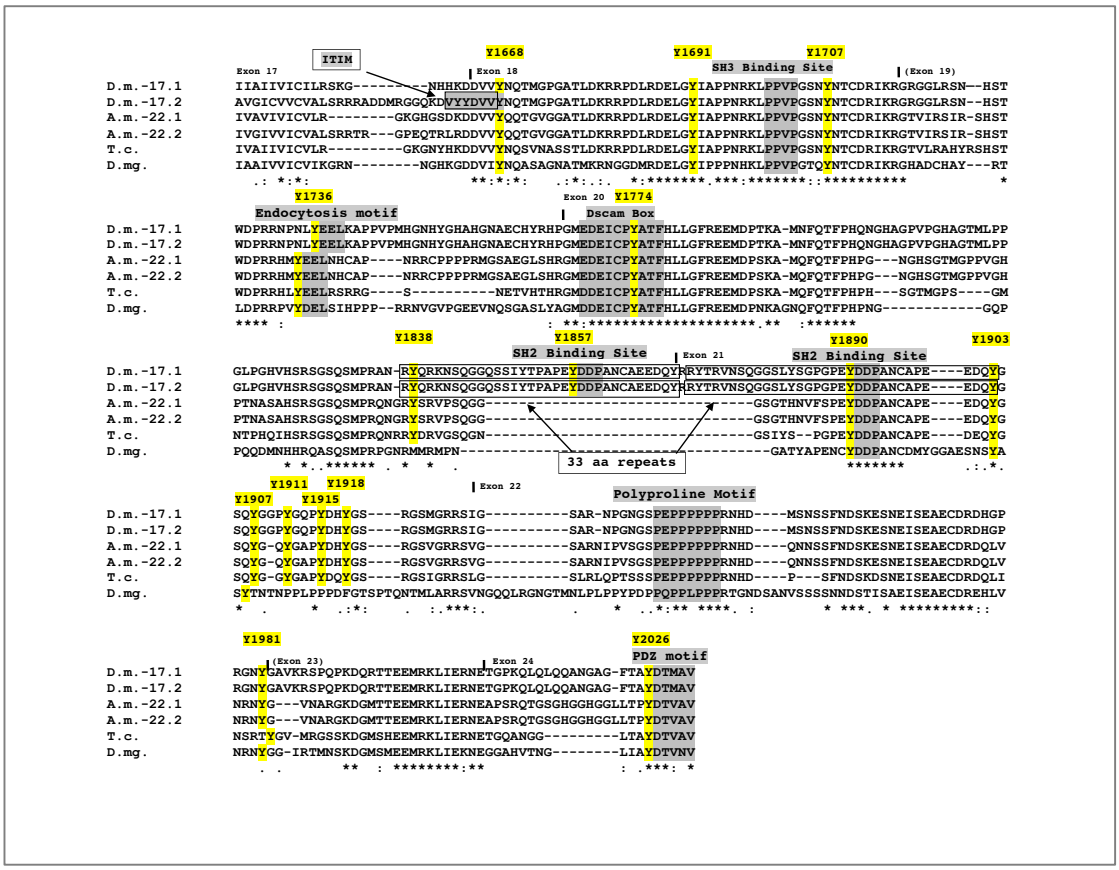

CHAPTER 3- FIGURE 1. **ALIGNMENT OF INVERTEBRATE DSCAM1 SEQUENCES REVEALS MANY CONSERVED TYROSINES.**

The grey boxes indicate signaling motifs reported in previous publications (Brites et al., 2008; Schmucker et al., 2000; Yang et al., 2012). The intracellular domain of Drosophila Dscam1 contains 21 tyrosines. Tyrosines considered to be important because of their conservation are indicated in yellow. This includes one tyrosine in the first SH2-binding site, which is part of a 33 aa conserved region (1857). Y1857, Y1890 and Y1981 were found to be potential RPTP69D substrate sites (Dascenco and Erfurth et al. 2015). However, dephosphorylation of these tyrosines appears to have distinct functions: Dephosphorylation of Y1857 and Y1890 inactivates Dscam1 signaling, while dephosphorylation of Y1981 leads to Dscam1 hyper-activation. The SH3-binding sites and SH2-binding sites are important for the interaction with the adaptor protein dock. Besides this, no other tyrosine in the Dscam1 intracellular domain has any proven signaling function as of today. Note the poly-tyrosine motif between Y1903 and Y1918. Despite its prominence, there is no assigned function.

The Dscam1 intracellular domains contains seven novel potential Y-based signaling motifs suggesting links to RTK signaling, transcription and translation

In an effort to assign functions to the remaining tyrosines of unknown function, we used the Elm Motif search tool (*http://elm.eu.org*) to discover novel signaling motifs centered around conserved tyrosines. In addition to the known two SH2-binding sites, we found ***seven novel tyrosine based signaling motifs*** listed in Chapter 3- Table 1 and Chapter 3- Figure 2.

They can be divided into the following ***three subclasses***:

(1) ***SH2 binding sites*** linking Dscam1 to signaling of the PTP ***corkscrew*** (CG3954) (Y1691) or phospholipase-gamma signaling (***small wings***) (Y691) as well as transcription factors (***Stat92E***) (1691 and Y1903). Interestingly, corkscrew and small wings (CG4200) have been found in the signaling pathways of most fly RTKS. Stat92E (CG4257) on the other hand is a transcriptional activator.

(2) Y-based sorting motifs important for the interaction with the ***AP-complex*** (Y1736, Y2026 and *Y1774*). The AP complex consists of a hetero-tetramer composed of two large subunits (adaptins, CG3002), a medium subunit (muA) and a small subunit (muS). Such a binding site would allow the binding of clathrin coated vesicles to the Dscam1 intracellular domain, affecting receptor mediated endocytosis. This finding is intriguing, as Dscam1 has been found in a complex of tyrosine phosphorylated proteins with the medium subunit of the AP-complex - known as AP-50- as well as with the sorting nexin SH3PX1.

(3) A binding motif for the translation initiation factor ***eIF4E*** (CG4035, CG10124, CG11392, CG8277, CG1422)

A second Dscam box?

To further pinpoint tyrosines important for Dscam1 signaling, we aligned the amino acid sequences of all Dscam paralogues in *Drosophila melanogaster* with the longest version of the intracellular domain of Dscam1. Earlier reports had identified a region known as the ***Dscam-box*** to be the only conserved stretch found in all Dscam paralogues (Andrews et al., 2008; Brites et al., 2013; Yang et al., 2012). This region contains a highly conserved tyrosine. It has been proposed that this signaling motif might be critical for an essential Dscam signaling function common to all Dscam family members. When I repeated such alignments with a special focus on conserved tyrosines I noticed ***a second Y-centered motif*** to be extremely conserved in the Dscam family: This *YXA* motif ***(*Y1691*) in exon 18*** lies right in front of the first SH3 binding site (Chapter 3- Figure 3) of the Dscam1 cytoplasmic domain. My *ELM* based sequence analysis suggests that it might be the center tyrosine of an SH2-binding site.

Another notable result of these alignments is the observation that the Dscam1 intracellular domain lacking exon 19 results in a very long conserved stretch (Chapter 3- Figure 2). Most cDNA based studies thus far have used the longest version of the Dscam1 intracellular domain, despite the fact that it is not very widely expressed *in vivo* (Yu et al., 2009). My alignments suggest that it might indeed valuable to include the shorter isoforms in further studies of Dscam1 signaling.

Y #	Motif	Function	Cellular Compartment	Consensus	Probability
Y1691	***YIAP***	SH2 binding site for *SH-PTP2/corkscrew and phospholipase C-gamma/small wing*	✓ Cytosol	(Y)[IV].[VILP]	2.454e-04
Y1691	***YIAP***	SH2 *binding site* for *STAT5/ Stat92E*	✓ Cytosol	(Y)[VLTFIC]..	3.296e-03
Y1736	***YEEL***	Tyrosine-based *sorting signal* responsible for the interaction with mu subunit of *AP (Adaptor Protein) complex*	✓ Plasma membrane, ✓ Clathrin-coated endocytic vesicle ✓ Cytosol	Y..[LMVIF]	2.587e-03
Y1774	***YATFHLL***	*Binding motif* for the dorsal surface of *eIF4E.*	✓ Cytosol	Y....L[VILMF]	1.891e-04
Y1774	***YATF***	Tyrosine-based *sorting signal* responsible for the interaction with mu subunit of *AP (Adaptor Protein) complex*	✓ Plasma membrane, ✓ Clathrin-coated endocytic vesicle ✓ Cytosol	Y..[LMVIF]	2.587e-03
Y1857	***YDDP***	SH2-*binding site*	✓ Cytosol	(Y)[QDEVAIL][DENPYHI][IPVGAHS]	8.729e-04
Y1890	***YDDP***	SH2-*binding site*	✓ Cytosol	(Y)[QDEVAIL][DENPYHI][IPVGAHS]	8.729e-04
Y1903	***YGSQ***	SH2 *binding motif* found in the cytoplasmic region of cytokine receptors that bind *STAT3/ Stat92E* SH2 domain.	✓ Cytosol	(Y)..Q	7.975e-04
Y2026	***YDTM***	Tyrosine-based *sorting signal* responsible for the interaction with mu subunit of *AP (Adaptor Protein) complex*	✓ Plasma membrane, ✓ Clathrin-coated endocytic vesicle, ✓ Cytosol	Y..[LMVIF]	2.587e-03

CHAPTER 3- TABLE 1. **TYROSINE BASED CONSERVED SIGNALING MOTIFS IN THE DSCAM1 INTRACELLULAR DOMAIN.**

The motifs were predicted with the ELM search tool. All information regarding the motifs was derived from the ELM and the SMART databases. Y#: Position of the tyrosine in the Dscam1 intracellular domain; Motif: Amino acid sequence considered as belonging to the motif; Function: molecular interaction mediated by the motif; Cell compartment: Subcellular region in which proteins carrying the motif are found; Consensus: Minimal consensus sequence; Probability: Indicates the likelihood that this amino acid sequence is more than a random occurrence.

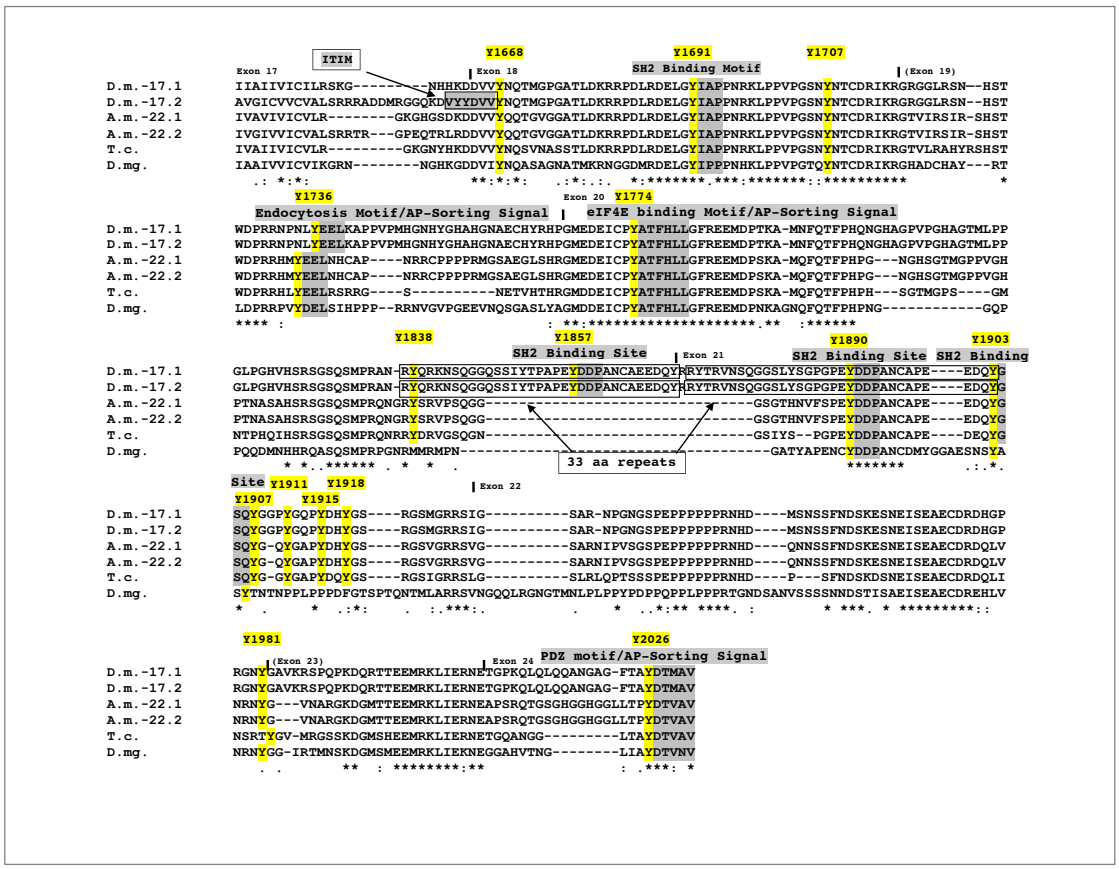

CHAPTER 3- FIGURE 2. **LOCATION OF NOVEL TYROSINE BASED SIGNALING MOTIFS IN THE DSCAM1 INTRACELLULAR DOMAIN.**

Note, that skipping of exon 19 results in a very long stretch of conserved amino acids (even though four extra amino acids are added to the transcript). The novel motifs can be divided into three main functional classes: (1) SH-2 binding sites; (2) interaction sites for the AP- complex; (3) interaction sites for components of the translational machinery

Development of a purification strategy to isolate tyrosine phosphorylated protein-complexes affected by Met-Dscam1 signaling (silver gel 1)

In order to better understand Dscam1 signaling, we decided to analyze the tyrosine phosphorylation events which are triggered by stimulation of the chimeric Met-Dscam1 receptor in S2 cells by phosphor-proteomics. The reason for choosing this approach instead of the classical receptor-complex purification strategy was the idea, that a focus on phosphorylated proteins might help us to pinpoint ***important key-molecules*** of the Dscam1 signaling pathway. Therefore, I optimized an immunoprecipitation based purification strategy for tyrosine-phosphorylated protein complexes. Even though anecdotal reports in the field suggest that antibody mediated enrichment of phosphorylated peptides is technically challenging and inefficient (e.g. Mann et al., 2002), I was encouraged by the fact that the cytoplasmic domain of the *Drosophila* Dscam1 receptor is ***highly tyrosine***

phosphorylated and that I could easily reproduce this finding in my own experiments (Muda et al., 2002; Schmucker et al., 2000) (see also Chapter 3- Figure 4 and Chapter 3- Figure 5). Furthermore, I was capable to efficiently purify large amounts of phosphorylated proteins by immunoprecipitation. For example, I purified tyrosine phosphorylated proteins with the 4G10 antibody from S2 cells and could not only reliably detect Dscam1 in a western blot, but I also noticed the presence of other proteins visible during ***Ponceau-staining*** of the nitrocellulose membrane after transfer of the immune-precipitates from SDS gels (data not shown).

CHAPTER 3- FIGURE 3. **ALIGNMENT OF THE FULL LENGTH DSCAM1 INTRACELLULAR DOMAIN WITH ALL KNOWN ISOFORMS OF DSCAM PARALOGUES IN *DROSOPHILA*.**

There are two highly conserved tyrosines present in all four the Dscam family paralogues (labeled in yellow). The YxA motif right in front of the first SH3-binding site (Y1691) might represent the center of an SH2-binding site (refer also to Chapter 3-Figure 2). The tyrosine (Y1774) is at the center of a sequence already known as the "Dscam box".

In order to conditionally activate Dscam1 signaling, I used a stable cell lines of S2 cells expressing the Met-Dscam1 chimeric receptor described in Chapter 2 and (Dascenco and Erfurth et al., 2015) (Chapter 3- Figure 5). Met-Dscam1 is a fusion product of the extracellular domain of the mouse cMet-receptor and the *Drosophila* transmembrane- and intracellular domain of Dscam1. The advantage of this assay is, that Dscam1 tyrosine

phosphorylation and signaling can be conditionally induced by addition of the Met-ligand HGF to the cell culture medium (Dascenco and Erfurth et al., 2015). There is no HGF in flies rendering the activation of Met-Dscam1 independent of any of the thousands of potential endogenous Dscam1 ligands.

In order to tackle the question which proteins and signaling complexes might be activated or inactivated in response to Met-Dscam1 activation, I optimized a ***large scale immunoprecipitation protocol.*** I used a buffer system based on *Tris*-buffer supplemented with NaCl, EDTA and 1% of detergent (Chapter 3- Figure 6). Important components of the protocol were: (1) The ***timing of the chimeric receptor phosphorylation***, (2) the choice of ***lysis and wash buffer***, (3) the ***ratio of antibody coated beads to sample volume*** and (4) the elution with ***sarcosyl containing elution*** buffer. After optimizing cell and protein amounts required, I conducted a pilot experiment in Met-Dscam1 expressing S2 cells. From the resulting silver stained SDS gel, I cut single bands for mass-spectrometric peptide fingerprint analysis.

We chose bands for the analysis that showed significant and clear changes in intensity (evaluated by eye) and analyzed them via LC-MS/MS peptide mass fingerprinting analysis ***(Taplin facility of Harvard University, Boston MA (Gygi lab)).*** The purification strategy, the resulting silver stained SDS-gel and the bands chosen for analysis are depicted in Chapter 3-Figure 6. Despite the fact, that I was only capable of purifying enough protein to be visualized by silver staining, we were able to detect sufficient peptides during the mass-spec fingerprinting to identify proteins with good confidence. The result of the first mass-spectrometry based fingerprinting experiment are listed in (Chapter 3- Tables 2-6).

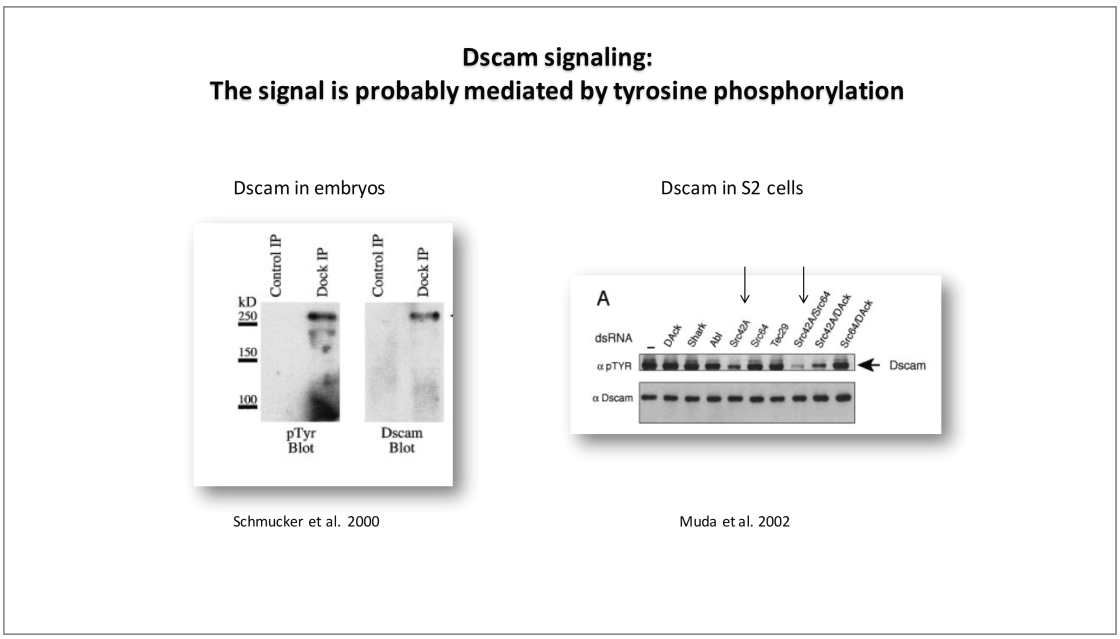

CHAPTER 3- FIGURE 4.**THE CYTOPLASMIC DOMAIN OF THE DSCAM1 RECEPTOR IS HEAVILY TYROSINE PHOSPHORYLATED.**

Left: Dscam1 is a highly tyrosine phosphorylated protein and belongs to a protein complex binding to the adaptor protein dock in Drosophila embryos. Dock is the invertebrate orthologue of vertebrate Nck proteins (figure taken from Schmucker et al., 2000). Right: Dscam1 in S2 cells is heavily tyrosine phosphorylated by tyrosine kinases of the Src family, with Src42A and Src64B being the main modifiers of Dscam1 tyrosine phosphorylation in hemocytes (figure taken from Muda et al., 2002).

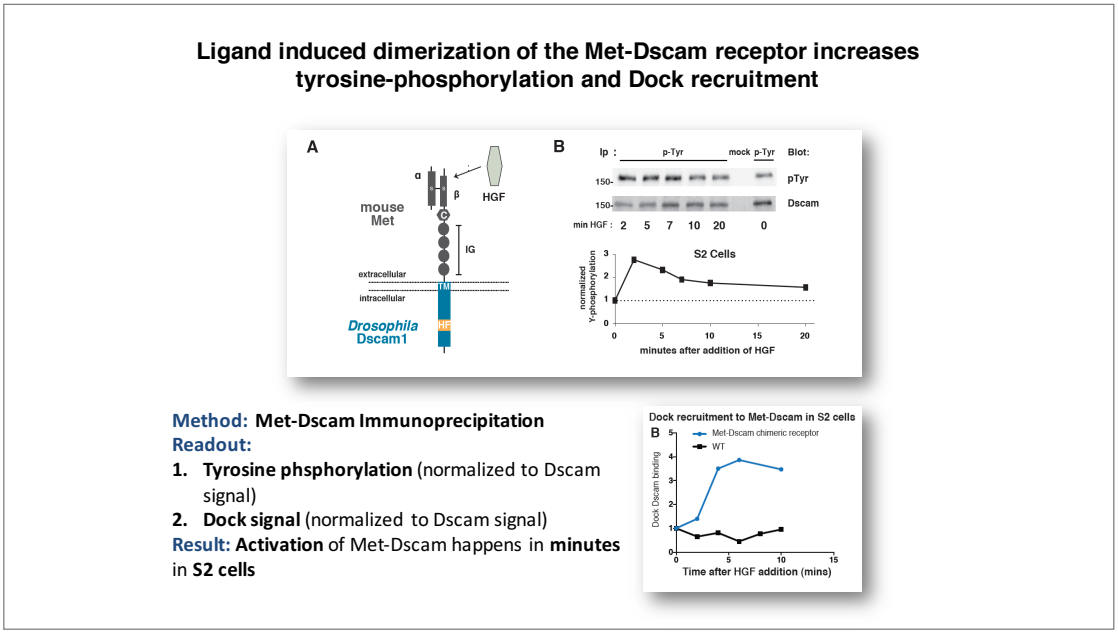

CHAPTER 3- FIGURE 5. **THE INTRACELLULAR DOMAIN OF MET-DSCAM1 IS HEAVILY TYROSINE PHOSPHORYLATED.**

The Met-Dscam1 chimeric receptor (Dascenco and Erfurth et al. 2015) can be activated by addition of HGF to the cell culture medium (A). It responds to ligand addition with quick increased tyrosine phosphorylation (B) and Dock recruitment (C).

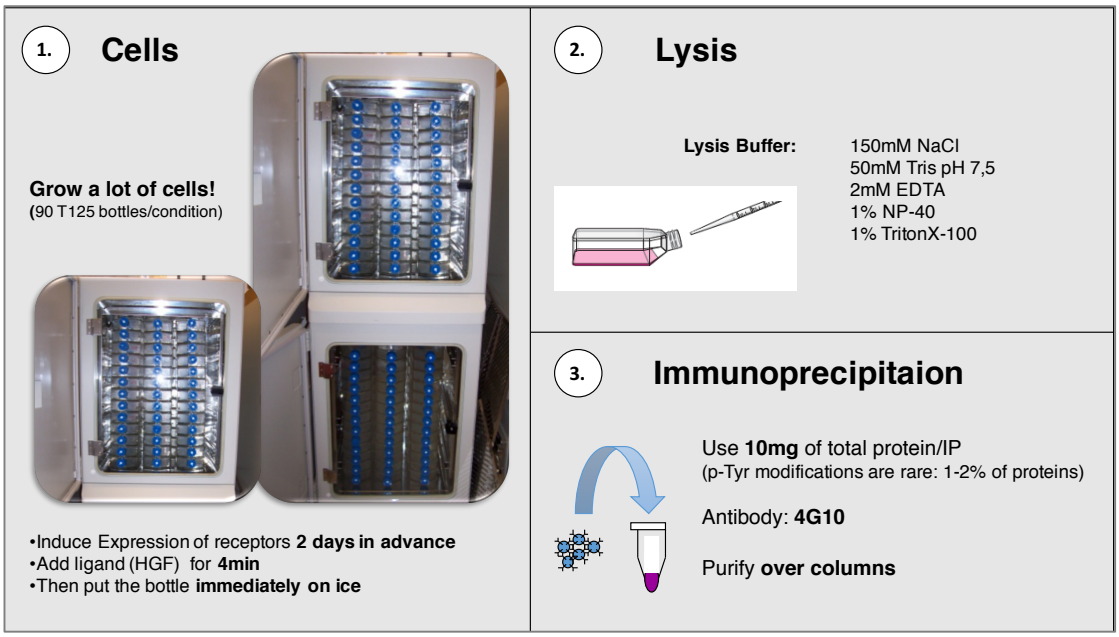

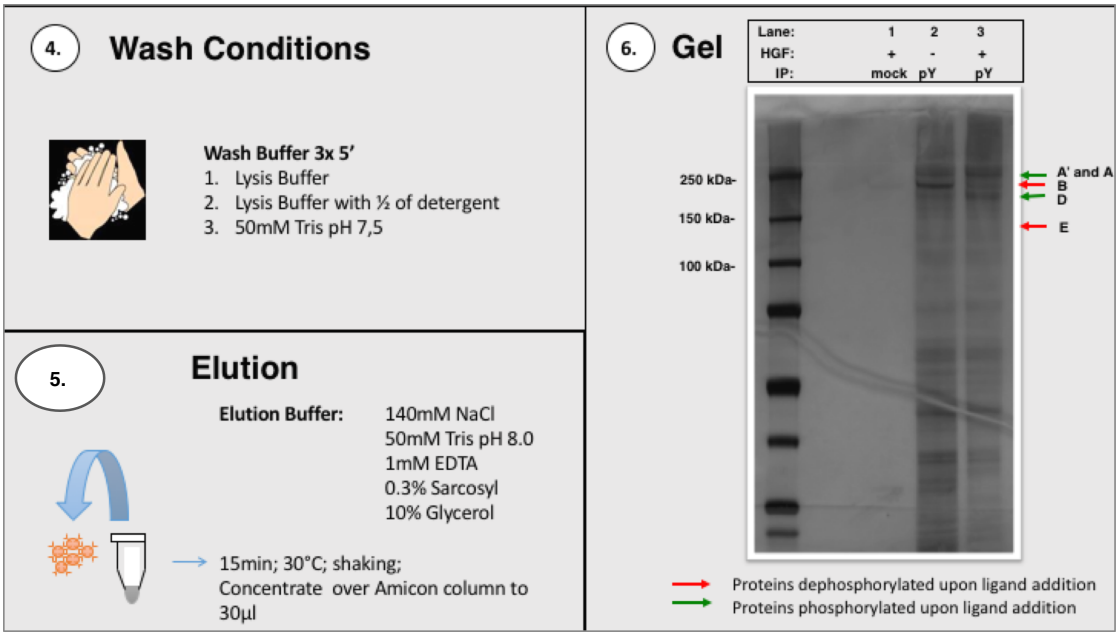

CHAPTER 3- FIGURE 6. **PURIFICATION STRATEGY TO OBSERVE THE EFFECT OF MET-DSCAM1 ACTIVATION ON TYROSINE PHOSPHORYLATED PROTEINS IN S2 CELLS.**

Efficient immunoprecipitation of tyrosine phosphorylated proteins affected by Met-Dscam1 signaling was possible by using an immunoprecipitation protocol employing the conditions shown above. Critical points of the experiment were the timing of the activation, the ratio of antibody coated beads to sample, the use of the right lysis and wash buffers as well as the elution via sarcosyl elution buffer. Bands significantly changing intensity under different experimental conditions were cut out and subject to MS-based peptide fingerprinting.

Results of the first silver gel

CHAPTER 3- TABLE 2. **BAND A CUT OUT FROM THE SILVER GEL AFTER PURIFICATION OF TYROSINE PHOSPHORYLATED PROTEINS.**

This 250 kDa band cut out from the third lane of silver gel 1, representing a protein complex existent in the presence of the Met-Dscam1 ligand HGF (+HGF). It was intended to be compared to Band A', the corresponding band in the sample without HGF (Lane 2). If these two bands correspond, the signal of the relevant proteins should be increased upon HGF activation. Blue: Identification with more than one unique peptide (Good confidence) Yellow: Protein also identified in other experiments in this dissertation. Grey: Identification by only one unique peptide.

Band	Protein	Human Orthologue	# of peptides identified	% of sequence covered by mass	% of sequence covered by aa count	MW in kDa	Protein Family	Paralogues
A	***Abelson tyrosine kinase*** *Abl, CG4032*	ABL1 and ABL2	**28**	**23,5**	**24,5**	170 predicted; 250 reported	***Tyrosine kinase***	Src64A Src42A
A	***Prosap*** *CG30483, CG8122*	SHANK1,SHANK2	**8**	**8,7**	**7,9**	199 predicted	***Synaptic scaffolding protein***	-
A	***Polychaetoid*** *pyd, ZO-1, CG31349, tam, Tamou, dzo-1, CG31349*	TJP1 and TJP2 and TJP3	**15**	**16.4**	**15.7**	Depending on isoform: 125.6-230.5 predicted	***Cell adhesion molecule; guanylate cyclase***	CG6509 (Dlg5)
A	***PDGF- and VEGF-receptor related*** *Pvr, VEGFR, stai, CG8222*	FLT1,FLT3, FLT4, KDR, PDGFRA, KIT,CSF1R	**6**	**7,2**	**7,0**	137,3 predicted	***Receptor tyrosine kinase***	Heartless (htl); breathless (btl)
A	***Clathrin heavy chain*** *Chc, CLH CG31349*	CLTC, CLTC1	**5**	**4,8**	**4,7**	191 predicted	***Clathrin heavy chain***	-
A	***Cheerio*** *cher, sko, FLN, CG3937*	FLNC	**4**	**2,3**	**2,2**	240	***Actin binding filamin***	jbug; CG5984
A	***Eukaryotic translation initiation factor*** *eIF4G, eIF-4G, delF4G CG10811*	EIF4G1, EIF4G3	**4**	**3,1**	**2,9**	211,1 predicted	***Translation initiation factor***	eIF4G2, NAT1
A	***RhoGAP15B*** *CG4937*	ARAP1, ARAP2,ARAP3	**3**	**1,9**	**1,9**	169,9	***Rho and ARF GTPase activator***	cenB1A, Asap1, cenG1A
A	***Down syndrome cell adhesion molecule 1*** *Dscam1, CG17800, Neu1, p270*	DSCAM, DSCAML1	**2**	**1,2**	**1,2**	220 predicted; 270 observed	***Cell adhesion molecule; axon guidance receptor***	Dscam2, Dscam3, Dscam4, Contactin, Neuroglian
A	***Glutamyl-prolyl-tRNA synthetase*** *Aats-glupro; EPRS, GluProRS, CG5394*	EPRS	**3**	**3,4**	**3,1**	Depending on isoform: 189 or 107,8 predicted	***Bifunctional glutamate/proline tRNA ligase***	-
A	***Collagen Type IV*** *Cg25C, Dcg1, CG4145*	COL7A1	**2**	**2**	**2**	174,3 predicted	***Collagen alpha IV chain (extracellular matrix)***	vkg
A	***v (2) k05816*** *CG3524*	FASN	**1**	**0,6**	**0,6**	265,9 predicted	***Fatty acid synthase***	CG3523, CG17374, CG12170
A	***c11.1*** *CG12132*	MRO, MROH8, MROH2B MROH1, MROH7, MROH2A, MROH5, MROH6, MROH7-TTC4	**1**	**1,0**	**0,9**	193,1 predicted	***Maestro like heat repeat containing protein***	-
A	***CG3523*** *FAS, Fatty acid synthase, BcDNA:gh07626, dFAS*	FASN	**1**	**0,5**	**0,5**	266,4 predicted	***Fatty acid synthase***	v(2)k05816, CG17374, CG12170
A	***Transport and Golgi organization*** *Tango1, CG11098*	MIA, CTAGE15, CTAGE6, CTAGE5, MIA3, CTAGE1, CTAGE4, CTAGE8, RP11-407N17.3	**1**	**1,0**	**0,9**	139,1 predicted	***MIA/OTOR family***	-

CHAPTER 3- TABLE 3. **BAND A' CUT OUT FROM THE SILVER GEL AFTER PURIFICATION OF TYROSINE PHOSPHORYLATED PROTEINS.**

This band was a 250 kDa band cut out from the second lane of silver gel 1, representing a protein complex existent in the absence of the ligand HGF (-HGF). It was intended to be compared to Band A, which appeared to be the corresponding band in the sample with HGF. If these two bands correspond, the signal of the relevant proteins should be increased upon HGF activation. Blue: Identification with more than one unique peptide (Good confidence) Yellow: Protein also identified in other experiments. Grey: Identification by only one unique peptide.

Band	Protein	Human Orthologue	# of peptides identified	% of sequence covered by mass	% of sequence covered by aa count	MW in kDa	Protein Family	Paralogues
A'	***Abelson tyrosine kinase*** *Abl, CG4032*	*ABL1 and ABL2*	**33**	**24,1**	**24,3**	170 predicted 250 reported	**Tyrosine kinase**	Src64A Src42A
A'	***Glutamyl-prolyl-tRNA synthetase*** *Aats-glupro; EPRS, GluProRS, CG5394*	*EPRS*	**9**	**8,8**	**9,1**	Depending on isoform: 189 or 107,8 predicted	**Bifunctional Glutamate/Proline tRNA ligase**	-
A'	***Cheerio*** *cher, sko, FLN, CG3937*	*FLN*	**5**	**2,7**	**2,7**	240	**Actin binding filamin**	jbug; CG5984
A'	***Polychaetoid*** *pyd, ZO-1, CG31349, tam, Tamou, dzo-1, CG31349*	*TJP1 and TJP2 and TJP3*	**14**	**12,2**	**12,2**	Depending on isoform: 125.6-230.5 predicted	**Cell adhesion molecule; Guanylate cyclase**	CG6509 (Dlg5)
A'	***Prosap*** *CG30483, CG8122*	*SHANK1,SHANK2*	**3**	**3,0**	**3,0**	199 predicted	**Synaptic scaffolding protein**	-
A'	***Eukaryotic translation initiation factor*** *eIF4G, eIF-4G, deIF4G CG10811*	*EIF4G1, EIF4G3*	**3**	**3,2**	**3,0**	211,1 predicted	**Translation initiation factor**	eIF4G2, NAT1
A'	***PDGF- and VEGF-receptor related*** *Pvr, VEGFR, stai, CG8222*	*FLT1,FLT3, FLT4, KDR, PDGFRA, KIT,CSF1R*	**4**	**3,7**	**3,7**	137,3 predicted	**Receptor tyrosine kinase**	Heartless (htl); breathless (btl)
A'	***Down syndrome cell adhesion molecule 1*** *Dscam1, CG17800, Neu1, p270*	*DSCAM, DSCAML1*	**2**	**3,9**	**3,4**	220 predicted; 270 observed	**Cell adhesion molecule; axon guidance receptor**	Dscam2, Dscam3, Dscam4, Contactin, Neuroglian
A'	***Elongation factor 1α48D*** *Ef1α48D, ef-1α, Ef1alpha48D, EF1α, EF, F1, CG8280*	*EEF1A1, EEF1A2*	**2**	**6,3**	**5,8**	50,3 predicted	**GTPase, translation elongation factor**	Ef1alpha100E
A'	***Phosphatidylinositol 3 kinase 68D*** *Pi3K68D, Pi3K, PI3K_68D, dPI3K, cpk, PI(3)K, CG11621*	*PIK3C2A, PIK3C2B, PIK3C2G*	**1**	**0,9**	**0,8**	210	**1-phosphatidylinositol-3-kinase activity; 1-phosphatidylinositol-4-phosphate 3-kinase activity; phosphatidylinositol 3-kinase activity;**	Pi3K92E, Pi3K59F
A'	***Clathrin heavy chain*** *Chc, CLH CG31349*	*CLTC, CLTC1*	**1**	**0,7**	**0,7**	191 predicted	**Clathrin heavy chain**	-
A'	***RhoGAP15B*** *CG4937*	*ARAP1, ARAP2,ARAP3*	**1**	**1,1**	**1,1**	169,9 predicted	**Rho and ARF GTPase activator**	cenB1A, Asap1, cenG1A
A'	***v (2) k05816*** *CG3524*	*FASN*	**1**	**0,6**	**0,6**	265,9 predicted	**Fatty acid synthase**	CG3523, CG17374, CG12170

CHAPTER 3- TABLE 4. **BAND B CUT OUT FROM THE SILVER GEL AFTER PURIFICATION OF TYROSINE PHOSPHORYLATED PROTEINS.**

This 250 kDa band cut out from the second lane (-HGF) of silver gel 1, representing a protein complex disappearing in the presence of the ligand HGF. A corresponding band in the sample with HGF (Lane 3) was much weaker. Blue: Identification with more than one unique peptide (Good confidence) Yellow: Protein also identified in other experiments in this dissertation. Grey: Identification by only one unique peptide.

Band	Protein	Abbreviation	# of identified peptides	% of sequence covered by aa count	% of sequence covered by mass	MW in kDa	Protein Family	Paralogue
B	***Phosphatidylinositol 3 kinase 68D*** *Pi3K68D, Pi3K, PI3K_68D, dPI3K, cpk, PI(3)K, CG11621*	PIK3C2A, PIK3C2B, PIK3C2G	**15**	**13,4**	**14**	210	**Phosphatidyl-Inositol-4-phosphate-3-kinase**	Pi3K92E, Pi3K59F
B	***Cheerio*** *cher, sko, FLN, CG3937*	FLN	**9**	**5,2**	**5,2**	240	**Actin binding filamin**	jbug; CG5984
B	***Prosap*** *CG30483, CG8122*	SHANK1,SHANK2	**7**	**7,4**	**6,5**	199 predicted	**Synaptic scaffolding protein**	-
B	***sponge*** *sp,CG31048, DmDOCK4, mat(3)6*	DOCK3, DOCK4	**6**	**4,3**	**4,2**	246,7 predicted	**Rho guanyl-nucleotide exchange factor**	mbc
B	***Polychaetoid*** *pyd, ZO-1, CG31349, tam, Tamou, dzo-1, CG31349*	TJP1, TJP2, TJP3	**12**	**12,5**	**12,3**	Depending on isoform: 125.6-230.5 predicted	**Cell adhesion molecule; guanylate cyclase**	CG6509 (Dlg5)
B	***viking*** *vkg, CG16858*	COL4A2, COL4A6, COL4A4	**4**	**2,3**	**2,1**	193,8 predicted	**Collagen alpha IV chain (extracellular matrix)**	Cg25C
B	***Clathrin heavy chain*** *Chc, CLH CG31349*	CLTC, CLTC1	**3**	**1,9**	**1,9**	191,2 predicted	**Clathrin heavy chain**	-
B	***Abelson tyrosine kinase*** *Abl, CG4032*	ABL1 and ABL2	**3**	**2,5**	**2,5**	180 reported	**Tyrosine kinase**	Src64A Src42A
B	***Pi3K92E*** *Dp110, PI3K, p110, dPI3K, PI(3)K, PI3K-Dp110, PI3K-92D, CG4141*	PIK3CB, PIK3CD	**1**	**1,1**	**1,0**	127 predicted	**Phosphatidyl-insositol-4,5-biphosphate-3-kinase**	Pi3K68D, Pi3K59F
B	***Tenascin major*** *b, odz, tenm, CG5723*	-	**1**	**0,4**	**0,4**	304,1 predicted 900,270, 70 and 55 observed	**Filamin binding Protein**	Cell adhesion; regulation of cell shape
B	***CG3523*** *FAS, Fatty acid synthase, BcDNA:gh07626, dFAS*	FASN	**1**	**0,5**	**05**	266,4 predicted	**Fatty acid synthase**	v(2)k05816, CG17374, CG12170
B	***Elongation factor 1a48D*** *Ef1a48D, ef-1a, Ef1alpha48D, EF1a, EF, F1, CG8280*	EEF1A1, EEF1A2	**1**	**1,7**	**1,9**	50,3 predicted	**GTPase, translation elongation factor**	Ef1alpha100E

CHAPTER 3- TABLE 5. **BAND D CUT OUT FROM THE SILVER GEL AFTER PURIFICATION OF TYROSINE PHOSPHORYLATED PROTEINS.**

This 170 kDa band was cut out from the third lane of silver gel 1, representing a protein complex existent in the presence of the ligand HGF (+HGF). There was a corresponding band in Lane 2 (-HGF). However, the signal was stronger in Lane 3 and therefore this band was chosen for analysis. Blue: Identification with more than one unique peptide (good confidence) Yellow: Protein also identified in other experiments in this dissertation. Grey: Identification by only one unique peptide.

Band	Protein	Human Orthologue	# of identified peptides	% of sequence covered by mass	% of sequence covered by aa count	MW in kDa	Protein Family	Paralogue
D	**Activated Cdc42 kinase** Ack, CG14992, DACK, p145	TNK2	**9**	**10,5**	**10,3**	118,4 predicted	**Protein tyrosine kinase**	PR2, hop, Fak56D, shark, EgfR
D	**Karyopherin β 3** Karyβ3, l(3)j3A4, Karybeta3, l(3)j7E8, CG1059	IPO5, RANBP6	**9**	**12,9**	**12,8**	123,6	**Importin subunit, protein transmembrane transporter**	-
D	**Abelson tyrosine kinase** Abl, CG4032	ABL1 ABL2	**9**	**7,3**	**7,2**	180 reported	**Tyrosine kinase**	Src64A Src42A
D	**moleskin** msk, dim-7, dim7, CIP-61, Imp7/8, CG7935	IPO7, IPO8	**7**	**9,0**	**8,8**	119,3 predicted	**Importin 7, Ran GTPase binding protein, protein transmembrane transporter**	-
D	**HEM-protein** kette, Nap1, kte, CG5837	NCKAP1, NCKAP1L	**5**	**6,5**	**6,3**	129,4 predicted	**Adaptor protein**	-
D	**Regulatory particle non-ATPase 2** Rpn2, p110, CG11888	PSMD1	**2**	**3,0**	**2,9**	113,2 predicted	**Proteasome regulatory subunit**	-
D	**Kinesin heavy chain** Khc, KIN, DmKHC, kinesin, DKH, kinesin-1, CG7765	KIF5A, KIF5B, KIF5C	**1**	**1,1**	**1,2**	110,4 predicted	**Microtubule motor protein, kinesin heavy chain protein,**	cos, Klp3A, Klp31E, Klp54D, pav, sub
D	**CG14516**	TRHDE	**1**	**1,1**	**1,2**	115,3 predicted	**Aminopeptidase, metallopeptidase**	CG3502, CG7653, CG31445, CG11951, SP1029, CG6071, CG9806, CG2111, sda, CG42335, CG5849, CG31198, CG31343, CG31233, CG40470, CG8774, CG8773, CG32473, CG4467, Psa
D	**Polychaetoid** pyd, ZO-1, CG31349, tam, Tamou, dzo-1, CG31349	TJP1, TJP2, TJP3	**1**	**0,5**	**0,6**	Depending on isoform: 125.6-230.5 predicted	**Cell adhesion molecule; guanylate cyclase**	CG6509 (Dlg5)

CHAPTER 3- TABLE 6. **BAND E CUT OUT FROM THE SILVER GEL AFTER PURIFICATION OF TYROSINE PHOSPHORYLATED PROTEINS.**

This 130 kDa band was cut out from the second lane of silver gel 1, representing a protein complex existent in the absence of the ligand HGF (-HGF). There was no corresponding band in Lane 3 representing tyrosine phosphorylated proteins in the absence of HGF. Blue: Identification with more than one unique peptide (good confidence) Grey: Identification by only one unique peptide.

Band	Protein	Human Orthologue	# of identified peptides	% of sequence covered by mass	% of sequence covered by aa count	MW in kDa	Protein Family	Paralogues
E	***specifically, Rac1-associated protein 1*** *CYFIP, sra1, DSra-1, PIR121, CG4931*	CYFIP1, CYFIP2	**46**	**32,1**	**31,6**	149,3 predicted	**Cytoplasmic GTP binding protein; subunit of the WRS complex**	-
E	***Abelson tyrosine kinase,*** *Abl, CG4032*	ABL1 ABL2	**11**	**12,0**	**11,3**	180 reported	**Tyrosine kinase**	Src64A Src42A
E	***Dynamin associated protein 160*** *Dap160, DAP-160, noncoding_4110, CG1099*	ITSN1, ITSN2	**8**	**10,6**	**10,2**	111,9 predicted 160 observed	**Intersectin**	Reps, Eps-15, CG9297, Past1
E	***Epidermal growth factor receptor pathway substrate clone 15*** *Eps-15, eps-15, CG16932*	EPS15, EPS15L1	**7**	**7,5**	**7,5**	134,4 predicted	**Protein present in clathrin coated vesicles**	CG9297, Past1, Reps, Dap160
E	***Polychaetoid*** *pyd, ZO-1, CG31349, tam, Tamou, dzo-1, CG31349*	TJP1, TJP2, TJP3	**14**	**13,2**	**12,8**	Depending on isoform: 125.6-230.5 predicted	**Cell adhesion Molecule; guanylate cyclase**	CG6509 (Dlg5)
E	***Protein kinase related to protein kinase N*** *Pkn, Dpkn, l(2)06736, l(2)45Ca, CG2049*	PKN1, PKN2, PKN3	**5**	**3,8**	**3,8**	166,8 predicted	**Protein serine/threonine kinase, PKC kinase related**	aPKC, Pkc98E, inaC, Pkc53E, Pkcdelta
E	***PDGF- and VEGF-receptor related*** *Pvr, VEGFR, stai, CG8222*	FLT1,FLT3, FLT4, KDR, PDGFRA, KIT,CSF1R	**2**	**2,2**	**2,1**	137,3 predicted	**Receptor tyrosine kinase**	Heartless (htl); breathless (btl)
E	***jaguar*** *jar, MHC95F, MyoVI, JAG, 95F, 95F MHC, CG5695*	MYO6	**2**	**2,1**	**2,0**	depending on isoform between 120 and 145	**Unconventional myosin type VI**	Myo31DF, Myo61F, Myo95E,
E	***Prosap*** *CG30483, CG8122*	SHANK1,SHANK2	**1**	**0,8**	**0,6**	199 predicted	**Synaptic scaffolding protein**	-
E	***Activated Cdc42 kinase*** *Ack, CG14992, DACK, p145*	TNK2	**1**	**0,9**	**1,1**	118,4 predicted	**Protein tyrosine kinase**	PR2, hop, Fak56D, shark, EgfR
E	***eIF3-S10*** *CG9805*	EIF3A	**1**	**1,2**	**1,3**	87,4 predicted	**Translation initiation factor**	-

The antibody purification strategy is compatible with quantitative mass-spectrometry (iTRAQ1)

In order to quantify the phosphorylation events induced by Met-Dscam1 activation, we tested the compatibility of our sample preparation with quantitative proteomic approaches. Quantifying phosphorylated protein complexes, requires the analysis of phosphorylation based signaling in greater detail (Mann et al., 2002): A protein might for example be part of different protein complexes which change upon stimulus addition. Furthermore, it is important to bear in mind that most phosphorylated proteins can be modified on more than one tyrosine residue. This means that dependent on the activation state a protein could exist as non-phosphorylated, slightly phosphorylated and heavily phosphorylated protein. The resulting "***phosphorylation code"*** might not be resolved in unsynchronized isolated experiments but could be detected in an experiment comparing different states of a conditionally inducible system. In order to perform quantitative experiments, I collaborated with ***Guillaume Adelmand*** and the ***Marto laboratory*** at the Dana-Farber Cancer Institute/Harvard Medical School to label sample peptides with low mass reporters, followed by multiplex LC-MS/MS analysis of the pooled sample, an approach known as ***iTRAQ.*** The iTRAQ-protocol is based on the labeling of the sample-peptides with ***isobaric iTRAQ-tags***. The tags are coupled to the N-terminus of protein peptides and to the epsilon-side chains of lysines. The term "*isobaric*" refers to the fact, that all labels contain the same nominal mass of 145 kDa (Gafken and Lampe, 2006). This is achieved by adding balancing groups to the reporter-labels. After peptide labeling, the samples were pooled and further processed for LC-MS/MS. Simultaneous detection of label and corresponding peptides can then be achieved at the so called ***MS/MS level***. At this step, the four balancing groups are separated from the labels. As a result, the four reporter groups appear in the lower molecular weight range of the mass-spectrum at m/z values of 114, 115, 116 and 117 (Gafken and Lampe, 2006). Their signal is far away from the spectra obtained for the fragmented peptides. Therefore, it is possible to simultaneously perform qualitative analysis of peptides and measure their distribution in the distinct samples by quantifying the abundance of the respective reporters (Gafken and Lampe, 2006). Nowadays, there are up to eight distinct iTRAQ-labels available. However, during my experiments we used a ***4-plex protocol*** routinely performed in the Marto-laboratory (Chapter 3-Figure 7).

The advantage of performing iTRAQ experiments is the ability to ***multiplex*** combined with superior ***sensitivity*** that arises from pooling the samples (Gafken and Lampe, 2006).

Furthermore, it is possible to ***label phosphor-peptides with the same efficiency*** as non-phosphorylated peptides (Gafken and Lampe, 2006). Therefore, we considered it to be an ideal approach for the analysis of my phosphor-tyrosine protein-complex purifications.

Results of the pilot iTRAQ-experiment (iTRAQ1)

A first proof-of principle experiment was conducted with a stable S2 cell line expressing Met-Dscam1 with the 17.1 intracellular domain (Cell line CG). We compared wild type S2 cells with the signal observed upon overexpression of the chimeric Met-Dscam1 receptor in the presence and absence of ligand. This experiment demonstrated that our ***quantitative approach*** to tyrosine phosphorylated protein complexes ***is feasible***. While abundance of detected proteins was low, we still could detect ***12 proteins*** in our p-tyrosine-immunoprecipitations, which were significantly regulated upon ligand addition (Chapter 3- Tables 7-9).

The translation elongation factor ***EF2*** (CG2238) was the only protein already present under wild type conditions, which was then significantly upregulated upon HGF addition (11.4 fold) (Chapter 3- Table7). All other proteins appeared only after expression of the Met-Dscam1 receptor. There were three proteins, namely ***RpL37a*** (CG9091), ***RpS16*** (CG4046) and ***Bicoid interacting protein*** (CG6046), which emerged in a tyrosine phosphorylated complex after addition of the ligand HGF (Chapter 3- Table 8). Notably, two of these three proteins are involved in ***translation***.

Eight other proteins responded not only to Met-Dscam1 overexpression but also to ligand addition (Chapter 3- Table 9). Of these, four were related to ***protein translation***, namely ***mfl*** (CG3333), ***stubarista*** (CG14792), ***L18A*** (CG6510) and ***Fmr1*** (CG6203). Two others suggest a ***link to the cytoskeleton*** in an actin (***α-Spectrin***; CG1977) and tubulin (***betaTub85D; CG9277***) dependent fashion. Importantly, ***betaTub85D*** is a paralogue of TUBB3, a protein known to physically interact with the vertebrate DSCAM protein (see also general introduction and Huang et al., 2015). α-Spectrin on the other hand, has been shown to interact with Dscam1 in a tissue specific manner (Dissertation Michael Hughes, Harvard University, 2007).

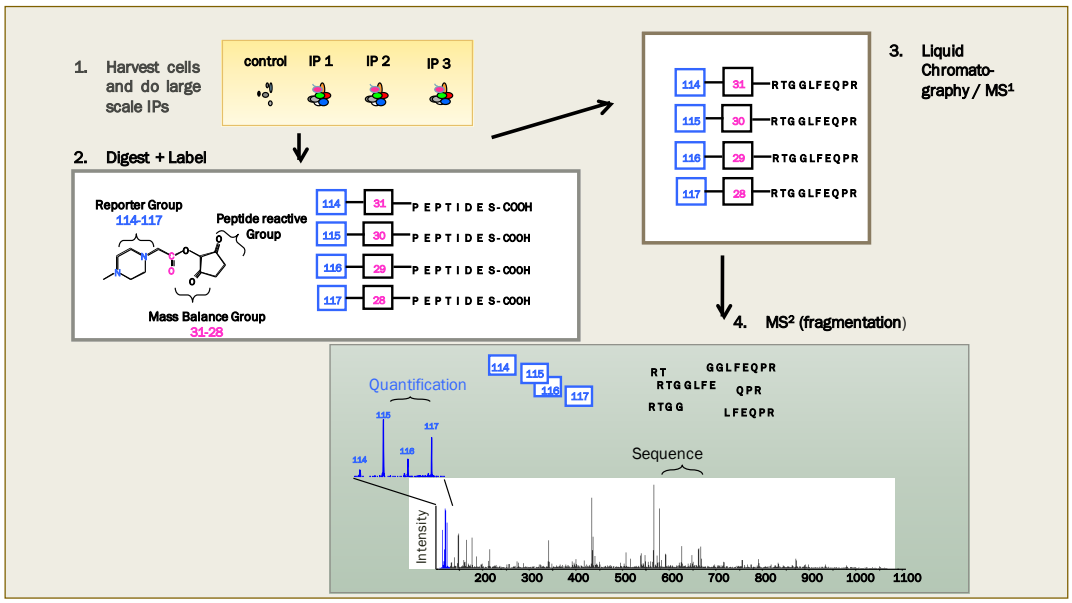

CHAPTER 3- FIGURE 7. **4-PLEX QUANTITATIVE MS ITRAQ EXPERIMENT USED TO STUDY DSCAM1 DEPENDENT TYROSINE-PHOSPHORYLATED COMPLEXES.**

I harvested the cells and purified the proteins by immunoprecipitation as described above. There were four different samples: Control=Mock IP; IP-1-3= IP of tyrosine phosphorylated protein complexes. I used a stable cell line expressing Met-Dscam1 under the control of a metallothionine promoter. This allowed us to compare the following conditions: IP1: Wild type S2 cells; IP2: S2 cells induced to express Met-Dscam1 for 2 days; IP3: S2 cells expressing Met-Dscam1 and treated with HGF ligand for four minutes. The samples from the immunoprecipitations were digested and labeled with iTRAQ reporters (Step2). Afterwards, the samples were pooled and subjected to LC-MS/MS. The low mass reporters were separated from their respective peptides during the second MS step, allowing for simultaneous peptide/protein identification and quantification (figure adapted from a slide I received from Gillaume Adelmand).

Finally, we detected ***three proteins***, which were ***not regulated at all***. This confirmed that our experimental conditions did indeed purify all types of tyrosine-phosphorylated proteins and that we did not globally change the phosphorylation state of every detected protein. The trust in the validity of our results is furthermore enhanced because the majority of identified proteins was detected in later experiments again.

Taken together, we have demonstrated that we can not only purify sufficient amounts of tyrosine phosphorylated protein complexes for mass spectrometry based fingerprinting analysis but that we also can expand the approach to quantitative multiplexing experiments, allowing to efficiently compare several experimental conditions. Even though we detected only a small number of proteins, we identified several candidate Dscam1 interactors as part of protein complexes significantly regulated upon Met-Dscam1 regulation. This suggests that besides the Dscam1 intracellular domain also other tyrosine phosphorylated proteins are stimulated upon Dscam1 activation.

CHAPTER 3- TABLE 7. **ITRAQ EXPERIMENT 1- PROTEINS REGULATED UPON LIGAND ADDITION.**

Note that EF2 is involved in mRNA-translation and that it also has been seen in later experiments. Yellow: This protein has been identified in another independent experiment as Dscam1 interactor.

Rank	Protein	Human orthologue	Unique peptides	Protein function	Paralogues	Mean signal S2 WT	Mean signal Met-Dscam1	Mean signal Met-Dscam1 +HGF	identified in other experiment?	Fold regulation
1.	***Elongation factor 2*** *Ef2b, EF2, CG2238*	EEF2	**1**	TRAFAC class translation factor GTPase superfamily.	CG4849	**0**	**1,73**	**19,73**	YES (iTRAQ 2)	**11,40**

CHAPTER 3- TABLE 8. ITRAQ **EXPERIMENT 1- PROTEINS ONLY APPEARING AFTER ADDITION OF HGF TO MET-DSCAM1.**

Note that two of the proteins identified are involved in translation and that all three proteins were also seen in later experiments, validating the results obtained. Yellow: This protein has been identified in another independent experiment as Dscam1 interactor.

Rank	Protein	Human orthologue	Unique peptides	Protein function	Paralogues	Mean signal S2 WT	Mean signal Met-Dscam1	Mean signal Met-Dscam1 +HGF	Identified in other experiment?
1.	***Ribosomal protein L37a*** *RpL37a, CG9091*	RPL37	**1**	Ribosomal protein L37e; Binds to the 23S rRNA	RpL37b	**0**	**0**	**63,81**	YES (iTRAQ 2)
2.	***Ribosomal protein S16*** *RpS16, CG4046*	RPS16	**1**	Ribosomal protein S9P;	-	**0,51**	**0**	**2,9**	YES (iTRAQ2)
3.	***Bicoid interacting protein 1*** *Bin1, dSAP18, SAP1, CG6046*	SAP18	**1**	SAP18 protein involved in the tethering of the SIN3 complex to core histone proteins.	-	**0**	**0**	**34,72**	YES (iTRAQ 2)

CHAPTER 3- TABLE 9. **ITRAQ EXPERIMENT 1: PROTEINS AFFECTED BY MET-DSCAM1 OVEREXPRESSION AS WELL AS LIGAND ADDITION.**

Note that four of the proteins identified (mfl, stubarista, L18A, Fmr1) are involved in translation. Five of the e proteins were also seen in later experiments, validating the results obtained. Yellow: This protein has been identified in another independent experiment as Dscam1 interactor.

Rank	Protein	Human orthologue	Unique peptides	Protein function	Paralogues	Mean signal S2 WT	Mean signal Met-Dscam1	Mean signal Met-Dscam1 +HGF	Identified in other experiment?	Fold regulation Met-Dscam1/S2 Wt	Fold regulation (Met-Dscam1^{+HGF}/ Met-Dscam1)
1.	***α-Spectrin*** *α-Spec, alpha-Spec, αSpec, l(3)dre3, α-spectrin, spectrin, Spec-α, l(3)04276, α-Spe, CG1977*	SPTAN	**2**	Spectrin	Actn, kst, beta-Spec, Msp-300	**0,5**	**0,36**	**12,75**	NO	**0,72**	**35,41**
2.	***Nucleolar protein at 60B*** *mfl, CG3333*	DKC1	**1**	Plays a central role in ribosomal RNA processing.	-	**0,39**	**0,14**	**3,18**	YES (iTRAQ 2)	**0,36**	**22,71**
3.	***stubarista*** *sta, RpSA, P40, EG:80H7.6, l(1)G0130, CG14792*	RPSA, RPSAP58	**1**	Ribosomal protein S2P. Required for the assembly and/or stability of the 40S ribosomal subunit.	-	**1,05**	**0,61**	**9,30**	YES (iTRAQ 2)	**0,58**	**15,25**
4.	***Ribosomal protein L18A*** *L18A, CG6510*	RPL18A	**2**	Ribosomal protein L18Ae	-	**0,28**	**0,55**	**6,105**	YES (iTRAQ 2)	**1,96**	**11,1**
5.	***β-Tubulin at 85D*** *B2t, betaTub85D, β2, β2t, CG9359* ***or β-Tubulin at 56D*** *β1, betaTub56D, β-Tub, β1-tub, β-Tub56D, β1tub, Tub CG9277*	TUBB2A, TUBB2B, RP11-683L23.1, TUBB6, TUBB8	**1**	Tubulin; GTP-binding	betaTub60D, betaTub97EF, CG32396	**0,78**	**0,92**	**8,83**	YES (iTRAQ 2)	**1,18**	**9,60**
6.	***Fmr1*** *dfmr1, FMRP, dFMRP, dFXR, dFMR, fmr, FXR, dfxr1, dmfr1, CG6203*	FMR1, FXR1, FXR2	**1**	RNA-binding protein that associates with translating ribosomes and acts as a negative translational regulator	-	**0,56**	**0,36**	**3,03**	NO	**0,64**	**8,41**
7.	***Heat shock protein cognate 4*** *Hsc70-4, Hsc4, Hsc70, BAP74, hsp70, CG4264*	HSPA8, HSPA2, HSPA6, HSPA1B, HSPA1A, HSPA1L	**3**	Heat shock protein 70	Hsc70-1, Hsp70Aa, Hsp68, Hsp70Bc, Hsp70Bb, Hsp70Bbb, Hsp70Ab, Hsc70-2, Hsp70Ba, CG7182, Hsc70-5, Hsc70-3	**1,64**	**0,31**	**1,51**	YES (iTRAQ 2)	**0,19**	**4,87**
8.	***Death related ICE-like caspase*** *ICE, CG7788*	CASP3, CASP6, CASP7	**1**	Peptidase C14A	Dcp-1, decay, Dredd, Nc	**0,49**	**1,52**	**5,06**	NO	**3,10**	**3,33**

iTRAQ experiment #2 (iTRAQ2)

Following the positive outcome of the first iTRAQ experiment, we doubled the input material to enhance the detection efficiency. For this experiment, we used a stable S2 cell line expressing the chimeric Met-Dscam1 receptor that harbors the 17.2 trans-membrane domain (Cell line EG).

We performed immunoprecipitation, digest, iTRAQ labeling and LC-MS/MS as described above. As a result, we identified a total of ***147 proteins*** in tyrosine-phosphorylated complexes (Chapter 3- Tables 10-12). This is a good yield considering that approximately 2% of the proteome consists of phosphorylated proteins at any given time and that the *Drosophila* genome is predicted to contain 13,918 coding genes (Ensemble release 78 based on Flybase release 5.46).

Results iTRAQ experiment #2

1. Results iTRAQ experiment 2: Overexpression of Met-Dscam1 elicits a clear signaling response

While ***17 proteins*** were ***totally unaffected*** by Met-Dscam1 expression and signaling (Chapter 3- Table 13), we found that Met-Dscam1 overexpression elicits a clear signaling response: The signal of ***109*** proteins changed upon overexpression of the chimeric Met-Dscam1 receptor (Chapter 3- Table 10), indicating that tyrosine phosphorylation plays an important role during Dscam1 signaling transduction. Notably, ***32*** of the proteins regulated upon Met-Dscam1 overexpression are proteins ***found in association with translating mRNAs*** and ribosomes, such as translation initiation factors, t-RNA-synthetases or ribosomal proteins. This is approximately one third of all proteins identified, emphasizing that ***translation is an important signaling target of the Dscam1 receptor***.

This result also confirms the validity of our first iTRAQ experiment: The majority of all identified proteins belonged to the family of translational regulators in both iTRAQ experiments. The reproducibility of our results was further demonstrated by the overlap of several proteins between both experiments (labeled in yellow in the respective tables). For example, the translational protein ***EF2*** and ***β-Tubulin at 85D*** were found in both experiments. The interaction with β-Tubulin at 85D might be a highly conserved feature of

Dscam signaling, since vertebrate DSCAM binds to TUBB3 in branching axons (Huang et al., 2015).

A second notable subgroup of proteins regulated upon Met-Dscam1 overexpression are proteins linked to the ***actin and tubulin cytoskeleton*** as well as molecular motor proteins. With 14 proteins they represent 13 % of all hits. Furthermore, I noticed a large subgroup related to ***protein folding, trafficking and degradation*** (16 hits/ 15%). Other important subgroups are ***kinases*** (5 hits), ***adaptor and scaffolding proteins*** (5 hits), and proteins linked to ***G-protein mediated signaling*** (6 hits). Strikingly, only ***one phosphatase*** was detected among all proteins purified and detected in tyrosine phosphorylated complexes.

CHAPTER 3- TABLE 10. **iTRAQ 2: PROTEINS THAT CHANGE PHOSPHORYLATION STATUS ALREADY UPON MET-DSCAM1 OVEREXPRESSION.**

There are 109 proteins in this subgroup, with representatives from the following functional protein families: Translation (32 hits), Protein folding, trafficking and degradation (16 hits), cytoskeletal proteins and molecular motors (14 hits), adaptor proteins and molecular scaffolds (5 hits), kinases (5hits), GTPase mediated signaling (6 hits). The indicated information regarding orthologues, paralogues, and protein function were assembled from the Ensemble Genome Browser, Flybase and Uniprot databases. Yellow: This protein has been identified in another independent experiment as Dscam1 interactor.

Rank	Protein	Human Orthologue	Peptides	Protein Family	Paralogues	Mean Signal S2 WT	Mean Signal Met-Dscam1	Mean Signal Met-Dscam1 +HGF	Identified in previous experiment?
1.	***Abelson tyrosine kinase*** *Abl, CG4032*	ABL1 ABL2	**10**	Tyrosine Kinase	Src64A Src42A	**7,95**	**13,04**	**12,41**	YES (first silver gel)
2.	***Cctγ*** *Cctgamma, Cctg, Y, TCPG_DROME, CG8977*	CCT3	**8**	TCP-1 chaperonin	-	**4,82**	**9,02**	**8,55**	NO
3.	***Clathrin heavy chain*** *Chc, CLH CG31349*	CLTC, CLTC1	**8**	Clathrin Heavy Chain	-	**8,01**	**11,99**	**11,29**	YES: ***1. iTRAQ 1*** 2. ***Michael Hughes*** proteomic analysis of Dscam1 binding partners in fly heads and S2 cells ***3. Binding partners of the Dscam1 cytoplasmic domain***
4.	***Cysteine proteinase-1*** *Cp-1, Dcp1, Dcp-1, Cath L, CG6692*	CTSL, CTSV	**14**	Cysteine-type endopeptidase	CG4847, CG6347, 26-29-p, CG11459, CG5367, CG12163, Swim, CtsB1	**5,28**	**7,39**	**7,53**	NO
5.	***HEM-protein*** *kette, Nap1, kte, CG5837*	NCKAP1, NCKAP1L	**9**	Adaptor Protein	-	**21,78**	**13,44**	**7,68**	YES
6.	***Heat shock protein cognate 4*** *Hsc70-4, Hsc4, Hsc70, BAP74, hsp70, CG4264*	HSPA8, HSPA2, HSPA6, HSPA1B, HSPA1A, HSPA1L	**8**	Heat Shock Protein	Hsc70-1, Hsp70Aa, Hsp68, Hsp70Bc, Hsp70Bb, Hsp70Bbb, Hsp70Ab, Hsc70-2, Hsp70Ba, CG7182, Hsc70-5, Hsc70-3	**1,45**	**2,26**	**2,29**	YES
7.	***Glutamyl-prolyl-tRNA synthetase*** *Aats-glupro; EPRS, GluProRS, CG5394*	EPRS	**5**	Bifunctional Glutamate/Proline tRNA Ligase	-	**5,34**	**8,62**	**7,84**	YES (iTRAQ 1)
8.	***Receptor of activated protein kinase C 1*** *Rack1, CG7111*	GNB2L1	**5**	Scaffolding Protein	-	**4,11**	**5,52**	**5,51**	NO
9.	***polo*** *CG12306, l(3)01673*	PLK1	**4**	Serine/threonine-protein kinase	SAK	**6,00**	**11,78**	**11,00**	NO
10.	***Ribosomal protein L8*** *RpL8, M(3)LS2, L8, CG1263*	RPL8	**3**	Ribosomal Protein	-	**23,00**	**8,19**	**7,23**	NO
11.	***Elongation factor 2*** *Ef2b, EF2, CG2238*	EEF2	**5**	Translation elongation factor, GTPase	CG4849	**6,37**	**11,96**	**11,73**	YES (iTRAQ1)
12.	***Ribosomal protein S27A*** *RpS27A, DUb80, l(2)04820, mfs48, CG5271*	RPS27A	**4**	Cleaved into the following two units: 1. Ubiquitin 2. 40S ribosomal protein S27a	-	**12,37**	**7,47**	**8,05**	NO

Rank	Protein	Human Orthologue	Peptides	Protein Family	Paralogues	Mean Signal S2 WT	Mean Signal Met-Dscam1	Mean Signal Met-Dscam1 +HGF	Identified in previous experiment?
13.	***X11Lβ*** *X11B, X11Lbeta, CG3267*	MCCC2	**4**	Synaptic and axonal adaptor protein (X11/Mint family)	-	**10,49**	**8,71**	**9,53**	NO
14.	***Gale*** *UDP-galactose 4'-epimerase, dGale, CG12030*	GALE	**6**	Bifunctional galactose 4 epimerase	CG7979	**5,08**	**10,11**	**9,55**	YES: Protein that binds to the Dscam1 cytoplasmic domain (Band H)
15.	***Actin 42A*** *Act42A, Actin, BAP47, C, CG12051*	ACTG1, ACTB	**3**	Actin related protein	Act5C, Act87E, Act88F, Act57B, Act79B, Arp87C, Arp53D	**29,04**	**5,13**	**9,95**	NO
16.	***α-Tubulin at 84D*** *alphaTub84D, α-Tub, α-tubulin, αTUB, Tub, α84D,CG2512*	TUBA3D, TUBA3E, TUBA3C	**4**	Tubulin alpha chain	alphaTub84B, alphaTub85E, alphaTub67C, CG7794	**12,00**	**24,03**	**23,89**	NO
17.	***sprint*** *sprint, CG33175, CG34414*	RIN1, RIN2, RIN3, RINL	**3**	Potential Ras effector protein. May function as a GEF.	-	**5,83**	**7,83**	**8,43**	NO
18.	***β-Tubulin at 85D*** *B2t, betaTub85D, β2, β2t, CG9359* ***or β-Tubulin at 56D*** *β1, betaTub56D, β-Tub, β1-tub, β-Tub56D, β1tub, Tub CG9277*	TUBB2A, TUBB2B, RP11-683L23.1, TUBB6, TUBB8	**4**	Tubulin, GTPase	betaTub60D, betaTub97EF, CG32396	**8,85**	**12,92**	**12,22**	YES (iTRAQ1)
19.	***adenosine 2*** *ade2,* *CG9127*	PFAS	**3**	Phosphoribosylformylglycinamidine synthase	-	**4,82**	**7,08**	**7,68**	NO
20.	***ade5*** *AIRc-SAICARs, CG3989*	PAICS	**3**	Phosphoribosylaminoimidazolesuccinocarboxamide synthase	CG40801	**2,74**	**9,79**	**9,29**	NO
21.	***Na^+ pump α-subunit*** *Atpα, Atpalpha, Na,K-ATPase, Na^+, K^+-ATPase α-subunit, ATPa, l(3)01164, NaK, CG5670*	-	**3**	Cation transport ATPase (P-type)	JYalpha, CG40625, CG3701, Ca-P60A, SPoCk	**6,28**	**7,66**	**7,47**	NO
22.	***Actin-related protein 2*** *Arp2, ARP14D, CG9901*	ACTR2	**3**	ATP-binding component of the Arp2/3 complex	-	**15,12**	**12,00**	**10,68**	NO
23.	***Ribosomal protein S3*** *RpS3, M(3)95A, M(3)w, S3, M(3R)w, dS3, CG6779*	RPS3	**3**	RNA binding protein	-	**6,28**	**11,04**	**11,37**	NO
24.	***twinstar*** *tsr, ntf, cofilin, Adf, D-cof, l (2) k05633,* *CG4254*	-	**3**	cofilin/actin depolymerizing homologue	CG6873	**5,54**	**7,02**	**6,02**	NO
25.	***Trip1*** *eIF3-S2, CG8882*	EIF3I	**2**	Component of the eukaryotic translation initiation factor 3 (eIF-3) complex.	wmd, CG10459	**2,75**	**4,51**	**4,69**	NO
26.	***chickadee*** *chic,* *sand, Chi, CG9553*	-	**2**	Binds to actin and affects the structure of the cytoskeleton.	-	**1,39**	**3,65**	**3,80**	NO
27.	***zipper*** *zip, MyoII, Myo, Myo II, MHC, nmMHC, E(br), Mhc-c, Myo-II, CG15792*	MYH9, MYH10, MYH14, MYH11	**2**	Non muscle myosin, heavy chain	Mhc	**22,42**	**6,28**	**4,42**	NO
28.	***Succinyl coenzyme A synthetase α-subunit*** *Scsα, Scsalpha, CG1065*	SUCLG1	**2**	Catalyzes the ATP- or GTP-dependent ligation of succinate and CoA to form Succinyl-CoA, Succinyl-CoA ligase.	CG6255, ATPCL	**8,43**	**10,57**	**8,78**	NO

Rank	Protein	Human Orthologue	Peptides	Protein Family	Paralogues	Mean Signal S2 WT	Mean Signal Met-Dscam1	Mean Signal Met-Dscam1 +HGF	Identified in previous experiment?
29.	***hippo*** *hpo, dMST* *CG11228*	STK3, STK4	**2**	STE20 Ser/Thr protein kinase	GckIII	**4,46**	**5,23**	**6,23**	NO
30.	***Ribosomal protein L3*** *RpL3, CG4863*	RPL3, RPL3L	**2**	Ribosomal protein L3P family; component of the large subunit of cytoplasmic ribosomes.	-	**9,58**	**5,83**	**5,67**	NO
31.	***Protostome-specific GEF*** *PsGEF, CG14045, EG:BACH7M4.1, EG:BACH7M4.2, CG14047, EG:BACH48C10.4, CG1404*	RAN	**2**	GTP-binding protein involved in nucleocytoplasmic transport; Rho GEF	ran-like	**8,57**	**7,09**	**7,06**	NO
32.	***Regulatory particle triple-A ATPase 6*** *Rpt6, pros45, p42C, DUG, CG1489*	PSMC5	**2**	AAA-ATPase; involved in the ATP-dependent degradation of ubiquitinated proteins.	Rpt6R	**8,80**	**15,90**	**16,73**	NO
33.	***Eukaryotic initiation factor 4a*** *eIF-4a, eIF4A, l(2L)162, l(2)gdh-4, CG9075*	EIF4A1, EIF4A2	**2**	DEAD box helicase; eIF4A subfamily; ATP-dependent RNA helicase which is a subunit of the eIF4F complex involved in cap recognition and is required for mRNA binding to ribosomes.	eIF4AIII	**5,63**	**11,15**	**11,46**	NO
34.	***FK506-binding protein FKBP59*** *FKBP59, dFKBP59, l(2)k00424, CG4535*	FKBP4, FKBP5	**2**	Peptidyl-prolyl cis-trans isomerase, FKBP-type;	shu, CG5482, CG30075, FK506-bp2	**4,67**	**7,50**	**10,75**	NO
35.	***Vacuolar H^+-ATPase 55kD subunit*** *Vha55,* *l(3)87Ca, SzA, l(3)j2E9, CG17369*	ATP6V1B1, ATP6V1B2	**2**	ATPase alpha/beta chain; non-catalytic subunit of the peripheral V1 complex of vacuolar ATPase. V-ATPase is responsible for acidifying a variety of intracellular compartments in eukaryotic cells.	-	**6,06**	**8,86**	**8,20**	NO
36.	***U2 small nuclear riboprotein auxiliary factor 50*** *U2af50, U2AF, dU2AF^{50}, dU2AF50, l(1)9-21, l(1)14Ca, l(1)14Cc, CG9998*	U2AF2	**2**	Splicing factor SR; Necessary for the splicing of pre-mRNA. Binds to the polypyrimidine tract of introns early during spliceosome assembly	LS2	**7,03**	**5,72**	**5,50**	NO
37.	***Thioredoxin reductase-1*** *Trxr-1, DmTR, DmTrxR-1, TrxR, Gr, DmTrxR, CG2151*	TXNRD2	**2**	lass-I pyridine nucleotide-disulfide oxidoreductase; the thioredoxin system is a major player in glutathione metabolism.	Trxr-2	**1,82**	**9,89**	**9,0**	NO
38.	***Ribosomal protein S5a*** *RpS5a, RpS5, M(1)15D, M(1)o, CG8922*	RPS5	**2**	Ribosomal protein S7P	RpS5b	**8,26**	**10,26**	**11,10**	NO
39.	***Ribosomal protein L23*** *RpL23, RpL17A, CG3661*	RPL23	**2**	Ribosomal protein L14P; myosin binding	-	**13,32**	**15,80**	**15,88**	NO
40.	*Ribosomal protein L18A* ***L18A, CG6510***	RPL18A	**2**	Ribosomal protein L18Ae	-	**7,52**	**4,45**	**3,71**	YES (iTRAQ1)
41.	***Ribosomal protein L10Ab*** *RpL10Ab, CG7283*	RPL10A	**2**	Ribosomal protein L1P	RpL10Aa	**12,89**	**9,78**	**9,28**	NO

2. *Results iTRAQ experiment 2: Activation of Met-Dscam1 affects translational regulators and the cytoskeleton*

HGF-ligand addition to Met-Dscam1 leads to the differential regulation of tyrosine phosphorylated protein-complexes centered around ***38 proteins*** (Chapter 3- Table 3). This is a significant number, taking in account that it represents approximately 26 % of all detected proteins. The functional protein classes represented in this group are: Proteins involved in ***mRNA translation*** (9 hits= 24%), ***cytoskeletal proteins and molecular motors*** (8 hits=21%), proteins involved in ***GTPase signaling*** (3 hits= 8%), proteins involved in protein folding, trafficking and degradation (3 hits= 8%) but only two kinases and one adaptor protein. ***Eight*** other proteins were both significantly regulated upon Met-Dscam1 overexpression and after ligand addition (Chapter 3-Table 12). Of these, ***two*** belong to the functional group of proteins involved in GTPase signaling and one is associated translational complexes (Chapter 3-Table 12).

CHAPTER 3- TABLE 11. **ITRAQ2: PROTEINS THAT ARE REGULATED UPON LIGAND ADDITION.**

There are 38 proteins in this subgroup, with representatives from the following functional protein families: Translation (9 hits), Protein Folding, trafficking and DEGRADATION (3 hits), cytoskeletal proteins and molecular motors (7 hits), GTPase signaling (3 hits). The indicated information regarding orthologues, paralogues, and protein function was assembled from the Ensemble Genome Browser, Flybase and Uniprot databases. Yellow: This protein has been identified in another independent experiment as Dscam1 interactor.

Rank	Protein	Human orthologue	# of identified different peptides	Protein function	Paralogues	Mean signal S2 WT	Mean signal S2 with MetDscam1	Mean signal S2 with Met-Dscam1 +HGF	Identified in previous experiment?	Relative signal increase after ligand addition
1.	***HEM-protein*** *kette, Nap1, kte, CG5837*	NCKAP1, NCKAP1L	**9**	Adaptor protein	-	**21,78**	**13,44**	**7,68**	YES	**0.57**
2.	***Actin 42A*** *Act42A, Actin, BAP47, C, CG12051*	ACTG1, ACTB	**3**	Actin related protein	Act5C, Act87E, Act88F, Act57B, Act79B, Arp87C, Arp53D	**29,04**	**5,13**	**9,95**	NO	**1.9**
3.	***Ribosomal protein L10*** *RpL10, Qm, DQM, L10, CG17521*	RPL10, RPL10L	**3**	Ribosomal protein L10e	-	**7,46**	**7,38**	**6,15**	NO	**0.833**
4.	***twinstar*** *tsr, ntf, cofilin, Adf, D-cof, l (2) k05633, CG4254*	-	**3**	Cofilin/actin depolymerizing protein	CG6873	**5,54**	**7,02**	**6,02**	NO	**0.85**
5.	***zipper*** *zip, MyoII, Myo, Myo II, MHC, nmMHC, E(br), Mhc-c, Myo-II, CG15792*	MYH9, MYH10, MYH14, MYH11	**2**	Non muscle myosin	Mhc	**22,42**	**6,28**	**4,42**	NO	**0.7**
6.	***Succinyl coenzyme A synthetase α subunit*** *Scsa, Scsalpha, CG1065*	SUCLG1	**2**	Succinyl-CoA ligase: Catalyzes the ATP- or GTP-dependent ligation of succinate and CoA during formation of Succinyl-CoA.	CG6255, ATPCL	**8,43**	**10,57**	**8,78**	NO	**0.83**
7.	***hippo*** *hpo, dMST CG11228*	STK3, STK4	**2**	STE20 Ser/Thr protein kinase	GckIII	**4,46**	**5,23**	**6,23**	NO	**1.19**

Rank	Protein	Human orthologue	# of identified different peptides	Protein function	Paralogues	Mean signal S2 WT	Mean signal S2 with MetDscam1	Mean signal S2 with Met-Dscam1 +HGF	Identified in previous experiment?	Relative signal increase after ligand addition
8.	***Sphingosine-1-phosphate lyase*** *Sply, SPL, l(2)05091, CG8946*	SGPL1	**2**	Cleaves phosphorylated sphingoid bases (PSBs), such as sphingosine-1-phosphate, into fatty aldehydes and phosphoethanolamine.	-	**6,70**	**7,35**	**8,26**	NO	**1.12**
9.	***FK506-binding protein FKBP59*** *FKBP59, dFKBP59, l(2)k00424, CG4535*	FKBP4, FKBP5	**2**	Peptidyl-prolyl cis-trans isomerase, FKBP-type: May have a role in photo transduction.	shu, CG5482, CG30075, FK506-bp2	**4,67**	**7,50**	**10,75**	NO	**1.43**
10.	***Ribosomal protein L18A*** *L18A, CG6510*	RPL18A	**2**	Structural constituent of ribosome	-	**7,52**	**4,45**	**3,71**	YES (iTRAQ 1)	**0.83**
11.	***Metallothionine A*** *MtnA, MTN, CG9470*	-	**2**	Metallothionine type 5: This protein binds cations of several transition elements.	-	**1,13**	**7,55**	**10,89**	NO	**1,443**
12.	***Myosin light chain cytoplasmic*** *Mlc-c, CG3201*	MYL1, MYL3, MYL4, MYL6, MYL6B,	**2**	Myosin light chain: Potentially calcium binding. Binds to myosin heavy chain.	Mlc1, CG17237	**45,83**	**4,20**	**1,02**	NO	**0,244**
13.	***Tcp1-like*** *T-cp1, T-cpl, Tcp1-like, CG5374*	TCP1	**1**	TCP-1 chaperonin: Assists the folding of proteins upon ATP hydrolysis. Known to play a role, in vitro, in the folding of actin and tubulin.	-	**7,19**	**11,84**	**9,84**	NO	**0,83**
14.	***Ribosomal protein L24*** *RpL24, CG9282*	RPL24	**1**	Ribosomal protein L24e	-	**5,57**	**5,00**	**6,71**	NO	**1,34**
15.	***hyperplastic discs*** *hyd, l(3)c43, c43, CG9484*	UBR5	**1**	E3 ubiquitin-protein ligase which accepts ubiquitin from an E2 ubiquitin-conjugating enzyme in the form of a thioester and then directly transfers the ubiquitin to targeted substrates.	HERC2	**3,64**	**6,14**	**4,93**	NO	**0,80**
16.	***Actin 88F*** *Act88F, Actin, E, CG5178*	ACTG1, ACTB	**1**	Actin	Act79B, Act87E, Act57B, Act42A, Act5C, Arp87C, Arp53D	**14,75**	**3,75**	**4,75**	NO	**1,27**
17.	***DISCO Interacting Protein 2*** *DIP2, CG7020*	DIP2A, DIP2B, DIP2C	**1**	DIP2 family; May provide positional cues for axon pathfinding and patterning in the central nervous system	-	**10,13**	**8,75**	**6,88**	NO	**0,79**
18.	***MRG15*** *dMrg15, DmMRG15, CG6363*	MORF4L1, MORF4L2	**1**	Part of the Tip60 chromatin-remodeling complex which is involved in DNA repair. Upon induction of DNA double-strand breaks, this complex acetylates phosphorylated H2AV in nucleosomes and exchanges it with unmodified H2AV.	-	**6,85**	**8,31**	**6,31**	NO	**0,76**
19.	***wicked*** *wcd, l(2)k07824, CG7989*	UTP18	**1**	WD repeat UTP18 protein: Component of a nucleolar small nuclear ribonucleoprotein particle (snoRNP). Thought to participate in the processing and modification of pre-ribosomal RNA.	-	**10,33**	**11,00**	**13,33**	NO	**1,21**
20.	***Vacuolar protein sorting 28*** *Vps28, dVps28, l(2)k16503, CG12770*	VPS28	**1**	VPS28 family protein: Component of the ESCRT-I complex, a regulator of vesicular trafficking.	-	**8,25**	**8,25**	**9,75**	NO	**1,18**
21.	***SH2 Ankyrin repeat kinase*** *shark, dtk7, CG18247*	ZAP70, SYK	**1**	Tyr protein kinase: May be involved in signal transduction on the apical surface of ectodermal epithelia regulating their polarity during invagination.	Ack, PR2, EgfR, Fak56D, hop	**10,67**	**9,00**	**10,67**	NO	**1,19**
22.	***flightless I*** *flil, fli, W2, fli-1, l(1)W-2, fltO, w-2, CG1484*	FLII	**1**	Villin/gelsolin family member: Interacting with	CG33232, Gel, qua	**26,83**	**5,33**	**4,33**	NO	**0,81**

Rank	Protein	Human orthologue	# of identified different peptides	Protein function	Paralogues	Mean signal S2 WT	Mean signal S2 with MetDscam1	Mean signal S2 with Met-Dscam1 +HGF	Identified in previous experiment?	Relative signal increase after ligand addition
				both the cytoskeleton and other cellular components.						
23.	***lethal (2) tumorous imaginal discs*** *l(2)tid, DnaJ, tid, l(2)nud, CG5504*	DNAJA3	**1**	DNAJ homologue: May act as a tumor suppressor	CG7387	**6,92**	**4,15**	**5,31**	NO	**1,28**
24.	***RNA polymerase II elongation factor*** *TfIIS, l(2)35Cf, DmS-II, BG:DS00929.12, CG3710*	TCEA1, TCEA2, TCEA3, TCEANC	**1**	TFS-II family protein: Necessary for efficient RNA polymerase II transcription elongation past template-encoded arresting sites.	CG8117	**2,40**	**4,90**	**3,70**	NO	**0,76**
25.	***Spt5*** *DSIF, dSpt5, CG7626*	SUPT5H	**1**	SPT5 family protein: Component of the DRB sensitivity-inducing factor complex (DSIF complex), which regulates transcription elongation by RNA polymerase II. DSIF enhances transcriptional pausing at sites proximal to the promoter, which may facilitate the assembly of an elongation competent RNA polymerase II complex. DSIF may also promote transcriptional elongation within coding regions.	-	**4,89**	**10,11**	**8,44**	NO	**0,73**
26.	***Small ribonucleoprotein particle protein SmD3*** *SmD3, guf, l(2)90/37, CG8427*	SNRPD3	**1**	snRNP core protein	-	**8,27**	**5,20**	**6,07**	NO	**1,17**
27.	***Ribosomal protein S4*** *RpS4, CG11276*	RPS4Y1, RPS4X, RPS4Y2, RPS4Y1, RPS4Y2	**1**	Ribosomal protein S4e family	-	**6,25**	**9,67**	**11,42**	NO	**1,18**
28.	***Ribosomal protein L4*** *RpL4, RpL1, CG5502*	RPL4	**1**	Ribosomal protein L4P	1	**11,75**	**6.00**	**4,75**	NO	**0,79**
29.	***capping protein beta*** *cpb, CG17158*	CAPZB	**1**	F-actin-capping protein beta subunit; F-actin-capping proteins bind in a Ca2+-independent manner to the fast growing ends of actin filaments (barbed end), thereby blocking the exchange of subunits at these ends. Unlike other capping proteins (such as gelsolin and severin), these proteins do not sever actin filaments.	-	**15,78**	**6,89**	**5,11**	NO	**0,74**
30.	***ATP synthase, γ subunit*** *ATPsyny, ATPsyn-gamma, ATPsyn-γ, CG7610*	ATP5C1	**1**	Mitochondrial membrane ATPase subunit: Produces ATP from ADP in the presence of a proton gradient across the membrane which is generated by electron transport complexes of the respiratory chain. F-type ATPases consist of two structural domains, F1 - containing the extramembraneous catalytic core, and F0 - containing the membrane proton channel, linked together by a central stalk and a peripheral stalk.	-	**4,80**	**4,20**	**5,40**	NO	**1,29**
31.	***Ribosomal protein S17*** *RpS17, M(3)67C, M(3)i, M(3)^{i55}, CG3922*	RPS17	**1**	Ribosomal protein S17e	-	**9,17**	**9,17**	**7,50**	NO	**0,82**
32.	***Ribosomal protein L11*** *RpL11, l(2)k16914, DL11, L11, CG7726*	RPL11	**1**	Ribosomal protein L5P: Binds to 5S ribosomal RNA.	-	**3,90**	**3,80**	**3,00**	NO	**0,79**
33.	***Ribonucleoside diphosphate reductase large subunit*** *RnrL, l(2)k06709, RNR1, CG5371*	RRM1	**1**	Ribonucleoside diphosphate reductase large chain: Provides the precursors necessary for DNA synthesis. Catalyzes the biosynthesis of deoxyribonucleotides from the corresponding ribonucleotides.	-	**3,50**	**4,86**	**5,93**	Yes: found in complex with Dscam1 cytoplasmic domain	**1,22**

Rank	Protein	Human orthologue	# of identified different peptides	Protein function	Paralogues	Mean signal S2 WT	Mean signal S2 with MetDscam1	Mean signal S2 with Met-Dscam1 +HGF	Identified in previous experiment?	Relative signal increase after ligand addition
34.	***Rho-like*** *RhoL, Mes1, DRhoL, Drac3, CG9366*	-	**1**	Small Rho GTPase superfamily member: family: Essential for the maturation of hemocytes.	Rac1, Rac2, Mtl , Cdc42	**6,20**	**6,00**	**5,00**	NO	**0,83**
35.	***Roughened*** *R, Rap1, Dras3, Rap, D-Rap1, CG1956*	RAP1A, RAP1B	**1**	Small RAS GTPase	Rap2L, Ras85D, Ric, Rala	**11,76**	**10,59**	**7,47**	NO	**0,71**
36.	***hoi-polloi*** *hoip, CG3949*	NHP2L1	**1**	Ribosomal protein L7Ae: Binds to the 5'-stem-loop of U4 snRNA and may play a role in the late stage of spliceosome assembly. The protein undergoes a conformational change upon RNA-binding.	-	**5,67**	**6,42**	**5,33**	NO	**0,83**
37.	***Rm62*** *Lip, Dmp68, p68, CG10279*	DDX17, DDX5	**1**	DEAD box helicase family member (DDX5/DBP2 subfamily): Involved in RNA interference (RNAi);	CG10777, CG10077, CG14443, CG7878	**6,55**	**6,91**	**5,45**	NO	**0,79**
38.	***Rac1*** *Rac, Drac1, Drac, DracA, DmRAC1, Rac GTPase, D-Rac, D-Rac1, Drac1a, CG2248*	RAC1, RAC2, RAC3	**1**	Small Rho GTPase	Rac2, Mtl, RhoL, Cdc42	**4,25**	**4,38**	**5,50**	NO	**1,26**

CHAPTER 3- TABLE 12. iTRAQ 2: PROTEINS REGULATED UPON OVEREXPRESSION AND UPON LIGAND BINDING.

There are 8 proteins in this subgroup, with representatives from the following functional protein families: Translation (1 hit), G-protein mediated signaling (2 hits). The indicated information regarding orthologues, paralogues, and protein function were assembled from the Ensemble Genome Browser, Flybase and Uniprot databases. Yellow: This protein has been identified in another independent experiment as Dscam1 interactor.

Rank	Protein	Human orthologue	Unique peptides	Protein function	Paralogues	Mean Signal S2 (WT)	Mean Signal S2 with Met-Dscam1	Mean Signal S2 with Met-Dscam1 +HGF	Identified in previous experiment?	Fold regulation Met-Dscam1/S2 Wt	Fold regulation Met-Dscam1^{+HGF}/Met-Dscam1
1.	***CG17896*** *EG:171D11.1*	ALDH6A1	**1**	Aldehyde dehydrogenase: Plays a role in valine and pyrimidine metabolism. Binds fatty acyl-CoA.	-	**3,90**	**6,05**	**4,19**	NO	**1,55**	**0,69**
2.	***CG10306***	EIF3K	**1**	eIF-3 (subunit K): Component of the eukaryotic translation initiation factor 3 (eIF-3) complex which is involved in protein synthesis and, together with other initiation factors, stimulates binding of mRNA and methionyl-tRNA to the 40S ribosome.	-	**8,00**	**9,50**	**12,00**	NO	**1,19**	**1,26**
3.	***Nucleostemin orthologue (H. sapiens) 1*** *Ns1, ns1, CG3983*	GNL3L, GNL3	**1**	TRAFAC class YlqF/YawG GTPase.	-	**12,00**	**13,82**	**10,82**	NO	**1,15**	**0,78**
4.	***G protein ß-subunit 13F*** *Gβ13F, Gbeta13F, Gβ, G-beta, Gb13F, Gbb, CG10545*	GNB1, GNB2, GNB4	**1**	WD repeat G protein (beta subunit): Guanine nucleotide-binding proteins (G proteins) are modulators or transducer in various transmembrane signaling systems.	Gbeta76C, Gbeta5, CG2812	**8,08**	**9,50**	**7,08**	NO	**1,18**	**0,75**
5.	***Nucleolar protein at 60B*** *mfl, CG3333*	DKC1	**1**	Pseudouridine synthase TruB: Plays a central role in ribosomal RNA processing. Probable catalytic subunit of H/ACA small nucleolar ribonucleoprotein (H/ACA snoRNP) complex, which catalyzes pseudouridylation of rRNA.	-	**10,40**	**5,60**	**4,47**	yes iTRAQ1	**0,54**	**0,80**
6.	***Succinate dehydrogenase, subunit A (flavoprotein)*** *SdHA, scs-fp, sdh, CG17246*	SDHA	**1**	FAD-dependent oxidoreductase 2 family member (FRD/SDH subfamily): Flavoprotein (FP) subunit of succinate dehydrogenase (SDH) that is involved in complex II of the mitochondrial electron transport chain and is responsible for transferring electrons from succinate to ubiquinone (coenzyme Q).	-	**4,80**	**7,20**	**8,80**	NO	**1,50**	**1,22**
7.	***Bicoid interacting protein 1***	SAP18	**1**	SAP18 family protein:	-	**22,60**	**4,00**	**3,00**	YES (iTRAQ1)	**0,18**	**0,75**

Rank	Protein	Human orthologue	Unique peptides	Protein function	Paralogues	Mean Signal S2 (WT)	Mean Signal S2 with Met-Dscam1	Mean Signal S2 with Met-Dscam1 +HGF	Identified in previous experiment?	Fold regulation Met-Dscam1/S2 Wt	Fold regulation Met-Dscam1^{+HGF}/Met-Dscam1
	Bin1, dSAP18, SAP18, CG6046			Involved in the tethering of the SIN3 complex to core histone proteins. Interacts with bicoid to repress transcription of bicoid target genes in the anterior tip of the embryo; a process known as retraction.							

39. Results iTRAQ experiment 2: Some control proteins are not affected by Met-Dscam1 signaling.

Some proteins detected in my second iTRAQ experiment did not significantly change tyrosine phosphorylation status. They are listed in the following table (Chapter 3- Table 13).

CHAPTER 3- TABLE 13. **ITRAQ2: PROTEINS THAT DO NOT CHANGE PHOSPHORYLATION STATUS.**

The indicated information regarding orthologues, paralogues, and protein function was assembled from the Ensemble Genome Browser, Flybase and Uniprot databases. Yellow: This protein has been identified in another independent experiment as a Dscam1 interactor.

Rank	Protein	Human orthologue	# of identified different peptides	Protein function	Paralogues	Mean signal S2 (WT)	Mean signal S2 with Met-Dscam1	Mean signal S2 with Met-Dscam1 +HGF	Identified in previous experiment?
1	***Ribosomal protein S2*** *RpS2, sop, l(2)03848, S2, CG5920*	RPS2	**3**	40S ribosomal protein	-	**9,39**	**9,18**	**9,09**	NO
2	***Ribosomal protein S3A*** *RpS3A, M(4)101, C3, M(4)57g, CG2168*	RPS3A	**3**	40S ribosomal protein S1/3	-	**9,67**	**9,75**	**9,08**	NO
3	***Ribosomal protein S16*** *RpS16, CG4046*	RPS16	**3**	Ribosomal protein S9P	-	**11,44**	**15,33**	**16,7**	YES (iTRAQ1)
4	***Eukaryotic initiation factor 2*** *eIF-2γ, CG6476, eIF2γ, eIF-2G, eIF2G, CG6476, CG43665*	EIF2S3, EIF2S3L	**3**	Eukaryotic translation initiation factor 2	-	**6,64**	**6,79**	**7,48**	YES (also found in complex with Dscam1 cytoplasmic domain)
5	***Lasp*** *CG3849*	-	**2**	Actin binding protein	-	**1,85**	**1,99**	**1,89**	NO
6	***Fibrillarin*** *Fib, CG9888*	FBL, FBLL1	**2**	Methyltransferase: Fibrillarin family	CG10909	**6,56**	**6,37**	**6,15**	NO
7	***rolled*** *rl, MAPK, ERK, dpERK, dERK, ERKA, pERK, ERK-A, Sem, dpMAPK, DmERK-A, CG12559*	MAPK1, MAPK3	**2**	CMGC Ser/Thr protein kinase family (MAP kinase subfamily)	nmo	**8,11**	**7,38**	**6,86**	NO
8	***lethal (1) G0020*** *l(1)G0020, CG1994*	NAT10	**2**	Polycomb group (PcG) protein	-	**11,85**	**11,08**	**10,15**	NO
9	***Ribosomal protein S20*** *RpS20, CG15693*	RPS20	**2**	Ribosomal protein S10P	-	**11,26**	**12,58**	**12,95**	NO

Rank	Protein	Human orthologue	# of identified different peptides	Protein function	Paralogues	Mean signal S2 (WT)	Mean signal S2 with Met-Dscam1 +HGF	Mean signal S2 with Met-Dscam1 +HGF	Identified in previous experiment?
10	***Rho1*** *RhoA, Rho, dRhoA, DRho1, Rho kinase, Rho GTPase, CG8416*	RHOA, RHOB, RHOC	**2**	Small GTPase: Has a role in regulating actin cytoskeletal organization.	CG34104, RhoBTB	**8,52**	**9,57**	**8,26**	NO
11	***Ribosomal protein S6*** *RpS6, S6, air8, l(1)air8, hen, CG10944*	RPS6	**1**	Ribosomal protein S6e	-	**8,10**	**7,10**	**7,00**	NO
12	***Host cell factor*** *Hcf, dHCF, Hcf1, CG1710*	HCFC1, HCFC2	**1**	May be involved in control of the cell cycle; temperature sensitive.	slim, CG3711, CG12081	**2,59**	**2,94**	**3,12**	NO
13	***Casein kinase II β subunit*** *CkIIβ, CKII, CK2, CK2β, CKIIbeta, And, DmCK2β, DmCKIIβ, βCK2, dCK2β, CK2beta, CG15224*	CSNK2B	**1**	Casein kinase 2 (subunit beta): Plays a complex role in regulating the basal catalytic activity of the alpha subunit.	CkIIbeta2, Ste12DOR, Ste:CG33244, Ste:CG33241, Ste:CG33246, Ste:CG33239, CG40635, Ste:CG33245, Ste:CG33247, Ste:CG33236, SteXh:CG42398, Ste:CG33243, Ste:CG33237, Ste:CG33242, Ste:CG33238, Ste:CG33240, Ssl	**11,19**	**11,11**	**10,78**	NO
14	***Ribosomal protein S29*** *RpS29, CG8495*	RPS29	**1**	Ribosomal protein S14P	-	**4,17**	**4,00**	**4,00**	NO
15	***Ras opposite*** *Rop, l(3)64Ah, CG15811*	STXBP1, STXBP2, STXBP3	**1**	STXBP/unc-18/SEC1 family protein	-	**8,56**	**8,89**	**8,56**	YES: proteins found in complex with Dscam1 cytoplasmic domain
16	***Ecdysone-inducible gene L3*** *ImpL3, LDH, IMP-L3, lincRNA.S4223, CG10160*	LDHA, UEVLD, LDHC, LDHAL6A, LDHAL6B	**1**	LDH/MDH superfamily protein	-	**1,35**	**1,47**	**1,37**	YES: protein that binds to Dscam1 cytoplasmic domain
17	***Hepatocyte growth factor regulated tyrosine kinase substrate*** *Hrs, l(2)23Ad, vps27, CG2903*	HGS	**1**	Essential role in endosome membrane invagination and formation of multi-vesicular bodies, MVBs. Required during gastrulation and appears to regulate early embryonic signaling pathways. Inhibits tyrosine kinase receptor signaling by promoting degradation of the tyrosine-phosphorylated, active receptor, potentially by sorting activated receptors into MVBs. The MVBs are then trafficked to the lysosome where their contents are degraded.	CG5168	**7,40**	**7,95**	**7,70**	NO

Purification of the Dscam1 signaling complex

My tyrosine-phosphor-proteomic experiments were conducted ***in S2 cells***. However, I was wondering if my candidate Dscam1 effectors would also play a role in neuronal cells. Therefore, I used an Ha-Flag tagged membrane tethered form of the Dscam1 intracellular domain (CD8-Dscam1) stably expressed in neuronal ***BG3C2 cells***, to purify the Dscam1 cytoplasmic signaling complex in CNS cells.

Purification of the Dscam1 receptor complex is not trivial as Dscam1 (like many other Ig-family CAMs) is a very "sticky protein" (see also Yang et al., 2012). During the lysis and immunoprecipitation, one needs to balance stringent washing conditions with the requirement to purify sufficient protein for mass-spectrometry based analysis. Initially, we pursued a tandem-purification strategy employing both the Ha and the Flag tag. Even though this method yielded very clean results, we were not able to enrich the complex enough to detect it in a Coomassie stained gel. We tried to analyze these silver stained samples by submitting them to the ***VIB mas-spectrometry facility in Ghent (Belgium)*** but found that the enrichment of protein was not sufficient for high confidence identification of proteins.

In the meantime, I discovered that we were able to purify the Dscam1 receptor complex very efficiently and with little background by utilizing magnetic Dynabeads carrying a secondary antibody. Therefore, we decided to pursue the further large scale purification of the Dscam1 receptor complex based on this type of beads lacking protein A or G (Chapter 3- Figure 8). We purified the Dscam1 cytoplasmic domain with magnetic Dynabeads (Life Technologies) coated with Flag-M2 antibody coupled to mouse secondary antibody. This allowed for very efficient purification of all our Ha-Flag tagged constructs via the Flag tag, because we could wash the immunoprecipitations with very gentle wash buffer (4x TBS; 1xTBST). The choice of Dynabeads cross-linked with secondary antibody over beads coated with protein-A or protein G was the ***most important aspect*** of the protocol, as it reduced the background of the immunoprecipitation significantly.

While we could have enhanced the stringency of the purification by using harsher washing conditions, we decided to wash as gentle as possible in order to preserve the Dscam1-complex as much as possible.

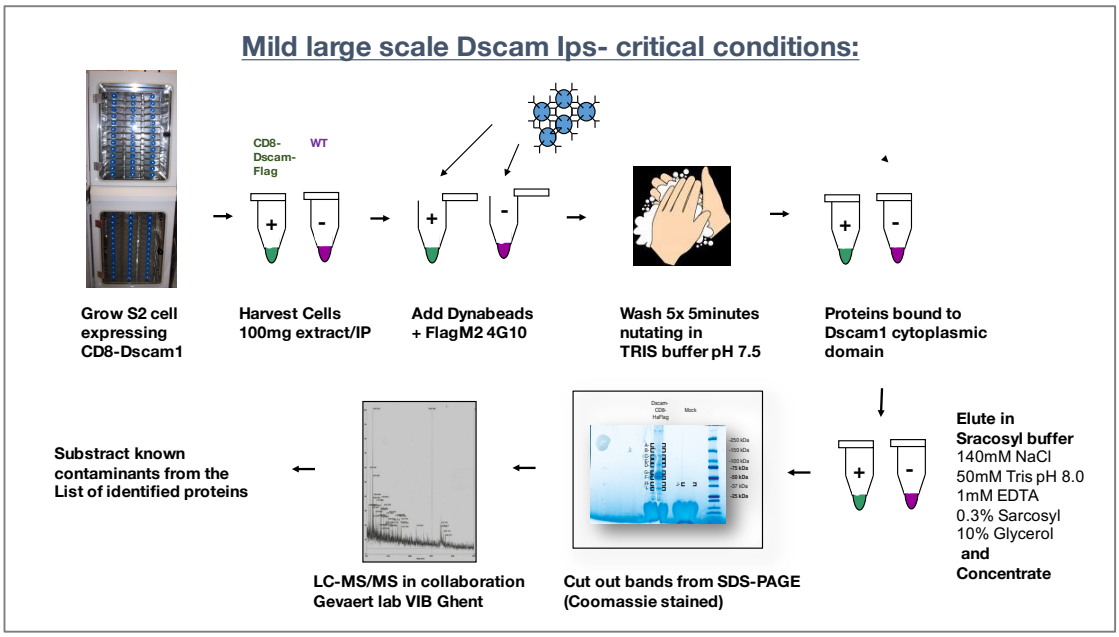

CHAPTER 3- FIGURE 8. **IP-CONDITIONS CHOSEN TO ANALYZE THE DSCAM1 CYTOPLASMIC RECEPTOR COMPLEX.**

Instead of using a tandem-affinity purification protocol that we initially designed to purify the Dscam1 receptor complex, we used a mild purification method based on anti-Flag antibody and Dynabeads. This allowed for efficient and clean purification of the Dscam1 signaling complex. Importantly, the proteins binding to the Flag-beads in an unspecific manner are known for the Drosophila proteome (Rees et al., 2011). Based on this, we subtracted unspecific interactors and obtained a list of potential Dscam1 signaling partners.

We were able to optimize the purification of the Dscam1 intracellular domain to such an extent that we could detect proteins of the Dscam1 receptor complex easily on a Coomassie gel and cut out bands for further analysis. The gel used for analysis is depicted in Chapter 3- Figure 9)

A second critical aspect of the protocol was the analysis of the raw data obtained from the mass-spectrometry facility: We omitted all hits for proteins that are commonly known to bind to the Flag-tag in an unspecific manner from the extensive list of potential interactors (Rees et al., 2011). Furthermore, I excluded all proteins as background that had ever appeared in any negative control of my own mass-spectrometry based experiments. Finally, I omitted all proteins from the analysis that were identified by less than three unique peptides. This threshold was chosen, because the known Dscam1 interactors ***Dock*** (three peptides), ***vap-33 protein*** (six peptides) and ***SH3PX1*** (three peptides) were identified by at least 3 unique peptides.

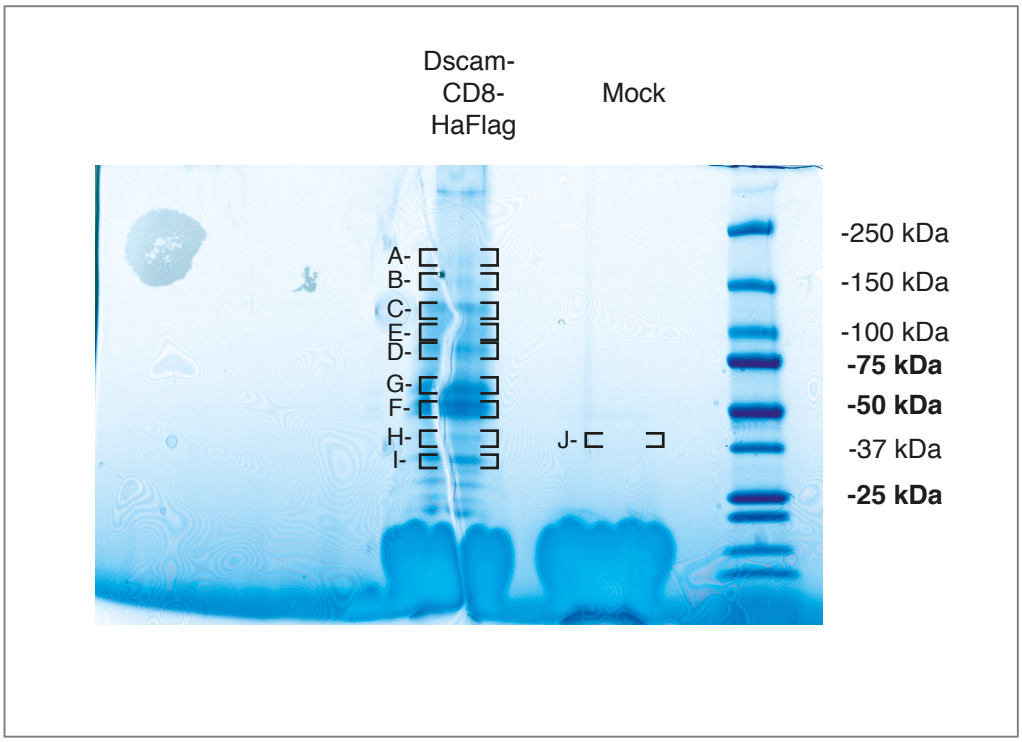

CHAPTER 3- FIGURE 9. **PURIFICATION OF MEMBRANE BOUND DSCAM1 SIGNALING COMPLEX.**

We used a membrane bound version of the full length Dscam1 cytoplasmic domain which was tagged with an HA-Flag- tag for our purification. The construct was stably expressed in BG3C2 cells. After elution with sarcosyl elution buffer, we separated the protein complexes over an SDS gel and stained with Coomassie. The brackets indicate, where we cut the gel in order to submit it for mass-spectrometry based fingerprinting analysis. Band A-I are proteins found associated with CD8-Dscam (cytoplasmic domain), while we cut out band J from a mock IP as a negative control.

Results of the purification of the Dscam1 receptor complex

1. *Summary of all identified proteins*

My analysis resulted in the identification of ***163 proteins*** that are potential Dscam1 receptor complex interactors. The identified proteins are listed in (Chapter 3-Table 14) ranked by their average peptide score. This score is used in order to evaluate with how much confidence a peptide of a given protein has been identified. It depends on the size of the proteome of a given model organism and the peptide sequence and quality. Generally, a higher score indicates a higher detection reliability. My list contains only proteins identified by at least three unique peptides. ***Importantly it includes not only Dscam1 itself but also all known Dscam1 interactors, such as dock, SH3-PX1 and vap-33*** but also other proteins that have been proposed to be connected with the Dscam1 complex, such as ***PTP61F***.

36 of the reported proteins were identified through the assignment ***of 10 or more unique peptides***. This is according to the mass-spectrometry facility in Ghent an indicator of recognition with high confidence. These proteins are listed in the following tables: Chapter 3- Tables 15, 17, 18, 20, 24, 26, 28 and 30. Nine of the identified proteins of the Dscam1 cytoplasmic complex might be of special interest as they also have been identified in the phosphor-proteomic experiments described earlier in this chapter. This could mean that they are important mediators of Dscam1 signaling or that they are common mass-spectrometry contaminants that I have not been able to predict during my analysis. The nine proteins are sorted by number of identified peptides according to the band from which they were purified and listed in the following tables: Chapter 3- Tables 25, 27, 29 and 31.

CHAPTER 3- TABLE 14. **PROTEINS BINDING TO THE DSCAM1 CYTOPLASMIC COMPLEX. LIST OF ALL IDENTIFIED PROTEINS SORTED BY THEIR AVERAGE MASCOT SCORE.**

*Proteins with more than 10 unique identified peptides are considered as identifications with very high confidence **(bold rows).** Proteins with three or more unique signature peptides are still considered as identified with relatively good confidence; information regarding protein function, orthologues and paralogues was extracted from the Uniprot and Ensemble Genome browser and Flybase databases. Further information regarding identified peptides, isoforms and raw data are to be found in the supplemental original data report.*

Rank	Band	Total spectral count	Max. Mas-cot score	Avg. peptide score	CG #	Name	Vertebrate orthologue	Paralogues
1.	*G*	**3**	**159**	119	CG13349	**Rpn13**	ADRM1	Rpn13R
2.	*G*	**3**	**156**	107	CG3059	**NTPase** Cd39-like NTPase	ENTPD5, ENTPD6	-
3.	*C*	**4**	**141**	95	CG1044	**dos** daughter of sevenless	GAB1, GAB2, GAB3, GAB4	-
4.	*F*	**7**	**120**	91	CG31694	**CG31694**	IFRD1, IFRD2	-
5.	*D*	**3**	**108**	90	CG14895	**Pak3**	-	stlk, fray mbt, Pak
6.	*H*	**6**	**151**	90	CG10203	**xl6** 9G8, Dxl6, d9G8, TN166, l(2)k00230, dx16,x16	SRSF7	Rbp1, Rbp1-like, Rsf1, B52, SF2
7.	*G*	**4**	**155**	88	CG10932	**CG10932**	ACAT1	CG9149, yip2
8.	*G*	**3**	**164**	85	CG31453	**pch2**	TRIP13	-
9.	*B*	**4**	**87**	82	CG8590	**Klp3A** Kinesin-like protein at 3A, mei-352, DmKlp3A, EG:BACR25B3.9, fs(1)M4	KIF4A, KIF4B	Khc, cos, Klp54D, pav, sub, Klp31E
10.	*C*	**9**	**142**	82	CG15100	p120, MRS	Methionyl-tRNA synthetase (MARS)	
11.	*F*	**7**	**99**	79	CG13849	**Nop56**	NOP56	-
12.	*F*	**3**	**116**	79	CG9285	**DipB** Dipeptidase B, Dip-B	-	S-Lap1, S-Lap2, S-Lap3, S-Lap4, S-Lap5, S-Lap6, S-Lap7, S-Lap8, grsm, loopin-1
13.	*F*	**10**	**113**	**78**	**CG5581**	**Ote** Otefin	-	bocksbeutel
14.	*G*	**3**	**115**	78	CG2048	**dco** discs overgrown, DBT, CKIε, l(3)dco, ck1ε, l(3)discs overgrown, l(3)dco-1, CK1epsilon,doubletime	CSNK1D, CSNK1E	CG12147, CG7094, CG9962, CG2577, CkIalpha, ball, Asator, CG8878, gish
15.	*C, E*	**6**	**87**	77	CG1453	**Klp10A**, DmKLP10A, Kif2A	KIF2A, KIF2B, KIF2C	Kl59D, Klp59C, Kif19A, Klp67A
16.	*H*	**5**	**106**	77	CG18174	**Rpn11**, p37B, DmS13	PSMD14	
17.	*A, B*	**11**	**109**	**75**	**CG4165**	**CG4165**	USP45, USP16	Khc, cos, Klp54D, pav, sub, Klp31E

Rank	Band	Total spectral count	Max. Mas-cot score	Avg. peptide score	CG #	Name	Vertebrate orthologue	Paralogues
18.	*E*	**3**	**83**	74	CG12876	**AliX** ALG-2 interacting protein X	PDCD6IP	Mop, RhP
19.	*F*	**3**	**81**	73	CG5165	**Pgm** Phosphogluconate mutase	PGM1, PGM5	
20.	*I*	**5**	**116**	73	CG34179	**CG34179**		
21.	*E*	**5**	**110**	72	CG9412	**rin** rasputin, Nts, rasp	GTPase activating SH3 domain binding protein, G3BP1, G3BP2	-
22.	*F*	**3**	**92**	72	CG42641	**Rpn3**, Regulatory particle non-ATPase 3, Dox-A2, CG10484, p58, l(2)37Bf	Proteasome 26S subunit	-
23.	*H*	**3**	**79**	72	CG8979	Putative proteasome inhibitor	Proteasome inhibitor subunit 1 (PI31)	-
24.	*I*	**13**	**103**	**72**	**CG5474**	**Signal sequence receptor β**	**Signal sequence receptor SSR2**	-
25.	*D*	**4**	**93**	71	CG9242	**bur** burgundy	Guanine monophosphate synthetase (GMPS)	-
26.	*C*	**5**	**113**	70	CG8571	**smid**, smallminded	Nuclear VCP-like protein (NVL)	-
27.	*G*	**4**	**109**	70	CG8309	**Tango7** Transport and Golgi organization 7	Eukaryotic translation initiation factor 3 (subunit M) (EIF3M)	-
28.	*G*	**3**	**84**	70	CG8003	**CG8003**	Ankyrin repeat and MYND domain containing 2 (ANKMY2)	-
29.	*H, I*	**5**	**87**	70	CG3931	**Rrp4**	Exosome component 2 (EXOSC2)	-
30.	*G*	**6**	**153**	69	CG5028	**CG5028**	Isocitrate dehydrogenase 3 (NAD+) gamma (IDH3G)	CG7755, CG6439
31.	*G*	**6**	**101**	69	CG4600	**yip2** yippee interacting protein 2	acetyl-CoA acyltransferase 2 (ACAA)	CG9149, CG10932
32.	*I*	**5**	**98**	69	CG5174	**CG5174**	Tumor protein D52-like 2 (TPD52, TPD52L2)	-
33.	*C*	**4**	**82**	68	CG13391	**Aats-ala** Alanyl-tRNA synthetase	AARS	Aats-ala-m
34.	*D, E*	**7**	**47**	68	CG4001	**Pfk** 6-phosphofructokinase, Phosphofructokinase	Phosphofructokinase, platelet protein (PFKP, PFKL, PFKM)	-
35.	*G*	**3**	**85**	68	CG31098	**CG31098**	-	CG11891, CG11878, CG33301, CG11892, CG10513, CG16898, CG31380, CG10514, CG11889, CG13658, CG9498, CG31436, CG31975, CG31300, CG7135, CG32195, CG13659, CG31370, CG13360,

Rank	Band	Total spectral count	Max. Mascot score	Avg. peptide score	CG #	Name	Vertebrate orthologue	Paralogues
								CG9497, CG11893, CG31104, CG31974, CG10560, CG10550, CG10553, CG31087, CHKov1, CG6830, CG10562, CG6908, CHKov2, CG10559, CG31099, CG31097, CG31102, CG6834, CG31288, CG18765
36.	*H*	**17**	**136**	**68**	**CG9543**	**εCOP**	**Coatomer protein complex subunit epsilon (COPE)**	**-**
37.	*H*	**12**	**128**	**68**	**CG8636**	**eIF3-S4**	**Eukaryotic translation initiation factor 3, subunit G (EIF3G)**	**CG10881**
38.	*B*	**7**	**115**	67	CG31739	**CG31739**	Aspartyl-tRNA synthetase 2 (mitochondrial) (DARS2)	-
39.	*D*	**6**	**102**	67	CG14788	**Ns3**, Nucleostemin 3	Large subunit GTPase 1 homolog (LSG1)	Ns4
40.	*E*	**3**	**82**	67	CG2929	**Pi4KIIα**	Phosphatidylinositol 4-kinase type 2 alpha	PI4K2A, PI4K2B, RP11-548K23.11, PI4K2B
41.	*H*	**3**	**88**	67	CG17904	**CG17904**	Nucleotide binding protein 1 (NUBP1)	CG3262
42.	*B, E*	**23**	**128**	**66**	**CG5820**	**Gp150**	**-**	**MstProx, Toll-4, chp, lbk, Toll-6, conv, CG7509, Con, 18w, CG7896, CG4168, CG32055, Tollo, atk, haf, Toll-7, CG18095, CG42346, Tehao, Tl, rdo, Lrt**
43.	*B, D, E*	**69**	**52**	**66**	**CG5353**	**Threonyl-tRNA synthetase**	**-**	**mRpL39**
44.	*C, E*	**7**	**92**	66	CG4260	**AP-2alpha** α-Adaptin,α-Ada, AP2, ada, D-αAda	Adaptor-related protein complex 2, alpha 2 subunit, (AP2A1, AP2A2)	-
45.	*E*	**12**	**113**	66	CG2910	**nito**, spenito,dOTT	RNA binding motif protein 15 (RBM15, RBM15E)	spen
46.	*G*	**8**	**111**	66	CG8340	upstream of RpIII128, **128up**	Developmentally regulated GTP binding protein 1 (DRG1)	-

Rank	Band	Total spectral count	Max. Mascot score	Avg. peptide score	CG #	Name	Vertebrate orthologue	Paralogues
47.	*G*	**4**	**100**	66	CG8890	**Gmd**, GDP-mannose 4,6-dehydratase	GDP-mannose 4,6-dehydratase, GMDS	-
48.	*D*	**16**	**148**	**65**	**CG9373**	**rumpelstiltskin, hrp59, hnRNP M**	**Heterogeneous nuclear ribonucleoprotein M (HNRNPN, MYEF2)**	**-**
49.	*E*	**5**	**82**	65	CG9209	**vap** vacuolar peduncle, RasGAP, D-RasGP	RAS p21 protein activator (GTPase activating protein) 1 (RASA1)	RasGAP1, CG42684
50.	*E*	**4**	**111**	65	CG4755	**RhoGAP92B**	Rho GTPase activating protein 17, ARHGAP44, SH3BP1, ARHGAP17	RhoGAP68F
51.	*F*	**6**	**87**	65	CG4561	**Aats-tyr**, Tyrosyl-tRNA synthetase	YARS	-
52.	*G*	**5**	**113**	65	CG7558	**Arp3** Actin-related protein 66B, ARP3, Arp66B	ARP3 actin-related protein 3 homolog, ACTR3, ACTR3B, ACTR3C	-
53.	*G*	**5**	**142**	65	CG1416	**CG1416**	AHA1(activator of heat shock 90kDa protein ATPase homolog), AHA2	-
54.	*B*	**16**	**118**	**64**	**CG4119**	**CG4119**	**RNA binding motif protein 25 (RBM25)**	**-**
55.	*D*	**4**	**79**	64	CG6756	**Tom70** Translocase of outer membrane 70	Translocase of outer mitochondrial membrane 70 homolog A (TOMM70A)	Unc-45, CG14894, spag, CG18472
56.	*D*	**3**	**80**	64	CG10206	**nop5**	NOP58 ribonucleoprotein homolog	
57.	*F*	**4**	**104**	64	CG6769	**CG6769**	zinc finger protein 622, ZNF622	-
58.	*G*	**74**	**120**	**64**	**CG31251**	**NudC-like**	**NUDCD3**	**nudC**
59.	*G*	**4**	**83**	64	CG1354	**CG1354**	Obg-like ATPase 1, OLA1	-
60.	*G, H, I*	**85**	**79**	**64**	**CG10160**	**ImpL3** Ecdysone-inducible gene L3, LDH	**Lactate dehydrogenase A, (LDHA), LDHB**	**CG13334**
61.	*E*	**10**	**96**	**63**	**CG9342**	**Mtp** Microsomal triacylglycerol transfer protein	**Microsomal triglyceride transfer protein (MTTP)**	**-**
62.	*F*	**18**	**89**	**63**	**CG4347**	**UGP** UGPase, UDPGPP	**UDP-glucose pyrophosphorylase 2 (UGP2)**	**-**
63.	*F, G*	**6**	**78**	63	CG10370	**Rpt5,** Tat-binding protein-1, p50, Rpt5, l(3)04210	Proteasome 26S subunit, ATPase, 3, (PSMC3)	-
64.	*F, G*	**8**	**50**	63	CG15602	**CG15602**	ZFYVE19	-
65.	*G*	**10**	**108**	**63**	**CG3724**	**Phosphogluconate dehydrogenase**	**Phosphogluconate dehydrogenase (PGD)**	**-**
66.	*H*	**5**	**75**	63	CG5313	**RfC3**, Replication factor C subunit 3	Replication factor C (activator 1) 5, 36.5kDa, (RFC5)	-

Rank	Band	Total spectral count	Max. Mascot score	Avg. peptide score	CG #	Name	Vertebrate orthologue	Paralogues
67.	*I*	**4**	**108**	63	CG8186	**Vha36-1,** Vacuolar H+ ATPase subunit 36-1	ATPase, H+ transporting, lysosomal 34kDa, V1 subunit D (ATP6V1D)	Vha36-2, Vha36-3
68.	*D*	**6**	**90**	62	CG9181	**PTP61F** Protein tyrosine phosphatase 61F	Protein tyrosine phosphatase, non-receptor type 1, PTPN1, PTPN2	l(1)G0232, csw, PTP52F, Ptp10D, PTP4e, Pez
69.	*D*	**3**	**71**	62	CG6757	**SH3PX1**	SNX9, SNX33, SNX18	-
70.	*F, G*	**12**	**70**	**62**	**CG5809**	**CaBP1**	**Protein disulfide isomerase family A, member 6 (PDIA6)**	**CG5027, prtp, CG9302**
71.	*F*	**3**	**67**	62	CG3613	**qkr58E-1,** quaking related 58E-1	KH domain containing, RNA binding, signal transduction associated 3, KHDRBS2, KHDRBS1, KHDRBS3	nsr, qkr54B, qkr58E-2, qkr58E-3, CG3927, CG4021, CG10384, how, SF1
72.	*H,I*	**10**	**87**	**62**	**CG9968**	**Annexin B11**	**Annexin A7, ANXA7**	**AnxB9, AnxB10**
73.	*F*	**49**	**118**	**61**	**CG2129**	**CG2129**	**ZNF276, ZNF653, ZNF692, ZFP91, ZFP91-CNTF, CTC-398G3.6**	**CG10959, CG18262, Plzf, CG15336**
74.	*I*	**10**	**85**	**61**	**CG4659**	**Signal recognition particle protein 54k, l(3)01418, Srp54**	**Signal recognition particle 54kDa (SRP54)**	**-**
75.	*C*	**5**	**91**	60	CG11661	**Nc73F** Neural conserved at 73EF, E1	Oxoglutarate dehydrogenase (OGDH, OGDHL)	-
76.	*D*	**4**	**107**	60	CG7791	**CG7791**	Mitochondrial intermediate peptidase (MIPEP)	-
77.	*D*	**3**	**69**	60	CG15811	**SEC1** Ras opposite, Rop	Syntaxin binding protein 1; STXBP1, STXBP2, STXBP3 ✓ **also identified in iTRAQ 2 as belonging to a tyrosine phosphorylated complex not affected by Met-Dscam1 signaling**	-

Rank	Band	Total spectral count	Max. Mascot score	Avg. peptide score	CG #	Name	Vertebrate orthologue	Paralogues
78.	*E*	**5**	**95**	60	CG5371	**RnrL** Ribonucleoside diphosphate reductase large subunit, l(2)k06709, RNR1	Ribonucleotide reductase M1 (RRM1) ✓ **also identified in iTRAQ 2 as belonging to a tyrosine phosphorylated complex affected by Met-Dscam1 signaling**	-
79.	*F*	**17**	**98**	**60**	**CG17259**	**Seryl-tRNA synthetase**	**SARS**	**-**
80.	*F*	**8**	**96**	60	CG4799	**Pen** Pendulin, oho31, imp-α2, Imp-alpha2, Kap-α2, Dimp-alpha2	Karyopherin alpha 2, KPNA2, KPNA7	Kap-alpha3, alphaKap4, Kap-alpha1
81.	*F, G*	**9**	**166**	60	CG9735	**Aats-trp** Tryptophanyl-tRNA synthetase	WARS	-
82.	*F*	**5**	**79**	60	CG12333	**CG12333**, WD repeat domain 37	WDR37	CG6724
83.	*G, H*	**13**	**82**	60	CG9946	**Eukaryotic translation Initiation Factor 2α**		
84.	*I*	**13**	**96**	60	CG7834	**CG7834** Electron transfer flavoprotein beta subunit	Electron-transfer-flavoprotein, beta (ETFB)	-
85.	*C, E*	**32**	**81**	**59**	**CG1009**	**Puromycin sensitive aminopeptidase**	**NPEPPS**	**-**
86.	*G*	**3**	**72**	59	CG8190	**eIF2B-γ**	EIF2B3	-
87.	*H*	**4**	**79**	59	CG2976	**Fnta** farnesyl transferase α	farnesyltransferase, CAAX box, alpha, FNTA	-
88.	*A*	**3**	**78**	58	CG1244	**MEP-1**	-	-
89.	*D*	**4**	**75**	58	CG33138	**AGBE**	glucan (1,4-alpha-), branching enzyme 1, GBE1	-
90.	*D*	**4**	**70**	58	CG3806	**eIF2B-ε**, EG:86E4.1, eIF2Bε	eukaryotic translation initiation factor 2B, subunit 5 epsilon, 82kDa, EIF2B5	-
91.	*F*	**8**	**77**	58	CG9987	**CG9987** chromosome 22 open reading frame 28	RTCB	-
92.	*F*	**5**	**102**	58	CG13425	**bl**, bancal, Hrb57A, Q18, Heterogeneous nuclear ribonucleoprotein at 57A	HNRNPK	ps, mub
93.	*F*	**3**	**69**	58	CG17002	**CG17002**	-	-
94.	*G*	**4**	**96**	58	CG33303	**CG33303** ribophorin I	RPN1	-
95.	*G*	**3**	**75**	58	CG10622	**Sucb**	succinate-CoA ligase, GDP-forming, beta subunit, SUCLG2	skap

Rank	Band	Total spectral count	Max. Mas-cot score	Avg. peptide score	CG #	Name	Vertebrate orthologue	Paralogues
96.	*A, B, C, D,E,F,G ,H*	20	73	57	CG17800	Dscam1	DSCAM	Dscam2, Dscam3, Dscam4
97.	*A, B*	7	47	57	CG8730	**drosha**	DROSHA	-
98.	*B*	3	81	57	CG32435	**C hb** chromosome bows, Mast, Orbit, CLASP, Orbit/MAST, MAST/Orbit, MESR7, v40	Cytoplasmic linker associated protein (CLASP1, CLASP2)	-
99.	*C*	12	97	57	**CG4062**	**Valyl-tRNA synthetase**	**VARS2, VARS**	**CG5660**
100.	*C*	11	126	57	**CG31012**	**cindr** CIN85 and CD2AP orthologue	**CIN85 (SH3-domain kinase binding protein 1) CD2AP, SH3KBP1, SH3D21**	-
101.	*D, F*	10	46	57	**CG3714**	**CG3714**	**NAPRT**	-
102.	*G*	6	89	57	CG6174	**Arp1** grid, Actin-related protein 87C	ARP1 actin-related protein 1 homolog A, centractin alpha, ACTR1B, ACTR1A	Arp53D, Act42A, Act5C, Act57B, Act79B, Act88F, Act87E
103.	*G*	3	69	57	CG7583	**CtBP** C-terminal Binding Protein, dCtBP, G9, l(3)G9	C-terminal binding protein 2, CTBP1, CTBP2	CG6287
104.	*D*	5	88	56	CG1691	**Imp** IGF-II mRNA-binding protein	Insulin-like growth factor 2 mRNA binding protein 1, IGF2BP2, IGF2BP3	-
105.	*D*	4	89	56	CG5692	**pins** rad, rapsynoid, raps	G-protein signaling modulator 2, GPSM2, GPSM1	CG43163
106.	*I*	5	81	56	CG8778	**CG8778**	Enoyl-CoA hydratase, ECHDC2, AUH	CG5611, CG5844, CG6543, CG9577, CG6984, HIPP1, CG13890
107.	*C*	6	83	55	CG6841	**CG6841** Prp6	PRP6 pre-mRNA processing factor 6 homolog (S. cerevisiae), PRPF6	-
108.	*D*	12	107	55	**CG1898**	**HBS1**	**HBS1-like**	**Elf**
109.	*G*	11	98	55	**CG4153**	**eIF-3p40,** Eukaryotic initiation factor 2β	**EIF2S2**	-
110.	*G, H*	10	93	55	**CG3609**	**CT12127**	**Dihydrodiol dehydrogenase (dimeric)(DHD)**	**CG3597, CG13280**
111.	*G, H*	6	84	55	CG9124	**eIF-3p40** Eukaryotic initiation factor 3 p40 subunit	EIF3H	-
112.	*B*	10	108	54	**cg33123**	**cg33123**	**Leucyl-tRNA synthetase, (LARS)**	-
113.	*C*	7	81	54	CG7935	**moleskin** msk, dim-7, dim7, CIP-61, Ran binding protein 7	Importin 7, IPO7, IPO8 ✓ **also found in first silver gel, in a tyrosine**	-

Rank	Band	Total spectral count	Max. Mascot score	Avg. peptide score	CG #	Name	Vertebrate orthologue	Paralogues
							phospho-rylated complex of proteins	
114.	***D***	**5**	**70**	54	CG2522	**Gtp-bp** GTP-binding protein	Signal recognition particle receptor (docking protein), (SRPR)	-
115.	***D***	**3**	**65**	54	CG5729	Dgp-1	GTP binding protein 1, (GTPBP1)	CG2017
116.	***E***	**17**	**88**	54	CG8165	**JHDM2** JmjC domain-containing histone demethylase 2	JMJD1C, HR, lysine (K)-specific demethylase 3B	-
117.	***E***	**15**	**95**	**54**	**CG4900**	**IRP1A, Iron regulatory protein 1A**	**Aconitase 1, soluble, (ACO1)**	**Irp-1b, Acon, CG4706**
118.	***F***	**12**	**102**	**54**	**CG6335**	**Histidyl-tRNA synthetase**	**HARS, HARS2**	**-**
119.	***G***	**3**	**78**	54	CG9453	**Spn42Da,** Serine protease inhibitor 4	serpin peptidase inhibitor, clade I (neuroserpin), member 1, SERPING1, SERPINA1, SERPINA2, SERPINA3, SERPINA4, SERPINA5, SERPINA6, SERPINA7, SERPINA9, SERPINA12, SERPINA11, SERPINA10, SERPIND1, SERPINF1	Spn42Db, Spn55B, nec, Spn43Ab, Spn43Aa, Spn42De, Spn38F, Spn42Dd, Spn42Dc, Spn28Db, Spn47C, Spn28Da, Spn28F, Spn28B, Spn88Ea, Spn88Eb, Spn27A
120.	***C, F,G***	**43**	**60**	**53**	**CG4816**	**qkr54B** quaking related 54B, Sam50	**KH domain containing, RNA binding, signal transduction associated 3 (KHDRBS3), KHDRBS1,**	**nsr, qkr58E-2, qkr58E-3, CG3927, CG4021, qkr58E-1, CG10384, how, SF1**
121.	***D***	**11**	**107**	**53**	**CG14813**	**δ-coatomer protein** CG14813, deltaCOP, EG:63B12.10, δ-Cop	**archain, ARCN1**	**-**
122.	***D***	**4**	**52**	53	CG6904	**Glycogen synthase** GlyS, GS	Glycogen synthase 1 (GYS1), GYS2 ✓ **also identified in iTRAQ 2 as a protein of tyrosine phospho-rylated protein complex affected by Met-Dscam1 signaling**	-
123.	***G***	**10**	**85**	**53**	**CG10149**	**Rpn6** Proteasome p44.5 subunits p42B	**Proteasome 26S subunit, non-ATPase, 11, PSMD11**	**-**
124.	***H***	**4**	**87**	53	CG2064	**CG2064**	Retinol dehydrogenase 12 (all-trans/9-cis/11-cis), DHRS12 ✓ ✓	CG2065, CG30491, CG30495, CG2070, CG3842, CG7675,

Rank	Band	Total spectral count	Max. Mascot score	Avg. peptide score	CG #	Name	Vertebrate orthologue	Paralogues
							✓ **(binds to vap-33)**	Wwox, CG11200, CG31235
125.	*E, C*	**12**	**97**	**52**	**CG13281**	**CAS/CSE1 segregation protein,** Exportin-2	**CSE1 chromosome segregation 1-like (CSE1L)**	**-**
126.	*H*	**4**	**74**	52	CG3181	**Ts**	Thymidylate synthetase (TYMS)	-
127.	*C*	**3**	**58**	51	CG6223	**Coat Protein (coatomer) β** βCOP, BetaCop, βCOP, β-COP	Coatomer protein complex, subunit beta 1 (COPB1)	-
							✓ **Also found in iTRAQ2 as a protein affected by Met-Dscam1 signaling**	
128.	*C*	**3**	**71**	51	CG5252	**Ranbp9**	Importin 9 (IPO9)	-
129.	*D*	**5**	**67**	51	CG9281	**CG9281**	ATP-binding cassette, sub-family F (GCN20), member 2 (ABCF2)	-
130.	*H*	**3**	**56**	51	CG9862	**Rae1**	RAE1, RNA export 1 homolog	CG12782, Bub3
131.	*A*	**3**	**63**	50	CG8290	**ADD1**	-	-
132.	*F*	**5**	**71**	50	CG2263	**CG2263** phenylalanine-tRNA ligase	FARSA	-
133.	*F*	**3**	**61**	50	CG3593	**r-l** rudimentary-like	Uridine monophosphate synthetase (UMPS)	-
134.	*H*	**6**	**60**	**50**	**CG5014**	**Vap-33-1**	**VAMP (vesicle-associated membrane protein)-associated protein B and C, VAPB, VAPA**	**fan**
135.	*A*	**3**	**54**	49	CG9012	**Chc** Clathrin heavy chain	Clathrin, heavy chain (Hc), CLTC, CLTCL1	-
136.	*B*	**4**	**93**	49	CG7961	**α-COP** α-coatomer protein	Coatomer protein complex, subunit alpha (COPA)	-
137.	*G*	**5**	**64**	49	CG11893	**CG11893**	-	CG31300, CG31104, CG31370, CG13659,CG31436, CG13658, CG9498, CG31975, CG7135, CG32195, CG13360, CG9497, CG31974, CG11891, CG11878, CG33301, CG11892, CG10513, CG16898, CG31380, CG31098, CG10514, CG11889, CG10560,

Rank	Band	Total spectral count	Max. Mas-cot score	Avg. peptide score	CG #	Name	Vertebrate orthologue	Paralogues
								CG10550, CG10553, CG31087, CHKov1, CG6830, CG10562, CG6908, CHKov2, CG10559, CG31099, CG31097, CG31102, CG6834, CG31288, CG18765
138.	*G*	**3**	**49**	49	CG10639	**CG10639**	L-2-hydroxyglutarate dehydrogenase	L2HGDH
139.	*E*	**8**	**77**	48	CG2658	**CG2658**	Spastic paraplegia 7 (pure and complicated autosomal recessive)(SPG7)	-
140.	*C, E*	**12**	**93**	**47**	**CG5787**	**CG5787**	**-**	**Pih1D1**
141.	*D*	**3**	**54**	47	CG9020	**Aats-arg,** Arginyl-tRNA synthetase	RARS	CG10092
142.	*H*	**15**	**95**	**47**	**CG12030**	**Gale**	**UDP-galactose-4-epimerase (GALE)**	**CG7979**
143.	*H*	**4**	**53**	47	CG11876	**CG11876** Pyruvate dehydrogenase E1β subunit	Pyruvate dehydrogenase (lipoamide) beta (PDHB)	CG17691
144.	*B*	**6**	**60**	46	CG14998	**ens** ensconsin	Microtubule-associated protein 7	-
145.	*E*	**5**	**55**	46	CG4878	**eIF3-S9**	Eukaryotic translation initiation factor 3, subunit B, (EIF3B)	-
146.	*G*	**3**	**56**	46	CG6950	**CG6950**	Cysteine conjugate-beta lyase 2 (CCBL2), CCBL1,	CG1461
147.	*C*	**4**	**52**	45	CG10333	**CG10333** DmRH19	DEAD (Asp-Glu-Ala-Asp) box polypeptide 23 (DDX23)	abs
148.	*F*	**5**	**59**	45	CG7619	**Rpn10,** Proteasome 54kD subunit, p54, S5A	Proteasome 26S subunit, non-ATPase, 4 (PSMD4)	-
149.	*D*	**5**	**58**	44	CG5064	Signal recognition particle protein 68	Signal recognition particle 68kDa	
150.	*F,G*	**14**	**53**	44	CG6476	**Srp-68** Suppressor of variegation 3-9	SRP68, signal recognition particle 68kDa ✓ **Also found in a tyrosine phosphory lated complex in iTRAQ minimally affected by Met-Dscam1 signaling**	-
151.	*F*	**3**	**47**	43	CG5482	**CG5482**	FK506 binding protein 8, 38kDa (FKBP8)	shu, FKBP59, FKBP506-bp2

Rank	Band	Total spectral count	Max. Mascot score	Avg. peptide score	CG #	Name	Vertebrate orthologue	Paralogues
152.	*G*	**4**	**54**	43	CG2922	**kra** extra bases, eIF-5C, elF-5C, l(3)03022	BZW1, BZW2 (basic leucine zipper and W2 domains 1-2)	-
153.	*A*	**3**	**45**	42	CG9206	**Gl** Glued, p150Glued, p150, p150/glued	Dynactin 1 (DCTN1)	CG9279, TBCB
154.	*G*	**3**	**48**	**42**	**CG3727**	**dock**	**NCK1, NCK2, NCK adaptor protein**	**drk**
155.	*H*	**3**	**43**	**42**	**CG5730**	**Annexin B9** AnxB9, AnnIX, AnxB9	**ANXA7, annexin A11** ✓ **also found in iTRAQ2 as a protein affected by Met-Dscam1 signaling**	**AnxB11, AnnX**
156.	*B, C*	**5**	**51**	41	CG33158	**CG33158**	EFTUD1 (elongation factor Tu GTP binding domain containing 1)	-
157.	*D*	**8**	**50**	41	CG32549	**CG32549**	5'-nucleotidase, cytosolic II, NT5DC4	CG1814, CG2277
158.	*G*	**3**	**49**	41	CG11183	**Dcp1** Decapping protein 1, Dcp1	DCP1A (decapping mRNA 1A), DCP1B	-
159.	*C*	**3**	**40**	40	CG3542	**CG3542**	PRP40 pre-mRNA processing factor 40 homolog A (PRPF40A), PRPF40B	CG42724
160.	*F*	**3**	**47**	40	CG17566	**γ-Tub** γ-Tubulin at 37C, fs(2)TW1, γTUB, γTub37CD,, γ-Tub37C, gammaTub37C	Tubulin, gamma 1(TUBG1), TUBG2	gammaTub23C
161.	*I*	**4**	**46**	39	CG9159	**Kr-h2** Kruppel homolog 2, Krh2	Transmembrane protein 33 (TMEM33)	-
162.	*D*	**4**	**38**	34	CG7757	**Prp3**	PRP3 pre-mRNA processing factor 3 homolog (PRPF3)	-
163.	*B, C*	**26**	**142**		**CG11471**	**Isoleucyl-tRNA synthetase**	**IARS**	**-**

2. *Proteins binding to Dscam1 cytoplasmic domain: Band A*

CHAPTER 3- TABLE 15. **LIST OF PROTEINS IDENTIFIED WITH HIGH CONFIDENCE AS BINDING PARTNERS OF THE DSCAM1 CYTOPLASMIC IN BG3C2 CELLS: BAND A**

This table contains all proteins with 10 or more unique peptides identified in band A of the Dscam1 cytoplasmic domain purification. The high cut-off guarantees high confidence of identification. Other proteins, identified with lower confidence, can be found in Chapter 3-Table 14 (identification via three and more peptides) and the supplementary file containing the raw data. Information regarding protein function, orthologues and paralogues was retrieved from the Uniprot, Ensemble and Flybase databases.

Band	Gene name	# of unique peptides	Max. MASCOT score	Human orthologue	Protein function	Paralogues	Identified in other experiment?
A	***Usp16-45*** CG4165, Ubiquitin specific protease 16/45, Usp45	**11**	**109**	USP45, USP16	Ubiquitin specific protease, zinc ion binding.	Khc, cos, Klp54D, pav, sub, Klp31E	**Yes** (Band B of this experiment)

CHAPTER 3- TABLE 16. **PROTEINS IDENTIFIED IN THE DSCAM1 CYTOPLASMIC RECEPTOR COMPLEX ALSO IDENTIFIED IN PHOSPHOR-PROTEOMIC EXPERIMENTS: BAND A**

This table contains proteins identified in Band A of the Dscam1cytoplasmic domain purification that also have been detected in other proteomic experiments. Information regarding protein function, orthologues and paralogues was retrieved from the Uniprot, Ensemble and Flybase databases.

#	Band	Gene name	# of unique peptides	Max. MASCOT score	Human orthologue	Protein function	Paralogues	Identified in other experiment?
1.	*A*	***Chc*** Clathrin heavy chain, CG9012	**3**	**54**	clathrin, heavy chain (Hc), CLTC, CLTCL1	Clathrin heavy chain	-	**Yes** (iTRAQ 1 and 2 and Michael Hughes proteomic analysis of Dscam1 signaling complex in S2 cells and fly heads)

3. *Proteins binding to the Dscam1 cytoplasmic domain: Band B*

CHAPTER 3- TABLE 17. **LIST OF PROTEINS IDENTIFIED WITH HIGH CONFIDENCE AS BINDING PARTNERS OF THE DSCAM1 CYTOPLASMIC DOMAIN IN BG3C2 CELLS: BAND B**

This table contains all proteins with 10 or more unique peptides identified in band B of the Dscam1 cytoplasmic domain purification. The high cut-off guarantees good confidence of identification. Other proteins, identified with lower confidence, can be found in Chapter 3-Table 14 (identified by three and more unique peptides) and in the supplementary file containing the raw data. Information regarding protein function, orthologues and paralogues was retrieved from the Uniprot, Ensemble and Flybase databases. Yellow: Proteins that have been identified in other experiments as well.

#	Band	Gene name	# of unique peptides	Max. MASCOT score	Human orthologue	Protein function	Paralogues	Identified in other experiment?
1.	*B*	***Threonyl-tRNA synthetase*** *CG5353, l (2) k04203, ThrRS*	**69**	**52**	-	Threonine-tRNA ligase; involved in neurogenesis	mRpL39	**YES** (Band D and E)
2.	*B*	***Isoleucyl-tRNA synthetase*** *CG11471, l(3)00827, IleRS, Aats-ile*	**26**	**142**	IARS	Cytoplasmic isoleucine-tRNA ligase; ATP binding	-	**YES**: (Band B and C)
3.	*B*	***Gp150*** *CG5820*	**23**	**128**	-	Leucine rich repeat transmembrane protein involved in RPTP signaling and compound eye development	MstProx, Toll-4, chp, lbk, Toll-6, conv, CG7509, Con, 18w, CG7896, CG4168, CG32055, Tollo, atk, haf, Toll-7, CG18095, CG42346, Tehao, Tl, rdo, Lrt	**YES** (Band E)
4.	*B*	***CG4119***	**16**	**118**	RBM25	mRNA binding protein, involved in splicing	-	NO
5.	*B*	***Usp16-45*** *CG4165, Ubiquitin specific protease 16/45, Usp45*	**11**	**109**	USP45, USP16	Ubiquitin specific protease, zinc ion binding,	Khc, cos, Klp54D, pav, sub, Klp31E	**Yes** (Band A)
6.	*B*	***leucyl-tRNA synthetase,*** *CG33123*	**10**	**108**	LARS	Leucine-tRNA ligase, involved in wound healing and neurogenesis	-	NO

4. *Proteins binding to the Dscam1 cytoplasmic domain: Band C*

CHAPTER 3- TABLE 18. **LIST OF PROTEINS IDENTIFIED WITH HIGH CONFIDENCE AS BINDING TO THE DSCAM1 CYTOPLASMIC DOMAIN IN BG3C2 CELLS: BAND C**

This table contains all proteins with 10 or more unique peptides identified from band C of the Dscam1 cytoplasmic domain purification. The high cut-off number guarantees good confidence of identification. Other proteins, identified with lower confidence, can be found in Chapter 3-Table 14 (identified with three and more peptides) and the supplementary file containing the raw data. Information regarding protein function, orthologues and paralogues was retrieved from the Uniprot, Ensemble and Flybase databases. Yellow: Proteins that have been identified in other experiments as well.

#	Band	Gene name	# of unique peptides	Max. MASCOT score	Human orthologue	Protein function	Paralogues	Identified in other experiment?
1.	*C*	***qkr54B*** *quaking related 54B, Sam50, CG4816*	**43**	**60**	KHDRBS1, KHDRBS3	Cytosolic mRNA binding protein with KH domain	nsr, qkr58E-2, qkr58E-3, CG3927, CG4021, qkr58E-1, CG10384, how, SF1	**YES** (Band F and G)
2.	*C*	***Puromycin sensitive aminopeptidase*** *PSA, dPSA, CG1009*	**32**	**81**	NPEPPS	Zinc ion binding metallopeptidase involved in proteolysis	-	**YES** (Band E)
3.	*C*	***Isoleucyl-tRNA synthetase*** *CG11471, l(3)00827, IleRS, Aats-ile*	**26**	**142**	IARS	Cytoplasmic isoleucine-tRNA ligase	-	**YES** (Band B)
4.	*C*	***Valyl-tRNA synthetase*** *CG4062*	**12**	**97**	VARS2, VARS	Cytoplasmic valine- and glutamate tRNA ligase, involved in neurogenesis	CG5660	NO
5.	*C*	***CAS/CSE1 segregation protein*** *Exportin-2, CG13281*	**12**	**97**	CSE1L	Export receptor for importin alpha. Mediates importin-alpha re-export from the nucleus to the cytoplasm after import substrates have been released into the nucleoplasm; Involved in neurogenesis and phagocytosis and apoptosis.	-	**YES** (Band E)
6.	*C*	***CG5787***	**12**	**93**	-	Microtubule associated protein	Pih1D1	**YES** (Band E)
7.	*C*	***cindr*** *CIN85 and CD2AP orthologue, CG31012*	**11**	**126**	SH3KBP1, CD2AP, SH3D21	SH3 domain containing protein; binds cell adhesion molecules, involved in actin filament organization, border cell migration, compound eye development, intercell bridging and receptor mediated endocytosis.	-	NO

CHAPTER 3- TABLE 19. **PROTEINS IDENTIFIED IN THE DSCAM1 CYTOPLASMIC RECEPTOR COMPLEX ALSO IDENTIFIED IN OTHER PHOSPHOR-PROTEOMIC EXPERIMENTS: BAND C**

This table contains proteins identified from band C of the Dscam1cytoplasmic domain purification that also have been detected in other proteomic experiments. Information regarding protein function, orthologues and paralogues was retrieved from the Uniprot, Ensemble and Flybase databases.

#	Band	Gene name	# of unique peptides	Max. MASCOT score	Human orthologue	Protein function	Paralogues	Identified in other experiment?
1.	*C*	***moleskin*** *msk, dim-7, dim7, CIP-61, Ran binding protein 7, CG7935*	**7**	**81**	Importin 7, IPO7, IPO8	Importin: protein transmembrane transporter; binds Ran GTPases; involved in compound eye development, EGFR signaling, regulation of neuronal apoptosis and RTK signaling.	-	**Also found in the first silver gel presented in this dissertation in a tyrosine phosphorylated complex of proteins.**
2.	*C*	***Coat Protein (coatomer) β*** *βCOP, BetaCop, βCOP, β-COP, CG6223*	**3**	**58**	Coatomer protein complex, subunit beta 1, COPB1	Complex that binds to dilysine motifs and reversibly associates with Golgi non-clathrin-coated vesicles which further mediate biosynthetic protein transport from the ER.	-	**Also found in iTRAQ2 as a protein affected by Met-Dscam1 signaling.**

5. *Proteins binding to the Dscam1 cytoplasmic domain: Band D*

CHAPTER 3- TABLE 20. **LIST OF PROTEINS IDENTIFIED WITH HIGH CONFIDENCE AS BINDING TO THE DSCAM1 CYTOPLASMIC DOMAIN IN BG3C2 CELLS: BAND D**

This table contains all proteins with 10 or more unique peptides identified in band D of the Dscam1 cytoplasmic domain purification. The high cut-off number guarantees good confidence of identification. Other proteins, identified with lower confidence, can be found in Chapter 3-Table 14 (identified by three and more peptides) and the supplementary file containing the raw data. Information regarding protein function, orthologues and paralogues was retrieved from the Uniprot, Ensemble and Flybase databases. Yellow: Proteins that have been identified in other experiments as well.

#	Band	Gene name	# of unique peptides	Max. MASCOT score	Human orthologue	Protein function	Paralogues	Identified in other experiment?
1.	*D*	***Threonyl-tRNA synthetase*** *CG5353, l(2)k04203, ThrRS*	**69**	**52**	-	Threonine-tRNA ligase; involved in neurogenesis.	mRpL39	**YES** (Band B and E)
2.	*D*	***Rumpelstiltskin*** *hrp59, hnRNP M, CG9373, rump*	**16**	**148**	HNRNPN, MYEF2	mRNA binding protein found at the 3'UTR; exists in nucleus and cytoplasm.	-	NO
3.	*D*	***δ-coatomer protein*** *CG14813, deltaCOP, EG:63B12.10, δ-Cop*	**11**	**107**	ARCN1	Belongs to the COPI vesicle coat and AP complex; involved in salivary gland migration, phagocytosis and retrograde vesicle mediated transport as well as protein secretion.	-	NO
4.	*D*	***HBS1*** *CG1898*	**12**	**107**	HBS1L	Cytosolic translation release factor; GTP binding with GTPase activity; important for termination of translation; involved in innate immune response.	Elf	NO

#	Band	Gene name	# of unique peptides	Max. MASCOT score	Human orthologue	Protein function	Paralogues	Identified in other experiment?
5.	*D*	***CG3714***	**10**	**46**	NAPRT	Cytosolic protein involved in step 1 of the sub-pathway that synthesizes nicotinate D-ribonucleotide from nicotinate.	-	**YES** (Band F)

CHAPTER 3- TABLE 21. **PROTEINS IDENTIFIED IN THE DSCAM1 CYTOPLASMIC RECEPTOR COMPLEX ALSO IDENTIFIED IN MY PHOSPHOR-PROTEOMIC EXPERIMENTS: BAND D**

This table contains proteins identified from band D of the Dscam1cytoplasmic domain purification that also have been detected in other proteomic experiments. Information regarding protein function, orthologues and paralogues was retrieved from the Uniprot, Ensemble and Flybase databases.

#	Band	Gene name	# of unique peptides	Max. MASCOT score	Human orthologue	Protein function	Paralogues	Identified in other experiment?
1.	*D*	***Rop*** *SEC1 Ras opposite, Rop, CG15811*	**3**	**69**	Syntaxin binding protein 1; STXBP1, STXBP2, STXBP3	Sec1-like protein; SNARE and Syntaxin binding; involved in neurotransmitter secretion and synaptic transmission, synaptic vesicle transport, priming and vesicle docking during exocytosis.	SEC1, Ras opposite, Rop	**Also identified in iTRAQ 2 as belonging to a tyrosine phosphorylated complex not affected by Met-Dscam1 signaling.**
2.	*D*	***Glycogen synthase*** *GlyS, GS, CG6904*	**4**	**52**	Glycogen synthase 1, GYS1, GYS2	Glycosyltransferase 3; transfers the glycosyl residue from UDPG to the non-reducing end of alpha-1,4-glucan.	-	**Also identified in iTRAQ 2 as a protein of tyrosine phosphorylated protein complex affected by Met-Dscam1 signaling.**

6. *Proteins binding to the Dscam1 cytoplasmic domain: Band E*

CHAPTER 3- TABLE 22. **LIST OF PROTEINS IDENTIFIED WITH HIGH CONFIDENCE AS BINDING TO THE DSCAM1 CYTOPLASMIC DOMAIN IN BG3C2 CELLS: BAND E**

This table contains all proteins with 10 or more unique peptides identified in band E of the Dscam1 cytoplasmic domain purification. The high cut-off number guarantees good confidence of identification. Other proteins, with lower confidence identification, can be found in Chapter 3-Table 14 (identified with three and more peptides) and the supplementary file containing the raw data. Information regarding protein function, orthologues and paralogues was retrieved from the Uniprot, Ensemble and Flybase databases. Yellow: Proteins that have been identified in other experiments as well.

#	Band	Gene name	# of unique peptides	Max. MASCOT score	Human orthologue	Protein function	Paralogues	Identified in other experiment?
1.	*E*	***Threonyl-tRNA synthetase*** *CG5353, l (2) k04203, ThrRS*	69	52	-	Threonine-tRNA ligase activity; involved in neurogenesis.	mRpL39	**YES** (Band B and D)
2.	*E*	***Puromycin sensitive aminopeptidase*** *PSA, dPSA, CG1009*	32	81	NPEPPS	Zinc ion binding metallopeptidase involved in proteolysis.	-	**YES** (Band C)
3.	*E*	***Gp150*** *CG5820*	23	128	-	Leucine rich repeat transmembrane protein involved in RPTP signaling and compound eye development.	MstProx, Toll-4, chp, lbk, Toll-6, conv, CG7509, Con, 18w, CG7896, CG4168, CG32055, Tollo, atk, haf, Toll-7, CG18095, CG42346, Tehao, Tl, rdo, Lrt	**YES** (Band B)
4.	*E*	***CAS/CSE1 segregation protein*** *Exportin-2, CG13281*	12	97	CSE1L	Export receptor for importin alpha. Mediates importin-alpha re-export from the nucleus to the cytoplasm after import substrates have been released into the nucleoplasm; Ran GTPase binding; involved in neurogenesis and phagocytosis and apoptosis.	-	**YES** (Band C)
5.	*E*	***CG5787***	12	93	-	Microtubule associated protein	Pih1D1	**YES** (Band C)
6.	*E*	***Mtp*** *Microsomal triacylglycerol transfer protein, dMTP CG9342*	10	96	MTTP	Lipid transport protein; involved in dendritogenesis and synaptic target recognition; found in lipid particles and the endomembrane system.	-	NO
7.	*E*	***IRP1A*** *Iron regulatory protein 1A, CG4900*	15	95	ACO1	Catalyzes the isomerization of citrate to isocitrate via cis-aconitate; iron and mRNA binding; involved in regulation of translational initiation.	Irp-1b, Acon, CG4706	NO

CHAPTER 3- TABLE 23. **PROTEINS IDENTIFIED IN THE DSCAM1 CYTOPLASMIC RECEPTOR COMPLEX ALSO IDENTIFIED IN OTHER PHOSPHOR-PROTEOMIC EXPERIMENTS: BAND E**

This table contains proteins identified from band E of the Dscam1cytoplasmic domain purification that also have been detected in other proteomic experiments. Information regarding protein function, orthologues and paralogues was retrieved from the Uniprot, Ensemble and Flybase databases.

#	Band	Gene name	# of unique peptides	Max. MASCOT score	Human orthologue	Protein function	Paralogues	Identified in other experiment?
1.	*E*	***RnrL*** *Ribonucleoside diphosphate reductase large subunit, l (2) k06709, RNR1, CG5371*	**5**	**95**	Ribonucleotide reductase M1, RRM1	Provides the precursors necessary for DNA synthesis. Catalyzes the biosynthesis of deoxyribonucleotides from the corresponding ribonucleotides.	-	**Also identified in iTRAQ 2 as belonging to a tyrosine phosphorylated complex affected by Met-Dscam1 signaling.**

7. *Proteins binding to the Dscam1 cytoplasmic domain: Band F*

CHAPTER 3- TABLE 24. **LIST OF PROTEINS IDENTIFIED WITH HIGH CONFIDENCE AS BINDING TO THE DSCAM1 CYTOPLASMIC DOMAIN IN BG3C2 CELLS: BAND F**

This table contains all proteins with 10 or more unique peptides identified in band F of the Dscam1 cytoplasmic domain purification. The high cut-off number guarantees good confidence of identification. Other proteins, identified with lower confidence, can be found in Chapter 3-Table 14 (identified via three and more peptides) and in the supplementary file containing the raw data. Information regarding protein function, orthologues and paralogues was retrieved from the Uniprot, Ensemble and Flybase databases. Yellow: Proteins that have been identified in other experiments as well.

#	Band	Gene name	# of unique peptides	Max. MASCOT score	Human orthologue	Protein function	Paralogues	Identified in other experiment?
1.	*F*	**CG2129**	**49**	**118**	ZNF276, ZNF653, ZNF692, ZFP91, ZFP91-CNTF, CTC-398G3.6	Metal and nucleic acid binding protein of unknown function.	CG10959, CG18262, Plzf, CG15336	NO
2.	*F*	**qkr54B** quaking related 54B, Sam50 CG4816	**43**	**60**	KHDRBS1, KHDRBS3	Cytosolic mRNA binding protein with KH domain.	nsr, qkr58E-2, qkr58E-3, CG3927, CG4021, qkr58E-1, CG10384, how, SF1	**YES** (Band C and G)
3.	*F*	**UGP** UGPase, UDPGPP, CG4347	**18**	**89**	UGP2	Cytosolic UDP-glucose pyrophosphorylase 2.	-	NO
4.	*F*	**seryl-tRNA synthetase** CG17259	**17**	**98**	SARS	Serine-tRNA ligase activity; ATP binding	-	NO

#	Band	Gene name	# of unique peptides	Max. MASCOT score	Human orthologue	Protein function	Paralogues	Identified in other experiment?
5.	*F*	**Histidyl-tRNA synthetase** CG6335	**12**	**102**	HARS, HARS2	Histidine-tRNA ligase; ATP binding.	-	NO
6.	*F*	**CaBP1** CG5809, calcium-binding protein 1, AAL28897, BG:DS09218.4, DmCaBP1	**12**	**70**	PDIA6	Isomerase found in lipid particles, ER and the endomembrane system; involved in apoptotic clearance, cell redox homeostasis and protein folding.	CG5027, prtp, CG9302	YES (Band G)
7.	*F*	**Otefin** Ote, CG5581	**10**	**113**	-	Transcriptional repressor	bocksbeutel	NO
8.	*F*	**CG3714**	**10**	**46**	NAPRT	Cytosolic protein involved in step 1 of the sub-pathway that synthesizes nicotinate D-ribonucleotide from nicotinate.	-	YES (Band D)

CHAPTER 3- TABLE 25. **PROTEINS IDENTIFIED IN THE DSCAM1 CYTOPLASMIC RECEPTOR COMPLEX ALSO IDENTIFIED IN MY PHOSPHOR-PROTEOMIC EXPERIMENTS: BAND F.**

This table contains proteins identified from band F of the Dscam1cytoplasmic domain purification that also have been detected in other proteomic experiments. Information regarding protein function, orthologues and paralogues was retrieved from the Uniprot, Ensemble and Flybase databases.

#	Band	Gene name	# of unique peptides	Max. MASCOT score	Human orthologue	Protein function	Paralogues	Identified in other experiment?
1.	*F*	***Srp-68*** *Suppressor of variegation 3-9, CG6476*	**14**	**53**	SRP68, signal recognition particle 68kDa	Eukaryotic translation initiation factor 2	-	✓ **Also found in a tyrosine phosphorylated complex in iTRAQ experiments, minimally affected by Met-Dscam1 signaling.** ✓ **Also found in band G of this experiment.**

6. Proteins binding to Dscam1 cytoplasmic domain: Band G

CHAPTER 3- TABLE 26. **LIST OF PROTEINS IDENTIFIED WITH HIGH CONFIDENCE AS BINDING TO THE DSCAM1 CYTOPLASMIC DOMAIN IN BG3C2 CELLS: BAND G**

This table contains all proteins with 10 or more unique peptides identified in band G *of the Dscam1 cytoplasmic domain purification. The high cut-off number guarantees good confidence of identification. Other proteins, identified with lower confidence, can be found in Chapter 3-Table 14 (identified with three and more peptides) and in the supplementary file containing the raw data. Information regarding protein function, orthologues and paralogues was retrieved from the Uniprot, Ensemble and Flybase databases. Yellow: Proteins that have been identified in other experiments as well.*

#	Band	Gene name	# of unique peptides	Max. MASCOT score	Human orthologue	Protein function	Paralogues	Identified in other experiment?
1.	*G*	***ImpL3*** *Ecdysone-inducible gene L3, LDH, CG10160*	**85**	**79**	LDHA, LDHB	Cytoplasmic protein and lactate dehydrogenase involved in the fermentation of pyruvate to lactate; involved in myoblast fusion.	CG13334	**YES** ✓ In iTRAQ2 as a protein minimally affected by Met-Dscam1 signaling. ✓ In bands B, H and I of this experiment.
2.	*G*	***NudC-like*** *CG31251*	**74**	**120**	NUDCD3	Chaperone found in Golgi; involved in nuclear migration.	nudC	NO
3.	*G*	***qkr54B*** *quaking related 54B, Sam50 CG4816*	**43**	**60**	KHDRBS1, KHDRBS3	Cytosolic mRNA binding protein with KH domain.	nsr, qkr58E-2, qkr58E-3, CG3927, CG4021, qkr58E-1, CG10384, how, SF1	**YES** (Band C and F)
4.	*G*	***CaBP1*** *CG5809, calcium-binding protein 1, AAL28897, BG:DS09218.4, DmCaBP1*	**12**	**70**	PDIA6	Isomerase found in lipid particles, ER and the endomembrane system; involved in apoptotic clearance, cell redox homeostasis and protein folding.	CG5027, prtp, CG9302	**YES** (Band F)
5.	*G*	***Eukaryotic initiation factor 2β*** *CG4153, eIF-2beta, eIF2β, eIF2β, eIF-2*	**11**	**98**	EIF2S2	Cytosolic translation initiation factor; functions in the early steps of protein synthesis by forming a ternary complex with GTP and initiator tRNA. This preinitiation complex mediates ribosomal recognition of a start codon during the scanning process of the leader region; binds t-RNA and GTP; associated to microtubules, involved in axonal midline choice.	-	NO
6.	*G*	***CG3724*** *Phosphogluconate dehydrogenase*	**10**	**108**	PGD	Involved in pentosephosphate pathway; catalyzes the oxidative decarboxylation of 6-phosphogluconate to ribulose 5-phosphate and CO2 with concomitant reduction of NADP to NADPH.	-	NO
7.	*G*	***CT12127*** *CG3609*	**10**	**93**	DHDH	Cytosolic oxidoreductase	CG3597, CG13280	**YES** (Band H)
8.	*G*	***Rpn6*** *Regulatory particle non-ATPase 6 Proteasome p44.5 subunit, p42B, CG10149*	**10**	**85**	PSMD11	Component of the 26S proteasome, a multiprotein complex involved in the ATP-dependent degradation of ubiquitinated proteins. In the complex, RPN6 is required for proteasome assembly.	alien	NO

CHAPTER 3- TABLE 27. **PROTEINS IDENTIFIED IN THE DSCAM1 CYTOPLASMIC RECEPTOR COMPLEX ALSO IDENTIFIED IN MY PHOSPHOR-PROTEOMIC EXPERIMENTS: BAND G**

This table contains proteins identified from band A of the Dscam1cytoplasmic domain purification that also have been detected in other proteomic experiments. Information regarding protein function, orthologues and paralogues was retrieved from the Uniprot, Ensemble and Flybase databases.

#	Band	Gene name	# of unique peptides	Max. MASCOT score	Human orthologue	Protein function	Paralogues	Identified in other experiment?
1.	*G*	***ImpL3*** *Ecdysone-inducible gene L3, LDH, CG10160*	**85**	**79**	LDHA, LDHB	Cytoplasmic protein; lactate dehydrogenase involved in the fermentation of pyruvate to lactate; involved in myoblast fusion.	CG13334	**YES** ✓ In iTRAQ experiment 2 as a protein not affected by Met-Dscam1 signaling. ✓ In band H and I of this experiment.
2.	*G*	***Srp-68*** *Suppressor of variegation 3-9, CG6476*	**14**	**53**	SRP68, signal recognition particle 68kDa	Eukaryotic translation initiation factor 2	-	**YES** 1. Also found in a tyrosine phosphorylated complex in iTRAQ experiments minimally affected by Met-Dscam1 signaling. 2. Also found in band H of this experiment.

7. Proteins binding to Dscam1 cytoplasmic domain: Band H

CHAPTER 3- TABLE 28. **LIST OF PROTEINS IDENTIFIED WITH HIGH CONFIDENCE AS BINDING TO THE DSCAM1 CYTOPLASMIC IN BG3C2 CELLS.**

This table contains all proteins with 10 or more unique peptides identified in band H of the Dscam1 cytoplasmic domain purification. The high cut-off number guarantees a high confidence degree of identification. Other proteins, identified with lower confidence, can be found in Chapter 3-Table 14 (identified with three and more peptides) and in the supplementary file containing the raw data. Information regarding protein function, orthologues and paralogues was retrieved from the Uniprot, Ensemble and Flybase databases. Yellow: Proteins that have been identified in other experiments as well.

#	Band	Gene name	# of unique peptides	Max. MASCOT score	Human orthologue	Protein function	Paralogues	Identified in other experiment?	
3.	***H***	***ImpL3*** *Ecdysone-inducible gene L3, LDH,CG10160*	**85**	**79**	LDHA, LDHB	Cytoplasmic protein; lactate dehydrogenase involved in the fermentation of pyruvate to lactate; involved in myoblast fusion.	CG13334	**YES** ✓ ✓	In iTRAQ 2 as a protein not affected by Met-Dscam1 signaling. In band G and I of this experiment.
4.	***H***	***εCOP*** *CG9543, epsilon COP, BcDNA:LD29885*	**17**	**136**	COPE	Coatomer protein complex, subunit epsilon; involved in ER to Golgi vesicle-mediated transport, intra-Golgi vesicle mediated transport and retrograde vesicle mediated transport.	-	NO	
5.	***H***	***Gale*** *CG12030*	**15**	**95**	GALE	Catalyzes two distinct but analogous reactions: The reversible epimerization of UDP-glucose to UDP-galactose and the reversible epimerization of UDP-N-acetylglucosamine to UDP-N-acetylgalactosamine; involved in larval lymph gland hematopoiesis.	CG7979	**YES** ✓	In iTRAQ 2 as protein in tyrosine phosphorylated complexes that are affected by Met-Dscam1 overexpression.
6.	***H***	***eIF3ga*** *CG8636, eIF3g paralogue a, eIF3-S4*	**12**	**128**	EIF3G	Component of the eukaryotic translation initiation factor 3 (eIF-3) complex which is involved in protein synthesis, and together with other initiation factors stimulates binding of mRNA and methionyl-tRNA to the 40S ribosome. This subunit can bind 18S rRNA.	CG10881	NO	
7.	***H***	***Annexin B11*** *CG9968*	**10**	**87**	ANXA7	Annexin; calcium-, phospholipid- and actin-binding protein involved in cell adhesion and regulation of cell shape.	AnxB9, AnxB10	**YES** ✓	Band I of this experiment.
8.	***H***	***CT12127*** *CG3609*	**10**	**93**	DHDH	Cytosolic oxidoreductase	CG3597, CG13280	**YES** ✓	Band G of this experiment.

CHAPTER 3- TABLE 29. **PROTEINS IDENTIFIED IN THE DSCAM1 CYTOPLASMIC RECEPTOR COMPLEX ALSO IDENTIFIED IN PHOSPHOR-PROTEOMIC EXPERIMENTS: BAND H**

This table contains proteins identified from band H of the Dscam1cytoplasmic domain purification that also have been detected in other proteomic experiments. Information regarding protein function, orthologues and paralogues was retrieved from the Uniprot, Ensemble and Flybase databases.

#	Band	Gene name	# of unique peptides	Max MASCOT score	Human orthologue	Protein function	Paralogues	Identified in other experiment?
1.	*H*	***ImpL3*** *Ecdysone-inducible gene L3, LDH, CG10160*	**85**	**79**	LDHA, LDHB	Cytoplasmic protein; lactate dehydrogenase involved in the fermentation of pyruvate to lactate; involved in myoblast fusion.	CG13334	**YES** ✓ In iTRAQ 2 as a protein not affected by Met-Dscam1 signaling. ✓ In band G and I of this experiment.
2.	*H*	***Gale*** *CG12030*	**15**	**95**	GALE	Catalyzes two distinct but analogous reactions: The reversible epimerization of UDP-glucose to UDP-galactose and the reversible epimerization of UDP-N-acetylglucosamine to UDP-N-acetylgalactosamine; involved in larval lymph gland hematopoiesis.	CG7979	**YES** ✓ In iTRAQ 2 as protein in tyrosine phosphorylated complexes that are affected by Met-Dscam1 overexpression.
3.	*H*	***Annexin B9*** *AnxB9, AnnIX, AnxB9, CG5730*	**3**	**43**	ANXA7, Annexin A11	Annexin; binds to beta-spectrin.	AnxB11, AnnX	**YES** ✓ Also found in iTRAQ2 as a protein affected by Met-Dscam1 signaling.

8. *Proteins binding to Dscam1 cytoplasmic domain: Band I*

CHAPTER 3- TABLE 30. **LIST OF PROTEINS IDENTIFIED WITH HIGH CONFIDENCE AS BINDING TO THE DSCAM1 CYTOPLASMIC DOMAIN IN BG3C2 CELLS: BAND I**

This table contains all proteins with 10 or more unique peptides identified from band I of the Dscam1 cytoplasmic domain purification. The high cut-off number guarantees high confidence of identification. Other proteins, identified with lower confidence, can be found in Chapter 3-Table 14 (identified by three and more signature peptides) and in the supplementary file containing the raw data. Information regarding protein function, orthologues and paralogues was retrieved from the Uniprot, Ensemble and Flybase databases. Yellow: Proteins that have been identified in other experiments as well.

#	Band	Gene name	# of unique peptides	Max. MASCOT score	Human orthologue	Protein function	Paralogues	Identified in other experiment?
1.	*I*	***ImpL3*** *Ecdysone-inducible gene L3, LDH, CG10160*	**85**	**79**	LDHA, LDHB	Cytoplasmic protein; lactate dehydrogenase involved in the fermentation of pyruvate to lactate; involved in myoblast fusion.	CG13334	**YES** ✓ In iTRAQ 2 as a protein not affected by Met-Dscam1 signaling. ✓ In band G and H of this experiment.
2.	*I*	***Signal sequence receptor β*** *CG5474*	**13**	**103**	SSR2	TRAP proteins are part of a complex whose function is to bind calcium to the ER membrane and thereby	-	NO

					regulate the retention of ER resident proteins.				
3.	*I*	***Annexin B11*** *CG9968*	**10**	**87**	ANXA7	Annexin; calcium-, phospholipid- and actin-binding protein involved in cell adhesion and regulation of cell shape.	AnxB9, AnxB10	**YES** ✓	In band H of this experiment.
4.	*I*	***Signal recognition particle protein 54k*** *l(3)01418, Srp54, CG4659*	**10**	**85**	SRP54	Signal recognition protein; binds 7S RNA and GTP; serves as GTPase; involved in targeting to membranes and ER.	-	NO	

CHAPTER 3- TABLE 31. **PROTEINS IDENTIFIED IN THE DSCAM1 CYTOPLASMIC RECEPTOR COMPLEX ALSO IDENTIFIED IN OTHER PHOSPHOR-PROTEOMIC EXPERIMENTS: BAND I**

This table contains proteins identified from band A of the Dscam1cytoplasmic domain purification that also have been detected in other proteomic experiments. Information regarding protein function, orthologues and paralogues was retrieved from the Uniprot, Ensemble and Flybase databases.

#	Band	Gene name	# of unique peptides	Max MASCOT score	Human orthologue	Protein function	Paralogues	Identified in other experiment?	
1.	*I*	***ImpL3*** *Ecdysone-inducible gene L3, LDH, CG10160*	**85**	**79**	LDHA, LDHB	Cytoplasmic protein; lactate dehydrogenase involved in the fermentation of pyruvate to lactate; involved in myoblast fusion.	CG13334	**YES** ✓ ✓	In iTRAQ 2 as a protein not affected by Met-Dscam1 signaling. In band G and H of this experiment.

The main group of proteins found in the Dscam1 signaling complex affects translation of mRNAs

Taken together, the number of proteins identified with ten or more peptides and of proteins identified in more than one proteomic experiments amounts to ***41 high confidence*** proteins. They can functionally be classified into the following subgroups as indicated in Chapter 3-Figure 10: ***Translational regulators***, proteins ***involving protein stability and trafficking***, ***cytoskeletal associated proteins***, ***proteins involved in phosphorylation signaling***, ***proteins involved in GTP mediated signaling***, protein involved in ***transcriptional pathways***, and ***adaptor proteins***.

Importantly, ***39% of the identified proteins are mRNA binding proteins and proteins involved in the regulation of translation***. Another 27% are involved in protein trafficking

and stability. 12% of the high confidence hits are proteins found in association with the cytoskeleton and 10% are involved in signaling mediated by phosphorylation. Other protein functions, such as adaptors, proteins involved in GTP and nuclear signaling were represented by smaller subgroups, while 21% of identified proteins could not be assigned to any functional term known to be involved in axon guidance or innate immune responses.

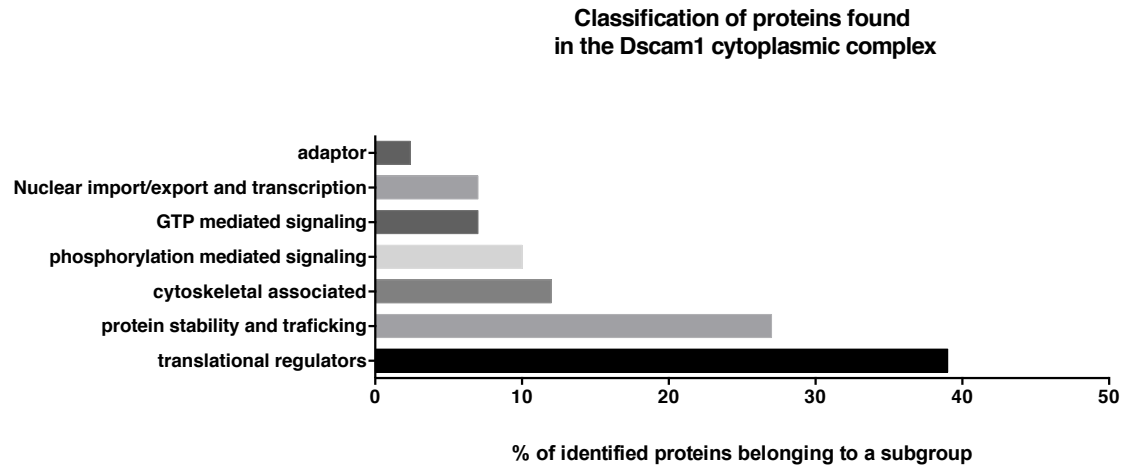

CHAPTER 3- FIGURE 10. **CLASSIFICATION OF THE PROTEINS IDENTIFIED WITH HIGH CONFIDENCE AS BELONGING TO THE DSCAM1 SIGNALING COMPLEX.**

The bars indicate the percentage of proteins linked to the respective GO-term annotation indicated on the left. (One protein can be linked to more than one GO-term). Note the high representation of proteins involved in translational regulation.

The cytoplasmic interactors of Dscam1 fall into at least three main protein complexes

I extended my bioinformatics analysis furthermore by analyzing all 163 identified potential Dscam1 interactors with the *flymine* tool. I used GO-term analysis (Gene ontology term analysis) to asses for biological function and subcellular localization. In line with the enrichment reported above, we found that biological processes involved in translation and protein localization were among the top 10 enriched GO-terms for the 163 potential Dscam1 interactors (Chapter 3- Figure 11).

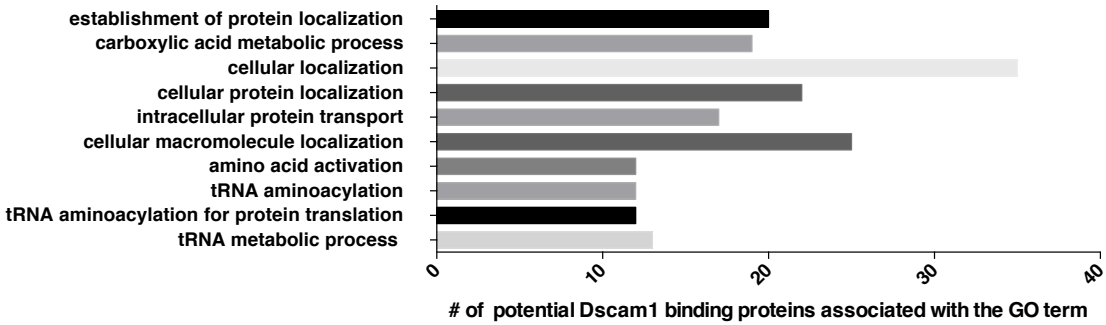

CHAPTER 3- FIGURE 11. **GO-TERM ANALYSIS OF 163 PROTEINS IDENTIFIED AS POTENTIAL BINDING PARTNERS OF THE DSCAM1 CYTOPLASMIC DOMAIN.**

Listed are ten most significantly enriched GO-terms for biological function obtained by Flymine analysis. Note the high representation of GO-terms associated with translation and protein localization. Significance was set at a max. p-value of 0.05 in a Holm-Bonfenorri test and the data distribution was compared to the default Flymine dataset.

Furthermore, I analyzed ***the subcellular localization*** of the 163 proteins found in complex with the Dscam1 cytoplasmic domain in BG3C2 cells. As expected, I found that the interactome points to ***membrane localization*** of Dscam1. However, the statistically significant enrichment of proteins associated with the ***endomembrane system*** points to a potential internalization of the receptor as well (Chapter 3- Figure 12).

In a last analytical step, I assessed protein-protein interactions on Flymine and obtained a regulatory network of physical interactions for the 163 proteins and their interaction partners depicted in Chapter 3- Figure 13. This analysis further confirms the notion of my GO-term analysis suggesting that Dscam1 belongs to ***at least three protein complexes***: Interestingly all of them contain some components of the translational machinery. The first complex is centered around translational initiation factors (eIF3 and eIF2). A second very large complex contains several amino-acyl-tRNA synthetases as well as kinesin and vap-33 and many components of membrane vesicles (e.g. COPI complex). A third complex is centered around regulatory components of the proteasome (Runs) and a potential fourth complex is connected to actin containing Annexins (Chapter 3- Figure 13).

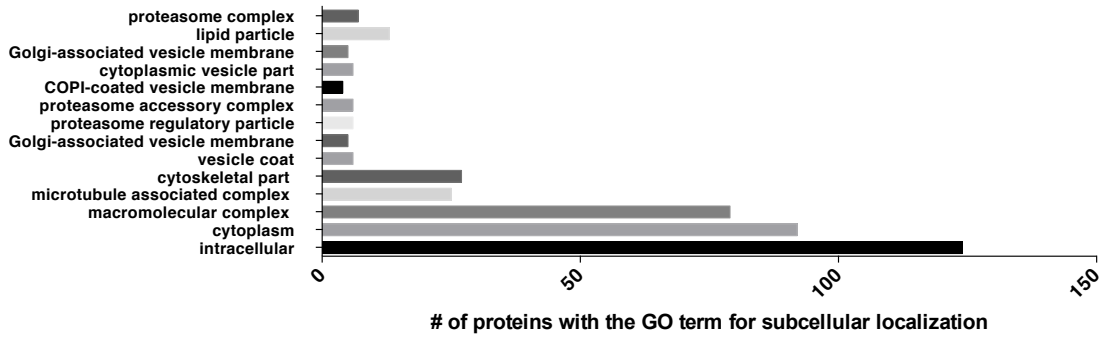

CHAPTER 3- FIGURE 12. **GO-TERM ANALYSIS OF 163 PROTEINS IDENTIFIED AS POTENTIAL BINDING PARTNERS OF THE DSCAM1 CYTOPLASMIC DOMAIN.**

Listed are most of the significantly enriched Go-terms for subcellular localization obtained by Flymine analysis. The bar represents the number of the 163 identified proteins linked to a given term. (One protein can be assigned to more than one term). Note the high representation of GO-terms associated with membrane vesicles and cytoskeleton. Significance was set at a max. p-value of 0.05 in a Holm-Bonfenorri test and the data was compared to the default Flymine dataset.

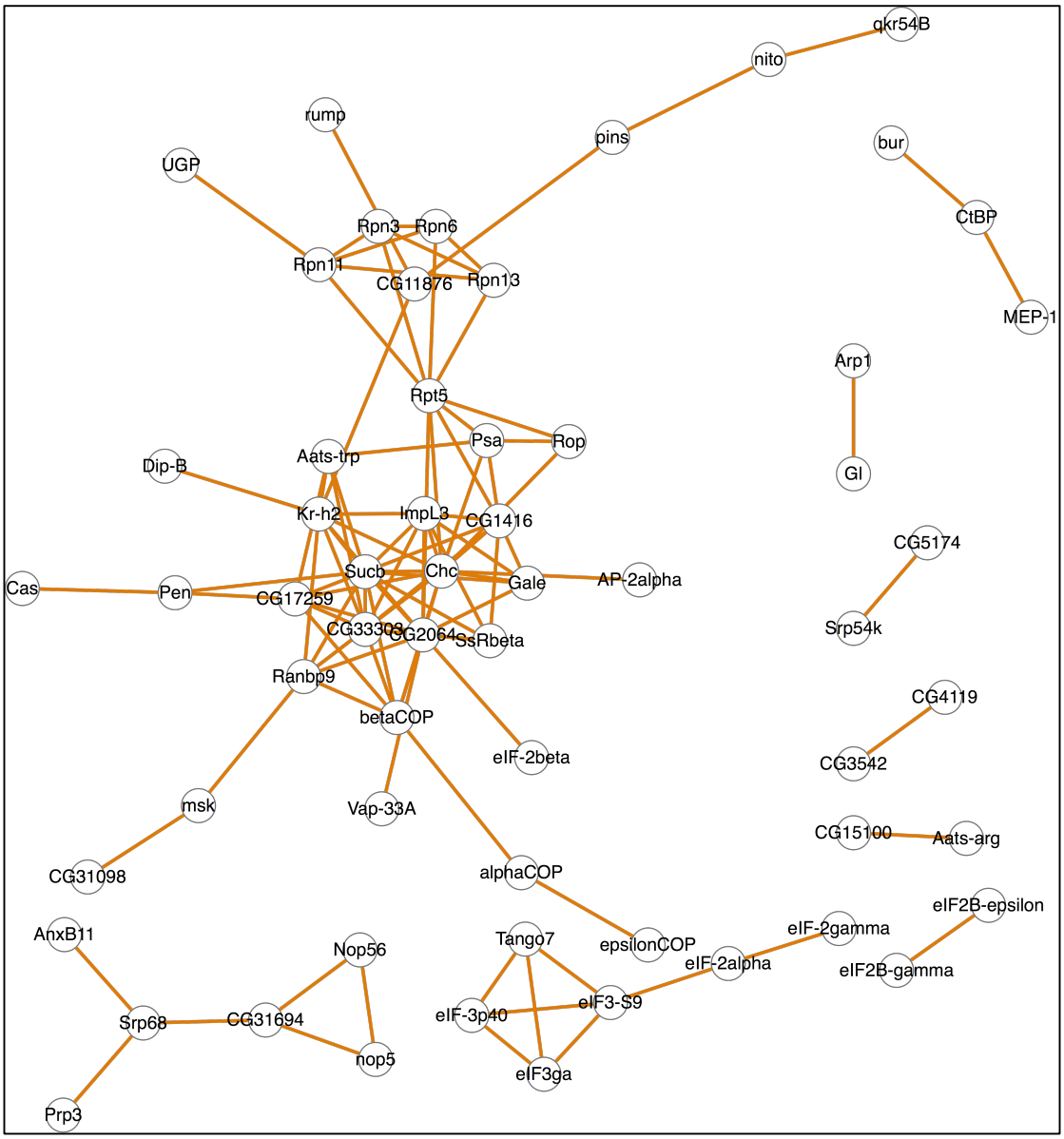

CHAPTER 3- FIGURE 13. **NETWORK ANALYSIS OF ALL PROTEINS DETECTED IN THE DSCAM1 CYTOPLASMIC COMPLEX REVEALS AT LEAST 3 LARGE PROTEIN SUB-COMPLEXES.**

The 163 proteins identified by mass-spectrometry based fingerprinting analysis of a Flag-purification of the Dscam1 cytoplasmic domain in BG3C2 cells were analyzed by Flymine and EasyN network analysis. Orange lines represent physical interactions. The analysis suggests the presence of Dscam1 in at least three distinct protein complexes: The first complex is centered around translational initiation factors (eIF3 and eIF2). A second very large complex contains several amino-acyl-tRNA synthetases as well as kinesin and vap-33 and many components of membrane vesicles (e.g. COPI complex). A third complex is centered around regulatory components of the proteasome (Runs) and a potential fourth complex is connected to actin containing Annexins.

Chapter 3- DISCUSSION

In this chapter I am reporting the combinatorial use of proteomic experiments aimed at resolving the Dscam1 signaling complex. Both, the proteomic data as well as a complementary sequence analysis searching for linear signaling motifs, point towards a direct physical interaction of the Dscam1 cytoplasmic domain with components of the ***translational machinery***, the ***cytoskeleton*** as well as the ***endomembrane system***. The proteomic analysis of tyrosine-phosphorylated proteins affected by Met-Dscam1 signaling clearly demonstrates an important role of tyrosine signaling for the Dscam1 pathway. In order to structure the discussion of my results, I am discussing my results in five distinct sub-chapters focused on: (1) ***Dscam1 signaling and translational regulation;*** (2) ***Dscam1 signaling to the cytoskeleton;*** (3) ***Dscam1 signaling and the endomembrane system;*** (4) ***Dscam1 signaling and tyrosine phosphorylation***; (5) ***unexpected new Dscam1 signaling targets.***

1. Dscam1 signaling and translational regulation

Dscam1 is a potential translational regulator and possibly directly recruits the translation initiation complex to the membrane

Components of the translational machinery are the most prominent Dscam1 signaling targets identified by the screens reported in this chapter. Both, the sequence analysis of signaling motifs in the intracellular domain and the purification of the Dscam1 signaling complex in neuronal BG3C2 cells point towards a direct physical interaction of the Dscam1 receptor with the translational machinery, especially the components of the translation initiation complex.

The observed interaction was not entirely surprising since regulation of Dscam1 signaling by the FMRP and DLK pathway have been reported recently. However, there is an important difference between the data presented in this dissertation and earlier published data regarding Dscam1 and translation in which both FMRP and DLK are proposed to act as *upstream regulatory elements* of Dscam1 expression and function (Cvetkovska et al., 2013; Kim et al., 2013). As opposed to previous studies, my data clearly suggests that the

interaction of Dscam1 with the local growth cone translational machinery does not solely occur on an mRNA level but more directly on a ***protein-protein level***.

Specifically, I would like to propose that Dscam1 interacts with the RNA unwinding eIF4F subunit. The eIF4F subunit refers to a complex formed by the three eIF4 translation initiation factors eIF4A, eIF4G and eIF4E. All three elongation factors belong to the family of RNA binding proteins. (Lasko, 2000). The scaffolding protein eIF4G and the DEAD box helicase eIF4A bind to each other (Hernández et al., 2004). Together with eIF4E, they form the ***eIF4F unit***, which unwinds RNA allowing the binding of the 40S ribosomal complex to the 5' cap of an mRNA (Hernández et al., 1998; 2004; 2005). This process might also involve ***eIF3 proteins***, which I interestingly also found to be affected by Met-Dscam1 signaling and as present in the Dscam1 signaling complex. The formation of the eIF4F complex is regulated by accessory proteins, such as 4E-binding proteins (4E-BPs) or Fmr1. This regulation often involves competition for the binding sites in eIF4E or eIF4G respectively (Papoulas et al., 2010).

Therefore, I find it notable that ***Fmr1*** (CG6203) was also among the strongly regulated proteins in my iTRAQ experiments (iTRAQ1). The Fmr1 signal was significantly upregulated upon overexpression and ligand addition to S2 cells expressing Met-Dscam1 receptor (Chapter 3-Table 9). Fmr1 mediated regulation of local protein translation is important for correct axon-guidance, -extension, -terminal arborization and -branching (Schenck et al., 2003; Cvetkovska et al., 2013; Kim et al., 2013; Morales et al., 2002). Fmr1 physically interacts with *Dscam1*-mRNA, a property critical for proper axon-arbor formation (Cvetkovska et al., 2013; Kim et al., 2013). Interestingly, Fmr1 has also been implicated in ***Sra-1*** mediated signaling transduction during axon guidance and synaptogenesis (Schenck et al., 2003). Sra-1, also known as CYFIP1 in vertebrates, was fingerprinted with high confidence (46 peptides) as belonging to a tyrosine phosphorylated protein-complex (Band E) only present in the absence of HGF (Chapter 3- Table 6). The observation that Fmr-1 is strongly upregulated upon ligand addition, while the Sra-1 signal disappears at the same time is intriguing and fits the known opposing roles of both proteins during axon guidance.

In summary, my data strongly supports the notion that Dscam1 interacts with components of the translation initiation machinery, specifically the ***eIF4F subunit*** necessary to unwind mRNA in order to allow ribosomes to bind to the target sequence. The wealth of

translational components identified not only in my purifications of the cytoplasmic domain but also in the phosphor-proteomic data suggests that in response to Dscam1 activation, mRNAs and the accompanying translational factors are recruited to the membrane, ***possibly via a direct binding site*** in the Dscam1 intracellular domain. Noticeably, translational components were identified in both proteomic experiments derived from ***hemocyte-like S2*** and ***neuronal BG3C2*** cells, suggesting that the interaction of Dscam1 with the translational machinery is not restricted to neuronal cells but might also play a role in immune cells, for example during phagocytosis.

Even though it is commonly accepted that axon guidance receptors affect the translation of locally stored mRNAs at the tip of growing neurites (Sutton and Schuman, 2006; Lin and Holt, 2008; Rodriguez et al., 2008; St Johnston, 2005), it has remained an open question, how this interaction is spatially regulated. In most cases it has been assumed that the link between guidance receptor and translational machinery is mediated via the cytoskeleton. A recent paper from the Holt laboratory just demonstrated that this is indeed the case: Netrin induced local protein synthesis is affected by both the presence of F-actin and of microtubules (Piper et al., 2015).

However, an alternative and shorter route of action has been proposed by the Flanagan lab: The guidance receptor DCC can recruit the translational machinery directly to the cytoplasmic domain, thereby affecting local translation specifically at hotspots of receptor activation (Tcherkezian et al., 2010). This model is extremely intriguing, because it allows for very specific spatial fine-tuning of protein expression. This might especially be interesting in such contexts of the Dscam1 receptor, which need to be tightly regulated in order to allow for correct neurite patterning.

Therefore, the physical link of the Dscam1 receptor to the translational machinery described above, would very locally affect translation, for example in specific growth cone filopodia. Importantly, the interaction with Fmr1 suggests an elegant ***novel auto-regulatory feedback mechanism***: Dscam1 translation is not just repressed by FMRP but the inhibition can also locally be regulated at the sites of Dscam1 activation, thereby providing a local and very specific signal to change Dscam1-expression with important consequences for the retraction-sensitivity of an axonal sub-compartment.

2. Dscam1 signaling to the cytoskeleton

Dscam1 affects the cytoskeleton via actin binding proteins

Axon guidance receptors signal to the actin cytoskeleton in order to affect neurite outgrowth, turning and branching. However, the exact molecular link to the cytoskeleton remains often unclear. In the case of the Dscam1 receptor, it has been proposed that the connection to cytoskeletal dynamics is mediated by the adaptor protein dock recruiting Pak kinase and small Ras-family-GTPases to the membrane (Schmucker et al., 2000). Small GTPases usually regulate the activity of actin cytoskeleton modifiers), such as the Arp2/3 complex or cofilin (reviewed in Hall and Lalli, 2010 and Heasman and Ridley, 2008). While Pak kinase is important for axonal targeting of Bolwigs nerve, it is dispensable for Dscam1 mediated dendrite self-repulsion (Hughes et al., 2007), suggesting that there might be context-specific distinct molecular mediators between Dscam1 and the cytoskeleton.

My proteomic analysis revels that Dscam1 interacts in S2 cells and in neuronal BG3C2 cells with the actin cytoskeleton. Important proteins identified as potential Dscam1 signaling targets are: ***Alpha-Spectrin*** (CG1977), ***Septin-1*** (*CG1403)***,*** ***Abl*** (CG4032), ***Elongation factor 1α48D*** (CG8280), ***Flightless*** (*CG1484, vilin*), ***Cheerio*** (Filamin, CG3937), the non-muscle myosin ***jaguar*** (CG5695), the ***Annexins B9 and B11*** (*CG5730***,** CG9968) and ***cindr*** (CG31012).

Most of these proteins belong to the large and conserved family of ***actin binding proteins*** (ABPs). These flexible molecules are characterized by the presence of one or more distinct actin binding sites and motifs, which can be distributed over the entire range of the often long proteins. ABPs are instrumental in regulating the mobility of the growth cone and therefore indispensable for axon guidance and branching (Bilimoria and Bonni, 2013). Indeed, some of the earliest studies of axonal branching in cell culture already demonstrate the importance of actin as signaling effector during NGF induced axonal branching of DRG neurons (reviewed in Bilimoria and Bonni, 2013; Pak et al., 2008). Therefore, actin binding proteins can be understood as the ultimate and central regulators of the structures formed by microfilaments: Some of them bundle filaments into fibers typically found in filopodia, while others crosslink the actin cytoskeleton in to mesh- or gel-like structures, thereby regulating the stiffness and speed of streaming in sub-compartments of the cytoplasm (Pak et al., 2008). At the synapse, the ABPs in pre- and post-synaptic compartments regulate the

availability and recycling of synaptic vesicles (Rust, 2015). Finally, ABPs also represent core components of cell adhesion sites, linking transmembrane receptors to the cytoskeleton, thereby mediating affinity to the extracellular matrix and other cells. This is an important aspect of developing traction for the directed movements of mobile cellular compartments, such as growth cones. In addition, ABPs are also critical for the motility of hemocytes and for the formation of membrane protrusions appearing during the phagocytosis of pathogens (Freeman and Grinstein, 2014; Le Floc'h and Huse, 2015).

Interestingly, several subclasses of ABPs are affected by Dscam1 signaling. This suggests that Dscam1 might exert differential effects based on the ABPs available in distinct cellular sub-compartments. Further studies will be needed to evaluate if and how these proteins are linked to Dscam1 function *in vivo*. Disappointingly, RNAi based knockdown of my cytoskeletal Dscam1 signaling candidates has not caused any striking phenotypes in the patterning of ms-neurons thus far (Dan Dascenco, personal communication). This fact, together with the observation that several actin binding proteins have been identified in my biochemical screen suggest, that strong compensatory mechanisms might be in place, allowing the neuron to pattern correctly even in absence of a specific ABP. For example, there are four paralogues of alpha-spectrin, one paralogue for EF1-alpha, three for flightless and two for cheerio, suggesting that more sophisticated genetic analysis will be necessary in the future to understand how Dscam1 regulates the activity of the actin cytoskeleton in a specific context.

Alpha-spectrin is a Dscam1 interactor identified with high confidence

Of the actin binding proteins identified above, I would like to emphasize ***alpha-spectrin*** (CG1977): Alpha-Spectrin is a rod-shaped molecule with one SH3-domain, capable of actin- and microtubule-binding (Sisson et al., 2000; Röper et al., 2002). Generally, multi-units of spectrins serve as linkers between transmembrane-receptors and the cytoskeleton in a submembraneous mesh described as the "cortical spectrin-network" (Dent et al., 2011; Röper et al., 2002). Such networks are prominent components of the molecular machinery ***at the base of filopodia*** (Gallo, 2013).

In my iTRAQ experiments aimed at identifying tyrosine phosphorylated proteins that are regulated upon activation of the chimeric Met-Dscam1 receptor, alpha-spectrin was one of

the top hits. The iTRAQ signal was almost 30x upregulated upon addition of ligand to the Met-Dscam1 receptor (Chapter 3-Table 9). In my Flag-based purification of the Dscam1 cytoplasmic domain from BG3C2 cells however, I did not detect alpha-spectrin. On the other hand, I observed that the physical interact or ***Chc*** (CG31349) was present Chapter 3-Table 14.

Interestingly, alpha-spectrin has been linked to Dscam1 signaling in a previous proteomic approach aiming at the purification of the Dscam1 signaling complex in S2 cells (Dissertation Michael Hughes, Harvard University 2007). During this set of experiments, it was shown that ***alpha- but not beta-spectrin*** binds in a tissue specific manner to the Dscam1 cytoplasmic domain. Furthermore, it was reported that ***RNAi mediated alpha-spectrin loss of function resembles Dscam1 gain of function in dendrites of multidendritic neurons*** (Dissertation Michael Hughes, Harvard University 2007). Furthermore, the spectrin interacting protein Chc was also detected in Michael Hughes' proteomic screen as part of the Dscam1 signaling complex.

Taken together, it enhances my confidence in the proteomic data reported above, that there is significant overlap between my own proteomic experiments and others. Not ***only alpha-spectrin,*** but also its physical interact or ***Chc*** and the protein ***EF1alpha48A*** are actin interactors identified in independent set of experiments. While the loss of function phenotype reported by Michael Hughes in multidendritic neurons is encouraging, it remains to be seen in the future if and how alpha-spectrin affects Dscam1 regulated axonal branching and guidance, especially because thus far only beta- and not alpha-spectrins have been implicated in neurite guidance decisions.

Dscam1 interacts with components of the SCAR/WAVE complex: Hem (Kette)

Two proteins identified in this experiment belong to the SCAR/WAVE complex: ***Hem*** (CG5837, kette) ***and Sra-1*** (CG4931, specifically Rac1-associated protein 1). I have discussed Sra-1 already in the paragraph dedicated to translational regulators. Therefore, I will focus this subchapter on Hem protein and the SCAR/WAVE complex.

The adaptor protein Hem (also known as kette or Nck-adaptor protein1) belongs to a highly conserved protein family typically expressed in the nervous system and in hematopoietic cells (Baumgartner et al., 1995). There are two *Hem* orthologues in humans but no

paralogues in *Drosophila.* Hem expression is ***strictly regulated*** with broad (maternal) expression detectable early during development and a spatially restricted expression pattern specific to the nervous system in later stages (Baumgartner et al., 1995).

Normally, Hem is found close to the membrane. It binds F-actin especially in ***lamellipodia***. Hem is involved in neuronal migration (Zhu and Bhat, 2011) as well as phagocytosis (Stroschein-Stevenson et al., 2005). In hemocytes, Hem is found predominantly in the cytosol even though it has six trans-membrane domains (Bogdan and Klämbt, 2003). Notable interaction partners of Hem are: ***Abl*** (Ku et al., 2009; Zhu and Bhat, 2011), ***dock*** (Hummel et al., 2003), ***PTP61F*** (Ku et al., 2009), ***Rac1*** (Hummel et al., 2000), ***Wasp*** (Bogdan and Klämbt, 2003; Bogdan et al., 2005; Schäfer et al., 2007), ***Fmr-1*** (Schenck et al., 2004) and ***Sra-1*** (Bogdan et al., 2004). This places Hem-protein in the middle of a number of known and potential Dscam1-interactants.

We identified *5 unique* peptides for Hem in band D (Chapter 3- Table 5) of my first silver gel. According to this result, Hem protein is part of a tyrosine phosphorylated protein-complex that is present in the presence of Met-Dscam1 chimeric receptor in S2 cells. Interestingly, we also identified Hem-protein as a strongly regulated target in the *second iTRAQ experiment.* This experiment was conducted with the 17.2 isoform of the chimeric receptor. We identified *9 unique peptides* characteristic for Hem (Chapter 3- Table 10 and Chapter 3- Table 11). The quantification of peptides suggests that overexpression of chimeric Met-Dscam1 leads to a reduced signal of a Hem-containing complex. Addition of the Met-Dscam1 ligand HGF leads to further strong reduction of the signal (Chapter 3- Table 11). Hem belongs also to and is a negative regulator of the pentameric ***SCAR/WAVE*** complex consisting of the following five components:

(1) SRA1 (also known as CYFIP1) or CYFIP2 (also known as p53-inducible protein 121 (PIR121) (fly homologue Sra-1 or CG4931)
(2) NCK associated protein 1 (NAP1) or its paralogue HEM1 (fly homologue Nap1 (CG5330) and Hem/Kette (CG5837))
(3) A nucleation promoting factor: WAVE1, WAVE2 or WAVE3 (fly homologue SCAR)
(4) Abl interact or 1 (ABI1), ABI2 or ABI3 (fly homologue Abi or CG9749)
(5) HSPC300 (also known as BRICK1) (fly homologue HSPC300 or CG30173)

The SCAR/WAVE complex is important for the initiation of actin filaments, a process known as actin nucleation. The complex is by default inactive but gets upon recruitment to actin activated. There are several distinct activation modes mediated by different classes of molecules, such as small GTPases, acidic phospholipids, kinases and clathrin-heavy-chain. In the context of this dissertation, the activation of the WAVE complex by tyrosine phosphorylation might be the most interesting (Mendoza, 2013). Such activation is typical for the ***lamellipodial edge***.

Of the other components in the SCAR/WAVE complex, we identified ***Sra-1*** (CG4931) with *46 peptides* in *band E* of the first silver gel (Chapter 3- Table 6). This means that Sra-1 is potentially part of a tyrosine phosphorylated protein-complex in S2 cells, which we enriched in our phosphor-tyrosine Ips. However, despite the good signal obtained in the IP we did not detect Sra-1 in any of our iTRAQ experiments, suggesting that either the detection threshold of the iTRAQ was too low (which is definitely the case in the first experiment), or that it is masked by other more prominent proteins that are regulated upon Met-Dscam1 expression and activation. Therefore, I cannot make any further conclusion regarding Sra-1 regulation.

Hem protein is also known to activate F-actin formation via Wasp (Bogdan and Klämbt, 2003). This is important for the formation of F-actin rich ***microspikes.*** It remains to be seen in the future, which aspect of Hem is important for Dscam1-function *in vivo*. RNAi mediated loss of Hem-function has resulted only in mild phenotypes in the axonal arborizations of ms-neurons (Dan Dascenco, personal communication). However, the terminal arborization and synapses of ms-neurons at the midline might be affected by loss of Hem (Olivier Urwyler, personal communication), suggesting that a more sophisticated analysis of Hem-Dscam1 interaction in the future might be rewarding.

Dscam1 interacts with the tubulin cytoskeleton

Vertebrate DSCAM has been shown to bind to polymerized tubulin in a Netrin dependent manner (Huang et al., 2015). This interaction lasts up to 20 min in cultured cortical neurons. It is dependent on Src kinases and important for the branch promoting function of DSCAM (Huang et al., 2015). The invertebrate orthologues of TUBB3 are ***betaTub56D***, ***betaTub60D***, ***betaTub85D***, ***betaTub97EF***. While no direct interaction of Dscam1 with tubulins has been reported as of yet, it has been reported that the Dscam1 intracellular

domain interacts directly with ***TBC-protein***, a co-factor important for the formation of alpha- and beta-tubulin heterodimers (Okumura et al., 2015). This interaction is required during the development of axonal and dendritic projections in olfactory neurons and mushroombody neurons (Okumura et al., 2015).

Interestingly, I identified ***betaTub*** in both of my iTRAQ experiments as significantly ***upregulated upon chimeric receptor expression and activation***. While the first iTRAQ experiment led solely to the identification of one signature peptide, I had four of them present in the second more efficient experiment, increasing my confidence in the result. The identified peptides were not sufficient to distinguish between the two beta tubulins ***56D and 85D***. (CG9277 and CG9359 respectively). Hence, it is very likely that at least one of them is present in the Dscam1 signaling complex. Further experiments are needed to validate and dissect this result.

My confidence in the notion that Dscam1 might interact with the tubulin cytoskeleton is enhanced by the fact that I purified the following 11 microtubule binding proteins together with the Dscam1 cytoplasmic domain: ***Rpn6*** (CG10149), ***CG10932 and its paralogue yip2*** (CG4600), ***Nc73EF*** (CG11661), ***ALiX*** (CG12876), ***Klp10A*** (CG1453), ***ens*** (CG14998), ***CG15100, gammaTub37C*** (CG17566), ***Rpn11*** (CG18174), ***chb*** (CG32435).

In addition, Michael Hughes reported tubulin as a potential binding partner of the Dscam1 receptor identified via large scale purifications of endogenous Dscam1 from adult fly heads and S2 cells (Dissertation Michael Hughes, Harvard University 2007).

In line with my hypothesis that Dscam1 might be of significance for the regulation of stabilized microtubules, I observed a punctate Dscam1 staining in *Drosophila* BG3C2 showing partial overlap with tubulin counter-staining (Chapter 3- Figure 14).

Taken together, the ***presence in two independent iTRAQ experiments*** as well as the identification of ***several microtubule binding proteins*** in the Dscam1 complex and the ***overlap with the published results*** for vertebrate DSCAM, make it very likely that *Drosophila* Dscam1 recruits polymerized tubulin to the cell surface upon signal- activation. This might be an important aspect for stabilizing filopodia, for example during axonal branching. Additional experiments are needed in the future, to fully understand the functional significance *in vivo*.

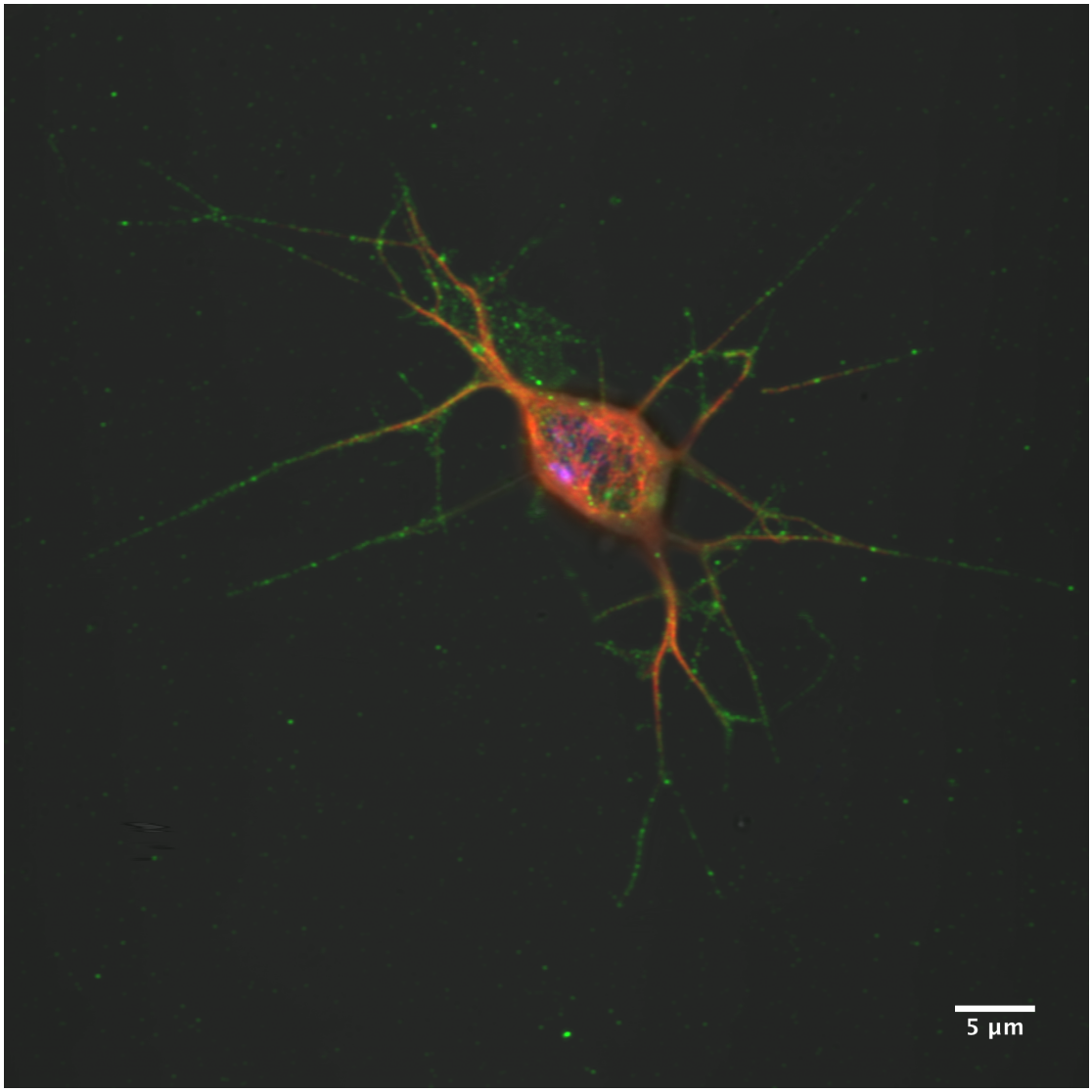

CHAPTER 3- FIGURE 14. **DSCAM1 CO-LOCALIZES PARTIALLY WITH TUBULIN.**

Red: Staining with anti-tubulin antibody; green: staining with anti-Dscam1 intracellular domain antibody (357). Note the linear arrangement of Dscam1 punctate along the neurites. Depicted is a BG3C2 cell differentiated on laminin for two days.

3. Dscam1 signaling and the endomembrane system

The candidate ***Chc*** (CG9012), identified in both of my own proteomic approaches as well as in the purification experiments conducted by Michael Hughes (Dissertation Michael Hughes, Harvard University 2007), links the Dscam1 receptor furthermore to the endomembrane system.

In addition to chc, I detected the following proteins linking Dscam1 to the endomembrane: ***The COP proteins*** (alpha, beta and delta and epsilon) (CG14813, CG6699, CG9543, CG7961) ***Rop*** (Ras-opposite, CG15811), ***Ap2-alpha*** (CG4260).

Receptor mediated endocytosis is an important way of modifying the amount of a guidance receptor present on the surface (reviewed in Bashaw and Klein, 2010). It is for example critical for the adaption of growth cones to guidance cues, fine-tuning the extend of a receptor signaling response. Fast desensitizing by removal of receptors via endocytosis is counterbalanced by a protein synthesis dependent re-equipment of the membrane. In Ephrin-Eph signaling, proteolytic cleavage coupled to endocytosis is indispensable for cell detachment and repulsion. Furthermore, mRNAs are shuttled between neuronal sub-compartments via COPI transport- complexes of vesicles containing FMRP (Todd et al., 2013).

Overall, I find it interesting that we observed a number of different vesicle associated proteins in the Dscam1 signaling complex. This could be important for a Dscam1-signaling model, in which the Dscam1 receptor is cleaved and endocytosed upon ligand binding in a manner similar to Eph-Ephrin receptor signaling**.** *Such a model would explain, how the strong homophilic adhesion observed in biochemical experiments in vitro is translated into a repulsive neurite response in vivo.* This hypothesis is supported by the cleavage of all my Dscam1 expression constructs (cDNA, genomic and chimeric receptor, tagged and untagged), whenever we expressed and immunoprecipitated them (data not shown). I tried to inhibit the cleavage in cell culture by means of different types of protease inhibitors but I was not able to obtain a convincing effect. Therefore, the class of proteases responsible for Dscam1 cleavage remains unknown.

However, the identification of different candidate proteases, such as ***Usp16-45*** (CG4165) and ***Regulatory particle triple-A ATPase 2*** (CG5289) might allow in the future for a more targeted RNAi approach *in vivo* and *in vitro*. It will be interesting to see if these specific

proteases also have roles in axon guidance. As of today, they only have been implicated been in the innate immune response of *Drosophila*.

In addition, I find it striking that we observe a potential link of the Dscam1 receptor not only to the endocytosis machinery but also to the translational machinery. In *Xenopus* it has been demonstrated that the sensitivity of growth cones to guidance cues is tightly regulated: Receptor mediated endocytosis removes activated receptors quickly from the membrane, stopping thereby the sensitivity for a certain guidance cue in the short term. Following a pause, the cone regains sensitivity by replacing the receptors in a protein synthesis dependent step. We have shown that Dscam1 signaling is extraordinarily sensitive to alterations of signal intensity (Dascenco and Erfurth et al., 2015; He et al., 2014a). The sensitivity of an axonal growth cone is defined by an intrinsic threshold depending on the number of Dscam1 isoforms present within a cell (He et al., 2014a), but depends also on the tyrosine phosphorylation status which can be dynamically regulated during development (Dascenco and Erfurth et al., 2015). Regulation of the growth cone sensitivity via Dscam1 receptor endocytosis would add another layer of control to the system, explaining for example why the anterior branches of the ms-neurons are stronger affected by Dscam1 hyper-activation than the posterior branches: Posterior branches are further away from the Dscam1 signaling hot-spot at the VNC entry point of the ms-axon, allowing the system to recover and reset.

4. Kinases and phosphatases interacting with Dscam1

We and others have shown that regulated phosphorylation is critical during Dscam1 signaling (Dascenco and Erfurth et al., 2015; Schmucker et al., 2000). In addition to the known kinases and phosphatases affected by Dscam1 signaling, I have also identified the following kinases and phosphatases as potential Dscam1 interactors: ***Pak3*** (*CG14895)*, ***Pvr*** (CG8222), ***Pfk*** (CG4001), ***Pi4KIIalpha*** (CG2929), ***PTP61F*** (CG9181).

The interaction between the Dscam1 receptor and the RTK Pvr is conserved between vertebrates and invertebrates

The receptor tyrosine kinase ***Pvr*** (CG8222) is the invertebrate orthologue of the two vertebrate receptors VEGFR and PDGFR. There is another paralogue annotated as ***CG3277***, belonging to the same protein family of "*split kinases* ". Pvr plays a role in cell migration (Bunt et al., 2010; Cho et al., 2002; Duchek et al., 2001; Mathieu et al., 2007; McDonald et al., 2006; Olofsson and Page, 2005; Wang et al., 2006), regulation of the actin cytoskeleton (Kiger et al., 2003), innate immunity (Kleino et al., 2005) and hemocyte development (Heino et al., 2001; Mondal et al., 2014; Tran et al., 2013; Zettervall et al., 2004). Virtually nothing is known regarding the orthologue CG3277. Pvr could be linked to known Dscam1 pathway interactors through its interaction with the adaptor protein ***dock***. In addition, Pvr is regulated by ***tyrosine phosphorylation***.

Here we report for the first time, an ***interaction between Dscam1 signaling and Pvr***. Based on the identification of Pvr as a protein which is part of tyrosine phosphorylated signaling complexes affected by Dscam1 signaling, we probed the interaction further. We found that endogenous Pvr physically interacts with Dscam1 in immunoprecipitations from lysates of BG3C2 cells (Chapter 3- Figure 15) expressing the chimeric Met-Dscam1 receptor or full length Dscam1. The binding to the Met-Dscam1 chimeric receptor was unaffected by addition of HGF to the cell culture medium. The RNAi mediated knockdown phenotype of *Pvr* in mechanosensory neurons is subtle (Derya Ayaz, unpublished data) and characterized by only mild growth defects in the terminal arborizations similar to the Fmr1 phenotypes reported by Cvetkovska et al., 2013.

Importantly, we found the interaction between Pvr and Dscam to be conserved between vertebrates and invertebrates. ***Vertebrate Flk1 receptor is capable of physical interacting with overexpressed vertebrate DSCAM*** in HEK-293 cells (Chapter 3- Figure 15) (Antheneh Argaw and Maria-Luise Erfurth, unpublished data). This was also noticed in primary cortical cells isolated from mouse embryos, where ***the interaction is weakened in the presence of VEGF*** (Antheneh Argaw, unpublished data).

Finally, I identified four motifs in the extracellular domain of DSCAM which resemble a ***VEGFR fingerprint*** (Chapter 3- Figure 16). These motifs are highly conserved (Chapter 3- Figure 17), suggesting that the DSCAM extracellular domain might be capable of interacting with VEGF. In addition, AP-tagged VEGF binds to DSCAM expressed in HEK-

293 cells in cell overlay assays (Anteneh Argaw, Carmen de Almodovar and Cathy Coulon; unpublished data). However, the interaction seems to be less robust than the interaction with Flk1.

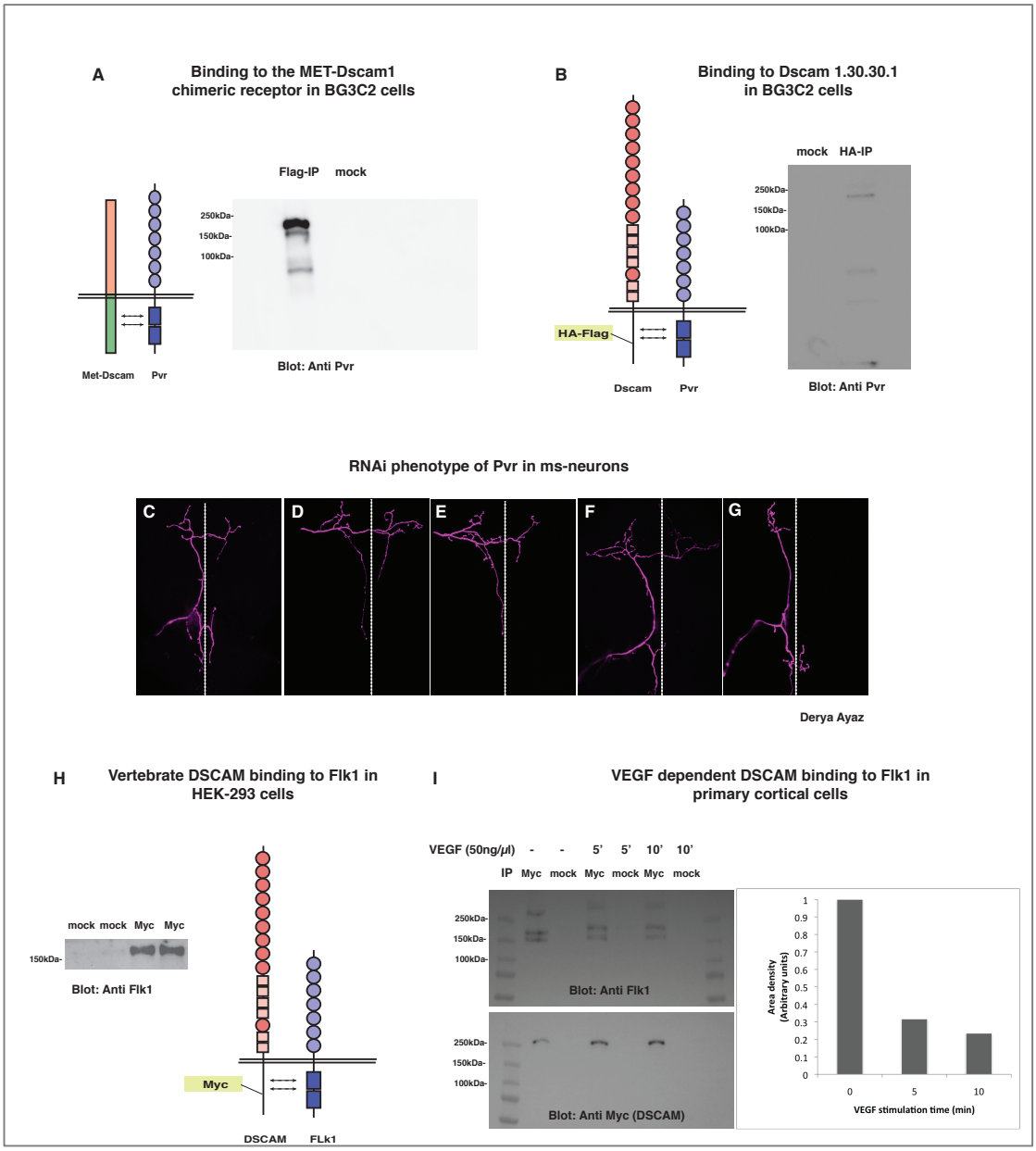

CHAPTER 3- FIGURE 15. **INTERACTION BETWEEN PVR AND DSCAM.**

(A) Endogenous Pvr can be detected in anti-Flag-immunoprecipitation of the chimeric Met-Dscam1 receptor in lysates of BG3C2 cells. (B) Endogenous Pvr can be detected in anti HA-Immunoprecipitation of full length Dscam1 receptor (isoform 1.30.30.1) expressed in BG3C2 cells. (C-G) RNAi phenotype of Pvr in pSC neurons. The core pattern is mostly unaffected. However, the terminal arborizations show abnormalities. (C) Normal (WT) pattern. (D-G) Abnormal arborization pattern. (H) Endogenous Flk1 can be detected in anti Myc-immunoprecipitation of vertebrate DSCAM receptor in lysates of HEK-293 cells. (I) DSCAM-FLK1-binding is dependent on the presence of VEGF (panel obtained from Anteneh Argaw).

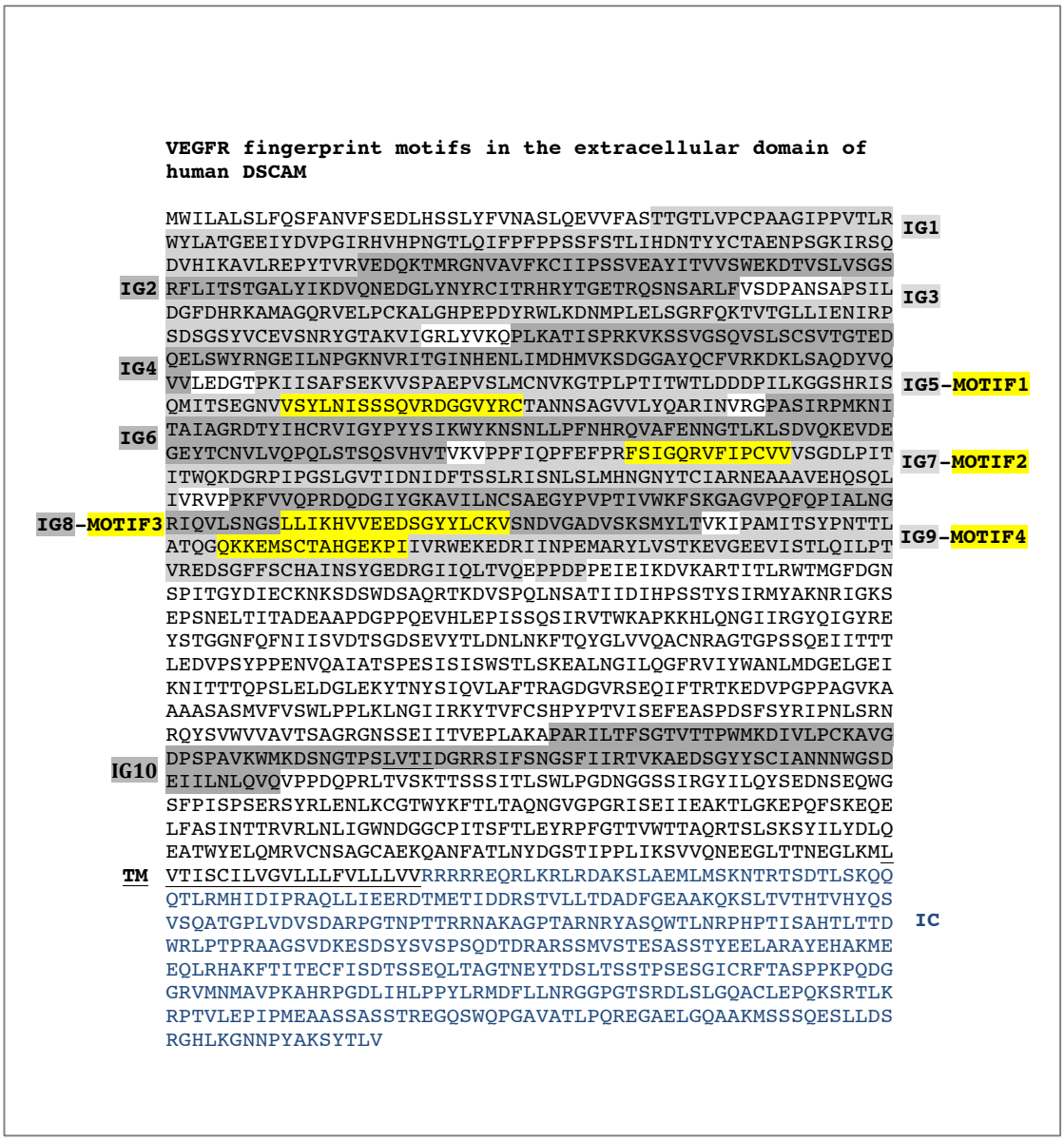

CHAPTER 3- FIGURE 16. **THE DSCAM EXTRACELLULAR DOMAIN CONTAINS REGIONS SIMILAR TO THE VEGFR FINGERPRINT.**

This fingerprint is an element that provides a signature typical for the vascular endothelial growth factor receptors. There are four motifs in the Dscam extracellular domain (yellow) which are highly conserved and which show high similarity to these fingerprint motifs. They are located in Ig 5,7,8 and 9. Grey: Ig-domains; underlined: Transmembrane domain (TM); blue: Intracellular domain (IC).

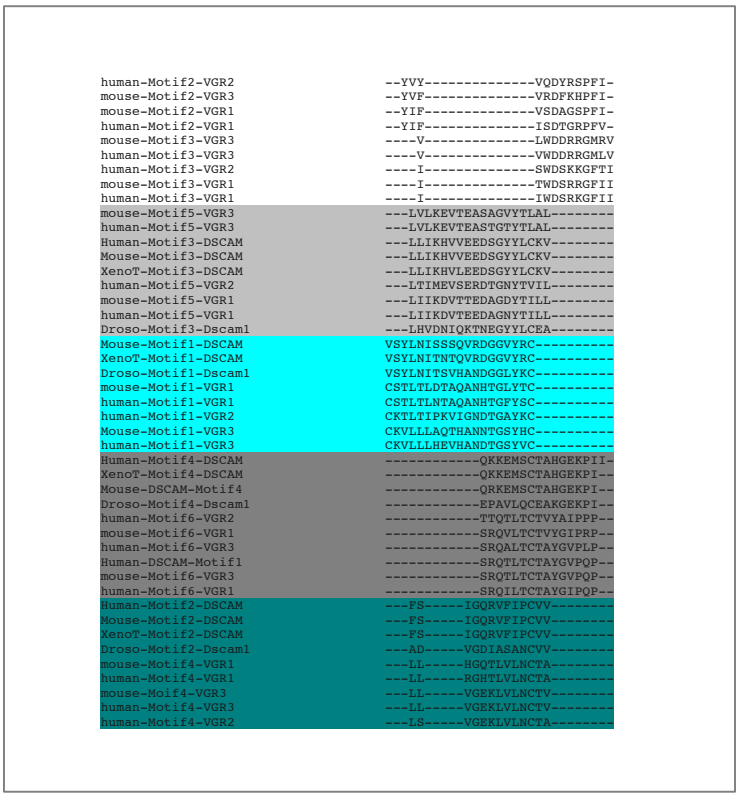

CHAPTER 3- FIGURE 17. **CLUSTAL OMEGA ALIGNMENT OF THE VEGFR FINGERPRINT MOTIFS IN DSCAM AND VEGFR.**

The four motifs predicted to be present in DSCAM have the highest similarity to the VEGFR fingerprint motifs 1 (light blue), 4 (green), 5 (light grey) and 6 (dark grey).

5. Other novel aspects regarding Dscam1 signaling

In addition to affecting local translation, the cytoskeleton and signaling pathways mediated by reversible tyrosine phosphorylation, I followed also up on two other novel aspects of Dscam1 signaling which I am going to present in the following sections dedicated to (A) Dscam1 interaction with the GEF sponge/DOCK4 and (B) the effect of Dscam1 signaling on the transcription of effector genes in the nucleus.

A. Dscam1 interacts with GTPase signaling by binding to the GEF Sponge/DOCK4

Several of the candidates identified in the proteomic screens point to a link between Dscam1 signaling and the ***signaling of Rho-GTPases***. We were especially interested in the GEF protein sponge, the invertebrate homologue of ***DOCK4/DOCK7*** proteins.

Sponge (CG31048) is an SH3 domain containing a GEF for the GTPases Rac or Rap. Sponge is a cytoplasmic protein found in membrane proximal compartments. It is involved in neuronal development (Biersmith et al., 2011) and differentiation (Eguchi et al., 2013). We found sponge in *band B* of my first silver gel in a fraction that was reduced/dephosphorylated upon ligand addition to the chimeric receptor (Chapter 3- Table 4). There were *six unique peptides*, which covered 4.2% of the entire amino acid sequence. We obtained antibody directed against the C-terminus of sponge from the ***Geisbrecht lab*** and could show that endogenous sponge protein ***binds to Met-Dscam1 in S2 cells and to full length Dscam1*** (isoform 1.30.30.1) ***in BG3C2 cells*** (Chapter 3- Figure 18). This interaction with the Met-Dscam1 receptor is activation dependent: Binding of sponge to the Met-Dscam1 chimeric receptor in the presence of HGF was slightly enhanced upon ligand addition (Quantified in Chapter 3- Figure 18). The RNAi phenotypes of sponge in mechanosensory neurons range from mild abnormalities in terminal arborizations to more *severe branching phenotypes with main branches of the core axonal pattern missing similar to a Dscam1 gain of function phenotype* (Derya Ayaz unpublished data). Further experiments will be needed in the future to understand the details and significance of this interaction.

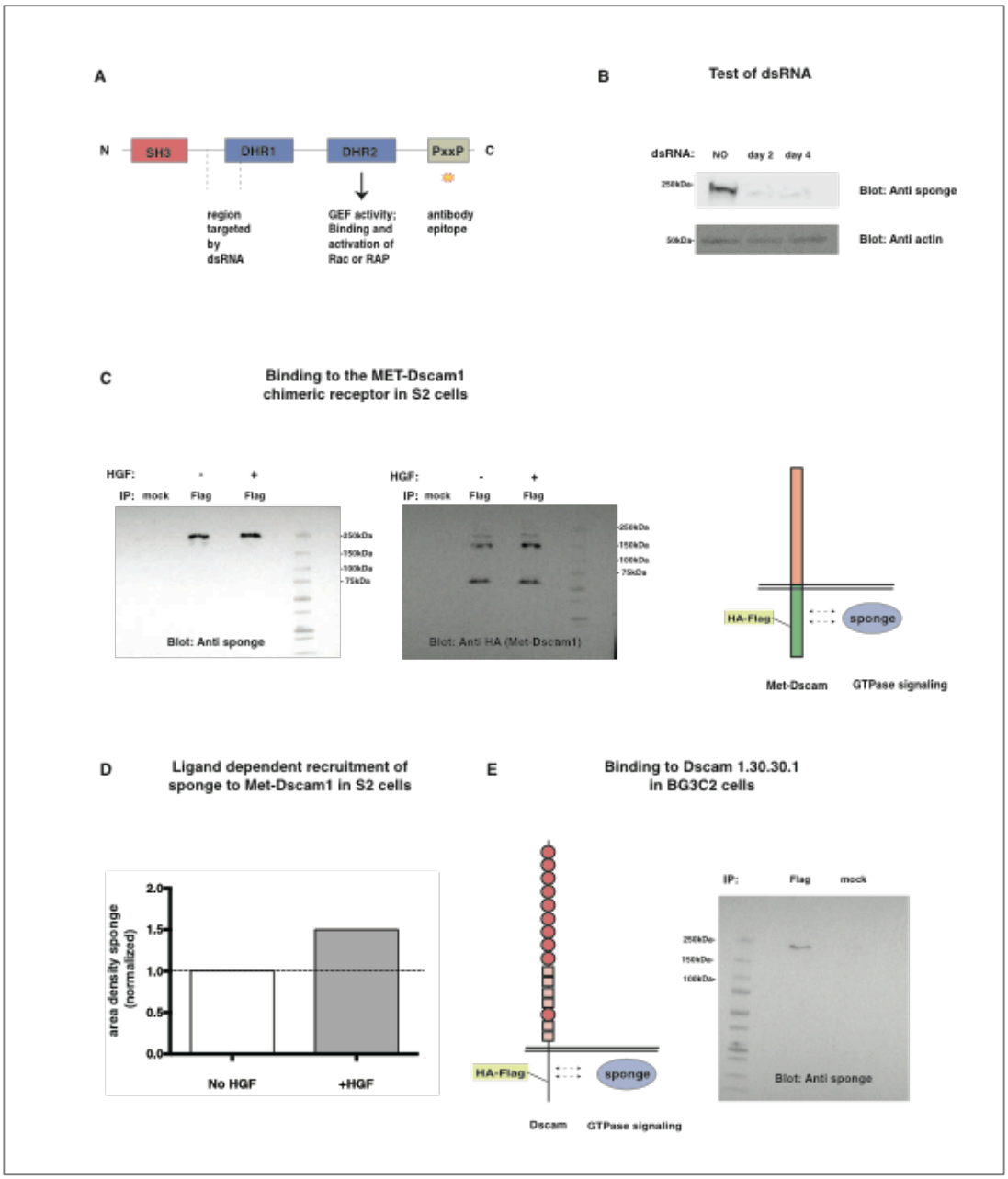

CHAPTER 3- FIGURE 18. **THE GEF SPONGE CAN BE FOUND IN THE DSCAM1-RECEPTOR COMPLEX.**

(A) Domain structure of the sponge protein. (B) Our dsRNA directed against sponge is specific. This test was important because there was some controversial sequence annotation on flybase at the time of performing these experiments. The antibody used was obtained from the Geisbrecht lab. (C) Sponge binds to the chimeric Met-Dscam1 receptor in S2 cells. Shown are immunoprecipitations of Met-Dscam1 via Ha-antibody. The blot was first developed with anti-sponge antibody, stripped, and then redeveloped with anti-Dscam1 antibody. (D) The interactions between Met-Dscam1 and sponge is activation dependent. Shown is the quantification of the area density of an immunoprecipitation based experiment as described under (C) in the presence and absence of the Met-Dscam1 ligand HGF. (E) Sponge binds to full length Dscam1 in BG3C2 cells. Shown is the immunoprecipitation of Dscam1 (Ha antibody) and the blot was developed with anti-sponge antibody.

B. Dscam1 surprisingly also interacts with transcriptional regulators

My sequence analysis of the Dscam1 intracellular domain suggests a potential physical interaction of the Dscam1 cytoplasmic domain with transcriptional activators, such as the protein Stat92E (CG4257). I identified two potential SH2-binding sites, which could facilitate such interaction (Y1691) and (Y1903).

Furthermore, I detected the transcription factor Stat92E as one protein belonging to a tyrosine phosphorylated signaling complex affected by overexpression of the chimeric Met-Dscam1 receptor (iTRAQ experiment 2, Chapter 3- Table 10).

Stat92E is a ***transcription factor.*** The protein also contains an *SH2 signaling-domain*, mediating cytoplasmic protein-protein interactions. Stat92E is involved in cell migration (Jang et al., 2009; Silver and Montell, 2001), hemocyte differentiation (Gao et al., 2009; Mondal et al., 2014), innate immunity (Avadhanula et al., 2009; Kim et al., 2007) and nervous system development (Li et al., 2003). The vertebrate orthologues of Stat92E are ***STAT6 and STAT5B***. Interestingly, there are at least four distinct isoforms of Stat92E: One long isoform is complemented by three shorter versions. Two of them lack either the very N-terminal or a small part of the sequence found in the longest isoform, while the last isoform is devoid of both variable regions. Stat92E can form homo- and heterodimers. Of the genetic interactions reported, ***Src42E and 64B***, ***PTP61F, Rac1***, ***csw*** and ***EGFR*** are notable because of their potential links to Dscam1 signaling.

Besides Stat92E we have identified ***two other transcriptional regulators*** in our proteomic experiments, namely the transcriptional corepressor ***groucho*** (CG8384) and the transcription elongation factor ***Spt5*** (CG7626).

A microarray study demonstrates that Dscam1 signaling affects transcription in S2 cells

Because there was little knowledge regarding Dscam1 signaling at the beginning of my PhD, I conducted several pilot experiments in order to understand how the receptor transmits its signal. Many signaling cascades convey the signal ultimately into the nucleus causing the expressional profile of a cell to change. This is often the case if the receptor is cleaved and an intracellular domain is translocated to the nucleus. Because of the long distance between the growth cone and the cell body, axon guidance receptors are classically

not thought to signal to the nucleus. However, it has recently been shown that some guidance receptors, such as DCC are capable of regulating transcription (Taniguchi et al., 2003). The Dscam1 receptor is proteolytically cleaved (Watson, 2005), suggesting that it might bear the capacity to transmit a signal away from the membrane. Furthermore, we identified a conserved potential Stat-binding site in the cytoplasmic domain of the intracellular domain. Additionally, we found importins and transcriptional regulators in the purifications of the Dscam1 cytoplasmic domain, further enhancing the notion that there might be a potential link to the nucleus. Therefore, I decided to conduct a microarray based preliminary experiment in order to investigate into the possibility that Dscam1 signals to the nucleus.

In order to study Dscam1 signaling and its effect on transcription, I utilized the chimeric Met-Dscam1 receptor with the transmembrane domain encoded by exon 17.1 (Cell line CG). I conducted the study in a S2 cell line stably expressing the chimeric receptor under control of a metallothionine inducible promoter. Therefore, I was able to profile three different basic conditions: I compared wild type cells with the effects of chimeric receptor expression and the effect exerted by activation of Met-Dscam1. In analogy to other microarray based expression studies regarding the innate immune response in *Drosophila* hemocytes (e.g. Boutros et al., 2002), I analyzed three distinct time points after ligand addition: ***20min, 2 hours and 6 hours***. I used "*Affymetrix Drosophila 2 expression arrays*". The goal of these experiments was to generally answer the question, if Dscam1-signaling could have any effect on transcription. There were two sets of experiments executed: One pilot experiment in May 2009 and another follow up in August 2009.

The analysis was conducted with the help of the ***Quackenbush lab*** (Dana-Farber Cancer Institute/ Harvard Medical School). The raw data of the assays was normalized with ***BIOTEQC*** and then further analyzed for visualization and statistical evaluation in *Multiexperiment Viewer* (MeV). We used *BETR* (Bayesian Estimation of Temporal Regulation) analysis to evaluate temporal regulation of transcription and found that the treatment with HGF leads to transcriptional changes with each of the time points representing an individual cluster in BETR. There were ***1249 significantly regulated genes*** (BETR: alpha=0.005) and ***GO term analysis with*** *EASE* resulted in the following top ten terms (sorted by probability scores):

#	Midgut development
1.	Octopamine Receptor Activity
2.	Defasciculation of Neuron
3.	G-protein Coupled Receptor Protein Signaling Pathway
4.	Proteasome Regulatory Particle, Base Subcomplex
5.	Regulation of Protein Catabolism
6.	Protein Hormone Receptor Activity
7.	Transmembrane Receptor Protein Tyrosine Phosphatase Activity
8.	Defasciculation of Motor Neuron

CHAPTER 3- TABLE 32. **TOP 10 GO TERMS ASSOCIATED WITH THE 1249 GENES REGULATED BY DSCAM1 SIGNALING.**

*The Go terms are ranked by their respective probability score. Note that the experiments were conducted in hemocyte like S2 cells. Still, GO terms associated with neuronal signaling, such as **"Defasciculation of Motor Neuron"** are found in the list. More detailed information can be found in the supplementary raw data files.*

Taken together, my data surprisingly suggests that Dscam1 signaling affects signaling not only locally at the growth cone but also the transcriptional level. In contrast to tyrosine phosphorylation mediated signals, this transcriptional response ***lasts longer than a few minutes***. It is striking that proteins linked to the GO-term "defasciculation of neuron" were among the top terms associated with the candidate genes, despite the fact that we used hemocyte like S2 cells for this study. Future studies should aim at comparing the response obtained in hemocytes to cells of neuronal origin in order to understand if this transcriptional response is solely a function of the immune system or if it is also meaningful during neurite guidance and branching.

Concluding remarks

The migrating growth cone of a developing neuron is a cellular subcompartment subjected to constantly changing environments. In order to form complex neuronal patterns, the neurite tip needs to acquire information regarding its surroundings as well as a sense of the location of sister-neurites derived from the same cell. Importantly, the growth cone needs to maintain flexibility: After reaching a guidance landmark, the signaling systems in the membrane needs to reset to maintain responsiveness towards novel guidance cues determining the next leg of the journey. The maintenance of homeostasis in such dynamically responsive signaling compartments requires the involved signaling systems to be regulated in a fast and reliable manner. One of these signaling mediators in axonal growth cones is the axon guidance receptor Dscam1, which mediates neurite self-recognition necessary for the formation of dendritic and axonal projections.

The aim of my studies was the dissection of the molecular mechanism determining the Dscam1 signaling pathway. Despite the important role of the Dscam1 receptor during axon guidance, branching and arborization as well as patterning, surprisingly little is known regarding the signaling-pathway. This might be due to the fact that the Dscam1 receptor can be activated by thousands of distinct ligands, hampering the systematic study of the pathway. To address these technical difficulties, I have developed a conditionally inducible Dscam1 signaling system based on a chimeric receptor (Met-Dscam1). This cell culture based system represents the starting point of most of my Dscam1 signaling related experiments presented in this dissertation: I have employed it for phosphor-proteomic and transcriptional analysis in hemocyte like S2 cells, complemented by proteomic analysis of the Dscam1 signaling complex in BG3C2 cells (Chapter 3). Furthermore, the chimeric receptor was my entry point into studying the regulation of Dscam1 signaling by tyrosine phosphorylation. It has been used in combination with full length cDNAs to pinpoint Dscam1 phosphorylation sites, and to characterize the important regulatory role of the phosphatase RPTP69D during Dscam1 signaling (Dascenco and Erfurth et al., 2015 and Chapter 2).

Generally, regulation of Dscam1 signaling appears to have an important role during the formation of complex neurite arborizations. For example, we have shown that in contrast to the "all-or-nothing reaction" during dendritic patterning of da-neurons, the patterning of

ms-neurons in the *Drosophila* VNC requires exquisitely precise regulation of Dscam1 signaling (Dascenco and Erfurth et al., 2015; He et al., 2014a and Chapter 1 and Chapter 2 of this dissertation). Both, loss and gain of Dscam1 function result in severe patterning phenotypes. We have developed a model for the function of Dscam1 signaling, which predicts that Dscam1 is necessary to expand a growth cone which is entering a branching hotspot by mediating repulsion between filopodia derived from the same cell (We named this step the "growth cone sprouting step" (He et al., 2014a)). However, Dscam1 activation at such a hotspot is necessary but not sufficient to fully form the three typical branches of ms-neuron which point into different directions. Instead, tight regulation of the Dscam1 mediated retraction mechanisms is necessary, to stabilize such filopodia/branches which are growing in the right directions. We propose, that such "branch selection" takes place in growth cone sub compartments, that are exposed to alternative Dscam1 ligands, such as the midline guidance cue Slit (Chapter 2 of this dissertation and Dascenco and Erfurth et al. 2015). Hence, Dscam1 mediated signaling is not only involved in the formation of uniform neurite patterns but is also used in combination with other guidance cues to establish non-symmetrical complex neurite arborizations.

The fast on/off response of Dscam1 signaling is mediated by tyrosine phosphorylation. We have shown that three tyrosine's in the Dscam1-cytoplasmic domain are critical for the regulation of Dscam1 signaling and the interaction with the Lar-family phosphatase RPTP696 (Chapter 2 of this dissertation and Dascenco and Erfurth et al. 2015). While dephosphorylation of the two SH2-binding sites within the Dscam1 cytoplasmic domain seems to be critical for midline branching of a main collateral branch in ms-neurons, we found that dephosphorylation of *Y1981* potentially hyperactivates the Dscam1 signal. In line with this, it was very hard to interpret double and triple Y>F mutations of the SH-2 binding sites together with *Y>F1981* which I generated in order to fully block the phosphorylation of the Dscam1 cytoplasmic domain (data not shown). I tried to predict the function of *Y1981* by means of several data mining tools, aimed at identifying linear binding motifs in the amino acid sequence of a receptor (e.g. *ELM* (*http://elm.eu.org*)). In addition, I also could not find any functional homology region for the amino acid stretch surrounding *Y1981* by mining the literature and in peptide and protein databases. Interestingly however, when I used an online protein modeling tool known as "*Robetta Full Chain Structure Prediction Server*" *(http://robetta.bakerlab.org)*, I was able to form a hypothesis regarding the function of Y1981: I submitted the amino acid sequence of the

longest version of the Dscam1 intracellular domain for *de novo* prediction and obtained models for the full intracellular domain as well as alternative models for five different stretches of it. These predictions need to be treated with caution as they are purely theoretical. However, in absence of any crystallographic data they still could provide us with some useful hints as to how the intracellular domain might be structured. When I modeled the C-terminus of Dscam1 (after the second SH2-domain), I noticed that four out of five potential models placed *Y1981* in a loop region between two alpha-helices (Chapter 3- Figure 19). Based on these model, one could speculate that phosphorylation of *Y1981* affects an important hinge region, affecting the interaction with other Dscam1 effectors. It will be interesting to follow up on these results in the future as better prediction tools or new crystal structures become available.

Importantly however, I have also created novel tools for the future study of Dscam1 signaling *in vivo*. All cDNA expression constructs that I cloned for the analysis of Dscam1 tyrosine phosphorylation are HA-Flag tagged. Hence, it will be possible to purify the Dscam1 receptor based on the protocols presented here from animals instead of cell culture. Furthermore, the signaling complex of the hyperactive Dscam1 isoform *YF1981* can be compared with the moderately signaling SH2-domain mutations and wildtype Dscam1 from cDNA as well as from flies expressing the HA-Flag tagged genomic Dscam1-Bac constructs that I created during my PhD.

My biochemical studies have shown that Dscam1 signaling is most likely regulated by a multitude of different molecular systems: There is the regulation by (1) ***alternative ligands*** and (2) by ***tyrosine phosphorylation*** of multiple tyrosines, which potentially also affect the conformation of the intracellular domain. Furthermore, I have shown a (3) physical link to the ***translational machinery*** and a regulatory link to ***FMRP protein***, suggesting that Dscam1 might be capable of regulating locally the translation of its own mRNA. (4) The co-purification of Dscam1 with proteins typically found in ***vesicles*** (e.g. the COPI complex) and the cleavage of the intracellular domain suggest furthermore, that the amount of receptor might be regulated by ***endocytosis and recycling*** of receptors. The last signaling mechanism was the most surprising to me: After co-purifying the Dscam1 cytoplasmic domain together with transcriptional regulators, I employed the Met-Dscam1 chimeric receptor system to demonstrate that activation of Dscam1 signaling changes the (5) ***transcriptional signature*** of S2 cells.

In the future it will be an enormously interesting task to dissect which molecular mechanisms are used in which cellular context. Our experiments in ms-neurons show that Dscam1 signaling differs significantly between axons and dendrites and that a correct ms-pattern only forms, if the Dscam1 signaling response is fine-tuned, for example by down regulating Dscam1 signaling in midline directed filopodia via Slit interactions with the Dscam1 extracellular domain. Such regulation ensures the maintenance of growth cone homeostasis and explains how Dscam1 is used during the development of non-uniform complex neurite patterns.

However, the molecular mechanisms mediating retractions are still in the dark: Is signaling mediated by homophilic attachment followed by protease mediated cleavage and receptor endocytosis? Or is the cytoskeleton mediating a more active retraction response? Furthermore, it will be interesting to compare the signaling events during pathogen phagocytosis and neurite patterning: Are there commonalities in the signaling pathways or are the pathways in hemocytes and neuronal cells completely independent of each other? For example, is there a transcriptional component of Dscam1 signaling in neurons? And if so- how is it utilized? Does it change the long term signature of a cell after reaching a certain landmark? Or is it just a function of maturing neurites? In respect to the immune system, it could be interesting to study the transcriptional response in regard to the immunological priming response that has been proposed to be mediated by Dscam1. Maybe such priming is not solely mediated by Dscam1 affecting the expression of selective Dscam1 isoforms, but by a general memory response of the immune cell allowing for a more effective immune response in the future. Finally, while writing this dissertation, I started to wonder, if priming of neurons might also play a role during the outgrowth and patterning of neurites. Is a neurite that has been retracted after encountering a sister neurite capable of re-growing into the same direction again or is there some kind of inhibition? And are both neurites retracted or is one of the two sister neurites the winner in a battle of Dscam1 signals? This leads to the last and maybe most intriguing question, namely how do filopodia finally get stabilized into mature branches? Such seemingly easy problems still represent challenging questions for modern neurobiology and can only be solved by combining careful experimental design, molecular biology, genetics and modern imaging technologies.

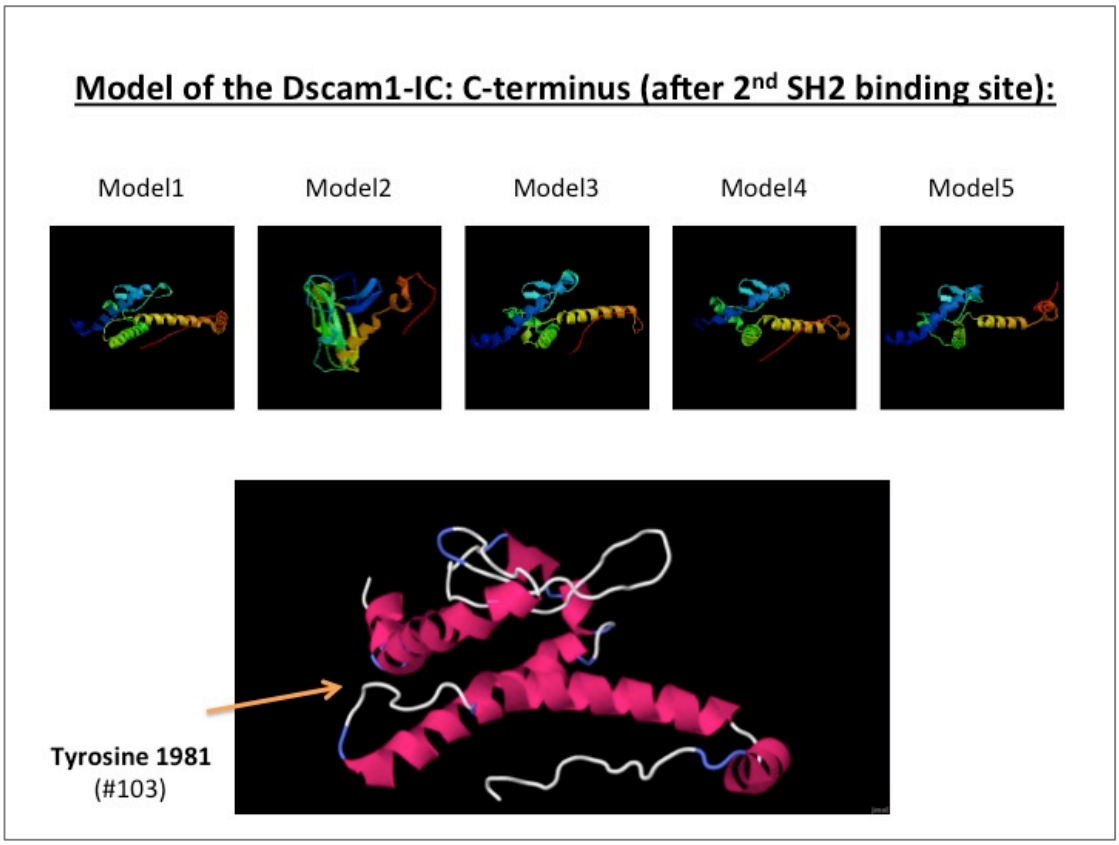

CHAPTER 3- FIGURE 19. **MODELING OF THE C-TERMINUS OF THE DSCAM1 CYTOPLASMIC DOMAIN WITH THE "ROBETTA FULL CHAIN STRUCTURE PREDICTION SERVER".**

The server can be found at: http://robetta.bakerlab.org. Note, that four out of five models place Y1981 in an exposed loop region, suggesting that phosphorylation might affect the capability of the cytoplasmic domain to interact with distinct signaling effectors by changing the conformation of the Dscam1 intracellular domain.

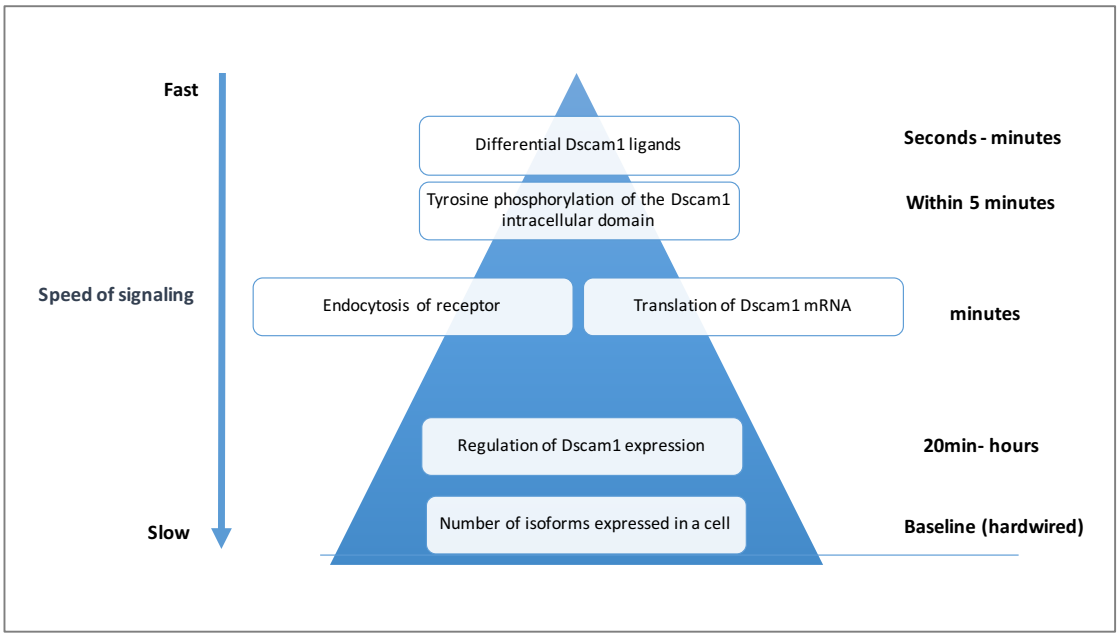

CHAPTER 3- FIGURE 20. **THE DIFFERENT LEVELS OF DSCAM1 REGULATION.**

Indicated are the different possibilities of regulating Dscam1 signaling strength. While we have shown that differential ligands and tyrosine phosphorylation play an important role in vivo (Dascenco and Erfurth et al., 2015; He et al., 2014a and Chapter 1 and 2 of this dissertation), future studies are needed to dissect the interaction with the endomembrane system, the translational and the transcriptional machinery.

General Material and Methods

This section supplements the materials and methods section of chapter 1 and chapter 2 of this dissertation.

Webpages and Databases

All webpages and databases used for this dissertation are listed in M&M- Table 1.

M&M TABLE 1. **WEBPAGES AND DATABASES USED.**

#	url	Name of the tool	Purpose
1.	*http://blast.ncbi.nlm.nih.gov/Blast.cgi*	**Blast**	Search for similar regions in biological sequences
2.	*https://dgrc.bio.indiana.edu/Home*	**Drosophila Genomics Resource Center**	Source for *Drosophila* cells and cDNAs
3.	*http://www.ebi.ac.uk/Tools/msa/clustalw2/*	**ClustalW2**	General purpose DNA or protein multiple sequence alignment program for **three or more** sequences
4.	*http://www.ebi.ac.uk/Tools/msa/clustalo/*	**Clustal Omega**	General purpose DNA or protein multiple sequence alignment program for **three or more** sequences
5.	*http://elm.eu.org*	**The Eukaryotic Linear Motif resource for Functional Sites in Proteins (ELM)**	Search for linear signaling motifs in protein sequences
6.	*http://www.ensembl.org/index.html*	**e! Ensemble**	Assignment of homologues and paralogues; analysis of Mass Spec Data, protein sequences and function
7.	*http://flybase.org*	**Flybase**	General information about any fly protein; analysis of Mass Spec Data
8.	*http://www.flyrnai.org*	**DRSC and Trip Drosophila RNAi screening center**	Information regarding use of dsRNA in flies
9.	*http://www.ncbi.nlm.nih.gov/pubmed*	**PubMed**	Literature Search
10.	*https://notendur.hi.is/bmo/Recombineering%20Website.htm*	**Recombineering Website**	Resources regarding recombineering
11.	*http://www.uniprot.org*	**Uniprot**	assignment of protein information, sequences and functions; analysis of Mass Spec Data
12.	*http://www.flymine.org*	**Flymine**	Detection of trends in proteomic data sets
13.	*Nobelprize.org*	**The official website of the Nobel Prize**	Information regarding Nobel laureates and their work
14.	*http://www.vega.org.uk/video/programme/38*		Information regarding the Nobel prize in physiology and medicine based on interviews at the Lindau Nobel prize Conference in Lindau 2003

#	url	Name of the tool	Purpose
15.	*www.Kinase.com*	**Webpage of the Manning Lab at Genentech**	Information regarding the eukaryotic kinome
16.	*http://robetta.bakerlab.org*	**Robetta Protein Prediction Server**	*De novo* prediction of protein folding based on the amino acid sequence.

Cell Culture

Buffers, materials and reagents used for Cell Culture

M&M TABLE 2. **BUFFER AND REAGENTS USED FOR CELL CULTURE.**

Name	Distributor	Purpose	Notes
Blasticidin S HCL	***Life Technologies***	Selection antibiotic	***Order # A1113903***
10x BPYE	***Home-made***	Bactopeptone and yeast extract ✓ 10g Yeast extract (Sigma-Aldrich) ✓ 25g Bactopeptone (Difco) ✓ Fill up with 1 l cell culture grade water (Life Technologies) ✓ Filter sterilize with a 0.2µm filter (BD) ✓ Aliquot in 15ml aliquots into sterile tubes (BD) ✓ Freeze at -20°C	
Blasticidin	***Life Technologies***	Selection antibiotic	***Order# 1012746***
Cell counter	***Biorad***		
Cell counter slides	***Biorad***		***Order #145-0015***
DMSO cell culture grade	***Sigma Aldrich***	Freezing cells	***Order # 1001997***
Microtest 96 Tissue Culture Plates	***Falcon***		***Order # 353072***
Copper Sulfate 10x	***Sigma-Aldrich***	✓ Make a 7.5 mM stock ✓ Filter through a 0.2µm filter ✓ Store at 4°C ✓ Use at a final conc. of 750µM	***Order # C8027-500G***
DPBS, no calcium, no magnesium	***Life Technologies***	Washing cells, diluting antibodies	***Order# 14190094***
Cell culture coated tissue culture flasks (T25, T75, T100)	***BD***	Growing cells in routine culture	***Order #430641***
0.2µm filter for 500ml and 50ml	***VWR***	Sterile filtration	
-20°C freezer		Storage of buffers, kits, FBS and DNA constructs	
L-Glutamine (200mM)	***Life Technologies***	Cell culture supplement	***Order # 25030081***
HGF	***R&D Systems***	Activation of Met-Dscam1	***Order # 2207-HG-025***
Heat inactivated FBS	***Life Technologies***	Cell culture supplement	***There is a large batch that has been tested in the -20° freezer***
Hygromycin	***BD***	Selection antibiotic	
27°C incubators		Cell storage	
Liquid nitrogen tanks			
M3 Medium	***Sigma***	Culture of neuronal cells	***Order #S3652-500ml***
Insulin	***Sigma***	Culture of neuronal cells	***Order# I9278***
Inverted microscope with 10x, 20x and 40x objectives	***Zeiss***	Observation of cells	
Blotting Grade Blocker (nonfat dry milk)	***Biorad***	Blocking solution for immunohistochemistry (5% weight/volume)	***#170-6404***

Penicillin-Streptomycin (5,000 U/mL)	***Life Technologies***	Antibiotic to avoid contamination	***Order #15070063***
Serological pipets 25ml, 10ml, 2ml	***VWR***	Pipetting	***Order # 1004987, 1004982, 1004986***
Sf-900™ II SFM medium	***Life Technologies***	Culture of hemocyte cell lines	***Order #10902-096***
Schneider's Drosophila Medium	***Life Technologies***	Culture of Drosophila cells	***Order #21720024***
2ml tubes for storage in liquid nitrogen	***VWR***		
15 and 50 ml sterile Falcon tubes	***VWR***	Storage of BPYE and FBS, centrifugation of cells	
Paraformaldehyde 32% solution 100ml	***Electron Microscopy Sciences***	Used as 10x stock for cell fixation buffer	***Order #15714-S***

Protocols for routine cell culture

General information regarding Drosophila cell cultures

S2 cell, Kc cells, Slit-expressing cells and BG3C2 cells were obtained from DGRC. Aliquots were stored in liquid Nitrogen. We thawed a fresh aliquot of cells ***every three month*** in order to avoid work with aged cells. Generally, we followed the ***guidelines given by*** *DGRC*, which can be found at the DGRC webpage (*https://dgrc.bio.indiana.edu/cells/Overview*).

Specifically, we grew cells during routine culture in a 27°C refrigerating incubator and kept them at a density of $1x10^6$-$1x10^8$. I mostly used T-flasks to grow my cells. The culture volume was determined by the surface area: The medium should be about 2-3 mm deep to permit good oxygen saturation. The speed of growth depends on the volume used within a culture vessel. Lower volumes lead to faster growth, while higher volumes inhibit growth.

The volumes recommend for the most common used tissue culture vessels are:

- 175 cm2 T flask: 27-35ml (Optimum 30ml)
- 75 cm2 T flask: 10-15ml (Optimum 12ml)
- 25 cm2 T flask: 3,5-5ml (Optimum 4ml)
- 6-well plate: 2ml (seal outside of plate with Parafilm to minimize evaporation)

In order to produce a lot of protein (e.g. for Slit purification), cells were grown in ***spinner bottles*** at high density at room temperature. Health and densities of all the cells were regularly checked (at least three times per week).

Drosophila cells are all semi-adherent on regular cell culture plastics and can be easily grown in the absence of any coating material. The hemocyte cell lines (S2 and Kc) form first a dense monolayer on the bottom of the dish and then release cells into suspension. At very high densities they form a suspension of clumping cells. There is no contact inhibition. However, it is important to keep the cells growing in the densities indicated above. Otherwise they will be very stressed and be hard to transfect.

CNS cells, such as BG3C2 attach at low densities to the bottom of the flask in small patches. *One can see neurites growing out and the patches connecting to each other as the densities* increase. At a certain point, healthy BG3C2 cells start to form round 3D structures looking like small "balls" consisting of cells. This is the optimal density for any type of experiment and it is advisable to keep the cells in this state.

Cells were generally kept in ***antibiotic free medium*** except in the first week after thawing and when using stable cell lines. There is no need of buffering the medium by CO_2 or for supplying extra humidity. Hence, *Drosophila* cells can be grown in ordinary air and even on the bench. S2 cells and Kc cells were grown in SF-900 Insect Medium (*Life Technologies*) supplemented with glutamate (*Life Technologies*). BG3C2 cells were grown in Schneider's medium (*Life Technologies*) supplemented with 10% FBS, 1x BPYE (bactopeptone and yeast extract) and Insulin (10mg/ml) (*Sigma*). An example for the way of healthy growing BG3C2 cells is shown in M&M- Figure 1.

Stable cell lines were routinely grown in the presence of Blasticidin (chimeric receptor expressing cells; Dscam cDNA expressing cells; PTP69D expressing cells) (*Life Technologies*) or Hygromycin (Slit expressing cells (*Sigma*)) to maintain selection pressure.

If constructs with a metallothionine promoter were used (Slit expressing cells and some chimeric receptor constructs) we induced expression three days before the experiment with by adding copper sulfate to a final concentration of 750µM.

Preparing FBS for cell culture (Heat inactivation)

The FBS we used since we arrived *in Leuven* was taken *from a batch purchased in December 2009 from Life Technologies* after testing different lots. The FBS used in Boston was an old batch from Life Technologies that had been purchased before my arrival. FBS was stored at -20°C:

1. Thaw a bottle over night
2. Heat in a 56°C water bath for 30 min
3. Sterile filter through a 0.2µm filter
4. Aliquot into 50ml sterile Falcon tubes
5. Freeze at -20° and label heat inactivated
6. Thaw 1 day before use in the fridge
7. Add one tube per 500ml medium

Transfections:

Cells were transfected with the ***Amaxa Nucleofector device***. For standard transfections we used ***2µg*** of a given plasmid/dsRNA in ***solution V*** with the program ***D-23***. Co-transfection of a single isoform of Dscam together with PTP69D required the use of less plasmid. Therefore, we transfected only 1µg per plasmid in order to obtain viable cells.

Freezing and thawing cells:

We followed the guidelines of the *DGRC* for freezing and thawing cells.

Differentiation of BG3C2 cells:

BG3C2 cells were differentiated by splitting them to a density of 1-2x10^6 cells/ml and by exposing them to differentiation medium. The differentiation medium is characterized by the absence of FBS and the presence of high concentrations of Insulin. Differentiation and neurite outgrowth happen faster on Laminin coated cover slips but can also achieved on cell culture plastics. After 10 days in differentiation medium the majority of BG3C2 cells is differentiated. An example for the differentiation process is depicted in M&M- Figure 1 and M&M- Figure 2.

Differentiation medium for BG3C2 cells:

- ✓ Schneider's medium
- ✓ 1xBPYE
- ✓ Insulin (100mg/ml)

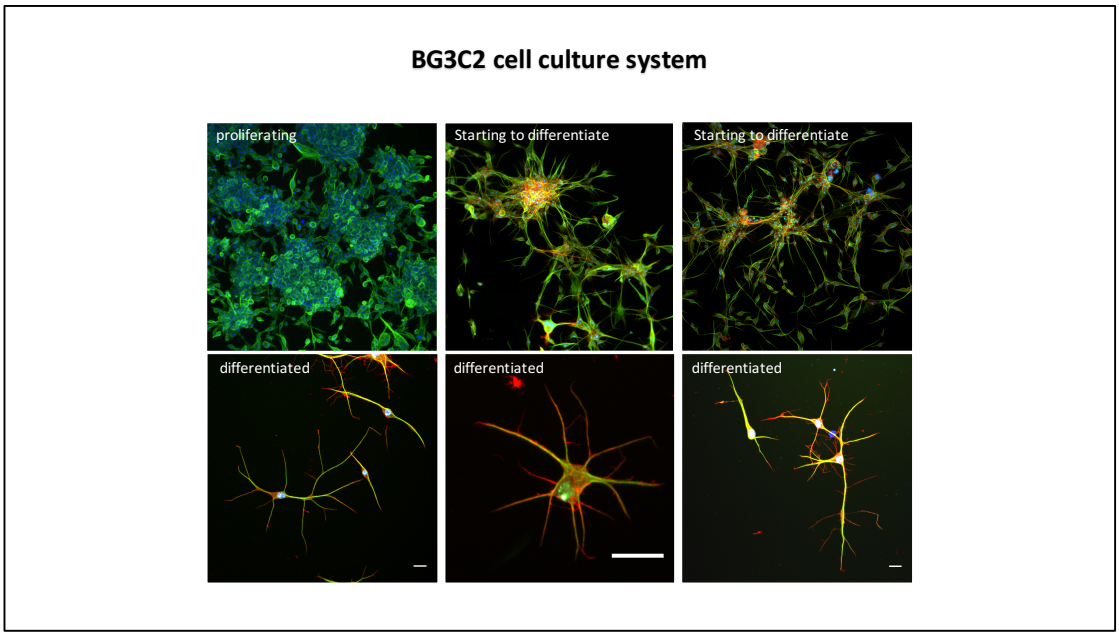

M&M FIGURE 1. **THE BG3C2 CELL CULTURE SYSTEM ALLOWS FOR THE DIFFERENTIATION OF CNS CELLS FROM ROUND PROGENITORS INTO NEURONS WITH SEVERAL NEURITES.**

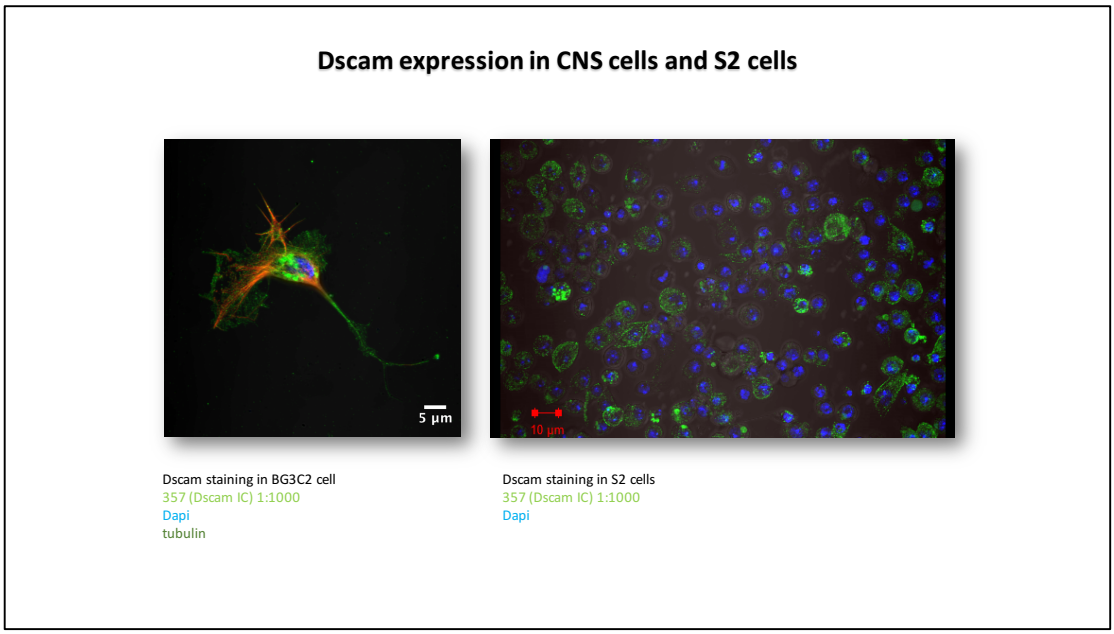

M&M FIGURE 2. **DIFFERENTIATION OF BG3C2 CELLS ALLOWS FOR THE BETTER CHARACTERIZATION OF SUBCELLULAR LOCALIZATION OF DSCAM1 IN COMPARISON WITH S2 CELLS.**

Cloning

Optimized protocol of bacterial recombineering

This is the protocol, I used to modify the ***73 kb genomic Dscam1*** locus including 5kb upstream of exon 1 to 6 kb downstream of exon 24 in the BAC vector P[acman] by means of recombination mediated genomic engineering (recombineering).

#	Equipment/Reagent needed
1.	**1% Agarose gels:** 96 well for screening and small gels for purification of linear template
2.	**Powerpac** to run agarose gels (e.g. Biorad #1645050)
3.	**Erlenmeyer flasks** to grow liquid bacterial cultures
4.	**Low salt LB medium** (contains only ***half of the usual concentration of NaCl***): ✓ 10 g Tryptone ✓ 5g NaCl ✓ 5g yeast extract ✓ fill up to one liter with dest. water ✓ autoclave
5.	**Antibiotics:** • Tetracycline (e.g. from Sigma Aldrich #T7660) • Ampicillin (e.g. from Sigma Aldrich #A9518-5G)
6.	**Incubators** which hold temperature ***reliably*** below ***32°C***
7.	**Water bath**
8.	**Centrifuge (capable of cooling)**
9.	50ml **Falcon tubes**
10.	**Electroporator:** Biorad Micropulser
11.	**Electroporation cuvettes** (0.1 cm)
12.	**Large LB-agar** plates with selection antibiotics
13.	**Nanodrop** or any other spectrophotometer allowing to measure the OD600 of cell cultures and OD260 of DNA samples
14.	**96 well plates** suitable for PCR
15.	**96 well plates** for bacterial culture
16.	**EPI300** electro-competent cells (epicenter)
17.	**Copy control solution** (epicenter)
18.	**SW102 recombineering competent *e. coli* cells:** ✓ Derived from the DY380 strain (to allow for galK positive/negative selection) (Warming et al., 2005) ✓ Further information can be found at the recombineering website : *https://notendur.hi.is/bmo/Recombineering%20Website.htm)*. ✓ ***Genotype of the DY380 strain***: F- *mcr*A Δ(*mrr-hsd*RMS-*mcr*BC) Φ80d*lac*Z M15 *ΔlacX74 deoR recA1 endA1 ara*D139 Δ (*ara, leu*) 7649 *galU galK rsp*L *nup*G [*λcI*857 (*cro-bio*A) <> *tet*]. ✓ Importantly, these bacteria contain a stably integrated defective λ-prophage that allows the expression of the three proteins needed for recombination from the strong ***pL phage promoter*** under control of the ***temperature-sensitive repressor cI857***. This allows the efficient expression of the proteins by simply shifting the cells from ***32°C to 42°C*** for 15 minutes. ✓ The SW102 strain is tetracycline ***(tet) resistant*** (12.5 µg/ml).
19.	**BAC vector P[acman] containing *the 73 kb Dscam1 genomic locus*** and flanking regions (Venken et al., 2006) (contains ***ampicillin*** resistance)
20.	**Linear dsDNA template** containing the Dscam1 modification flanked by homology arms (see below for instructions how to prepare it)

M&M TABLE 3. **MATERIALS NEEDED FOR BACTERIAL RECOMBINEERING.**

Instruction for the preparation of dsDNA recombineering template:

- ✓ The area to be modified should be surrounded by ***500-600 bp*** complementary region in a linear dsDNA construct.
- ✓ The "*overlap arms*" of the "*insert*" should be ***500-600 bp***. It is possible to use smaller arms but it is ***a lot*** easier to use longer overlaps.
- ✓ Prepare the "insert" by PCR. I am usually using KOD polymerase as proof reading polymerase according to manufacturer's recommendations.
- ✓ If amplifying from a plasmid, ***digest remaining plasmid with DpnI. Then run the PCR product on an agarose gels*** and cut out PCR product from gel to ensure that no residual template is disturbing during later steps of the recombineering protocol. Elute PCR product ***as concentrated as possible in nuclease free dest. water***.
- ✓ Measure DNA concentration on the Nanodrop.

Preparation of recombineering and electrocompetent cells:

#	Step
1.	Grow a starter culture of SW102 cells transformed with the Dscam1- P[acman] BAC vector overnight in a shaking incubator (250-300 rpm). ***Make sure the temperature does not exceed 32°C!***
2.	Dilute the starter culture 1/1000 in 500ml ***low salt LB*** and grow them in a glass Erlenmeyer flask in a shaking incubator (250-300 rpm) until they reach and OD_{600} of ≈0.6 (about three to four hours). ***Make sure the temperature does not exceed 32°C!***
3.	In the meantime: a) Prepare a water bath at 42°C b) Precool the centrifuge to 4°C c) Precool enough ddH_2O, cuvettes and 50ml tubes in the fridge d) Prepare an ice water-mix for cooling
4.	Once the cell reach the desired OD_{600} induce expression of the proteins needed for recombineering by ***gently swirling the flask in the 42°C water bath***
5.	Immediately afterwards cool the cells in the ice-water bath. Swirl for a couple of seconds and incubate at least another ***30 min***. From now on it is critical to ***keep the cells always cold.***
6.	Spin cells at 4000g, 15 minutes, 4°C
7.	Discard supernatant and ***gently*** resuspend in 500ml chilled ddH_2O (First add about 100ml and gently tap and flick to resuspend the pellet. Then add slowly more water. ***Take your time and treat the cells gently***. Resuspension should become easier and take shorter time with each wash step.)
8.	Spin cells at 4000g, 15 minutes, 4°C
9.	Discard supernatant and ***gently*** resuspend in 250ml chilled ddH_2O
10.	Spin cells at 4000g, 15 minutes, 4°C
11.	Discard supernatant and ***gently*** resuspend in 20ml chilled ddH_2O
12.	Spin cells at 4000g, 15 minutes, 4°C
13.	Discard supernatant and ***gently*** resuspend in 1,5 ml chilled ddH_2O
14.	By this time the pellet should be fluffy, white and very easy to resuspend (It should have become easier to resuspend the pellet with every wash step)

Electroporation of linear dsDNA template into SW102 cells containing the 73kb genomic Dscam1 Bac-construct

#	Step
1.	Mix 15µl of cells with ***750 ng - 1 µg*** of linear dsDNA template transfer to 0.1 mm ***pre-cooled cuvette***. (Keep 40 µl of cells that are not electroporated as a negative control for the PCR screen.) Tap the mixture to the bottom of the cuvette.
2.	Electroporate: ***1.75kV, time const.: 4.0 msec.***
3.	***Immediately*** after electroporation add 1 ml of LB and transfer the mixture into a fresh tube.
4.	Recover the cells and allow for recombination by gently rotating/shaking for ***1-3 hours,*** 32°C (Many protocols use only 1h recovery. But in my hands the efficiency increases if I leave it longer). Pre-warm LB plates with appropriate antibiotic.
5.	Streak out 50 µl on a ***large LB agar plate*** (tet and amp) and incubate overnight. Usually the cells need a little longer to grow than for normal cloning. If streaked out at 5 pm one day, the should be ready for further analysis by noon of the next day. ***Keep the rest of the liquid culture*** (store it at 4°C) ***to use it as a positive control in the PCR screen.***

PCR based screening for the selection of recombination positive pools of colonies of SW102 cells with the modified genomic Dscam1 Bac-construct

#	Step
1.	Optimize diagnostic PCR by using untransfected liquid culture as negative control and electroporated/recombined liquid culture as positive control: a) I have successfully used ***Amplitaq and Invitrogen Taq*** for screening by colony PCR (Amplitaq is a little more sensitive) b) I always used a primer combination with one ***primer specific to the dsDNA*** donor cassette (inside primer) and ***one primer lying in the unmodified Dscam1 locus*** (outside primer), resulting in a PCR product of about ***1kb size*** c) Note: It is ***a lot easier*** to screen with a good PCR for presence of a band than for size differences! Therefore, it is worth the effort to optimize a good and robust PCR reaction and to reorder primer sets in case the PCR is not very reliable. This will save a lot of effort in the long run
2.	Optimize PCR conditions by running a gradient PCR for the positive and the negative control. a) I am usually setting up 12x ***20µl reactions*** and added ***0.2 µl of liquid culture*** to each tube. b) ***Add 5 minutes*** for the initial denaturation step in order to break up the bacterial sample sufficiently.
3.	Run diagnostic optimized colony PCRs on ***pooled samples*** (96 well format) a) Prepare PCR mastermix for 96 reactions and distribute it into the wells of a 96 well PCR plate b) Prepare 10ml of LB medium with Tet and Amp and distribute 100µl aliquots into a 96 well sterile tissue culture plate c) I ***always*** included one positive control and one negative control from the liquid cultures (0.2 µl) d) Use sterile toothpicks or a 10µl sterile pipette tips to select colonies for PCR: • Touch 3-4 colonies on the LB plate streaked out after recombination and dib toothpick into the PCR mastermix of one well. • Incubate a few minutes • Transfer toothpick to the matching well of the 96 well tissue culture plate filled with LB • Incubate a few minutes • Discard toothpicks • Seal PCR plates thoroughly and run diagnostic PCR • Seal LB plate and incubate three to 4 hours at room temp. with gentle shaking (until a slight with precipitate is visible on the bottom of some wells) • Prepare 96 well agarose gel
4.	After finishing the PCR identify positive wells by running an agarose gel (usually I got 3-10 positive wells if the recombineering worked very well; But I also got 1-2 in worse cases.)
5.	Streak out the cells from the positive wells and incubate over night at 32°C

PCR based screening for recombination positive single colonies of SW102 cells with modified Dscam1 genomic Bac-construct

#	Step
1.	Run diagnostic optimized colony PCRs on ***single samples*** (96 well format) a) Prepare PCR mastermix for 96 reactions and distribute it into the wells of a 96 well PCR plate b) Prepare 10ml of LB medium with Tet and Amp and distribute 100µl aliquots into a 96 well sterile tissue culture plate. c) I ***always*** included one positive control and one negative control from the liquid cultures (0.2 µl) d) Use sterile toothpicks or a 10µl sterile pipette tips to select ***single*** colonies for PCR as described above
2.	Seal PCR plates thoroughly and run diagnostic PCR
3.	Prepare 96 well agarose gel
4.	Seal LB plate and incubate three to 4 hours at room temp. with gentle shaking (until a slight with precipitate is visible on the bottom of some wells)
5.	After finishing the PCR identify positive wells by running an agarose gel (usually I got 3-10 positive wells if the recombineering worked very well; But I also got 1-2 in worse cases.)
6.	Streak out the cells from the positive wells and incubate over night at 32°C
7.	Pick 10 colonies the next day and repeat diagnostic PCR to ***make sure that really a single colony has been picked*** a) If all 10 colonies are positive inoculate 10ml liquid culture and grow over night to make glycerol stocks b) If not all colonies are positive streak out a positive well again and repeat diagnostic PCR the next day; Then grow liquid culture and make glycerol stock

DNA preparation for embryo injection and sequencing:

#	Step
1.	For sequencing and retransformation, I used the Invitrogen Maxiprep kit with the BAC protocol • Inoculate 300ml of LB with Tet and Amp from the glycerol stock of the positive recombineering clone obtained above • Add copy control solution (Epicenter) according to protocol • Perform Maxiprep according to protocol • Elute in 500 water • Check DNA quality and concentration with the Nanodrop
2.	Sequence target region to ensure that everything has worked out well
3.	Use 1µg of DNA to electroporate ***EPI300 cells*** (Epicenter). Transformation into EPI300 cells guarantees that the DNA quality is very good for injection. • Settings: ***1.75kV, time const.: 4.0 msec***
4.	Streak out on an LB plate (tet and Amp) and incubate over night
5.	Pick a single colony, verify by diagnostic PCR and inoculate liquid culture to make glycerol stock
6.	For Injection I use the Epicenter Bac-Maxiprep kit (Epicenter)
7.	Inoculate 100ml of LB with Tet and Amp from the glycerol stock of the positive recombineering clone obtained above
8.	Add copy control solution (Epicenter) according to protocol
9.	Perform Maxiprep according to protocol
10.	Dilute the pellet in 50µl EB buffer by rotating the tube over night
11.	Heat DNA to 90°C and slowly cool back to room temperature
12.	Centrifuge 10 minutes at full speed in a microcentrifuge
13.	Filter DNA through a 0.2µl filter
14.	Check DNA concentration and quality on the Nanodrop
15.	Store at ***4°C*** until injection (***Do not freeze!***)

Preparation of fly embryo injections:

- ✓ Expand fly stocks with integrase and landing site early enough
- ✓ Prepare apple plates
- ✓

Instructions for the preparation of the apple plates:

The quality of Apple plates can make a big difference in embryo collections. Apple plates vary depending on the sugar content and the type of juice used. While I used grape fruit juice in the US, I optimized the following protocol after coming to Belgium. I found it to be very good and I hope that Minute Maid apple juice is almost everywhere available:

#	Step
1.	125ml apple juice (Minute Maid)
2.	125ml Water
3.	3g Sucrose
4.	7.5g Difco Agar
5.	Heat in the microwave until completely dissolved (or autoclave). Stir in between on the heat plate.
6.	Add 5ml EtOH and 5ml Acetic Acid.
7.	Poor into plates
8.	Dry the plates over night at room temperature. **They are the best if you use them the next day.** Streak a little acetic acid and yeast-paste on them before putting them into the fly cage.
9.	Transfer flies 2 days before injection into cages and exchange plates regularly
10.	Make sure not to add too many flies per cage but rater use more cages
11.	Transfer flies 1 day before injection to the 18°C room and exchange plates regularly
12.	On the day of injection exchange plates hourly until injections start
13.	After starting injections collect embryos every 30 minutes

Pulling injection needles for embryo injections:

The quality of the injection needles is very important for the injection workflow. One wants a sharp needle that does not bend but is also not too brittle. I based my injection needles on the bee stinger needle described in chapter 3 of the Sutter "Pipette cookbook" (Oesterle, 2011). However, to adjust to the needs of fly embryo injections, I aimed for a short tubby taper with a very thin small tip.

Tips for needle pulling:

1. Use box filament 2.5 x 2.5 box filament (FB255B)
    a. Make sure the box filament is well aligned and realign when necessary!
    b. Check humidity of the room in order to get reproducible results.
2. Use the following glass (with filament): BF100-50-10 (1.0 x 0.5)
3. Add 10-20 additional pull units and increase delay by 10-20 units
4. Pull many needles at the same time in order to maintain quality of a batch
5. A reference needle can be found in Dietmar's office

Embryo injections:

1. Collect embryos with the help of a paint brush and a filter and wash all the yeast off
2. Preclear cover slips by dipping them into ethanol
3. Use a small drop of glycerol to fix the cover slip on a slide
4. Align embryos on the cover slips in rows of 10
    a. Embryos move easy in a small film of water
    b. Use a pair of old dull forceps to push the embryos around
    c. Leave some space between the rows. This ensures that if the row does not stick well enough to the cover slip not everything is lost
5. Gently dry them off and store in humidified chamber (plate with wet paper towel) until injection
6. Add ethanol to clear the embryos
7. Gently inject (DNA conc. between 500ng and 1µg/µl) with a small amount of DNA
    a. If you are new to injections, you can visualize the flow of DNA with food dye.
8. Kill all embryos that are too old by stabbing them
9. Transfer cover slip to a small vial containing food

Cloning of the chimeric receptor expression constructs:

cDNA for mouse c-Met receptor was obtained from the Birchmeier lab. The chimeric receptor was created by overlap-fusion PCR. We fused amino acids 1-929 of the mouse c-Met ORF to amino acids 1590-2031 of Dscam 1.30.30.2. For the HA-Flag tagged version of the Met-Dscam chimeric receptor we added a Flag-Ha tag between amino-acids 1957 and 1958 of the intracellular domain of Dscam. For details see Supplemental Figure 1. The chimeric receptor was cloned into pIB-V5-HIS and in pMT-V5-HIS for expression in cells in such a way that there was a stop codon before the V5-His tag.

PTP69D expression constructs:

cDNA for HA-tagged RPTP69D in pUAS-attB was obtained from DGRC (UFO0693). For the HA-tagged cell culture expression constructs the insert was PCR amplified with two primers from the vector backbone and cloned into pIV-V5-HIS (Invitrogen). For the V5-tagged versions the full ORF except the stop-codon was amplified and cloned in frame with the V5 tag into pIB-V5-HIS.

Constructs obtained by mutagenesis:

Point mutations were generated by standard PCR methods (Quick change mutagenesis). 25ng of plasmid were 12x cycled with KOD polymerase. All primers used are listed in M&M Table 4.

M&M TABLE 4. **PRIMER USED FOR MUTAGENESIS PROJECTS.**

Name of construct	Primer A	Primer B
PTP69D DA1	CCTAACGTGGAAGGCCTTCATGGCACC	GGTGCCATGAAGGCCTTCCACGTTAGG
PTP69D DA2	GGTTGGCCCACCGTGGCCGGAGAAGTTCC	GGAACTTCTCCGGCCACGGTGGGCCAACC
Dscam 18 YF1	GTACTACGATGTAGT TTTCAATCAGACAATGGGACC	GGTCCCATTGTCTGATTGAAAACTACATCGTAGTAC
Dscam 18YF2	GGATGAGCTCGGATTCATCGCCCCGCCCAACC	GGTTGGGCGGGGCGATGAATCCGAGCTCATCC
Dscam 18YF3	CGTTCCCG GATCCAACTT TAATACCTGTGACC	GGTCACAGGTATTAAAGTTGGATCCGGGAACG
Dscam 19YF	CGCAATCCCAACCTGTTCGAGGAGCTGAAG G	CCTTCAGCTCCTCGAACAGGTTGGGATTGCG
Dscam 20YF1	GGAAGATGAAATCTGCCCCTTTGCCACGTTCCACC	GGTGGAACGTGGCAAAGGGGCAGATTTCATCTTCC
Dscam 20YF2	CGATGCCTCGGGCCAATCGATTCCAGCGA AAGAACAGCC	GGCTGTTCTTTCGCTGGAATCGATTGGCCCGAGGCATCG
Dscam SH2-1	CACGCCAGCTCCCGAATTCGATGATCCCGCCAAC	GTTGGCGGGATCATCGAATTCGGGAGCTGGCGTG
Dscam SH2-2	GGACCCGGACCCGAATTCGACGATCCCGCCAACTGC	GCAGTTGGCGGGATCGTCGAATTCGGGTCCGGGTCC
Dscam 21YF1	CCGAAGAGGATCAGTTCGGCTCCCAGTACGGAGG	CCTCCGTACTGGGAGCCGAACTGATCCTCTTCGG
Dscam 21YF2	*CAGTACGGCTCCCAGTTCGGAGGACCCTATGG*	CCATAGGGTCCTCCGAACTGGGAGCCGTACTG
Dscam 21YF3	*CCAGTACGGAGGACCCTTTGG*ACAGCCCTATGATCA CTACG	CGTAGTGATCATAGGGCTGTCCAAAGGGTCCTCCGTACTGG
Dscam 21YF4	*CCTATGG*ACAGCCCTTTGATCACTACGGTTCC	GGAACCGTAGTGATCAAAGGGCTGTCCATAGG
Dscam 21YF5	CAGCCCTATGATCA CTTCGGTTCC CGGGGATCC	GGATCCCCGGGAACCGAAGTGATCATAGGGCTG
Dscam 22YF	CCA CGGACCACGC GGAAACTTCG GAGCAGTGAA GCGATCTCC	GGAGATCGCTTCACTGCTCCGAAGTTTCCGCGTGGTCCGTGG
Dscam 24YF	CGTCGATTCACAGC CTTCGATACT ATGGCAGTG	CACTGCCATAGTATCGAAGGCTGTGAATCGACG

ds-RNAs and Taqman probes used

To produce ds-RNAs, S2 cells were harvested in Trizol and total RNA was prepared from them by purification over a spin column (*Life Technologies*). Remaining DNA was digested on the column by incubation with RNAse free DNAse (*Life Technologies*). 250ng of the resulting total RNA were used for reverse transcription using iScript (*Biorad*). The resulting cDNA was used to amplify the DNA templates for the *in vitro* transcription reaction with the MEGAScript RNAi kit (*Ambion*). Primers were designed based on dsRNAs published by DRSC (*http://www.flyrnai.org*). Each primer contained a T7 transcription start site. Efficiency of dsRNA was tested by real time PCR using Taqman probes (ABI). Primer sequences and Taqman assays are listed in M&M- Table 5.

M&M TABLE 5. **LIST OF PRIMERS USED TO AMPLIFY TEMPLATE FOR DSRNAS AND TAQMAN ASSAYS USED FOR QUANTITATIVE RT-PCR.**

Target name	CG#	Forward primer	Reverse primer	Length of dsRNA	*Taqman assay #*
PTP69D	CG10975	TaatacgactcactatagggAAGAATTCTTCGAAGAATCGATGAACCC	TaatacgactcactatagggAGTCTAGAACCTTGTGGGGGTATGTGAA	549	***Dm01822667_m1***
PTP69D	CG10975	TaatacgactcactatagggTACTGGCCACAGCAGATGAG	TaatacgactcactatagggTTTCGCTGTGCACGTATTTC	511	***Dm01822667_m1***
Dscam1	CG17800	GAATTAATACGACTCACTATAGGGAGAGCGTGGAAGAGGGCAC	GAATTAATACGACTCACTATAGGGAGAGACCGCTTCAGAGGATTG	685	***Dm01811763_m1***
Src42A	CG44128	TaatacgactcactatagggACTCAACGTTAACCAACCGC	TaatacgactcactatagggAGAAGAATGCCAAAGCTCCA	439	***Dm01811572_m1***
Src64B	CG7524	TaatacgactcactatagggTGCTGGCCGAGGAGAA	TaatacgactcactatagggGAGCAAACGGCATAGAGG	581	***Dm01843457_m1***
Lar	CG10443	TaatacgactcactatagggATGGGTCTGCAGATGACAG	TaatacgactcactatagggCCACGGCGAGTGGATTG	930	***Dm01817891_m1***
Lar	CG10443	TaatacgactcactatagggTGGGATCCACCAACTAGGG	TaatacgactcactatagggTACTGTAACCTTTTCACTAAGAC	504	***Dm01817891_m1***
PTP99A	CG11516	TaatacgactcactatagggGGAGCATGGAGCACAAACT	TaatacgactcactatagggACTGTGGAGCAGGGGTATC	663	***Dm02134665_m1***
PTP99A	CG11516	TaatacgactcactatagggGGTCGCACTGGCACATAC	TaatacgactcactatagggATTGTGGTCCCAGACCATCT	507	***Dm02134665_m1***
PTP10D	CG1817	TaatacgactcactatagggCAACAGTGCGTGTCCTCA	TaatacgactcactatagggGCAATATCGAAGTCATTGTACT	502	***Dm01799345_m1***
PTP52F	CG18243	TaatacgactcactatagggCATTCCGAGTGATGAGCTTA	TaatacgactcactatagggCCTTGATGGCCGCCTTG	506	***Dm01826072_g1***
PTP61F	CG9181	TaatacgactcactatagggCGCTGAAGAACCCCTCATTA	TaatacgactcactatagggGTAATCCTCATCGCTGTCCG	310	***Dm01832108_m1***
Abl	CG4032	TaatacgactcactatagggTGACAAGCTCAACATCCTGC	TaatacgactcactatagggAGGTGTCCTCCTCCGATTTT	500	***Dm01843165_m1***
PTP4E	CG6899	TaatacgactcactatagggTCCACCCGCACCATGC	TaatacgactcactatagggCGGTGAATGTGTAATTGTGATA	511	***Dm01824621_m1***

Other methods- molecular biology

M&M TABLE 6. **LIST OF ENZYMES USED FOR MOLECULAR BIOLOGY**

Name	Distributor	Purpose	Notes
Amplitaq (DNA Polymerase, 1000 units' w/ buffer II)	ABI	Colony PCRs	# N8080172
Gibson Assembly Mastermix	Fermentas	Seamless Cloning	Order #E2611S
DpnI Fast Digest	Fermentas/Thermo Scientific	Digest of unmethylated DNA	Order #FD1703
dNTPs 1.0ml 10mM of each	Fermentas	PCR	Order #R0192
100bp ladder	Fermentas	Judging size of DNA fragments	Order #sm0243
1kb ladder	Fermentas	Judging size of DNA fragments	Order # sm0311
KOD Polymerase	Novagen	High fidelity PCRs, cloning	Order # 71086
Fast digest SpeI	Fermentas	Cloning	Order# 1017588
Fast Digest NotI	Fermentas	Cloning	Order # FD0594
iScript	Biorad	Reverse transcriptions	Order # 170-8890
TaqMan® Universal PCR Master Mix, no AmpErase® UNG	Life Technologies	RT-PCRs	Order # 4324018
Nuclease-Free Water	Ambion	Dilution of enzymatic reactions	Order # AM9937

M&M TABLE 7. **LIST OF OTHER REAGENTS AND KITS USED FOR MOLECULAR BIOLOGY**

Name	Distributor	Purpose	Notes
Agarose	Fisher Scientific	DNA and RNA analysis	Order # BP1356-500
Ready Agarose 96 Plus Gel, TAE, 1.0% plus ethidium bromide, 4 x 26-well (96 plus)	Biorad	Screening of 96 well gels e.g. for recombineering	Order # 1669
UltraPure™ Agarose	Life Technologies	DNA and RNA analysis	Order # 16500500
Bacto yeast extract	BD	Reagent for different buffers	Order # 212750
BOROSILICATE with filament O.D. 1.0mm, I.D.: 0.5mm	Sutter	Glass for pulling injection needles	Order # BF100-50-10
Filter Tubes -Spin-X Centrifuge Tube Filter 0.2µm Cellulose acetate	Costar	Filtering of plasmid and bacmid constructs before injection or cell transfection	Order # 8160
Fontax #5AC, Super Fine Tips, Anti-Capillary	Electron Microscopy Sciences	Loading injection needles	Order # 72730-F
Quick Gel Extraction Kit (Pure Link)	Life Technologies	Purification of DNA from agarose gels	Order # K210012
PCR Purification Kit (Pure Link)	Life Technologies	Purification of DNA	Order # K3100-01
PCR Sealers Microseal 'A' Film	Biorad	96 well PCRs	Order # MSA5001
PureLink® Quick Plasmid Miniprep Kit	Life Technologies	Plasmid minipreps	Order # K210010
PureLink® HiPure Plasmid Filter Maxiprep Kit	Life Technologies	Plasmid maxipreps	Order # K210016
TOPO® TA Cloning® Kit for Subcloning, with TOP10 E. coli, without manual	Life Technologies	Cloning with TA overhangs	Order # KNM450001
TRIzol® Reagent	Life Technologies	Cell lysis for RNA purification	Order # 15596026
Tryptone	Acros	For making media	Order# 61184-5000

Protein biochemistry

M&M TABLE 8. **LIST OF ANTIBODIES USED FOR PROTEIN WORK**

Name	Distributor	Epitope	species of origin	Notes
Alexa Fluor® 488 Goat Anti-Rat IgG (H+L) Antibody	Life Technologies	Rat IgG (H+L)	Goat	Order # A11006
Alexa Fluor® 488 Goat Anti-Mouse IgG (H+L) Antibody, highly cross-adsorbed	Life Technologies	Mouse IgG (H+L)	Goat	Order # A11029
Alexa Fluor® 488 Goat Anti-Rabbit IgG (H+L) Antibody, highly cross-adsorbed	Life Technologies	Rabbit IgG (H+L)	Goat	Order # A11034
GFP Rabbit IgG Polyclonal Antibody Fraction	Life Technologies	GFP	Rabbit	Order # A11122
Alexa Fluor® 633 Goat Anti-Mouse IgG (H+L), highly cross-adsorbed	Life Technologies	Mouse IgG (H+L)	Goat	Order # A21052
Alexa Fluor® 633 Goat Anti-Rabbit IgG (H+L), highly cross-adsorbed	Life Technologies	Rabbit IgG (H+L)	Goat	Order # A21071
Alexa Fluor® 633 Goat Anti-Rat IgG (H+L)	Life Technologies	Rat IgG (H+L)	Goat	Order # A21094
Alexa Fluor® 555 Goat Anti-Mouse IgG (H+L), highly cross-adsorbed	Life Technologies	Mouse IgG (H+L)	Goat	Order # A21424
Alexa Fluor® 555 Goat Anti-Rabbit IgG (H+L), highly cross-adsorbed	Life Technologies	Rabbit IgG (H+L)	Rabbit	Order # A21429
357	Schmucker Lab	*Drosophila* Dscam1 full length intracellular domain	Rabbit	Reusable in WB; pre-absorb before IHC for best results
358	Schmucker Lab	*Drosophila* Dscam1 full length intracellular domain	Rabbit	Reusable in WB
19545	Schmucker Lab	*Drosophila* Dscam1 EC	Rabbit	reusable for WB
19546	Schmucker Lab	*Drosophila* Dscam1 EC	Rabbit	reusable for WB
4G10 Platinum	Millipore	Phosphotyrosine	Mouse	Do not use in Corning 50ml tubes to avoid background!
Phosphor-Tyrosine 100	Cell Signaling	Phosphotyrosine	Mouse	
anti-Dock	Zipursky Lab	*Drosophila* Dock	Rabbit	
anti-Dock	Bogdan Lab	*Drosophila* Dock	Rabbit	
Anti-actin	abcam	Actin	Mouse	Order # ab3280
anti-mouse-HRP	Jackson Laboratories	Mouse IgG	Goat	
anti-rabbit-HRP	Jackson Laboratories	Rabbit IgG	Goat	
anti-guinea-pig HRP	Jackson Laboratories	Guinea pig IgG	Goat	
anti-goat HRP	Jackson Laboratories	Goat IgG	Donkey	
3F10	Roche	HA Epitope Tag	Rat	
Pierce HA Antibody-HRP	Pierce	HA Epitope Tag	Mouse	
M2	Flag	Flag epitope Tag	Mouse	New batches of this antibody do not work anymore (since 2009)
V5 Tag Mouse Monoclonal Antibody	Life Technologies	V5 Epitope Tag	Mouse	Reusable Order # R96025
anti-Slit	Hybridoma Bank	*Drosophila* Slit protein	Mouse monoclonal	Block with BCA for best results
anti-Pvr	Carmeliet lab	*Drosophila* Pvr	Guinea pig	
anti-Myc	Thermo Scientific	Myc Epitope tag	Mouse monoclonal	
3F11	Hybridoma Bank	*Drosophila* RPTP69D	mouse monoclonal	Block with BCA for best results

Name	Distributor	Epitope	species of origin	Notes
Dynabeads® M-280 Sheep Anti-Mouse IgG	Life Technologies	Mouse IgG	sheep	Best for immunoprecipitation involving CAMS

M&M TABLE 9. **LIST OF BUFFERS AND SOLUTIONS USED FOR PROTEIN WORK**

Name	Stock solution	Composition	Notes
Pierce ECL Western Blotting Substrate	A+B	Mix solution A and B 1:1	Order # 32209
TBS	10x TBS	✓ 150mM NaCl ✓ 25mM Tris (with preferred pH)	
Phosphatase inhibitor cocktails 1+2			Use in experiments involving phosphorylation. Sigma
TBST	10x TBS	Add 0.1% Tween20 to 1xTBS	
BupH TBS	Pouches	1 BupH Tris Buffered Saline Pack (Pierce) per 500ml H_2O	For Mass Spec experiments
FU Buffer/HU Buffer	4x stocks in -20 freezer	✓ 200mM Tris pH 6.8 ✓ 8 M Urea ✓ 5% SDS ✓ 0.1 M EDTA ✓ 15mg/ml DTT ✓ add a little Bromophenol-blue for color	Filter through a 0.2micrometer filter and store in aliquots at -20
5% milk or BSA blocking buffer	Powder (Biorad)	Dilute weight/volume in PBS or TBS usually 5%	Order # 170-6404 Departmental stock
PBS	10x PBS	Make 1x PBS by diluting the 10x stock	
PBST	10x PBS	Add 0.1% Tween20 to 1xTBS	
DPBS		DPBS, no calcium, no magnesium (Life Technologies)	For IHC and cell culture Order # 14190094
DPBST		DPBS + 0.1% Triton	FOR IHC
Pierce Protease Inhibitor Tablets, EDTA-free	100x (Pierce)	Add as needed to protein lysates	Order # 88266
Precision Plus Protein Ladder	Biorad		Order # 161-0373
pTyr Lysis and IP buffer		✓ 150mM NaCl ✓ 50mM Tris pH 7,5 ✓ 2mM EDTA ✓ 0.5% NP-40 ✓ 0.5% TritonX-100	Add protease and phosphatase inhibitors before each use. Store at 4 degrees.

M&M TABLE 10. **LIST OF OTHER REAGENTS AND KITS USED FOR PROTEIN WORK**

Name	**Distributor**	**Purpose**	**Notes**
Amicon Ultra-15 Centrifugal Filter Unit with Ultracel-100 membrane	Millipore	Concentration of proteins and buffer exchange	Order # UFC910024
Blotting paper- extra thick	Biorad	Western blotting	Order # 1703967
Blotting Grade Blocker (nonfat dry milk)	Biorad	Blocking solution for immunohistochemistry and Westernblots	Order # 170-6404
BSA	Sigma Aldrich	e.g. for blocking buffer	Order # A-9418
Ponceau S solution 0.1% in 5% acetic acid	Sigma-Aldrich	Fixation and visualization of proteins on nitrocellulose membranes	Order # P71070-1L
SDS gel (4-20% TGX; 10 wells)	Biorad	SDS Page	Order #456-1093
Supported Nitrocellulose 0.2µm	Biorad	Western blots	Order # 162-0097
Sodium Chloride (molecular biology grade)	Sigma Aldrich	Component of many buffers (e.g. Lysis buffers, TBS, PBS)	Order # S3014

Western Blotting:

The protein complexes were mixed with FU buffer and separated on SDS gels (*Biorad*) and blotted semidry to 0.2 µm Nitrocellulose membranes (*Biorad*). Protein transfer was visualized by Ponceau red. Membranes were then blocked with 5% milk (*Biorad*) in TBS and further incubated with the appropriate primary and secondary detection antibodies diluted in 5% milk (*Biorad*). Washes after antibody incubation were performed in TBST. The last wash before visualization was done with TBS. The protein bands were visualized using ECL Western Blotting Substrate (*Pierce*) and imaged with a Chemi-Doc-IT imager (*UVP*). Area density measurements on the raw images were executed with Vision-Works-LS software (*UVP*).

Immunoprecipitations:

S2 cells were harvested 24h-48h post-transfection and lysed in RIPA buffer containing protease inhibitors (*Pierce*) and - if necessary- phosphatase inhibitors (*Sigma*). BG3C2 cells were harvested five days' post-transfection and lysed in the same lysis buffer. The lysates were incubated with beads pre-coated with the immunoprecipitation antibody. Depending on the experiment we used agarose beads coated with anti-Ha-antibody (*Sigma*) anti-Flag-M2-antibody (*Sigma*) or magnetic beads (*Dynabeads; Life Technologies*) coated with anti-Ha-3F10-antibody (*Roche*), anti-V5 antibody (*Life Technologies*), anti-Slit-antibody (*Hybridoma Bank*), anti-Dscam1-intracellular-domain-antibody (*357*) or anti-Dscam1-extracellular domain-antibody (*19545*). 150µl of lysate was incubated with the antibody-coupled beads and afterwards extensively washed. The protein complexes were eluted in FU buffer and separated on 7.5 percent SDS gels (*Biorad*) and blotted semidry to nitrocellulose membranes (*Biorad*). The membranes were incubated with the appropriate primary and secondary detection antibodies.

Primary antibodies in addition to the mentioned IP-antibodies were 4G10-anti-phosphotyrosine-antibody, anti-Dock-antibody (*Zipursky lab*) and anti-actin-antibody. HRP coupled secondary antibodies were obtained from Jackson Laboratories. We also used some primary antibodies coupled directly to HRP (anti-HA-HRP and pY20-HRP (*Pierce*)). The protein bands were visualized using HRP substrate from Pierce and imaged with the Chemi-Doc-IT imager from *UVP*. Area density measurements on the raw images were executed with Vision-Works-LS software (*UVP*)

Supplementary information

List of abbreviations

TABLE 1. **LIST OF ABBREVIATIONS**

Number	Abbreviation	Full term	Group
1.	***A***	Alanine	Amino acid
2.	***ABP***	Actin binding protein	Protein family
3.	***ADP***	adenosine diphosphate	Small molecule
4.	***A. mellifera***	*Apis mellifera*	Species
5.	***Amp***	Ampicillin	Antibiotic
6.	***A. gambiae***	*Anopheles gambiae*	Species
7.	***ANOVA***	Analysis of variance	Statistical method
8.	***AP***	Alkaline phosphatase	Enzyme
9.	***APF***	after puparium formation	Developmental stage in flies
10.	***AP complex***	Adaptor protein complex	Protein complex important in endocytosis
11.	***aSc neuron***	Anterior scutellar neuron	Cell type
12.	***ATP***	Adenosine tri-phosphate	Small molecule
13.	***BAC***	Bacterial artificial chromosome	Vector/Chromosome
14.	***BETR***	Bayesian Estimation of Temporal Regulation	Statistical method
15.	***Bla***	Blasticidin	Antibiotic
16.	***BMP***	Bone morphogenic protein	Protein
17.	***CAM***	Cell adhesion molecule	Protein family
18.	***CamKII***	Calcium-modulated kinase II	Protein
19.	***cAMP***	Cyclic adenosine monophosphate	Small molecule
20.	***Carb***	Carbenicillin	Antibiotic
21.	***cDNA***	complementary DNA	DNA
22.	***C. elegans***	*Caenorhabditis elegans*	Species
23.	***cGMP***	*cyclic guanosine mono-phosphate*	Small signaling molecule
24.	***CNS***	*Central nervous system*	Part of the nervous system
25.	***CT***	Cytoplasmic tail	Protein domain
26.	***CPEB1***	cytoplasmic polyadenylation element binding protein	Protein name
27.	***D***	Aspartic Acid	Amino Acid
28.	***D>A***	Aspartate to alanine mutation	Technique
29.	***da-neuron***	dendritic arborization neuron	Cell type
30.	***Dc***	dorso-central	Location in the body
31.	***DCC***	Deleted in colorectal cancer	Receptor protein
32.	***D1, D2***	Phosphatase domain 1, phosphatase domain 2	Protein domain
33.	***D. melanogaster***	*Drosophila melanogaster*	Species
34.	***D. magna***	*Daphnia magna*	Species
35.	***DSCAM***	Down Syndrome Cell Adhesion Molecule	Gene/Protein name
36.	***DSCAML1***	Down Syndrome Cell Adhesion Molecule Like 1	Gene/Protein name
37.	***DSCR***	Down syndrome critical region	Cytogenic region
38.	***dsDNA***	double-stranded DNA	DNA
39.	***dsRNA***	double-stranded DNA	RNA

Number	Abbreviation	Full term	Group
40.	***eIF***	Elongation initiation factor	Protein subclass
41.	***EGF(R)***	Epidermal growth factor (receptor)	Protein name
42.	***ELISA***	Enzyme-linked immunosorbent assay	Technique
43.	***EphR***	Eph receptor	Protein/receptor name
44.	***FGF(R)***	Fibroblast growth factor (receptor)	Protein name
45.	***FLP***	Flippase	Enzyme
46.	***FLPD***	Flipped out	Technique/ Allele name
47.	***FN(III) domain***	Fibronectin (III) domain	Protein subdomain
48.	***FMRP***	Fragile-X mental retardation protein	Protein name
49.	***FRT***	Flippase recognition target	DNA sequence
50.	***GAP***	GTPase activating protein	Protein family
51.	***GEF***	Guanine nucleotide exchange	Protein family
52.	***GFP***	Green fluorescent protein	Protein name
53.	***GO term***	Gene ontology term	term describing gene/protein attribute
54.	***GOF***	Gain of function	Functional level
55.	***GPCR***	G-protein coupled receptor	Protein/receptor family
56.	***GTP***	Guanosine triphosphate	Small molecule
57.	***HA-tag***	Hemagglutinin tag	Protein sequence
58.	***HGF***	Hepatocyte growth factor	Protein/ligand
59.	***H. medicinalis***	*Hirudo medicinalis*	Species
60.	***HSPG***	Heparan sulfate proteoglycan	Protein family
61.	***Ig-CAM***	Immunoglobulin cell adhesion molecule	Protein family
62.	***Ig-domain***	Immunoglobulin domain	Protein domain
63.	***IHC***	Immunohistochemistry	Technique
64.	***IP***	Immunoprecipitation	Technique
65.	***IPT-domain***	Ig-like, plexins, transcription factor domain	Protein domain
66.	***Ig-SF***	Immunoglobulin superfamily	Protein family
67.	***ITAM***	Immunoreceptor tyrosine based activation motif	Linear protein signaling motif
68.	***ITIM***	Immunoreceptor tyrosine based inhibitory motif	Linear protein signaling motif
69.	***iTRAQ***	Isobaric tag for relative and absolute quantification	Peptide labeling technique used in quantitative mass spectrometry based fingerprinting experiments
70.	***JNK***	c-Jun N-terminal kinase	Protein family
71.	***Kan***	Kanamycin	Antibiotic
72.	***KD***	Knockdown	Expression Level
73.	***LAR***	Leucocyte common antigen receptor	Protein/receptor family
74.	***LOF***	Loss of function	Function level
75.	***LRR***	Leucine rich repeat	Protein domain
76.	***MAPK***	Map kinase	Protein family
77.	***MAPK Ak2***	MAP kinase activated protein-kinase-2	Protein name
78.	***MAPKK***	Map kinase kinase	Protein name
79.	***MAPKKK***	Map kinase kinase kinase	Protein name
80.	***MARCM***	Mosaic analysis with repressible marker	Technique
81.	***MB***	Mushroom body	Part of the nervous system
82.	***MeV***	Multiexperiment Viewer	Program for the analysis of microarray data
83.	***MLC***	Myosin light chain	Protein domain/family
84.	***m. muculus***	*Mus muculus*	Species
85.	***MS-neuron***	Mechanosensory neuron	Cell type
86.	***MSP domain***	cytoplasmic major-sperm protein domain	Protein domain
87.	***NADH***	Nicotinamide adenine dinucleotide	Small molecule
88.	***NADPH***	Nicotinamide adenine dinucleotide phosphate	Small molecule

Number	Abbreviation	Full term	Group
89.	***NGF***	Nerve growth factor	Protein name
90.	***Pak***	p21 activated kinase	Protein name
91.	***Pcdhs***	Protocadherins	Gene/Protein family
92.	***pDC neuron***	posterior dorsocentral	Cell type
93.	***PDZ***	post synaptic density protein, Drosophila disc large tumor suppressor and zonula occludens-1 protein	Protein family/ domain
94.	***PH domain***	Pleckstrin-homology domain	Protein domain
95.	***PH domain***	Phox homology domain	Protein subdomain
96.	***PID***	Phosphotyrosine interacting domain	Protein domain
97.	***PI3K***	Phosphoinositide 3-kinase	Protein family
98.	***PiP2***	Phosphatidylinositol (4,5)-biphosphate	Protein
99.	***PiP3***	Phosphatidylinositol (3,4,5)-biphosphate	Protein
100.	***PKA***	Protein kinase A	Protein family
101.	***PKG***	Protein kinase G	Protein family
102.	***PNS***	Peripheral nervous system	Part of the nervous system
103.	***PTSD***	Post-Traumatic Stress Disorder	Disease
104.	***PTB***	Phosphotyrosine binding	Protein domain
105.	***PRR***	Pattern recognition receptor	Protein family
106.	***pSC neuron***	posterior scutellar neuron	Cell type
107.	***Pen-Strep***	Penicillin-Streptomycin	Antibiotic combination
108.	***Recombineering***	recombination mediated genomic engineering	Technique
109.	***RGC***	Retinal ganglion cell	Cell type
110.	***RNAi***	RNA interference	Technique
111.	***ROK***	Rho associated kinase	Protein family
112.	***RPTP***	Receptor tyrosine phosphatase	Protein family
113.	***RTK***	Receptor tyrosine kinase	Protein family
114.	***RT-PCR***	Real Time Quantitative PCR	Technique
115.	***Sc***	Scutellar	Anatomical localization in the fly
116.	***SEM***	Standard error of the means	Statistical method
117.	***SFK***	Src-family kinases	Protein family
118.	***SH2/3 domain***	Src-homology 2/3 domain	Protein domain
119.	***Slit2-N***	Slit2 N-terminal domain	Protein domain
120.	***S. maritima***	*Strigamia maritima*	Species
121.	***SFK***	Src family kinase	Protein family
122.	***SH2 domain***	Src-homology domain	Protein domain
123.	***T. castaneum***	*Tribolium castaneum*	Species
124.	***tet***	Tetracycline	Antibiotic
125.	***UAS***	Upstream activating sequence	DNA sequence
126.	***VDRC***	Vienna Drosophila research center	Fly resource
127.	***VNC***	Ventral nerve cord	Part of the nervous system of flies
128.	***WASP***	Wiskott Aldrich protein	Protein family
129.	***WB***	Western blot	Technique
130.	***WT***	Wild type	Genotype
131.	***Y-phosphorylation***	Tyrosine phosphorylation	Posttranslational protein modification
132.	***Y***	Tyrosine	Amino Acid
133.	***Y>F***	tyrosine to phenylalanine mutation	Technique

List of supplementary files

M&M TABLE 11. LIST OF SUPPLEMENTARY FILES.

The following files can be found on the supplementary CD:

#	Content	Folder/File name
1.	Amino acid sequences of the cytoplasmic domains of 62 different species used for ELM analysis	Dscam sequences
2.	Microarray Data	Microarrays
3.	Proteomic Data	Experiments conducted in Ghent

Acknowledgments

The work summarized in this dissertation is the result of my time as member of the Schmucker laboratory in Boston and in Leuven. In my time as graduate student I have had the privilege to work together and exchange ideas with many talented, creative and inspiring colleagues. I have learned to grow ideas in the constant exchange with others, and I have become better in communicating, discussing and defending my work. During this time, I have turned from a rather introvert biochemist into a person pursuing her passion for neuroscience, and thanks to the influence of many colleagues, I have adopted the fruit fly as my model organism of choice. I am thankful for the encouragement, the late night discussions and the different angles that each of you provided, however there are a few people who had a big impact on the way how I pursue my work which deserve a special mentioning in this dedicated section.

First, I would like to thank my supervisors ***Prof. Schmucker*** and ***Prof. Rose-John for*** supervising my research and the work towards this dissertation: ***Professor Rose-John***, I am immensely appreciating your support over the years, the continued contact and your interest in my work.

Dietmar, we have spent quite some time working together and it has been an enormous learning experience for me. I am grateful for the academic freedom that I had in your lab to explore my many areas of interest. Due to your decision to move from Boston to Leuven I had the opportunity to experience the academic culture in two different countries. I also saw what it takes to set up a new laboratory. Last but not least, you have taught me how important it is to not only do sound experiments but also to present them in meaningful and intuitive way. It was a long way from my first departmental seminar to the defense of this dissertation. I have always taken pride in being a member of the Schmucker lab and I will take away a wealth of personal and scientific memories and experiences.

My time in the Schmucker lab would also not have been the same without my colleagues and friends. I am fondly remembering the relatively small lab in Boston and the many laughs, discussions and good times I have shared with ***Akhila, Rachel, Jenny, Jing, Christoph and Xuyen***. Akhila in particular, had a very big impact on my scientific thinking, for which I am very grateful.

The "***Nerds and Geeks***" were my closest friends in Leuven and I am grateful to have such a fantastic group of people in my life! 2015 was a difficult year but it also made me realize what an exceptional group of friends I have. For example, I spent an entire evening at the Heilig Haart emergency room surrounded by friends in person and on the phone. That was a painful but memorable evening making me realize how privileged I am. Thank you for checking in on me constantly when I was sick and for all your support!

Especially, I would like to thank ***Tineke*** for being my closest co-worker who also has become a real friend. I think we made a fantastic team and I am happy that we still manage to stay in touch!

I am also very thankful to my colleague and friend ***Dan***, who worked on the PTP69D project together with me. Dan, I immensely appreciate your good spirit, your humor, your fairness and your sharp mind. It has been a pleasure to work so closely together and I hope that we will maintain our collaboration in the future!

The balance between work and life is always difficult to maintain in our job. However, there were some people who made sure that I enjoyed life outside the lab: In Boston, I made memories thanks to my friends ***Arndt, Maren and Markus*** and ***Marie*** but also because I was visited by the old crowd from Kiel, namely ***Johanna, Maren, Salvinia and Hendrik***, my sister ***Elisabeth*** and my brother ***Hartwig.***

Thank you also to my friend ***Kate*** for being my weekend refuge, for many memories and laughs, for your continued friendship, for spending the last evening before Belgium with me and for letting little Jimmy move to Belgium. The last couple of years would not have been possible without your support!

My brother ***Hartwig*** was another bulwark of support by listening to me in uncounted phone calls by encouraging me and by believing in me. You have also played an important part in making a new home here in Belgium! The same is true for my sister ***Elisabeth*** and my ***parents***: Thank you for always having an open ear in times of doubt and thank you for believing in me unconditionally. Thank you for always grounding me by pointing out that there is a life beyond science and for keeping me supplied with literature and food for thoughts.

A special thanks goes to my friends ***Sonja and Derya***. ***Sonja***, we have shared desks and benches for a long time and I will always fondly remember our Germany trips, our dinners

and all the good memories we both made in Belgium. ***Derya,*** you have had a big impact on my scientific thinking. Your love for science has been an inspiration to me. The uncounted discussions and your friendship made the transition to Belgium a lot easier!

Finally, I would like to sincerely thank the ***Boehringer Ingelheim Fonds***, Foundation for Basic Research in medicine (BIF), for their financial and general support. The sponsorship by the BIF did not only allow me to work undistracted on my PhD project but also enabled me to participate in many inspiring meetings. In addition, I also appreciate your continued interest in my work and the personal encouragement and support over the years!

See The Sky About To Rain

SEE THE SKY ABOUT TO RAIN,
BROKEN CLOUDS AND RAIN.
LOCOMOTIVE, PULL THE TRAIN,
WHISTLE BLOWING
THROUGH MY BRAIN.
SIGNALS CURLING ON AN OPEN PLAIN,
ROLLING DOWN THE TRACK AGAIN.
SEE THE SKY ABOUT TO RAIN.

SOME ARE BOUND FOR HAPPINESS,
SOME ARE BOUND TO GLORY
SOME ARE BOUND TO LIVE WITH LESS,
WHO CAN TELL YOUR STORY?

SEE THE SKY ABOUT TO RAIN,
BROKEN CLOUDS AND RAIN.
LOCOMOTIVE, PULL THE TRAIN,
WHISTLE BLOWIN'
THROUGH MY BRAIN.
SIGNALS CURLIN' ON AN OPEN PLAIN,
ROLLIN' DOWN THE TRACK AGAIN.
SEE THE SKY ABOUT TO RAIN.

I WAS DOWN IN DIXIE LAND,
PLAYED A SILVER FIDDLE
PLAYED IT LOUD AND THEN THE MAN
BROKE IT DOWN THE MIDDLE.
SEE THE SKY ABOUT TO RAIN.

Song performed by Neil Young.
Album: "Life at Massey Hall 1971" (2007)

Curriculum Vitae: Maria-Luise Erfurth

Address:	Mechelsestraat 161 bus 102 3000 Leuven Belgium
Date of birth:	25.3.1979
Place of birth:	Kiel
Nationality:	German

Education:

Doctoral student	Kiel University, Kiel, Germany and KU Leuven, Leuven, Belgium	March 2006- today January 2014- today
Diplom	Kiel University, Kiel, Germany Degree: Dipl. biochem.	March 2006
Abitur	Kieler Gelehrtenschule	July 1998

Working Experience:

Scientist	Molecular Neurogenomics Group Department of Molecular Genetics VIB and University of Antwerp Belgium	July 2015- today
PhD Researcher	Neuronal Wiring Laboratory Vesalius Research Center VIB and KU Leuven Belgium	October 2009-July 2015
PhD Researcher	Schmucker Laboratory Dana-Farber Cancer Institute Harvard Medical School USA	March 2006-October 2009
Diploma Student	Just Laboratory Institute for Biochemistry Kiel University Germany	March 2005-January 2006
Visiting Student	Fitch Laboratory New York University USA	November 2002-March 2003

Publications

Dascenco D*, **Erfurth ML*,** Izadifar A, Song M, Sachse S, Bortnick R, Urwyler O, Petrovic M, Ayaz D, He H, Kise Y, Thomas F, Kidd T, Schmucker D. "Slit and Receptor Tyrosine Phosphatase 69D Confer Spatial Specificity to Axon Branching via Dscam1" Cell (2015).

**** Equal contribution of first authors***

He H*, Kise Y*, Izadifar A, Urwyler O, Ayaz D, Parthasarthy A, Yan B, **Erfurth ML**, Dascenco D, Schmucker D. "Cell-Intrinsic Requirement of Dscam1 Isoform Diversity". Science (2014)

Langen M, Koch M, Yan J, De Geest N, **Erfurth ML**, Pfeiffer BD, Schmucker D, Moreau Y, Hassan BA. "Mutual inhibition among postmitotic neurons regulates robustness of brain wiring in Drosophila". Elife (2013)

Schwanbeck R, Schroeder T, Henning K, Kohlhof K, Rieber N, **Erfurth ML**, Just U. "Notch Signaling in Embryonic and Adult Myelopoiesis ". Cells Tissues Organs (2008)

Erfurth ML "Investigating Dscam signaling". B.I.F. FUTURA (2007)

Haikala V*, Schnell B, Claussen J, Forstner F, He H, **Erfurth ML**, Borst A, Schmucker D, Reiff D. "Altering dendritic field morphology of visual interneurons through Dscam1 affects dendritic physiology and optomotoric behavior" (Nature Neuroscience- under revision)

Oliva C., Soldano A, De Geest N, Mora N, Claeys A, **Erfurth ML**, Ramaekers A, Dascenco D, Schmucker D, Sanchez-Soriano N, Hassan B. (Developmental Cell- under revision)

Honors and Awards

Travel Stipend: Boehringer Ingelheim Fonds to attend CSHL Axon Guidance Meeting	September 2014
Travel Stipend: CSHL to attend CSHL Axon Guidance Meeting	September 2014
Long Term PhD Fellowship: Boehringer Ingelheim Fonds	December 2006- March 2009
Student Representative (CAU Kiel) 53rd Lindau Nobel Laureate Meeting	June 30th- July 4th 2003

General References

Abdallah, A.M., Zhou, X., Kim, C., Shah, K.K., Hogden, C., Schoenherr, J.A., Clemens, J.C., and Chang, H.C. (2013). Activated Cdc42 kinase regulates Dock localization in male germ cells during Drosophila spermatogenesis. Dev. Biol. *378*, 141–153.

Agarwala, K.L., Ganesh, S., Amano, K., Suzuki, T., and Yamakawa, K. (2001a). DSCAM, a highly conserved gene in mammals, expressed in differentiating mouse brain. Biochem. Biophys. Res. Commun. *281*, 697–705.

Agarwala, K.L., Ganesh, S., Tsutsumi, Y., Suzuki, T., Amano, K., and Yamakawa, K. (2001b). Cloning and functional characterization of DSCAML1, a novel DSCAM-like cell adhesion molecule that mediates homophilic intercellular adhesion. Biochem. Biophys. Res. Commun. *285*, 760–772.

Agarwala, K.L., Nakamura, S., Tsutsumi, Y., and Yamakawa, K. (2000). Down syndrome cell adhesion molecule DSCAM mediates homophilic intercellular adhesion. Brain Res. Mol. Brain Res. *79*, 118–126.

Ahmed, G., Shinmyo, Y., Ohta, K., Islam, S.M., Hossain, M., Naser, I.B., Riyadh, M.A., Su, Y., Zhang, S., Tessier-Lavigne, M., et al. (2011). Draxin inhibits axonal outgrowth through the netrin receptor DCC. J. Neurosci. *31*, 14018–14023.

Alberts, B., Johnson, A., Lewis, J., Morgan, D., Raff, M., Roberts, K., and Walter, P. (2014). Molecular Biology of the Cell, Sixth Edition (Garland Science).

Alves-Sampaio, A., Troca-Marín, J.A., and Montesinos, M.L. (2010). NMDA-mediated regulation of DSCAM dendritic local translation is lost in a mouse model of Down's syndrome. J. Neurosci. *30*, 13537–13548.

Amano, K., Fujii, M., Arata, S., Tojima, T., Ogawa, M., Morita, N., Shimohata, A., Furuichi, T., Itohara, S., Kamiguchi, H., et al. (2009). DSCAM deficiency causes loss of pre-inspiratory neuron synchroneity and perinatal death. Journal of Neuroscience *29*, 2984–2996.

Amano, K., Yamada, K., Iwayama, Y., Detera-Wadleigh, S.D., Hattori, E., Toyota, T., Tokunaga, K., Yoshikawa, T., and Yamakawa, K. (2008). Association study between the Down syndrome cell adhesion molecule (DSCAM) gene and bipolar disorder. Psychiatric Genetics *18*, 1–10.

Anastassiou, D., Liu, H., and Varadan, V. (2006). Variable window binding for mutually exclusive alternative splicing. Genome Biol. *7(1)*: R2.

Andrews, G.L., Tanglao, S., Farmer, W.T., Morin, S., Brotman, S., Berberoglu, M.A., Price, H., Fernandez, G.C., Mastick, G.S., Charron, F., et al. (2008). Dscam guides embryonic axons by Netrin-dependent and-independent functions. Development *135*, 3839–3848.

Armitage, S.A.O., Sun, W., You, X., Kurtz, J., Schmucker, D., and Chen, W. (2014). Quantitative Profiling of Drosophila melanogaster Dscam1 Isoforms Reveals No Changes in Splicing after Bacterial Exposure. PLoS ONE *9*, e108660.

Ashley-Koch, A.E., Garrett, M.E., Gibson, J., Liu, Y., Dennis, M.F., Kimbrel, N.A., Beckham, J.C., and Hauser, M.A. (2015). Genome-wide association study of posttraumatic stress disorder in a cohort of Iraq–Afghanistan era veterans. Journal of Affective Disorders *184*, 225–234.

Avadhanula, V., Weasner, B.P., Hardy, G.G., Kumar, J.P., and Hardy, R.W. (2009). A novel system for the launch of alphavirus RNA synthesis reveals a role for the Imd pathway in arthropod antiviral response. PLoS Pathog *5*, e1000582.

Azevedo, F., and Carvalho, L. (2009). Equal numbers of neuronal and nonneuronal cells make the human brain an

isometrically scaled-up primate brain. Journal of Comparative Neurology *513*:532-541.

Barlow, G.M., Micales, B., Lyons, G.E., and Korenberg, J.R. (2001). Down syndrome cell adhesion molecule is conserved in mouse and highly expressed in the adult mouse brain. Cytogenet. Cell Genet. *94*, 155–162.

Bashaw, G.J., and Goodman, C.S. (1999). Chimeric axon guidance receptors: the cytoplasmic domains of slit and netrin receptors specify attraction versus repulsion. Cell *97*, 917-926.

Bashaw, G.J. and Klein R. (2010). Signaling from Axon Guidance Receptors. Cold Spring Harb. Perspect. Biol. *2*, a001941.

Bateman, A., Eddy, S.R., and Chothia, C. (1996). Members of the immunoglobulin superfamily in bacteria. Protein Science *5*, 1939–1941.

Baumgartner, S., Martin, D., Chiquet-Ehrismann, R., Sutton, J., Desai, A., Huang, I., Kato, K., and Hromas, R. (1995). The HEM Proteins: A Novel Family of Tissue-specific Transmembrane Proteins Expressed from Invertebrates Through Mammals with an Essential Function in Oogenesis. Journal of Molecular Biology *251*, 41–49.

Bellen, H.J., Tong, C., and Tsuda, H. (2010). 100 years of Drosophila research and its impact on vertebrate neuroscience: a history lesson for the future. Nat. Rev. Neurosci. *11*, 514–522.

Bernard, C. (1974). Lectures on the phenomena common to animals and plants. Vol. 2, No. 1. Charles C Thomas Pub Ltd.

Bianco, A., Poukkula, M., Cliffe, A., Mathieu, J., Luque, C.M., Fulga, T.A., and Rørth, P. (2007). Two distinct modes of guidance signalling during collective migration of border cells. Nature *448*, 362–365.

Bianconi, E., Piovesan, A., Facchin, F., Beraudi, A., Casadei, R., Frabetti, F., Vitale, L., Pelleri, M.C., Tassani, S., Piva, F., et al. (2013). An estimation of the number of cells in the human body. Ann. Hum. Biol. *40*, 463–471.

Biersmith, B., Liu, Z.C., Bauman, K., and Geisbrecht, E.R. (2011). The DOCK protein sponge binds to ELMO and functions in Drosophila embryonic CNS development. PLoS ONE *6*, e16120.

Bilimoria, P.M., and Bonni, A. (2013). Molecular control of axon branching. The Neuroscientist *19*, 16–24.

Blank, M., Fuerst, P.G., Stevens, B., Nouri, N., Kirkby, L., Warrier, D., Barres, B.A., Feller, M.B., Huberman, A.D., Burgess, R.W., et al. (2011). The Down Syndrome Critical Region Regulates Retinogeniculate Refinement. J. Neurosci. *31*, 5764–5776.

Boehm, T. (2007). Two in one: dual function of an invertebrate antigen receptor. Nat Immunol *8*, 1031–1033.

Bogdan, S., and Klämbt, C. (2003). Kette regulates actin dynamics and genetically interacts with Wave and Wasp. Development *130*, 4427–4437.

Bogdan, S., Grewe, O., Strunk, M., Mertens, A., and Klämbt, C. (2004). Sra-1 interacts with Kette and Wasp and is required for neuronal and bristle development in Drosophila. Development *131*, 3981–3989.

Bogdan, S., Stephan, R., Lobke, C., Mertens, A., Klämbt, C. (2005). Abi activates WASP to promote sensory organ development. Nat. Cell Biol. *7(10)*: 977--984

Boutros, M., Agaisse, H., and Perrimon, N. (2002). Sequential activation of signaling pathways during innate immune responses in Drosophila. Developmental Cell *3*, 711–722.

Brehélin, M., and Roch, P. (2008). Specificity, learning and memory in the innate immune response. Inv. Surv. J. *5*: 103-109.

Brites, D., McTaggart, S., Morris, K., Anderson, J., Thomas, K., Colson, I., Fabbro, T., Little, T.J., Ebert, D., and Pasquier, Du, L. (2008). The Dscam homologue of the crustacean Daphnia is diversified by alternative splicing like in

insects. Mol Biol Evol *25*, 1429–1439.

Brites, D., Brena, C., Ebert, D., and Pasquier, Du, L. (2013). MORE THAN ONE WAY TO PRODUCE PROTEIN DIVERSITY: DUPLICATION AND LIMITED ALTERNATIVE SPLICING OF AN ADHESION MOLECULE GENE IN BASAL ARTHROPODS. Evolution *67*, 2999–3011.

Brose, K., Bland, K.S., Wang, K.H., Arnott, D., Henzel, W., Goodman, C.S., Tessier-Lavigne, M., and Kidd, T. (1999). Slit proteins bind Robo receptors and have an evolutionarily conserved role in repulsive axon guidance. Cell *96*, 795–806.

Brown, V., Jin, P., Ceman, S., Darnell, J.C., O'Donnell, W.T., Tenenbaum, S.A., Jin, X., Feng, Y., Wilkinson, K.D., Keene, J.D., et al. (2001). Microarray identification of FMRP-associated brain mRNAs and altered mRNA translational profiles in fragile X syndrome. Cell *107*, 477–487.

Bunt, S., Hooley, C., Hu, N., Scahill, C., Weavers, H., and Skaer, H. (2010). Hemocyte-secreted type IV collagen enhances BMP signaling to guide renal tubule morphogenesis in Drosophila. Developmental Cell *19*, 296–306.

Burnett, G., and Kennedy, E.P. (1954). The enzymatic phosphorylation of proteins. J. Biol. Chem. *211*, 969–980.

Celotto, A.M., and Graveley, B.R. (2001). Alternative splicing of the Drosophila Dscam pre-mRNA is both temporally and spatially regulated. Genetics *159*, 599–608.

Chambers, M.C., and Schneider, D.S. (2012). Pioneering immunology: insect style. Curr. Opin. Immunol. *24*, 10–14.

Chen, B.E., Kondo, M., Garnier, A., Watson, F.L., Püettmann-Holgado, R., Lamar, D.R., and Schmucker, D. (2006). The molecular diversity of Dscam is functionally required for neuronal wiring specificity in Drosophila. Cell *125*, 607–620.

Cheng, H.J., Nakamoto, M., Bergemann, A.D., and Flanagan, J.G. (1995). Complementary gradients in expression and binding of ELF-1 and Mek4 in development of the topographic retinotectal projection map. Cell *82*, 371–381.

Chiang, Y.-A., Hung, H.-Y., Lee, C.-W., Huang, Y.-T., and Wang, H.-C. (2013). Shrimp Dscam and its cytoplasmic tail splicing activator serine/arginine (SR)-rich protein B52 were both induced after white spot syndrome virus challenge. Fish Shellfish Immunol. *34*, 209–219.

Chipman, A.D., Ferrier, D.E.K., Brena, C., Qu, J., Hughes, D.S.T., Schroeder, R., Torres-Oliva, M., Znassi, N., Jiang, H., Almeida, F.C., et al. (2014). The First Myriapod Genome Sequence Reveals Conservative Arthropod Gene Content and Genome Organisation in the Centipede Strigamia maritima. PLOS Biol *12*(11), e1002005.

Cho, N.K., Keyes, L., Johnson, E., Heller, J., Ryner, L., Karim, F., and Krasnow, M.A. (2002). Developmental control of blood cell migration by the Drosophila VEGF pathway. Cell *108*, 865–876.

Chou, P.-H., Chang, H.-S., Chen, I.-T., Lee, C.-W., Hung, H.-Y., and Han-Ching Wang, K.C. (2011). Penaeus monodon Dscam (PmDscam) has a highly diverse cytoplasmic tail and is the first membrane-bound shrimp Dscam to be reported. Fish Shellfish Immunol. *30*, 1109–1123.

Chou, P.-H., Chang, H.-S., Chen, I.-T., Lin, H.-Y., Chen, Y.-M., Yang, H.-L., and Wang, K.C.H.-C. (2009). The putative invertebrate adaptive immune protein Litopenaeus vannamei Dscam (LvDscam) is the first reported Dscam to lack a transmembrane domain and cytoplasmic tail. Dev. Comp. Immunol. *33*, 1258–1267.

Cieśla, J., Frączyk, T., and Rode, W. (2011). Phosphorylation of basic amino acid residues in proteins: important but easily missed. Acta Biochim. Pol. *58*, 137–148.

Clemens, J.C., Ursuliak, Z., Clemens, K.K., Price, J.V., and Dixon, J.E. (1996). A Drosophila protein-tyrosine phosphatase associates with an adapter protein required for axonal guidance. J. Biol. Chem. *271*, 17002–17005.

Cohen, P. (2000). The regulation of protein function by multisite phosphorylation--a 25 year update. Trends in Biochemical Sciences *25*, 596–601.

Cohen, P. (2002a). The origins of protein phosphorylation. Nat. Cell Biol. *4*, E127–E130.

Cohen, P. (2002b). Protein kinases--the major drug targets of the twenty-first century? Nat Rev Drug Discov *1*, 309–315.

Corty, M.M., Matthews, B.J., and Grueber, W.B. (2009). Molecules and mechanisms of dendrite development in Drosophila. Development *136*, 1049–1061.

Crayton, M., Powell, B., Vision, T., and Giddings, M. (2006). Tracking the evolution of alternatively spliced exons within the Dscam family. BMC Evol. Biol. *6*, 16.

Cui, S., Lao, L., Duan, J., Jin, G., and Hou, X. (2013). Tyrosine phosphorylation is essential for DSCAML1 to promote dendrite arborization of mouse cortical neurons. Neurosci. Lett. *555*, 193–197.

Cvetkovska, V., Hibbert, A.D., Emran, F., and Chen, B.E. (2013). Overexpression of Down syndrome cell adhesion molecule impairs precise synaptic targeting. Nat Neurosci *16*, 677–682.

Dai, Z., and Peng, H.B. (1998). A role of tyrosine phosphatase in acetylcholine receptor cluster dispersal and formation. J. Cell Biol. *141*, 1613–1624.

Damasio, A. (2003). Looking for Spinoza: Joy, sorrow, and the feeling brain. Houghton Mifflin Harcourt. ISBN: 978-0156028714

Darnell, J.C., Van Driesche, S.J., Zhang, C., Hung, K.Y.S., Mele, A., Fraser, C.E., Stone, E.F., Chen, C., Fak, J.J., Chi, S.W., et al. (2011). FMRP stalls ribosomal translocation on mRNAs linked to synaptic function and autism. Cell *146*, 247–261.

Dascenco, D., Erfurth, M.-L., Izadifar, A., Song, M., Sachse, S., Bortnick, R., Urwyler, O., Petrovic, M., Ayaz, D., He, H., et al. (2015). Slit and Receptor Tyrosine Phosphatase 69D Confer Spatial Specificity to Axon Branching via Dscam1. Cell *162*, 1140–1154.

de Andrade, G.B., Kunzelman, L., Merrill, M.M., and Fuerst, P.G. (2014). Developmentally dynamic colocalization patterns of DSCAM with adhesion and synaptic proteins in the mouse retina. Mol. Vis. *20*, 1422–1433.

Dent, E.W., Gupton, S.L., and Gertler, F.B. (2011). The growth cone cytoskeleton in axon outgrowth and guidance. Cold Spring Harb Perspect Biol.

Desai, C.J., Sun, Q., and Zinn, K. (1997). Tyrosine phosphorylation and axon guidance: of mice and flies. Curr. Opin. Neurobiol. *7*, 70–74.

Dickson, B.J. (2002). Molecular mechanisms of axon guidance. Science *298*, 1959–1964.

Dinkel H, Van Roey K, Michael S, Davey NE, Weatheritt RJ, Born D, Speck T, Krüger D, Grebnev G, Kuban M, Strumillo M, Uyar B, Budd A, Altenberg B, Seiler M, Chemes LB, Glavina J, Sánchez IE, Diella F, Gibson TJ. (2014). The eukaryotic linear motif resource ELM: 10 years and counting. Nucleic Acids Research *42*: D259-66.

Dong, Y., Taylor, H.E., and Dimopoulos, G. (2006). AgDscam, a Hypervariable Immunoglobulin Domain-Containing Receptor of the Anopheles gambiae Innate Immune System. PLOS Biol *4*, e229.

Drescher, U., Kremoser, C., Handwerker, C., Löschinger, J., Noda, M., and Bonhoeffer, F. (1995). In vitro guidance of retinal ganglion cell axons by RAGS, a 25 kDa tectal protein related to ligands for Eph receptor tyrosine kinases. Cell *82*, 359–370.

Duchek, P., Somogyi, K., Jékely, G., Beccari, S., and Rørth, P. (2001). Guidance of cell migration by the Drosophila PDGF/VEGF receptor. Cell *107(1)*: 17-26.

Eckhart, W., Hutchinson, M.A., and Hunter, T. (1979). An activity phosphorylating tyrosine in polyoma T antigen immunoprecipitates. Cell *18 (4)*: 925-33.

Eguchi, K., Yoshioka, Y., Yoshida, H., Morishita, K., Miyata, S., Hiai, H., and Yamaguchi, M. (2013). The Drosophila DOCK family protein sponge is involved in differentiation of R7 photoreceptor cells. Exp. Cell Res. *319*, 2179–2195.

Fan, X., Labrador, J.P., Hing, H., and Bashaw, G.J. (2003). Slit stimulation recruits Dock and Pak to the roundabout receptor and increases Rac activity to regulate axon repulsion at the CNS midline. Neuron *40*, 113–127.

Fischer, E.H., and Krebs, E.G. (1955). Conversion of phosphorylase b to phosphorylase a in muscle extracts. J. Biol. Chem. *216*, 121–132.

Fischer, E.H., Tonks, N.K., and Charbonneau, H. (1989). Protein tyrosine phosphatases: a novel family of enzymes involved in transmembrane signalling. Adv. Second Messenger Phosphoprotein Res. *24*: 273-9.

Freeman, S.A., and Grinstein, S. (2014). Phagocytosis: receptors, signal integration, and the cytoskeleton. Immunol. Rev. *262*, 193–215.

Fuerst, P.G., Bruce, F., Rounds, R.P., Erskine, L., and Burgess, R.W. (2012). Cell autonomy of DSCAM function in retinal development. Dev. Biol. *361*, 326–337.

Fuerst, P.G., Bruce, F., Tian, M., Wei, W., Elstrott, J., Feller, M.B., Erskine, L., Singer, J.H., and Burgess, R.W. (2009). DSCAM and DSCAML1 function in self-avoidance in multiple cell types in the developing mouse retina. Neuron *64*, 484–497.

Fuerst, P.G., Koizumi, A., Masland, R.H., and Burgess, R.W. (2008). Neurite arborization and mosaic spacing in the mouse retina require DSCAM. Nature *451*, 470–U478.

Gafken, P.R., and Lampe, P.D. (2006). Methodologies for characterizing phosphoproteins by mass spectrometry. Cell Communication & Adhesion *13*, 249–262.

Gallo, G. (2013). More than one ring to bind them all: recent insights into the structure of the axon. Dev Neurobiol. *73*, (11):799-805.

Gao, H., Wu, X., and Fossett, N. (2009). Upregulation of the Drosophila Friend of GATA gene U-shaped by JAK/STAT signaling maintains lymph gland prohemocyte potency. Mol. Cell. Biol. *29*, 6086–6096.

Gergely, J., Pecht, I., and Sármay, G. (1999). Immunoreceptor tyrosine-based inhibition motif-bearing receptors regulate the immunoreceptor tyrosine-based activation motif-induced activation of immune competent cells. Immunol. Lett. *68*, 3–15.

Golgi, C. (1873). On the structure of the brain grey matter. Gazzetta Medica Italiana. Lombardia *33*:244-6.

Graveley, B.R. (2005). Mutually exclusive splicing of the insect Dscam pre-mRNA directed by competing intronic RNA secondary structures. Cell *123*, 65–73.

Graveley, B.R., Kaur, A., Gunning, D., Zipursky, S.L., Rowen, L., and Clemens, J.C. (2004). The organization and evolution of the dipteran and hymenopteran Down syndrome cell adhesion molecule (Dscam) genes. Rna *10*, 1499–1506.

Grossman, T.R., Gamliel, A., Wessells, R.J., Taghli-Lamallem, O., Jepsen, K., Ocorr, K., Korenberg, J.R., Peterson, K.L., Rosenfeld, M.G., Bodmer, R., et al. (2011). Over-expression of DSCAM and COL6A2 cooperatively generates congenital heart defects. PLoS Genet. *7*, e1002344.

Grueber, W.B., and Sagasti, A. (2010). Self-avoidance and tiling: Mechanisms of dendrite and axon spacing. Cold Spring Harb Perspect Biol *2*, a001750–a001750.

Grueber, W.B., Ye, B., Moore, A.W., Jan, L.Y., and Jan, Y.N. (2003). Dendrites of distinct classes of Drosophila sensory neurons show different capacities for homotypic repulsion. Curr. Biol. *13*, 618–626.

Guan, K.-L., and Rao, Y. (2003). Signalling mechanisms mediating neuronal responses to guidance cues. Nat. Rev. Neurosci. *4*, 941–956.

Guruharsha, K.G., Obar, R.A., Mintseris, J., Aishwarya, K., Krishnan, R.T., VijayRaghavan, K., and Artavanis-Tsakonas, S. (2014). Drosophila Protein interaction Map (DPiM). Fly *6*, 246–253.

Hall, A., and Lalli, G. (2010). Rho and Ras GTPases in axon growth, guidance, and branching. Cold Spring Harb. Perspect. Biol. *2* (2): a001818.

Han, S.M., Tsuda, H., Yang, Y., Vibbert, J., Cottee, P., Lee, S.-J., Winek, J., Haueter, C., Bellen, H.J., and Miller, M.A. (2012). Secreted VAPB/ALS8 major sperm protein domains modulate mitochondrial localization and morphology via growth cone guidance receptors. Developmental Cell *22*, 348–362.

Hassan, B.A., and Hiesinger, P.R. (2015). Beyond Molecular Codes: Simple Rules to Wire Complex Brains. Cell *163*, 285–291.

Hatta, K., Okada, T.S., and Takeichi, M. (1985). A monoclonal antibody disrupting calcium-dependent cell-cell adhesion of brain tissues: possible role of its target antigen in animal pattern formation. Proc. Natl. Acad. Sci. U.S.A. *82*, 2789–2793.

Hattori, D., Chen, Y., Matthews, B.J., Salwinski, L., Sabatti, C., Grueber, W.B., and Zipursky, S.L. (2009). Robust discrimination between self and non-self neurites requires thousands of Dscam1 isoforms. Nature *461*, 644–648.

Hatzihristidis, T., Desai, N., Hutchins, A.P., Meng, T.-C., Tremblay, M.L., and Miranda-Saavedra, D. (2015). A Drosophila-centric view of protein tyrosine phosphatases. FEBS Lett. *589*, 951–966.

He, H., Kise, Y., Izadifar, A., Urwyler, O., Ayaz, D., Parthasarthy, A., Yan, B., Erfurth, M.-L., Dascenco, D., and Schmucker, D. (2014a). Cell-intrinsic requirement of Dscam1 isoform diversity for axon collateral formation. Science *344*, 1182–1186.

He, R., Yu, Z., Zhang, R., and Zhang, Z. (2014b). Protein tyrosine phosphatases as potential therapeutic targets. Acta Pharmacologica Sinica *35*(10):1227-46.

Heasman, S.J., and Ridley, A.J. (2008). Mammalian Rho GTPases: new insights into their functions from in vivo studies. Nat. Rev. Mol. Cell Biol. *9*, 690–701.

Hedgecock, E.M., Culotti, J.G., and Hall, D.H. (1990). The unc-5, unc-6, and unc-40 genes guide circumferential migrations of pioneer axons and mesodermal cells on the epidermis in C. elegans. Neuron *4*, 61–85.

Heino, T.I., Kärpänen, T., Wahlström, G., Pulkkinen, M., Eriksson, U., Alitalo, K., and Roos, C. (2001). The Drosophila VEGF receptor homolog is expressed in hemocytes. Mech. Dev. *109*, 69–77.

Hendriks, W.J.A.J., Elson, A., Harroch, S., Pulido, R., Stoker, A., and Hertog, den, J. (2013). Protein tyrosine phosphatases in health and disease. Febs J. *280*, 708–730.

Hernández, G., del Mar Castellano, M., Agudo, M., and Sierra, J.M. (1998). Isolation and characterization of the cDNA and the gene for eukaryotic translation initiation factor 4G from Drosophila melanogaster. Eur. J. Biochem. *253*, 27–35.

Hernández, G., Altmann, M., Sierra, J.M., Urlaub, H., Diez del Corral, R., Schwartz, P., and Rivera-Pomar, R. (2005). Functional analysis of seven genes encoding eight translation initiation factor 4E (eIF4E) isoforms in Drosophila. Mech. Dev. *122*, 529–543.

Hernández, G., Lalioti, V., Vandekerckhove, J., Sierra, J.M., and Santarén, J.F. (2004). Identification and characterization of the expression of the translation initiation factor 4A (eIF4A) from Drosophila melanogaster. Proteomics *4*, 316–326.

Hing, H., Xiao, J., Harden, N., Lim, L., and Zipursky, S.L. (1999). Pak functions downstream of Dock to regulate photoreceptor axon guidance in Drosophila. Cell *97*, 853–863.

Huang, H., Shao, Q., Qu, C., Yang, T., Dwyer, T., and Liu, G. (2015). Coordinated interaction of Down syndrome cell adhesion molecule and deleted in colorectal cancer with dynamic TUBB3 mediates Netrin-1-induced axon branching. Neuroscience *293*, 109–122.

Hughes, M.E., Bortnick, R., Tsubouchi, A., Bäumer, P., Kondo, M., Uemura, T., and Schmucker, D. (2007). Homophilic Dscam interactions control complex dendrite morphogenesis. Neuron *54*, 417–427.

Huh, G.S., Boulanger, L.M., Du, H., Riquelme, P.A., Brotz, T.M., and Shatz, C.J. (2000). Functional requirement for class I MHC in CNS development and plasticity. Science *290*, 2155–2159.

Hulpiau, P., and van Roy, F. (2009). Molecular evolution of the cadherin superfamily. The International Journal of Biochemistry & Cell Biology *41*, 349–369.

Hummel, T., Leifker, K., and Klämbt, C. (2000). The Drosophila HEM-2/NAP1 homolog KETTE controls axonal pathfinding and cytoskeletal organization. Genes & Development *14*, 863–873.

Hummel, T., Vasconcelos, M.L., Clemens, J.C., Fishilevich, Y., Vosshall, L.B., and Zipursky, S.L. (2003). Axonal targeting of olfactory receptor neurons in Drosophila is controlled by Dscam. Neuron *37*, 221–231.

Hung, H.-Y., Ng, T.H., Lin, J.-H., Chiang, Y.-A., Chuang, Y.-C., and Wang, H.-C. (2013). Properties of Litopenaeus vannamei Dscam (LvDscam) isoforms related to specific pathogen recognition. Fish Shellfish Immunol. *35*, 1272–1281.

Hunter, T. (2009). Tyrosine phosphorylation: thirty years and counting. Current Opinion in Cell Biology *21*, 140–146.

Hunter, T. (2014). The genesis of tyrosine phosphorylation. Cold Spring Harb Perspect Biol *6*(5), a020644.

Isakov, N. (1998). ITAMs: immunoregulatory scaffolds that link immunoreceptors to their intracellular signaling pathways. Recept. Channels *5*, 243–253.

Ishii, N., Wadsworth, W.G., Stern, B.D., Culotti, J.G., and Hedgecock, E.M. (1992). UNC-6, a laminin-related protein, guides cell and pioneer axon migrations in C. elegans. Neuron *9*, 873–881.

Jan, Y.N., and Jan, L.Y. (2010). Branching out: mechanisms of dendritic arborization. Nat. Rev. Neurosci. *11(5):* 316-28.

Jang, A.C.-C., Chang, Y.-C., Bai, J., and Montell, D. (2009). Border-cell migration requires integration of spatial and temporal signals by the BTB protein Abrupt. Nat. Cell Biol. *11*, 569–579.

Jin, X.-K., Li, W.-W., Wu, M.-H., Guo, X.-N., Li, S., Yu, A.-Q., Zhu, Y.-T., He, L., and Wang, Q. (2013). Immunoglobulin superfamily protein Dscam exhibited molecular diversity by alternative splicing in hemocytes of crustacean, Eriocheir sinensis. Fish Shellfish Immunol. *35*, 900–909.

Johnson, K.G., and Van Vactor, D. (2003). Receptor protein tyrosine phosphatases in nervous system development. Physiological Reviews *83*, 1–24.

Johnson, K.N., van Hulten, M.C.W., and Barnes, A.C. (2008). "Vaccination" of shrimp against viral pathogens: phenomenology and underlying mechanisms. Vaccine *26*, 4885–4892.

Julien, S.G., Dubé, N., Hardy, S., and Tremblay, M.L. (2011). Inside the human cancer tyrosine phosphatome. Nat. Rev. Cancer *11*, 35–49.

Kaipa, B.R., Shao, H., Schäfer, G., Trinkewitz, T., Groth, V., Liu, J., Beck, L., Bogdan, S., Abmayr, S.M., and Onel, S.F. (2013). Dock mediates Scar-and WASp-dependent actin polymerization through interaction with cell adhesion molecules in founder cells and fusion-competent myoblasts. J. Cell. Sci. *126*, 360–372.

Kalil, K., and Dent, E.W. (2014). Branch management: mechanisms of axon branching in the developing vertebrate CNS. Nat. Rev. Neurosci. *15*, 7–18.

Kennedy, T.E., Serafini, T., De la Torre, J.R., and Tessier-Lavigne, M. (1994). Netrins are diffusible chemotropic factors for commissural axons in the embryonic spinal cord. Cell *78*, 425–435.

Kenny, N.J., Shen, X., Chan, T.T.H., Wong, N.W.Y., Chan, T.F., Chu, K.H., Lam, H.-M., and Hui, J.H.L. (2015).

Genome of the Rusty Millipede, Trigoniulus corallinus, Illuminates Diplopod, Myriapod, and Arthropod Evolution. Genome Biol Evol *7*, 1280–1295.

Khongphinitbunjong, K., de Guzman, L.I., Tarver, M.R., Rinderer, T.E., Chen, Y., and Chantawannakul, P. (2015). Differential viral levels and immune gene expression in three stocks of Apis mellifera induced by different numbers of Varroa destructor. Journal of Insect Physiology *72*, 28–34.

Kidd, T., Bland, K.S., and Goodman, C.S. (1999). Slit is the midline repellent for the robo receptor in Drosophila. Cell *96*, 785–794.

Kiger, A.A., Baum, B., Jones, S., Jones, M.R., Coulson, A., Echeverri, C., and Perrimon, N. (2003). A functional genomic analysis of cell morphology using RNA interference. J. Biol. *2*, 27.

Kim, J.H., Wang, X., Coolon, R., and Ye, B. (2013). Dscam Expression Levels Determine Presynaptic Arbor Sizes in Drosophila Sensory Neurons. Neuron *78*, 827–838.

Kim, L.K., Choi, U.Y., Cho, H.S., Lee, J.S., Lee, W.-B., Kim, J., Jeong, K., Shim, J., Kim-Ha, J., and Kim, Y.-J. (2007). Down-regulation of NF-kappaB target genes by the AP-1 and STAT complex during the innate immune response in Drosophila. PLOS Biol *5*, e238.

Kleino, A., Valanne, S., Ulvila, J., Kallio, J., Myllymäki, H., Enwald, H., Stöven, S., Poidevin, M., Ueda, R., Hultmark, D., et al. (2005). Inhibitor of apoptosis 2 and TAK1-binding protein are components of the Drosophila Imd pathway. Embo J *24*, 3423–3434.

Kohmura, N., Senzaki, K., Hamada, S., Kai, N., Yasuda, R., Watanabe, M., Ishii, H., Yasuda, M., Mishina, M., and Yagi, T. (1998). Diversity Revealed by a Novel Family of Cadherins Expressed in Neurons at a Synaptic Complex. Neuron *20*, 1137–1151.

Kolodkin, A.L., and Tessier-Lavigne, M. (2011). Mechanisms and molecules of neuronal wiring: a primer. Cold Spring Harb Perspect Biol *3*, a001727–a001727.

Kolodkin, A.L., Matthes, D.J., and Goodman, C.S. (1993). The semaphorin genes encode a family of transmembrane and secreted growth cone guidance molecules. Cell *75*, 1389–1399.

Krebs, E.G., and Fischer, E.H. (1956). The phosphorylase b to a converting enzyme of rabbit skeletal muscle. Biochim. Biophys. Acta *20*, 150–157.

Ku, H.Y., Wu, C.L., Rabinow, L., Chen, G.C., and Meng, T.C. (2009). Organization of F-actin via concerted regulation of Kette by PTP61F and dAbl. Mol. Cell. Biol. *29*, 3623–3632.

Kurtz, J., and Franz, K. (2003). Innate defence: Evidence for memory in invertebrate immunity. Nature *425*, 37–38.

Lasko, P. (2000). The drosophila melanogaster genome: translation factors and RNA binding proteins. J. Cell Biol. *150*, F51–F56.

Le Floc'h, A., and Huse, M. (2015). Molecular mechanisms and functional implications of polarized actin remodeling at the T cell immunological synapse. Cellular and Molecular Life Sciences *72*(3): 537-56.

Lefebvre, J.L., Kostadinov, D., Chen, W.V., Maniatis, T., and Sanes, J.R. (2012). Protocadherins mediate dendritic self-avoidance in the mammalian nervous system. Nature *488*, 517–521.

Li, H.S., Chen, J.H., Wu, W., Fagaly, T., Zhou, L., Yuan, W., Dupuis, S., Jiang, Z.H., Nash, W., Gick, C., et al. (1999). Vertebrate slit, a secreted ligand for the transmembrane protein roundabout, is a repellent for olfactory bulb axons. Cell *96*, 807–818.

Li, H.-L., Huang, B.S., Vishwasrao, H., Sutedja, N., Chen, W., Jin, I., Hawkins, R.D., Bailey, C.H., and Kandel, E.R. (2009). Dscam mediates remodeling of glutamate receptors in Aplysia during de novo and learning-related synapse formation. Neuron *61*, 527–540.

Li, J., Li, W., Calhoun, H.C., Xia, F., Gao, F.-B., and Li, W.X. (2003). Patterns and functions of STAT activation during Drosophila embryogenesis. Mech. Dev. *120*, 1455–1468.

Li, S., Sukeena, J.M., Simmons, A.B., Hansen, E.J., Nuhn, R.E., Samuels, I.S., and Fuerst, P.G. (2015). DSCAM promotes refinement in the mouse retina through cell death and restriction of exploring dendrites. J. Neurosci. *35*, 5640–5654.

Li, W., Fan, J., and Woodley, D.T. (2001). Nck/Dock: an adapter between cell surface receptors and the actin cytoskeleton. Oncogene *20*, 6403–6417.

Lin, A.C., and Holt, C.E. (2008). Function and regulation of local axonal translation. Curr. Opin. Neurobiol. *18*, 60–68.

Liu, G., Li, W., Wang, L., Kar, A., Guan, K.-L., Rao, Y., and Wu, J.Y. (2009). DSCAM functions as a netrin receptor in commissural axon pathfinding. Proc. Natl. Acad. Sci. U.S.A. *106*, 2951–2956.

Loewen, C.J.R., Roy, A., and Levine, T.P. (2003). A conserved ER targeting motif in three families of lipid binding proteins and in Opi1p binds VAP. Embo J *22*, 2025–2035.

Logue, M.W., Smith, A.K., Baldwin, C., Wolf, E.J., Guffanti, G., Ratanatharathorn, A., Stone, A., Schichman, S.A., Humphries, D., Binder, E.B., et al. (2015). An analysis of gene expression in PTSD implicates genes involved in the glucocorticoid receptor pathway and neural responses to stress. Psychoneuroendocrinology *57*, 1–13.

Lowery, L.A., and Van Vactor, D. (2009). The trip of the tip: understanding the growth cone machinery. Nat. Rev. Mol. Cell Biol. *10*(5), pp.332-343.

Luo, Y., Raible, D., and Raper, J.A. (1993). Collapsin: a protein in brain that induces the collapse and paralysis of neuronal growth cones. Cell *75*, 217–227.

Ly, A., Nikolaev, A., Suresh, G., Zheng, Y., Tessier-Lavigne, M., and Stein, E. (2008). DSCAM is a netrin receptor that collaborates with DCC in mediating turning responses to netrin-1. Cell *133*, 1241–1254.

Malnic, B., Godfrey, P.A., and Buck, L.B. (2004). The human olfactory receptor gene family. Proc. Natl. Acad. Sci. U.S.A. *101*, 2584–2589.

Mandell, J.W., and Banker, G.A. (1998). Selective blockade of axonogenesis in cultured hippocampal neurons by the tyrosine phosphatase inhibitor orthovanadate. Journal of neurobiology *35(1)*, pp.17-28.

Mann, M., Ong, S.E., Grønborg, M., Steen, H., Jensen, O.N., and Pandey, A. (2002). Analysis of protein phosphorylation using mass spectrometry: deciphering the phosphoproteome. Trends Biotechnol. *20*, 261–268.

Manning, G., Whyte, D.B., Martinez, R., Hunter, T., and Sudarsanam, S. (2002a). The protein kinase complement of the human genome. Science *298*, 1912–1934.

Manning, G., Plowman, G.D., Hunter, T., and Sudarsanam, S. (2002b). Evolution of protein kinase signaling from yeast to man. Trends in Biochemical Sciences *27*, 514–520.

Manser, E., Leung, T., Salihuddin, H., Zhao, Z.S., and Lim, L. (1994). A brain serine/threonine protein kinase activated by Cdc42 and Rac1. Nature *367*, 40–46.

Mason, C.A., and Wang, L.C. (1997). Growth cone form is behavior-specific and, consequently, position-specific along the retinal axon pathway. The Journal of Neuroscience. *17*(3), pp.1086-1100.

Mathieu, J., Sung, H.-H., Pugieux, C., Soetaert, J., and Rørth, P. (2007). A sensitized PiggyBac-based screen for regulators of border cell migration in Drosophila. Genetics *176*, 1579–1590.

Matthews, B.J., Kim, M.E., Flanagan, J.J., Hattori, D., Clemens, J.C., Zipursky, S.L., and Grueber, W.B. (2007). Dendrite self-avoidance is controlled by Dscam. Cell *129*, 593–604.

Maynard, K.R., and Stein, E. (2012). DSCAM contributes to dendrite arborization and spine formation in the developing cerebral cortex. Journal of Neuroscience *32*, 16637–16650.

McDonald, J.A., Pinheiro, E.M., Kadlec, L., Schupbach, T., and Montell, D.J. (2006). Multiple EGFR ligands participate in guiding migrating border cells. Dev. Biol. *296*, 94–103.

Meijers, R., Püettmann-Holgado, R., Skiniotis, G., Liu, J.-H., Walz, T., Wang, J.-H., and Schmucker, D. (2007). Structural basis of Dscam isoform specificity. Nature *449*, 487–491.

Meister, M. (2004). Blood cells of Drosophila: cell lineages and role in host defence. Curr. Opin. Immunol. *16*, 10–15.

Mendoza, M.C. (2013). Phosphoregulation of the WAVE regulatory complex and signal integration. Seminars in Cell & Developmental Biology *24*, 272–279.

Millard, S.S., Lu, Z., Zipursky, S.L., and Meinertzhagen, I.A. (2010). Drosophila dscam proteins regulate postsynaptic specificity at multiple-contact synapses. Neuron *67*, 761–768.

Miller, W.T. (2012). Tyrosine kinase signaling and the emergence of multicellularity. Biochim. Biophys. Acta *1823*, 1053–1057.

Missler, M., and Südhof, T.C. (1998a). Neurexins: three genes and 1001 products. Trends Genet. *14*, 20–26.

Missler, M., and Südhof, T.C. (1998b). Neurexophilins form a conserved family of neuropeptide-like glycoproteins. J. Neurosci. *18*, 3630–3638.

Mitne-Neto, M., Silva, H., and Richieri-Costa, A. (2004). A mutation in the vesicle-trafficking protein VAPB causes late-onset spinal muscular atrophy and amyotrophic lateral sclerosis. The American Journal of Human Genetics, *75*(5), pp.822-831.

Miura, S.K., Martins, A., Zhang, K.X., Graveley, B.R., and Zipursky, S.L. (2013). Probabilistic splicing of Dscam1 establishes identity at the level of single neurons. Cell *155*, 1166–1177.

Mondal, B.C., Shim, J., Evans, C.J., and Banerjee, U. (2014). Pvr expression regulators in equilibrium signal control and maintenance of Drosophila blood progenitors. Elife *3*, e03626.

Montesinos, M.L. (2014). Roles for DSCAM and DSCAML1 in central nervous system development and disease. Adv Neurobiol *8*, 249–270.

Morales Diaz, H.D. (2014). Down syndrome cell adhesion molecule is important for early development in Xenopus tropicalis. Genesis *52*, 849–857.

Morales, J., Hiesinger, P.R., Schroeder, A.J., Kume, K., Verstreken, P., Jackson, F.R., Nelson, D.L., and Hassan, B.A. (2002). Drosophila fragile X protein, DFXR, regulates neuronal morphology and function in the brain. Neuron *34*, 961–972.

Muda, M., Worby, C.A., Simonson-Leff, N., Clemens, J.C., and Dixon, J.E. (2002). Use of double-stranded RNA-mediated interference to determine the substrates of protein tyrosine kinases and phosphatases. Biochem. J. *366*, 73–77.

Neduva, V., and Russell, R.B. (2005). Linear motifs: evolutionary interaction switches. FEBS Lett. *579*, 3342–3345.

Negro, A., Brunati, A.M., and Donella-Deana, A. (2002). Multiple phosphorylation of α-synuclein by protein tyrosine kinase Syk prevents eosin-induced aggregation. The FASEB Journal, *16*(2), pp.210-212.

Neugebauer, K.M., Tomaselli, K.J., Lilien, J., and Reichardt, L.F. (1988). N-cadherin, NCAM, and integrins promote retinal neurite outgrowth on astrocytes in vitro. J. Cell Biol. *107*, 1177–1187.

Neves, G., and Chess, A. (2004). Dscam-mediated self- versus non-self-recognition by individual neurons. Cold Spring Harb. Symp. Quant. Biol. *69*, 485–488.

Neves, G., Zucker, J., Daly, M., and Chess, A. (2004). Stochastic yet biased expression of multiple Dscam splice variants by individual cells. Nat. Genet. *36*, 240–246.

Ng, T.H., Chiang, Y.A., Yeh, Y.C., and Wang, H.C. (2015). Reprint of "Review of Dscam-mediated immunity in shrimp and other arthropods." Dev. Comp. Immunol. *48*, 306–314.

Ng, T.H., Hung, H.-Y., Chiang, Y.-A., Lin, J.-H., Chen, Y.-N., Chuang, Y.-C., and Wang, H.-C. (2014). WSSV-induced crayfish Dscam shows durable immune behavior. Fish Shellfish Immunol. *40*, 78–90.

Nguyen, L.K., Matallanas, D., and Croucher, D.R. (2013). Signalling by protein phosphatases and drug development: a systems-centred view. Febs Journal*, 280(2), pp.751-765.*

Obenauer, J.C., Cantley, L.C., and Yaffe, M.B. (2003). Scansite 2.0: Proteome-wide prediction of cell signaling interactions using short sequence motifs. Nucleic acids research, *31*(13), pp.3635-3641.

Oesterle, A. (2011). P-1000 & P-97 Pipette Cookbook, Sutter Instrument Co, http://www.sutter.com/PDFs/pipette_cookbook.pdf

Okumura, M., Sakuma, C., Miura, M., and Chihara, T. (2015). Linking Cell Surface Receptors to Microtubules: Tubulin Folding Cofactor D Mediates Dscam Functions during Neuronal Morphogenesis. Journal of Neuroscience *35*, 1979–1990.

Olofsson, B., and Page, D.T. (2005). Condensation of the central nervous system in embryonic Drosophila is inhibited by blocking hemocyte migration or neural activity. Dev. Biol. *279*, 233–243.

Olson, S., Blanchette, M., Park, J., Savva, Y., Yeo, G.W., Yeakley, J.M., Rio, D.C., and Graveley, B.R. (2007). A regulator of Dscam mutually exclusive splicing fidelity. Nature Structural & Molecular Biology *14*, 1134–1140.

Owen, D.J., and Evans, P.R. (1998). A structural explanation for the recognition of tyrosine-based endocytotic signals. Science *282*, 1327–1332.

Pak, C.W., Flynn, K.C., and Bamburg, J.R. (2008). Actin-binding proteins take the reins in growth cones. Nat. Rev. Neurosci. *9*, 136–147.

Papoulas, O., Monzo, K.F., Cantin, G.T., Ruse, C., Yates, J.R., Ryu, Y.H., and Sisson, J.C. (2010). dFMRP and Caprin, translational regulators of synaptic plasticity, control the cell cycle at the Drosophila mid-blastula transition. Development *137*, 4201–4209.

Park, J.W., Parisky, K., Celotto, A.M., Reenan, R.A., and Graveley, B.R. (2004). Identification of alternative splicing regulators by RNA interference in Drosophila. Proc. Natl. Acad. Sci. U.S.A. *101*, 15974–15979.

Paterson, W.D., and Stewart, J.E. (1979). Rate and duration of phagocytic increase in lobsters induced by Pseudomonas perolens endotoxin. Dev. Comp. Immunol. *3*, 353–357.

Pawson, T., Gish, G.D., and Nash, P. (2001). SH2 domains, interaction modules and cellular wiring. Trends Cell Biol. *11*, 504–511.

Pawson, T. (2004). Specificity in signal transduction: from phosphotyrosine-SH2 domain interactions to complex cellular systems. Cell *116*, 191–203.

Pennetta, G., Hiesinger, P.R., Fabian-Fine, R., Meinertzhagen, I.A., and Bellen, H.J. (2002). Drosophila VAP-33A directs bouton formation at neuromuscular junctions in a dosage-dependent manner. Neuron *35*, 291–306.

Pham, L.N., and Schneider, D.S. (2008). Evidence for specificity and memory in the insect innate immune response. Insect Immunology, (Elsevier), pp. 97–127.

Pierschbacher, M.D., and Ruoslahti, E. (1983). Cell attachment activity of fibronectin can be duplicated by small synthetic fragments of the molecule. Nature, 309(5963), p.30.

Piper, M., Lee, A.C., van Horck, F.P.G., McNeilly, H., Lu, T.B., Harris, W.A., and Holt, C.E. (2015). Erratum to: Differential requirement of F-actin and microtubule cytoskeleton in cue-induced local protein synthesis in axonal growth cones. Neural Dev *10*, 3.

Powell, A., Pope, E.C., Eddy, F.E., Roberts, E.C., Shields, R.J., Francis, M.J., Smith, P., Topps, S., Reid, J., and Rowley, A.F. (2011). Enhanced immune defences in Pacific white shrimp (Litopenaeus vannamei) post-exposure to a vibrio vaccine. J. Invertebr. Pathol. *107*, 95–99.

Purohit, A.A., Li, W., Qu, C., Dwyer, T., Shao, Q., Guan, K.L., and Liu, G. (2012). Down syndrome cell adhesion molecule (DSCAM) associates with uncoordinated-5C (UNC5C) in netrin-1-mediated growth cone collapse. J. Biol. Chem. *287*, 27126–27138.

Rees, J.S., Lowe, N., Armean, I.M., Roote, J., Johnson, G., Drummond, E., Spriggs, H., Ryder, E., Russell, S., Johnston, D.S., et al. (2011). In vivo analysis of proteomes and interactomes using parallel affinity capture (iPAC) coupled to mass spectrometry. Molecular & Cellular Proteomics *10*, M110.002386–M110.002386.

Richter, J.D., and Sonenberg, N. (2005). Regulation of cap-dependent translation by eIF4E inhibitory proteins. Nature *433*, 477–480.

Riddell, C.E., Garces, J., and Adams, S. (2014). Differential gene expression and alternative splicing in insect immune specificity. BMC genomics, *15*(1), p.1.

Rimer, J., Cohen, I.R., and Friedman, N. (2014). Do all creatures possess an acquired immune system of some sort? Bioessays *36*, 273–281.

Rodriguez, A.J., Czaplinski, K., Condeelis, J.S., and Singer, R.H. (2008). Mechanisms and cellular roles of local protein synthesis in mammalian cells. Current Opinion in Cell Biology *20*, 144–149.

Rogers, M.V., Buensuceso, C., Montague, F., and Mahadevan, L. (1994). Vanadate stimulates differentiation and neurite outgrowth in rat pheochromocytoma PC12 cells and neurite extension in human neuroblastoma SH-SY5Y cells. Neuroscience *60*(2), pp.479-494.

Röper, K., Gregory, S.L., and Brown, N.H. (2002). The "spectraplakins": cytoskeletal giants with characteristics of both spectrin and plakin families. J. Cell. Sci. *115*, 4215–4225.

Ruan, W., Pang, P., and Rao, Y. (1999). The SH2/SH3 adaptor protein dock interacts with the Ste20-like kinase misshapen in controlling growth cone motility. Neuron *24*, 595–605.

Rust, M.B. (2015). ADF/cofilin: a crucial regulator of synapse physiology and behavior. Cellular and Molecular Life Sciences, *72*(18), pp.3521-3529.

Sadd, B.M., and Schmid-Hempel, P. (2006). Insect Immunity Shows Specificity in Protection upon Secondary Pathogen Exposure. Current Biology *16*, 1206–1210.

Sadowski, I., Stone, J.C., and Pawson, T. (1986). A noncatalytic domain conserved among cytoplasmic protein-tyrosine kinases modifies the kinase function and transforming activity of Fujinami sarcoma virus P130gag-fps. Mol. Cell. Biol. *6*, 4396–4408.

Saito, Y., Oka, A., Mizuguchi, M., Motonaga, K., Mori, Y., Becker, L.E., Arima, K., Miyauchi, J., and Takashima, S. (2000). The developmental and aging changes of Down"s syndrome cell adhesion molecule expression in normal and Down"s syndrome brains. Acta Neuropathol. *100*, 654–664.

Sanes, J.R., and Zipursky, S.L. (2010). Design principles of insect and vertebrate visual systems. Neuron *66*, 15–36.

Sawaya, M.R., Wojtowicz, W.M., Andre, I., Qian, B., Wu, W., Baker, D., Eisenberg, D., and Zipursky, S.L. (2008). A double S shape provides the structural basis for the extraordinary binding specificity of Dscam isoforms. Cell *134*, 1007–1018.

Schäfer, G., Weber, S., Holz, A., and Bogdan, S. (2007). The Wiskott–Aldrich syndrome protein (WASP) is essential for myoblast fusion in Drosophila. Developmental biology, *304*(2), pp.664-674.

Schenck, A., Bardoni, B., Langmann, C., and Harden, N. (2003). CYFIP/Sra-1 controls neuronal connectivity in Drosophila and links the Rac1 GTPase pathway to the fragile X protein. Neuron, *38*(6), pp.887-898.

Schenck, A., Qurashi, A., Carrera, P., Bardoni, B., Diebold, C., Schejter, E., Mandel, J.-L., and Giangrande, A. (2004). WAVE/SCAR, a multifunctional complex coordinating different aspects of neuronal connectivity. Dev. Biol. *274*, 260–270.

Schmucker, D., and Chen, B. (2009). Dscam and DSCAM: complex genes in simple animals, complex animals yet simple genes. Genes & Development *23*, 147–156.

Schmucker, D., Clemens, J.C., Shu, H., Worby, C.A., Xiao, J., Muda, M., Dixon, J.E., and Zipursky, S.L. (2000). Drosophila Dscam is an axon guidance receptor exhibiting extraordinary molecular diversity. Cell *101*, 671–684.

Schnorr, J.D., Holdcraft, R., Chevalier, B., and Berg, C.A. (2001). Ras1 interacts with multiple new signaling and cytoskeletal loci in Drosophila eggshell patterning and morphogenesis. Genetics *159*, 609–622.

Serafini, T., Kennedy, T.E., Gaiko, M.J., and Mirzayan, C. (1994). The netrins define a family of axon outgrowth-promoting proteins homologous to C. elegans UNC-6. Cell, *78*(3), pp.409-424.

Shen, L., Xiao, Z., Pan, Y., Fang, M., Li, C., Chen, D., Wang, L., Xi, Z., Xiao, F., and Wang, X. (2011). Altered expression of Dscam in temporal lobe tissue from human and experimental animals. Synapse *65*, 975–982.

Shi, L., Yu, H.H., Yang, J.S., and Lee, T. (2007). Specific Drosophila Dscam Juxtamembrane Variants Control Dendritic Elaboration and Axonal Arborization. Journal of Neuroscience *27*, 6723–6728.

Silver, D.L., and Montell, D.J. (2001). Paracrine signaling through the JAK/STAT pathway activates invasive behavior of ovarian epithelial cells in Drosophila. Cell *107*, 831–841.

Silver, J., and Rutishauser, U. (1984). Guidance of optic axons in vivo by a preformed adhesive pathway on neuroepithelial endfeet. Dev. Biol. *106*, 485–499.

Sisson, J.C., Field, C., Ventura, R., Royou, A., and Sullivan, W. (2000). Lava lamp, a novel peripheral golgi protein, is required for Drosophila melanogaster cellularization. J. Cell Biol. *151*, 905–918.

Soba, P., Zhu, S., Emoto, K., Younger, S., Yang, S.-J., Yu, H.-H., Lee, T., Jan, L.Y., and Jan, Y.N. (2007). Drosophila sensory neurons require Dscam for dendritic self-avoidance and proper dendritic field organization. Neuron *54*, 403–416.

Sperry, R.W. (1963). Chemoaffinity in the orderly growth of nerve fiber patterns and connections. Proc. Natl. Acad. Sci. U.S.A. *50*, 703–710.

St Johnston, D. (2005). Moving messages: the intracellular localization of mRNAs. Nat. Rev. Mol. Cell Biol. *6*, 363–375.

Stein, E., and Tessier-Lavigne, M. (2001). Hierarchical organization of guidance receptors: silencing of netrin attraction by slit through a Robo/DCC receptor complex. Science *291*, 1928–1938.

Sterne, G.R., Kim, J.H., and Ye, B. (2015). Dysregulated Dscam levels act through Abelson tyrosine kinase to enlarge presynaptic arbors. Elife *4*, p. e05196.

Stroschein-Stevenson, S.L., Foley, E., O'Farrell, P.H., and Johnson, A.D. (2005). Identification of Drosophila Gene Products Required for Phagocytosis of Candida albicans. PLOS Biol *4*, e4.

Su, Y.C., Maurel-Zaffran, C., Treisman, J.E., and Skolnik, E.Y. (2000). The Ste20 kinase misshapen regulates both photoreceptor axon targeting and dorsal closure, acting downstream of distinct signals. Mol. Cell. Biol. *20*, 4736–4744.

Sun, L.O., Jiang, Z., Rivlin-Etzion, M., Hand, R., Brady, C.M., Matsuoka, R.L., Yau, K.-W., Feller, M.B., and Kolodkin,

A.L. (2013a). On and Off Retinal Circuit Assembly by Divergent Molecular Mechanisms. Science *342*, 1241974–1241974.

Sun, W., You, X., Gogol-Döring, A., He, H., Kise, Y., Sohn, M., Chen, T., Klebes, A., Schmucker, D., and Chen, W. (2013b). Ultra-deep profiling of alternatively spliced Drosophila Dscam isoforms by circularization-assisted multi-segment sequencing. Embo J *32*, 2029–2038.

Sutton, M.A., and Schuman, E.M. (2006). Dendritic protein synthesis, synaptic plasticity, and memory. Cell *127*, 49–58.

Taniguchi, Y., Kim, S.-H., and Sisodia, S.S. (2003). Presenilin-dependent "gamma-secretase" processing of deleted in colorectal cancer (DCC). J. Biol. Chem. *278*, 30425–30428.

Tcherkezian, J., Brittis, P.A., Thomas, F., Roux, P.P., and Flanagan, J.G. (2010). Transmembrane receptor DCC associates with protein synthesis machinery and regulates translation. Cell *141*, 632–644.

Todd, A.G., Lin, H., Ebert, A.D., Liu, Y., and Androphy, E.J. (2013). COPI transport complexes bind to specific RNAs in neuronal cells. Hum. Mol. Genet. *22*, 729–736.

Tomaselli, K.J., Neugebauer, K.M., Bixby, J.L., Lilien, J., and Reichardt, L.F. (1988). N-cadherin and integrins: two receptor systems that mediate neuronal process outgrowth on astrocyte surfaces. Neuron *1*, 33–43.

Tonks, N.K., Diltz, C.D., and Fischer, E.H. (1988). Characterization of the major protein-tyrosine-phosphatases of human placenta. Journal of Biological Chemistry *263(14)*:6731-7.

Tonks, N.K. (2013). Special issue: Protein phosphatases: from molecules to networks: introduction. Febs J. *280*, 323–323.

Tran, T.A., Kinch, L., Peña-Llopis, S., Kockel, L., Grishin, N., Jiang, H., and Brugarolas, J. (2013). Platelet-derived growth factor/vascular endothelial growth factor receptor inactivation by sunitinib results in Tsc1/Tsc2-dependent inhibition of TORC1. Mol. Cell. Biol. *33*, 3762–3779.

Trowsdale, J., and Parham, P. (2004). Mini-review: defense strategies and immunity-related genes. Eur. J. Immunol. *34*, 7–17.

Tsuda, H., Han, S.M., Yang, Y., Tong, C., Lin, Y.Q., Mohan, K., Haueter, C., Zoghbi, A., Harati, Y., Kwan, J., et al. (2008). The amyotrophic lateral sclerosis 8 protein VAPB is cleaved, secreted, and acts as a ligand for Eph receptors. Cell *133*, 963–977.

Turk, B.E. (2008). Understanding and exploiting substrate recognition by protein kinases. Curr Opin Chem Biol *12*, 4–10.

Tutor, A.S., Prieto-Sánchez, S., and Ruiz-Gómez, M. (2014). Src64B phosphorylates Dumbfounded and regulates slit diaphragm dynamics: Drosophila as a model to study nephropathies. Development *141*, 367–376.

Ullrich, B., Ushkaryov, Y.A., and Südhof, T.C. (1995). Cartography of neurexins: more than 1000 isoforms generated by alternative splicing and expressed in distinct subsets of neurons. Neuron *14*, 497–507.

Venken, K.J.T., He, Y., Hoskins, R.A., and Bellen, H.J. (2006). P[acman]: a BAC transgenic platform for targeted insertion of large DNA fragments in D. melanogaster. Science *314*, 1747–1751.

Wang, F., Nemes, A., Mendelsohn, M., and Axel, R. (1998). Odorant receptors govern the formation of a precise topographic map. Cell *93*, 47–60.

Wang, J., Zugates, C.T., Liang, I.H., Lee, C., and Lee, T.M. (2002). Drosophila Dscam is required for divergent segregation of sister branches and suppresses ectopic bifurcation of axons. Neuron *33*, 559–571.

Wang, J., Ma, X., Yang, J.S., Zheng, X., Zugates, C.T., Lee, C.-H.J., and Lee, T. (2004). Transmembrane/juxtamembrane domain-dependent Dscam distribution and function during mushroom body neuronal morphogenesis. Neuron *43*, 663–

672.

Wang, J., Wang, L., Gao, Y., Jiang, Q., Yi, Q., Zhang, H., Zhou, Z., Qiu, L., and Song, L. (2013). A tailless Dscam from Eriocheir sinensis diversified by alternative splicing. Fish Shellfish Immunol. *35*, 249–261.

Wang, X., Li, G., Yang, Y., Wang, W., Zhang, W., Pan, H., Zhang, P., Yue, Y., Lin, H., Liu, B., et al. (2012). An RNA architectural locus control region involved in Dscam mutually exclusive splicing. Nature Communications *3*, 1255.

Wang, X., Bo, J., Bridges, T., Dugan, K.D., Pan, T.-C., Chodosh, L.A., and Montell, D.J. (2006). Analysis of cell migration using whole-genome expression profiling of migratory cells in the Drosophila ovary. Developmental Cell *10*, 483–495.

Warming, S., Costantino, N., Court, D.L., Jenkins, N.A., and Copeland, N.G. (2005). Simple and highly efficient BAC recombineering using galK selection. Nucleic Acids Res. *33*, e36–e36.

Watkins, T.A., Wang, B., Huntwork-Rodriguez, S., Yang, J., Jiang, Z., Eastham-Anderson, J., Modrusan, Z., Kaminker, J.S., Tessier-Lavigne, M., and Lewcock, J.W. (2013). DLK initiates a transcriptional program that couples apoptotic and regenerative responses to axonal injury. Proc. Natl. Acad. Sci. U.S.a. *110*, 4039–4044.

Watson, F.L. (2005). Extensive Diversity of Ig-Superfamily Proteins in the Immune System of Insects. Science *309*, 1874–1878.

Watthanasurorot, A., Jiravanichpaisal, P., Liu, H., Söderhäll, I., and Söderhäll, K. (2011). Bacteria-Induced Dscam Isoforms of the Crustacean, Pacifastacus leniusculus. PLoS Pathog *7*, e1002062.

Wojtowicz, W.M., Flanagan, J.J., Millard, S.S., Zipursky, S.L., and Clemens, J.C. (2004). Alternative splicing of Drosophila Dscam generates axon guidance receptors that exhibit isoform-specific homophilic binding. Cell *118*, 619–633.

Wojtowicz, W.M., Wu, W., Andre, I., Qian, B., Baker, D., and Zipursky, S.L. (2007). A vast repertoire of Dscam binding specificities arises from modular interactions of variable Ig domains. Cell *130*, 1134–1145.

Wojtowicz, W.M. (2008). The Drosophila Dscam gene encodes a vast repertoire of neuronal recognition molecules. Dissertation, University of California, Los Angeles.

Worby, C.A., Simonson-Leff, N., Clemens, J.C., Kruger, R.P., Muda, M., and Dixon, J.E. (2001). The sorting nexin, DSH3PX1, connects the axonal guidance receptor, Dscam, to the actin cytoskeleton. J. Biol. Chem. *276*, 41782–41789.

Worby, C.A., Simonson-Leff, N., Clemens, J.C., Huddler, D., Muda, M., and Dixon, J.E. (2002). Drosophila Ack targets its substrate, the sorting nexin DSH3PX1, to a protein complex involved in axonal guidance. J. Biol. Chem. *277*, 9422–9428.

Wu, C.-L., Buszard, B., Teng, C.-H., Chen, W.-L., Warr, C.G., Tiganis, T., and Meng, T.-C. (2011). Dock/Nck facilitates PTP61F/PTP1B regulation of insulin signalling. Biochem. J. *439*, 151–159.

Wu, D.Y., and Goldberg, D.J. (1993). Regulated tyrosine phosphorylation at the tips of growth cone filopodia. J. Cell Biol. *123*, 653–664.

Wu, Q., and Maniatis, T. (1999). A striking organization of a large family of human neural cadherin-like cell adhesion genes. Cell *97*, 779–790.

Wu, W., Ahlsen, G., Baker, D., Shapiro, L., and Zipursky, S.L. (2012). Complementary chimeric isoforms reveal Dscam1 binding specificity in vivo. Neuron *74*, 261–268.

Wu, Y.Y., and Bradshaw, R.A. (1993). Effect of nerve growth factor and fibroblast growth factor on PC12 cells: inhibition by orthovanadate. J. Cell Biol. *121*, 409–422.

Yaffe, M.B. (2002). Phosphotyrosine-binding domains in signal transduction. Nat. Rev. Mol. Cell Biol. *3*, 177–186.

Yamagata, M., and Sanes, J.R. (2008). Dscam and Sidekick proteins direct lamina-specific synaptic connections in vertebrate retina. Nature *451*, 465–U466.

Yamakawa, K., Huot, Y.K., Haendelt, M.A., Hubert, R., Chen, X.N., Lyons, G.E., and Korenberg, J.R. (1998). DSCAM: a novel member of the immunoglobulin superfamily maps in a Down syndrome region and is involved in the development of the nervous system. Hum. Mol. Genet. *7*, 227–237.

Yan, D., Wu, Z., Chisholm, A.D., and Jin, Y. (2009). The DLK-1 Kinase Promotes mRNA Stability and Local Translation in C. elegans Synapses and Axon Regeneration. Cell *138*, 1005–1018.

Yan, K.S., Kuti, M., and Zhou, M.M. (2002). PTB or not PTB -- that is the question. FEBS Lett. *513*, 67–70.

Yang, J.S.-J., Bai, J.-M., and Lee, T. (2008). Dynein-Dynactin Complex Is Essential for Dendritic Restriction of TM1-Containing Drosophila Dscam. PLoS ONE *3*, e3504.

Yang, Z., Huh, S.U., Drennan, J.M., Kathuria, H., Martinez, J.S., Tsuda, H., Hall, M.C., and Clemens, J.C. (2012). Drosophila Vap-33 Is Required for Axonal Localization of Dscam Isoforms. J. Neurosci. *32*, 17241–17250.

y Cajal, S.R. (1890). Sur l'origine et les ramifications des fibres nerveuses de la moelle embryonnaire. Gustav Fischer.

y Cajal, S.R.Y. (1906). Nobel Lecture: The Structure and Connexions of Neurons. Retrieved Feb, 27, p.2013. p.2013.

Yimlamai, D., Konnikova, L., Moss, L.G., and Jay, D.G. (2005). The zebrafish down syndrome cell adhesion molecule is involved in cell movement during embryogenesis. Dev. Biol. *279*, 44–57.

Yu, H.-H., Yang, J.S., Wang, J., Huang, Y., and Lee, T. (2009). Endodomain diversity in the Drosophila Dscam and its roles in neuronal morphogenesis. J. Neurosci. *29*, 1904–1914.

Zettervall, C.-J., Anderl, I., Williams, M.J., Palmer, R., Kurucz, E., Ando, I., and Hultmark, D. (2004). A directed screen for genes involved in Drosophila blood cell activation. Proc. Natl. Acad. Sci. U.S.A. *101*, 14192–14197.

Zhan, X.L., Clemens, J.C., Neves, G., Hattori, D., Flanagan, J.J., Hummel, T., Vasconcelos, M.L., Chess, A., and Zipursky, S.L. (2004). Analysis of Dscam diversity in regulating axon guidance in Drosophila mushroom bodies. Neuron *43*, 673–686.

Zhang, G., and Neubert, T.A. (2011). Comparison of three quantitative phosphoproteomic strategies to study receptor tyrosine kinase signaling. J. Proteome Res. *10*, 5454–5462.

Zhang, L., Huang, Y., Chen, J.Y., Ding, Y.Q., and Song, N.N. (2015). DSCAM and DSCAML1 regulate the radial migration and callosal projection in developing cerebral cortex. Brain Research *1594*, 61-70.

Zhu, H., Hummel, T., Clemens, J.C., Berdnik, D., Zipursky, S.L., and Luo, L. (2006). Dendritic patterning by Dscam and synaptic partner matching in the Drosophila antennal lobe. Nat Neurosci *9*, 349–355.

Zhu, Z., and Bhat, K.M. (2011). The Hem protein mediates neuronal migration by inhibiting WAVE degradation and functions opposite of Abelson tyrosine kinase. Dev. Biol. *357*, 283–294.

Zipursky, L.S. and Grueber, W.B. (2013). The Molecular Basis of Self-Avoidance. Annu. Rev. Neurosci. *36*, 547–568.